

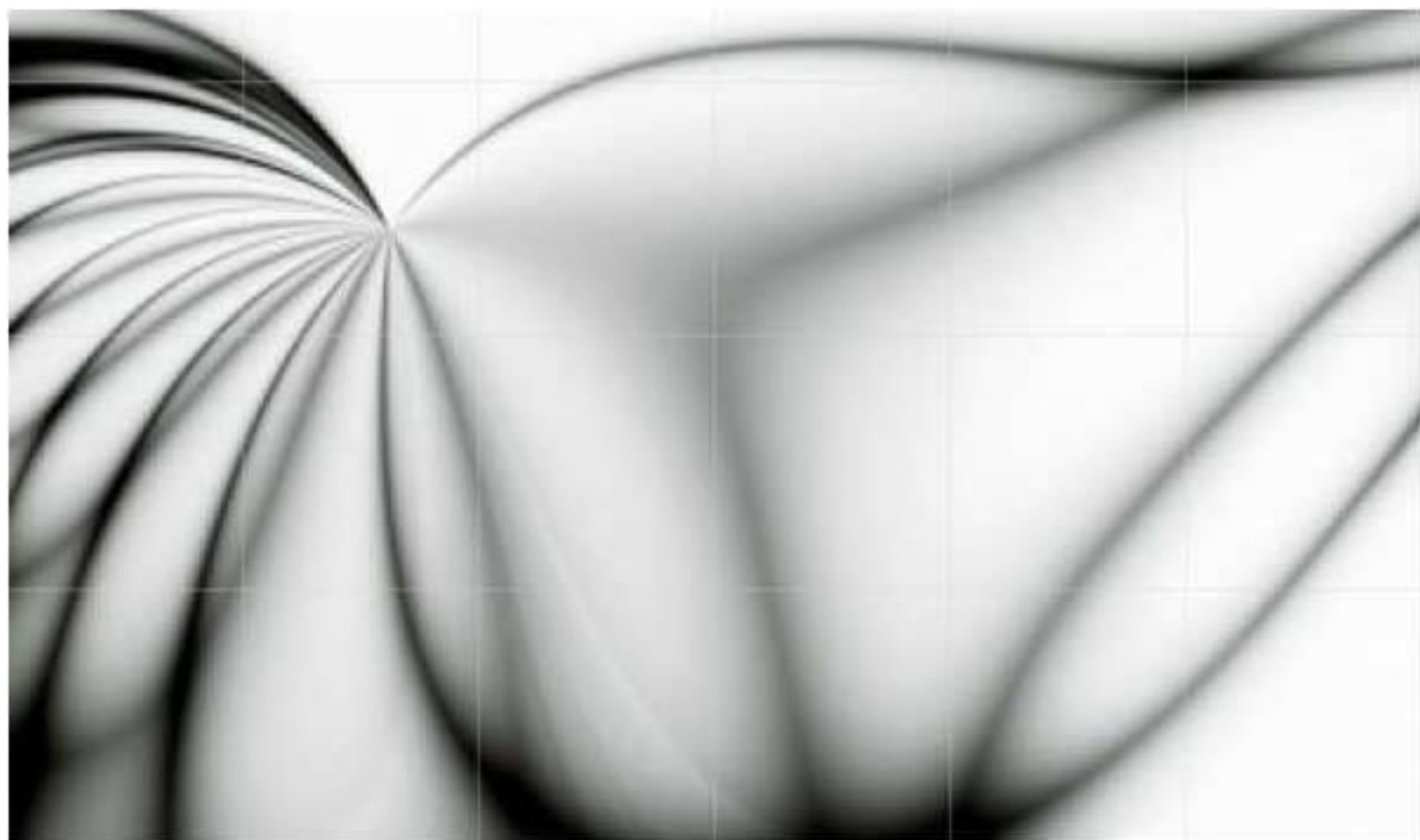
**IJOCTA**

An International Journal of  
Optimization and Control:  
Theories & Applications  
2010

**ISSN:2146-0957**  
**eISSN:2146-5703**

**Volume:9 Number:3**  
**December 2019**  
**Special Issue**

# **An International Journal of Optimization and Control: Theories & Applications**



**[www.ijocta.com](http://www.ijocta.com)**





www.ijocta.com  
info@ijocta.com

Publisher & Owner (*Yayımcı & Sahibi*):

Prof. Dr. Ramazan YAMAN  
Istanbul Gelisim University, Faculty of  
Engineering and Architecture,  
Department of Industrial Engineering,  
Avcilar, Istanbul, Turkey  
*İstanbul Gelişim Üniversitesi, Mühendislik  
ve Mimarlık Fakültesi, Endüstri  
Mühendisliği Bölümü, Avcılar, İstanbul,  
Türkiye*

ISSN: 2146-0957

eISSN: 2146-5703

Press (*Basımevi*):

Bizim Dijital Matbaa (SAGE Publishing),  
Kazım Karabekir Street, Kültür Market,  
No:7 / 101-102, İskitler, Ankara, Turkey  
*Bizim Dijital Matbaa (SAGE Yayıncılık),  
Kazım Karabekir Caddesi, Kültür Çarşısı,  
No:7 / 101-102, İskitler, Ankara, Türkiye*

Date Printed (*Basım Tarihi*):

December 2019

*Aralık 2019*

Responsible Director (*Sorumlu Müdür*):

Prof. Dr. Ramazan YAMAN

IJOCTA is an international, bi-annual,  
and peer-reviewed journal indexed/  
abstracted by (*IJOCTA, yılda iki kez  
yayımlanan ve aşağıdaki indekslerde  
taranan/dizinenen uluslararası hakemli  
bir dergidir*):

Cabell's Directories, DOAJ, EBSCO  
Databases, JournalSeek, Google Scholar,  
Index Copernicus, International  
Abstracts in Operations Research,  
JournalTOCs, Mathematical Reviews  
(MathSciNet), ProQuest, Scopus,  
Ulakbim Engineering and Basic Sciences  
Database (Tubitak), Ulrich's Periodical  
Directory, and Zentralblatt Math.



iThenticate and [ijocta.balikesir.edu.tr](http://ijocta.balikesir.edu.tr)  
are granted by Balikesir University.

# An International Journal of Optimization and Control: Theories & Applications

Volume: 9, Number: 3 (Special Issue)

December 2019

## Editor in Chief

**YAMAN, Ramazan** – Istanbul Gelisim University / Turkey

## Area Editor (Applied Mathematics & Control)

**OZDEMIR, Necati** - Balikesir University / Turkey

## Area Editors (Engineering Applications)

**DEMIRTAS, Metin** - Balikesir University / Turkey

**MANDZUKA, Sadko** - University of Zagreb / Croatia

## Area Editors (Fractional Calculus & Applications)

**BALEANU, Dumitru** - Cankaya University / Turkey

**POVSTENKO, Yuriy** - Jan Dlugosz University / Poland

## Area Editors (Optimization & Applications)

**WEBER, Gerhard Wilhelm** – Poznan University of Technology / Poland

**KUCUKKOC, Ibrahim** - Balikesir University / Turkey

## Editorial Board

**AGARWAL, Ravi P.** - Texas A&M University Kingsville / USA

**AGHABABA, Mohammad P.** - Urmia University of Tech. / Iran

**ATANGANA, A.** - University of the Free State / South Africa

**AYAZ, Fatma** - Gazi University / Turkey

**BAGIROV, Adil** - University of Ballarat / Australia

**BATTINI, Daria** - Università degli Studi di Padova / Italy

**CAKICI, Eray** - IBM / Turkey

**CARVALHO, Maria Adelaide P. d. Santos** - Institute of Miguel Torga / Portugal

**CHEN, YangQuan** - University of California Merced / USA

**DAGLI, Cihan H.** - Missouri University of Science and Technology / USA

**DAI, Liming** - University of Regina / Canada

**EVIRGEN, Firat** - Balikesir University / Turkey

**ISKENDER, Beyza B.** - Balikesir University / Turkey

**JANARDHANAN, M. N.** - University of Leicester / UK

**JONRINALDI** - Universitas Andalas, Padang / Indonesia

**KARAOGLAN, Aslan Deniz** - Balikesir University / Turkey

**KATALINIC, Branko** - Vienna University of Technology / Austria

**MACHADO, J. A. Tenreiro** - Polytechnic Institute of Porto / Portugal

**NANE, Erkan** - Auburn University / USA

**PAKSOY, Turan** - Selcuk University / Turkey

**SULAIMAN, Shamsuddin** - Universiti Putra Malaysia / Malaysia

**SUTIKNO, Tole** - Universitas Ahmad Dahlan / Indonesia

**TABUCANON, Mario T.** - Asian Institute of Technology / Thailand

**TEO, Kok Lay** - Curtin University / Australia

**TORIJA, Antonio J.** - University of Granada / Spain

**TRUJILLO, Juan J.** - Universidad de La Laguna / Spain

**WANG, Qing** - Durham University / UK

**XU, Hong-Kun** - National Sun Yat-sen University / Taiwan

**YAMAN, Gulsen** - Balikesir University / Turkey

**ZAKRZHEVSKY, Mikhail V.** - Riga Technical University / Latvia

**ZHANG, David** - University of Exeter / UK

## Technical Editor

**AVCI, Derya** - Balikesir University, Turkey

## English Editors

**INAN, Dilek** - Balikesir University / Turkey

## Editorial Assist Team

**CETIN, Mustafa** - Balikesir University / Turkey

**ONUR, Suat** - Balikesir University / Turkey

**UCMUS, Emine** - Balikesir University / Turkey



# An International Journal of Optimization and Control: Theories & Applications

Volume: 9 Number: 3 (Special Issue)  
December 2019



## CONTENTS

- 1 On the numerical solution for third order fractional partial differential equation by difference scheme method  
Mahmut Modanli
- 6 Investment evaluation of wind turbine relocation  
Hasan Huseyin Yildirim, Sakir Sakarya
- 15 Simulation of glucose regulating mechanism with an agent-based software engineering tool  
Sevcan Emek, Vedat Evren, Şebnem Bora
- 21 A comparison of some control strategies for a non-integer order tuberculosis model  
Tuğba Akman Yıldız
- 31 A new auxiliary function approach for inequality constrained global optimization problems  
Nurullah Yilmaz, Ahmet Sahiner
- 39 Analysis of boride layer thickness of borided AISI 430 by response surface methodology  
Turker Turkoglu, Irfan Ay
- 45 An application of fuzzy linear modeling: prediction of uncertainty for beta-glucan content  
Özlem Türkşen, Suna Ertunç
- 52 On the explicit solutions of fractional Bagley-Torvik equation arises in engineering  
Zehra Pinar
- 59 Application of precedence constrained travelling salesman problem model for tool path optimization in CNC milling machines  
Ilker Kucukoglu, Tulin Gunduz, Fatma Balkancioglu, Emine Chousein Topal, Oznur Sayim
- 69 Maintenance of the latent reservoir by pyroptosis and superinfection in a fractional order HIV transmission model  
Ana R Carvalho, Carla M Pinto, João N Tavares
- 76 The DRBEM solution of Cauchy MHD duct flow with a slipping and variably conducting wall using the well-posed iterations  
Cemre Aydin, Münevver Tezer-Sezgin
- 86 Approximate controllability of nonlocal non-autonomous Sobolev type evolution equations  
Arshi Meraj, Dwijendra Narain Pandey
- 95 A Boiti-Leon Pimpinelli equations with time-conformable derivative  
Kamal Ait Touchent, Zakia Hammouch, Toufik Mekkaoui, Canan Unlu



RESEARCH ARTICLE

# On the numerical solution for third order fractional partial differential equation by difference scheme method

Mahmut Modanlı

*Harran University, Faculty of Art and Science, Department of Mathematics, Turkey*  
*mmodanli@harran.edu.tr*

ARTICLE INFO

Article History:  
*Received 15 August 2018*  
*Accepted 10 December 2018*  
*Available 19 March 2019*

Keywords:  
*Third order fractional partial differential equation*  
*Exact solution*  
*Stability estimate*  
*Difference scheme*

AMS Classification 2010:  
*34A08; 34K37; 74G15*

ABSTRACT

The third order fractional partial differential equations is obtained the exact solution depending on initial-boundary value problem. The exact solution and its stability estimates theorem is proved for this equation. Difference schemes are presented for the third order fractional partial differential equation. The stabilities of these difference schemes for this problem are given. The numerical solutions of the third order fractional partial differential equation defined by Caputo fractional derivative for fractional orders  $\alpha = 0.1, 0.5, 0.9$  are calculated by these methods. The exact solutions are compared with the numerical results and it is shown that the given method is effective.



## 1. Introduction

The theory of fractional differential equations becomes one of the most interesting and attractive topics and has shown an increasing development. Differential equations involving fractional order derivatives are used to model a variety of systems has important applied sciences and engineering aspects. In applied sciences, this frame of derivatives are used to model a variety of systems, of which the important applications lie in field of viscoelasticity, electrode-electrolyte polarization, heat conduction, electromagnetic waves, diffusion equation and so on [1,2].

Finite difference methods in particular became very popular and a large number of schemes has been published very recently. Consequently it becomes important to understand how they compare in terms of accuracy, stability and computing times. In [3–7], fractional differential transform method (FDTM) and modified fractional differential transform method (MFDTM) to solve third-order dispersive partial differential equations were studied by various authors. Third order partial

differential equations were investigated in [8], [9], and [10]. In [11], the initial value problem for the third order partial differential equation with time delay with self adjoint positive operator of a Hilbert space was investigated. Finally, some paper implemented several on the numerical solutions of the fractional differential equations in recent years [12–18].

Now, we shall give the following basic definitions for this study.

**Definition 1.** The Caputo fractional derivative  $D_t^\alpha u(t, x)$  of order  $\alpha$  depended on time is defined as:

$$\begin{aligned} \frac{\partial^\alpha u(t, x)}{\partial t^\alpha} &= D_t^\alpha u(t, x) & (1) \\ &= \frac{1}{\Gamma(n - \alpha)} \int_0^t \frac{1}{(t - p)^{\alpha - n + 1}} \frac{\partial^\alpha u(p, x)}{\partial p^\alpha} dp, \\ &(n - 1 < \alpha < n), \end{aligned}$$

and for  $\alpha = n \in N$  defined as:

$$D_t^\alpha u(t, x) = \frac{\partial^\alpha u(t, x)}{\partial t^\alpha} = \frac{\partial^n u(t, x)}{\partial t^n}.$$

**Definition 2.** First-order approximation method computing the problem (1) given by the formula:

$$D_t^\alpha U_n^k \cong g_{\alpha, \tau} \sum_{j=1}^k w_j^{(\alpha)} (U_n^{k-j+1} - U_n^{k-j}), \quad (2)$$

where  $g_{\alpha, \tau} = \frac{1}{\Gamma(2-\alpha)\tau^\alpha}$  and  $w_j^{(\alpha)} = j^{1-\alpha} - (j-1)^{1-\alpha}$ . From the above facts, we have the following approximation [19]:

$$\frac{\partial^\alpha u(t_k, x_n)}{\partial t^\alpha} = g_{\alpha, \tau} \left[ w_1 U_n^k - w_k U_n^0 + \sum_{j=1}^{k-1} (w_{k-j+1} - w_{k-j}) u_n^j \right]. \quad (3)$$

In this work, we consider the third order fractional partial differential equation depend on initial boundary value problem

$$\begin{cases} \frac{\partial^3 u(t, x)}{\partial t^3} + \frac{\partial^\alpha u(t, x)}{\partial t^\alpha} - \frac{\partial^2 u(t, x)}{\partial x^2} + u(t, x) = f(t, x), \\ 0 < x < L, 0 < t < T, 0 < \alpha < 1, \\ u(0, x) = \varphi(x), u_t(0, x) = \psi(x), \\ u_{tt}(0, x) = \sigma(x), 0 \leq t \leq T, \\ u(t, X_L) = u(t, X_R) = 0, X_L < x < X_R. \end{cases} \quad (4)$$

For the problem (4), basic definitions are given. The exact solution of the problem (4) and its stability inequalities are investigated. The first order of difference schemes of the problem (4) are constructed. The theorem of stability estimates for the solution of difference schemes for initial-boundary value problem for this partial differential equation are obtained. The results of numerical experiments are presented and are compared with exact solutions. These results obtained with Matlab programming showed that the method gives good results for this problem.

## 2. The exact solution and stability for third order fractional partial differential equation

Consider the equation (4) the following abstract form

$$\begin{cases} \frac{d^3 u(t)}{dt^3} + Au(t) = F(t), (0 < t < T), \\ u(0) = \varphi, u'(0) = \psi, u''(0) = \sigma, \end{cases} \quad (5)$$

in a Hilbert space  $H = L_2[0, L]$ . Here  $f(t) = f(t, x)$  is abstract function defined on  $[0, T]$  with values in  $H = L_2[0, L]$ .  $\varphi = \varphi(x)$  and  $\psi = \psi(x)$  are the elements of  $H = L_2[0, L]$ .  $u(t) = u(t, x)$  is unknown abstract function defined on  $[0, T]$  with values in  $H = L_2[0, L]$ .

$A : D(A) \rightarrow H$  is the differential operator defined by formula

$$Au(x) = -u''(x) + u(x)$$

with domain

$$D(A) = \{u : u_x, u_{xx} \in L_2[0, L]; u(0) = u(L) = 0\}.$$

Here,  $F(t) = f(t) - D_t^\alpha u(t)$ .

Now, we shall get the formula for the solution of the problem (5). Using the method [8], we write the problem (5) as the following first order linear differential equations:

$$\begin{cases} \frac{du(t)}{dt} - aBu(t) = w(t), \\ \frac{dw(t)}{dt} - \bar{a}Bw(t) = v(t), \\ \frac{dv(t)}{dt} + Bv(t) = F(t), \end{cases} \quad (6)$$

where  $B = A^{1/3}$ . Using the initial conditions of the problem (5) and the formula (6), we get new initial conditions for the formula (5) as the following:

$$\begin{cases} w(0) = u'(0) - aBu(0) \\ v(0) = u''(0) - Bu'(0) + B^2(0). \end{cases} \quad (7)$$

Here,  $a = \frac{1}{2} + i\frac{\sqrt{3}}{2}$  and  $\bar{a} = \frac{1}{2} - i\frac{\sqrt{3}}{2}$ .

Integrating the formula (6) and using the initial conditions of the formula (7), we obtain

$$u(t) = R_1 u(0) + R_2 u'(0) + R_3 u''(0) + \int_0^t R_4 f(s) ds - \int_0^t R_4 D_s^\alpha u(s) ds. \quad (8)$$

Here

$$\begin{aligned}
 R_1 &= \frac{\bar{a}e^{aA^{1/3}t} - ae^{\bar{a}A^{1/3}t}}{\bar{a} - a} + \frac{e^{-A^{1/3}t} - e^{aA^{1/3}t}}{(a+1)(\bar{a}+1)} \\
 &\quad + \frac{e^{\bar{a}A^{1/3}t} - e^{aA^{1/3}t}}{(\bar{a}+1)(\bar{a}-a)}, \\
 R_2 &= \frac{e^{aA^{1/3}t} - e^{\bar{a}A^{1/3}t}}{(\bar{a}-a)A^{1/3}} - \frac{e^{-A^{1/3}t} - e^{aA^{1/3}t}}{(a+1)(\bar{a}+1)A^{1/3}} \\
 &\quad - \frac{e^{\bar{a}A^{1/3}t} - e^{aA^{1/3}t}}{(\bar{a}+1)(\bar{a}-a)A^{1/3}}, \\
 R_3 &= \frac{e^{-A^{1/3}t} - e^{aA^{1/3}t}}{(a+1)(\bar{a}+1)A^{2/3}} + \frac{e^{\bar{a}A^{1/3}t} - e^{aA^{1/3}t}}{(\bar{a}+1)(\bar{a}-a)A^{2/3}}, \\
 R_4 &= -\frac{e^{-A^{1/3}(t-s)} - e^{aA^{1/3}(t-s)}}{(a+1)(\bar{a}+1)A^{2/3}}.
 \end{aligned}$$

**Lemma 1.** *The following inequalities are satisfied:*

$$\begin{cases} \|R_1\|_H \leq M(\delta), & \|R_2\|_H \leq M(\delta) \\ \|R_3\|_H \leq M(\delta), & \|R_4\|_H \leq M(\delta). \end{cases} \quad (9)$$

**Lemma 2.** *For  $t \geq 0$  of the following estimates hold:*

$$\left\| e^{-A^{1/3}t} \right\| \leq e^{-\delta^{1/3}t} \quad (10)$$

The proof of this Lemma is supported the spectral representation of unit self-adjoint positive definite operator  $A$  in a Hilbert space  $H$ .

**Lemma 3.** *Suppose that  $\varphi \in D(A)$ ,  $\psi \in D(A^{2/3})$ ,  $\sigma \in D(A^{1/3})$ ,  $D_t^\alpha u(t)$  and  $f(t)$  are continuously differentiable on  $[0, T]$ . Then, there are the following stability inequality for the formula (8)*

$$\begin{aligned}
 \|D_t^\alpha u(t)\|_H &\leq M \left\{ \|\varphi\|_H + \left\| A^{-1/3}\psi \right\|_H \right. \\
 &\quad + \left\| A^{-2/3}\sigma \right\|_H \\
 &\quad \left. + \max_{0 \leq t \leq T} \left\| A^{-2/3}f(t) \right\|_H \right\}. \quad (11)
 \end{aligned}$$

**Proof.** Taking the first derivative of the problem (8) and using the following formula for fractional derivative of order  $0 < \alpha < 1$ , we find

$$D_t^\alpha u(t) = \frac{1}{\Gamma(1-\alpha)} \int_0^t \frac{u'(p)dp}{(t-p)^\alpha}, \quad \text{where } u(0) = 0, \quad (12)$$

which implies that the proof of this lemma is completed.  $\square$

**Theorem 1.** *Let  $\varphi \in D(A)$ ,  $\psi \in D(A^{2/3})$ ,  $\sigma \in D(A^{1/3})$  and  $f(t)$  be continuously differentiable on  $[0, T]$ . Then, there is a unique solution*

*of problem (5) and the following stability inequalities hold:*

$$\begin{aligned}
 &\max_{0 \leq t \leq T} \|u(t)\|_H \\
 &\leq M \left\{ \|\varphi\|_H + \left\| A^{-1/3}\psi \right\|_H + \left\| A^{-2/3}\sigma \right\|_H \right. \\
 &\quad \left. + \max_{0 \leq t \leq T} \left\| A^{-2/3}f(t) \right\|_H \right\}, \quad (13)
 \end{aligned}$$

$$\begin{aligned}
 &\max_{0 \leq t \leq T} \left\| \frac{d^3 u(t)}{dt^3} \right\|_H + \max_{0 \leq t \leq T} \|Au(t)\|_H \\
 &\leq M \left\{ \|A\varphi\|_H + \left\| A^{2/3}\psi \right\|_H + \left\| A^{1/3}\sigma \right\|_H \right. \\
 &\quad \left. + \max_{0 \leq t \leq T} \|f'(t)\|_H + \|f(0)\|_H \right\} \quad (14)
 \end{aligned}$$

are valid, where  $M$  is independent on  $f(t)$ ,  $t \in [0, T]$ ,  $\varphi$ ,  $\psi$ , and  $\sigma$ .

**Proof.** From (9), (10) and (8), the proof of the formula (13) and (14) are completed.  $\square$

### 3. Constructed difference scheme and its stability

Let us choose  $h = \frac{L}{M}$  for  $x$ -axis and  $\tau = \frac{T}{N}$  for  $t$ -axis as grid mess in the difference scheme method. In this case, we have

$x_n = x_L + nh$ ;  $n = 1, 2, \dots, M$ ,  $t_k = k\tau$ ,  $k = 1, 2, \dots, N$ . Applying the formula (2) for the fractional partial differential equation (4), we construct the following the first order difference schemes

$$\begin{cases} \frac{U_n^{k+2} - 3U_n^{k+1} + 3U_n^k - U_n^{k-1}}{\tau^3} \\ + g_{\alpha, \tau} \sum_{j=1}^k w_j^{(\alpha)} (U_n^{k-j+1} - U_n^{k-j}) + U_n^k \\ - \frac{1}{2h^2} [U_{n+1}^{k+1} - 2U_n^{k+1} + U_{n-1}^{k+1} + U_{n+1}^k \\ - 2U_n^k + U_{n-1}^k] \\ = f_n^k = f(t_k, x_n), \\ U_0 = \varphi, \\ \frac{U_1 - U_0}{\tau} = \psi. \end{cases} \quad (15)$$

**Theorem 2.** *Suppose that the assumption  $A \geq \delta$  holds and  $\varphi \in D(A)$ ,  $\psi \in D(A^{2/3})$  and  $\sigma \in D(A^{1/3})$ . Then, for the solution of difference scheme (15) the following stability estimates*

$$\begin{aligned} & \max_{1 \leq k \leq N} \left\| \frac{U_n^{k+2} - 3U_n^{k+1} + 3U_n^k - U_n^{k-1}}{\tau^3} \right\|_H \\ & + \max_{1 \leq k \leq N} \|Au_k\|_H \\ \leq & M(\delta) \left\{ \|A\varphi\|_H + \|A^{2/3}\psi\|_H + \|A^{1/3}\sigma\|_H \right. \\ & \left. + \max_{0 \leq t \leq T} \left\| \frac{f_k - f_{k-1}}{\tau} \right\|_H + \|f_1\|_H \right\}, \end{aligned}$$

hold, where  $M(\delta)$  is independent of choosing  $\tau$ ,  $\varphi$ ,  $\psi$ ,  $\sigma$  and  $f_k$ ,  $1 \leq s \leq N - 1$ .

The proof of Theorem 2 is based on the formulas for the solution of difference schemes (15), on the estimates for the step operators and on the self-adjointness and positivity of operator  $A$ .

### 4. Numerical experiments

#### Example

Investigate the following third order fractional partial differential equation for initial boundary value problems

$$\left\{ \begin{aligned} & \frac{\partial^3 u(t,x)}{\partial t^3} + \frac{\partial^\alpha u(t,x)}{\partial t^\alpha} - \frac{\partial^2 u(t,x)}{\partial x^2} + u(t,x) \\ & = \sin x(4 + 6 \frac{t^{3-\alpha}}{\Gamma(4-\alpha)} + 2t^3), \\ & 0 < x < \pi, 0 < t < 1, 0 < \alpha \leq 1, \\ & u(0,x) = -\sin x, \\ & u_t(0,x) = 0, u_{tt}(0,x) = 0, 0 \leq t \leq 1, \\ & u(t,0) = u(t,\pi) = 0, 0 \leq x \leq \pi. \end{aligned} \right. \quad (16)$$

This problem has the exact solution of as  $u(t,x) = (t^3 - 1) \sin x$ .

For the numerical solution of problem (16), we applied difference schemes method to (10). By the help of modified Gauss elimination method, we compute the maximum norm of error of the numerical solution as

$$\varepsilon = \max_{\substack{n = 0, 1, \dots, M \\ k = 0, 1, 2, \dots, N}} |u(t,x) - U(t_k, x_n)|,$$

where  $U_n^k = U(t_k, x_n)$  is the numerical solution and  $u(t,x)$  is the exact solution. The error analysis table gives our the error analysis for difference schemes method.

**Table 1.** Error analysis table.

| $\tau = \frac{1}{N}, h = \frac{pi}{M}$ |          |        |
|--|----------|--------|
| The difference scheme (16)             |          |        |
|  | $\alpha$ |        |
| $N = M = 40$                           | 0.1      | 0.0722 |
|  | 0.5      | 0.0711 |
|  | 0.9      | 0.0692 |
| $N = M = 80$                           | 0.1      | 0.0365 |
|  | 0.5      | 0.0359 |
|  | 0.9      | 0.0349 |
| $N = M = 160$                          | 0.1      | 0.0183 |
|  | 0.5      | 0.0180 |
|  | 0.9      | 0.0188 |
| $N = M = 240$                          | 0.1      | 0.0122 |
|  | 0.5      | 0.0120 |
|  | 0.9      | 0.0213 |
| $N = 625, M = 25$                      | 0.1      | 0.0047 |
|  | 0.5      | 0.0112 |
|  | 0.9      | 0.0247 |

### 5. Conclusion

The exact solution of the third order fractional partial differential equation is examined. The abstract theorem on the stability estimate for the solution of the initial boundary value problems for the third order fractional equations is established. The first order of accuracy difference schemes for the numerical solution of the initial-boundary value problems for the third order fractional equations are presented. Stability estimates for the solution of difference schemes for the initial-boundary value problems for the third order fractional equations are obtained. The Matlab implementation of the first order of accuracy difference schemes for the approximate solution of the initial boundary value problem for the third order fractional equations are presented. Taking into consideration the results of numerical examples, applications of the theorems are shown.

### References

- [1] Hilfer, R. (2000). *Applications of fractional calculus in physics*. Singapore: Word Scientific Company.
- [2] Caputo, M. (1967). Linear models of dissipation whose Q is almost frequency independent Part II. *Geophysical Journal of the Royal Astronomical Society banner*, 13(5), 529-539.
- [3] Djidjeli, K., & Twizell, EH. (1991). Global extrapolations of numerical methods for solving a third-order dispersive partial differential equations. *International Journal of Computer Mathematics*, 41(1-2), 81-89.

- [4] Wazwaz A.M. (2003). An analytic study on the third-order dispersive partial differential equation. *Applied Mathematics and Computation*, 142(23), 511-520.
- [5] Twizell, E.H. (1984). *Computational methods for partial differential equations*. Ellis Horwood, New York: Chichester and John Wiley and Sons.
- [6] Lewson, J.D., & Morris, J.LI. (1978). The extrapolation of first-order methods for parabolic partial differential equations I. *SIAM Journal on Numerical Analysis*, 15(6), 1212-1224.
- [7] Mengzhao, Q. (1983). Difference scheme for the dispersive equation. *Computing*, 31(3), 261-267.
- [8] Ashyralyev, A., & Simsek, S.N. (2017). An operator method for a third order partial differential equation. *Numerical Functional Analysis and Optimization*, 38(10), 1341-1359.
- [9] Apakov, Y.P. (2012). On the solution of a boundary-value problem for a third-order equation with multiple characteristics. *Ukrainian Mathematical Journal*, 64(1), 1-12.
- [10] Belakroum, K., Ashyralyev, A., Guezane-Lakoud, A., & Lukashov, A. (2016). A note on the nonlocal boundary value problem for a third order partial differential equation, *AIP Conference Proceedings*, 1759:1, 020021, Online publication date: 10-Aug-2016.
- [11] Ashyralyev, A., Hincal, E., & Ibrahim, S. (2018). Stability of the third order partial differential equations with time delay, *AIP Conference Proceedings*, 1997(1), 02086.
- [12] Baskonus, H.M., & Bulut, H. (2015). On the numerical solutions of some fractional ordinary differential equations by fractional Adams-Bashforth-Moulton method. *Open Mathematics*, 13(1).
- [13] Baskonus, H.M., Mekkaoui, T., Hammouch, Z., & Bulut, H. (2015). Active control of a chaotic fractional order economic system. *Entropy*, 17(8), 5771-5783.
- [14] Baskonus, H.M., & Bulut, H. (2016). Regarding on the prototype solutions for the nonlinear fractional-order biological population model. *AIP Conference Proceedings*, 1738(1), p.290004.
- [15] Baskonus, H.M., Hammouch, Z., Mekkaoui, T., & Bulut, H. (2016). Chaos in the fractional order logistic delay system: circuit realization and synchronization. *AIP Conference Proceedings*, 1738(1), p.290005.
- [16] Gencoglu, M.T., Baskonus, H.M., & Bulut, H. (2017). Numerical simulations to the nonlinear model of interpersonal Relationships with time fractional derivative. *AIP Conference Proceedings*, 1798(1), p.020103.
- [17] Ozdemir, N., Avci, D., & Iskender, B.B. (2011). The numerical solutions of a two-dimensional space-time Riesz-Caputo fractional diffusion equation. *An International Journal of Optimization and Control: Theories & Applications (IJOCTA)*, 1(1), 17-26.
- [18] Evirgen, F. (2016). Analyze the optimal solutions of optimization problems by means of fractional gradient based system using VIM. *An International Journal of Optimization and Control: Theories & Applications (IJOCTA)*, 6(2), 75-83.
- [19] Karatay, I., Bayramoglu, S.R., & Sahin, A. (2013). A new difference scheme for time fractional heat equation based on the Crank-Nicholson method. *Fractional Calculus and Applied Analysis*, 16, 892-910.

**Mahmut Modanlı** is an Assistant Professor in Harran University of Department of Mathematics. He has been a faculty member since 2016. His research interests lie in the area of applied mathematics, Matlab programming, numerical analysis, fractional partial differential equations. He has two sons and one daughter.



RESEARCH ARTICLE

## Investment evaluation of wind turbine relocation

Hasan Huseyin Yildirim <sup>a\*</sup> , Sakir Sakarya <sup>b</sup> 

<sup>a</sup> Department of Banking and Finance, Balikesir University, Turkey

<sup>b</sup> Department of Economics and Administrative Sciences, Balikesir University, Turkey  
[hhyildirim@balikesir.edu.tr](mailto:hhyildirim@balikesir.edu.tr), [sakarya@balikesir.edu.tr](mailto:sakarya@balikesir.edu.tr)

### ARTICLE INFO

#### Article history:

Received: 18 December 2018

Accepted: 11 February 2019

Available Online: 19 March 2019

#### Keywords:

Energy

Wind energy

Energy investment valuation

Energy investment decisions

#### AMS Classification 2010:

00A69, 91G50, 37N40

### ABSTRACT

Energy has become one of the most important building blocks of many changes in the world, and it still maintains this quality. The demand for natural resources and energy continues to increase daily. For this reason, the supply of reliable and sustainable energy has become an important issue that concerns and occupies mankind. Of the renewable energy sources, wind energy is a clean, reliable and inexhaustible source of energy with low operating costs. Turkey is a rich nation in terms of wind energy potential. In this context, the profitability of investments made in utilising domestic and renewable energy potential is important. Investment efficiency is a very important issue before and during the investment period due to the fact that wind energy investments are high cost investments. In this study, a solution will be proposed for the replacement of inefficient wind turbines which have been installed. In the ideal solution of the issue, the remaining lifetime of the wind turbine which is to be replaced and capacity utilization at the new location of the turbine will be used as key input factors. The results showed that it was important for the relocation decision to be made early for the investment to be more profitable. In the event of delayed decisions to relocate the turbine, a high capacity factor is expected in the new location. If a high capacity factor is not achieved, the relocation of the turbine will be meaningless and losses will be incurred for the investor. Also according to the results of the analysis, in the first two years, the turbine operating at a low capacity of 19% and 17% is profitable if it works at 26% capacity until the end of its economic life when change is made in the third year.



### 1. Introduction

Countries aiming for sustainability in economic growth and development ensure the reliability of energy supplies. For countries to provide their energy needs uninterruptedly, it is important for domestic and renewable energy sources to be utilised. In Turkey, which is one of the developing countries, the economic change experienced in recent years has led to a rapid increase in demand in the energy sector, as it has in other sectors. While electricity production in Turkey showed an average annual increase of 3.6% between the years 1970 and 2000, electricity production increased annually by 8.9% on average between the years 2000 and 2017. In this regard, Turkey was one of the OECD countries in which energy demand increased the most rapidly. Electricity production in Turkey in 2017 increased by 5.6% to 294.8 GWh compared with the previous year. 37% of this production was obtained

from natural gas, 33% was obtained from coal, 20% from hydraulic energy, 6% from wind energy, 2% from geothermal energy and 2% from other sources [1]. In 2017, approximately 70% of electricity production came from fossil sources, namely coal, liquid fuels and natural gas, while about 28% was obtained from renewable energy sources. When evaluating Turkey's 2017 energy situation, the high rate of energy use from fossil sources leads to environmental problems such as greenhouse gas emissions. Furthermore, the fact that a high percentage of the required energy is provided by imports has a negative effect on the balance of payments in a national economic sense. Between the years 1996 and 2017, energy imports made up an average of 20% of total annual imports. In 2017, total imports amounted to 234,156 million US dollars, 16% of which consisted of energy imports of 37,194 million US dollars. The 2015 foreign trade deficit was 76,736 million US dollars. If Turkey's energy needs were

\*Corresponding author

obtained from domestic sources instead of imported sources, the foreign trade deficit would be reduced by approximately 48%. Considering the overall picture of energy in Turkey in recent years, providing the required energy from domestic and renewable sources has become essential.

With regard to renewable energy potential, Turkey is a country with high potential for obtaining electricity production from wind and solar energy. According to the criteria specified, wind potential at a height of 50 metres on Turkey's wind atlas ranges from good to excellent, approaching 48 GW [2]. By July 2018, Turkey's wind-based energy capacity had reached 7 GW [3]. Turkey's wind-based power is about 15% of the energy potential that can be obtained from wind.

In meeting increasing energy needs, energy sources that reduce dependence on foreign sources and cause fewer environmental problems should be used within the energy portfolio. For these reasons, increasing domestic and renewable energy sources is essential for Turkey, and this will also provide many benefits for the national economy. Within the scope of the 2015-2019 Strategic Plan prepared by the Ministry of Energy and Natural Resources, based on the diversification of resources in energy consumption with continuous, sustainable, environmentally friendly, good quality, reliable and low-cost energy for final consumers, the greatest possible utilisation of domestic and renewable energy sources was included among the main aims. Accordingly, the 2015-2019 Strategic Plan consists of 8 themes, 16 aims and 62 targets. In the 2015-2019 Strategic Plan, in the area of Energy and Natural Resources, common development needs such as good governance and stakeholder interaction, regional and international activity, technological research, development and innovation, and improvement of the investment environment are emphasised, while in the Energy field, security of supply and energy efficiency and saving are given priority. Moreover, in the field of Natural Resources, the subjects of security of supply of raw materials and efficient and effective use of raw materials are given attention. The subject of sustainability, which is regarded as an indispensable approach in the process of acquiring energy and natural resources for the economy and of their consumption, is designed not as a separate theme, but as a framework which covers all the themes [4].

As can be seen in the 2015-2019 Strategic Plan prepared by the Ministry of Energy and Natural Resources, sustainability as a framework is aimed for and a Turkey that benefits from domestic and renewable natural resources is targeted by diversification of energy sources to ensure security of supply. The use of domestic and renewable energy sources ensures diversification of resources within the energy portfolio, thereby allowing important progress to be made in reducing dependence on foreign energy sources and developing an environment that provides security of energy supply [5]. When considering why domestic and renewable energy is needed and why the

prepared strategic targets are frequently deliberated, the importance of financial support for investments in renewable energy sources is stressed.

The increase in wind energy investments in Turkey and the world is striking. Is the main reason for this increase the fact that wind energy is an alternative energy source for meeting the needed and ever-increasing demand for energy? Or is it the fact that investments in wind energy are economically profitable? The answer to both questions explains the interest that there is in investment in wind power plants (WPP).

Before wind energy investments are begun, two basic analyses need to be made. The first of these is the technical analysis, which includes technical components such as the place where the investment is to be made, the investment capacity, the choice of turbines to be used in the investment, etc. The second analysis to be made is the financial analysis of the investment, which determines whether the investment is economically profitable or not. In both the technical and the financial analyses, there are a number of uncertain variables which affect the investment.

In evaluating a wind energy project in an economic sense, a project estimate of the installation costs must be made. In the technical evaluation of a WPP investment, the subjects in which there is insufficient knowledge and uncertainties regarding the WPP investment are factors such as when it will be completed, when the installation of the investment will begin, when the installation period of the investment will be completed, future changes in prices of materials to be used in the investment and how long the supply of the turbine from the manufacturer will take. Businesses have to make decisions under the existence of uncertainties like these. It is important for companies to make decisions that are as correct as possible and that will gain the most profit.

In this study, alternatives are discussed related to the relocation of 8 wind turbines for which adequate wind measurements had not been made in the technical analysis of WPP investments and which had been installed in unproductive locations. In the relocation of the 8 wind turbines that had been installed in unproductive locations and were operating at low capacity, the minimum required capacity of the new location was determined. Moreover, the capacity of the new location created for a return to profitability was determined separately for each year up to the end of the economic life of the turbine. In this way, it was revealed in which year and at what capacity a turbine that had been installed in the wrong place could be turned into a profitable investment in its new place of installation.

## 2. Literature review

Despite the increasing interest in renewable energy technologies, following the literature review conducted, it was observed that few studies have been conducted regarding economic assessment of investments in this field. Some of the studies that

evaluate WPP investments in an economic sense are included below. It is considered that this study will also contribute to the literature.

In a study by Desrochers and Blanchard [6] to examine the cost effectiveness of wind energy, one year's hourly data for wind turbines were utilised. In their study, with the aid of the model established, the energy production capacities of different types of wind turbines were compared by means of simulation. It was concluded that the lower the investment constraints and the higher the production, the higher the rate of wind energy that could be absorbed by the system. With the system they developed, the inputs of different wind turbines into the system in terms of energy and capacity can be calculated [6].

In a study carried out by Venetsanos et al. [7], the net present value (NPV) and real options (RO) methods were used to evaluate wind energy for Greece, a country which has high potential in terms of renewable energy. It was determined that since investments in wind power plants involved high uncertainties, it would be beneficial to use the RO method as a complement to the NPV method [7].

In his study conducted in 239 locations selected from different states of the USA, using Monte Carlo simulation, Liberman [8] examined the payback periods of WPP investments for the locations depending on meteorological wind data. Due to the different prevailing wind speeds of the locations, the payback periods for the investments to be made in the locations were different. In areas with high wind speeds, the payback periods for the wind energy investments were shorter than in areas with low wind speeds [8].

In their study, Özerdem et al. [9] calculated the technical and economic feasibility of investments in wind power plants for the Izmir region in Turkey. For the technical feasibility study, wind speed, prevailing wind direction and temperature data were utilized. For the economic feasibility study, three different scenario groups for investment were examined with regard to net present value (NPV), internal rate of return (IRR) and payback period (PBP). The study revealed that the cost of the installed capacity per kWh had different characteristics as a function of capacity. It was concluded that the larger the capacity, the smaller the cost per kWh. It was also determined that investments with high installed capacity had high IRR [9].

In the study by Vardar and Çetin [10], the unit kWh energy cost generated by wind energy in 14 selected locations in Turkey was calculated. To calculate the unit kWh energy production cost, data and power curves for three turbines selected from the regions were utilized. The results revealed that the most advantageous and economic location was Bozcaada [10].

Moran and Sherrington [11] calculated the contribution to the local area of investment in a wind power plant in Scotland by examining the positive and negative

factors through NPV analysis. It was revealed that despite all the expenditure, a wind power plant created a net increase in welfare [11].

Madlaner and Wenk (2008) investigated the installed energy capacity of Switzerland and compared the NPVs of the energy sources with Monte Carlo simulation (MCS). By utilizing the outputs obtained with the MCS analysis, the optimum energy portfolio created from the types of energy sources in certain proportions was calculated [12].

In their study, Williams et al. [13] simulated the benefits to be obtained from investment in and operation of wind power plants for two different regions in Northern Arizona. An attempt was made to estimate the uncertainties related to the investment with the MCS applied. In this way, an attempt was made to determine the benefits to be obtained from economic activity during and after the WPP investment period for the economy of both regions [13].

In a study conducted by Vardar and Çetin [14], the unit kWh cost generated from wind energy in 22 selected locations in Turkey was calculated. To calculate the unit kWh energy production cost, data and power curves for three turbines selected from the regions were utilized. The results revealed that the most advantageous and economic location was Kumköy [14].

Ay [15] attempted to determine in what ways different financing choices affected the results of wind energy investments. In the study, economic evaluations were made in two different situations, namely one that took account of depreciation and one that did not. The economic evaluation results were different for the two different situations. When depreciation was taken into account in the economic evaluation, cash flows were higher. Therefore, it was concluded that depreciation is an important factor that needs to be taken into account in economic evaluation of investments [15].

In Hamamcıoğlu's study [16], the wind energy potential of the region was determined by using data obtained from a wind measurement station installed on the Campus of Yıldız Technical University. Next, the annual amount of energy that would be produced by two wind turbines with different capacities was calculated with the WASP program. In two different scenarios, the unit electricity cost that would be obtained was analyzed with economic evaluation criteria like payback period and internal rate of return methods. The analysis results revealed that investment made in accordance with the two scenarios would yield profits [16].

In their study, Frølund and Obling [17] conducted an economic evaluation of WPP investments by comparing discounted cash flows (DCF) and real options valuation (ROV) approaches. In the economic evaluation of WPP investments, it was concluded that both methods were successful and usable methods [17].

Cardell and Anderson [18] simulated power generation costs at different wind speeds. In the scenarios created

for the study, it was determined that domestic wind generation was correlated with wind speed [18].

In the study conducted by RehmAn et al. [19], an economic evaluation of a 20-MW wind power plant investment in the eastern region of Saudi Arabia was carried out. According to the technical assessments conducted, the planned location of the wind power plant investment had a 33.7% capacity. When all the input costs affecting the investment were considered, the production cost of the investment per kWh was calculated as \$2.94. It was concluded that in the area to be measured and thereabouts, a wind power plant investment could be developed [19].

By establishing a model based on uncertain environmental factors for a 13-GW WPP investment to be set up in Turkey, Ertürk [20] calculated the NPV of the investment. Considering the tariffs in the Renewable Energy Law of 2005 in Turkey, it was concluded that provided the wind speed in the location of the WPP investment was 7.5 m/s and over, the investment could be economically profitable [20].

Using RETScreen analysis software, Doğan et al. [21] performed a cost analysis for 3 wind power plants with 1-MW, 5-MW and 10-MW power levels in Hatay province. As a result, it was concluded that in an economic sense, wind power plant investments with a capacity of at least 2 MV and above should be preferred based on bank interest income [21].

Using the MCS method for the economic evaluation of WPP investments, Khindanova [22] obtained the distribution of the net present value (NPV), which is an output variable, by modelling the stochastic variables of electricity price and cost uncertainties. The NPV distribution obtained gives the wind power plant investor the opportunity for a deeper assessment when compared with a single point estimate of NPV or different scenario outputs. The method employed allows the wind power plant investor to acquire knowledge about risk measurements such as standard deviation, skewness, kurtosis and extreme NPV values that may be created [22].

Özçelik [23] examined the investment profitability of 4 locations in Turkey by considering cash flows that affect wind energy investments. Using the NPV and IRR methods of project evaluation, it was determined that of the locations examined, investments made in Karaburun (Izmir) and Samandağ (Hatay) would be profitable [23].

### 3. Research method

To evaluate the suitability of an investment project, all the expenditure and income of the project must be taken into account. To determine the economic suitability of wind energy investments, feasibility studies of the economic factors must first be carried out at the financial analysis stage. For a WPP investment to be made, it must first be placed in a competitive position with other alternative projects. A feasible WPP investment must be profitable for the producer and

provide cheaper energy for the consumer compared to other energy sources.

In economic analyses carried out for WPP projects, payback period, project profitability and productivity, and net present value obtained throughout economic life are calculated [24].

In this study, alternatives related to the relocation of 8 wind turbines are discussed, as shown in Figure 1. For this aim, analyses of a WPP investment that maintains its activity in Balıkesir province in the Southern Marmara region have been made by utilizing actual data. The data for eight 3 MW wind turbines in the installed plants of the wind power company have been used in the study. The 8 turbines selected are turbines that function in the same WPP area and have been relocated because they were low capacity. One of the codes of the turbines analyzed is identified as WTG34, as seen in Figure 1.

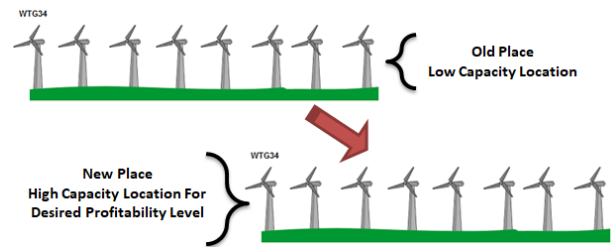


Figure 1. Relocation of wind turbines

In the case of relocation of the 8 wind turbines installed in unproductive locations and operating at low capacity, the minimum capacity required at the new location was determined.

In the implementation section of the study, the payback period method, which is a test of economic profitability of a WPP investment, was used. There are two different types of calculation in the payback period method. The first of these is the method that does not take the time value of money into account (Eq. (1)). With this method, the year in which the cash inflows and cash outflows of the investment are equalized is calculated without accounting for the discount factor (resource cost of the investment) [25].

$$\sum_{t=0}^n R_i = \sum_{t=0}^n C_i \quad (1)$$

The second method, however, takes the time value of money into account (Eq. (2)). With this method, the year in which the cash inflows and cash outflows of the investment are equalized is calculated after discounting [26].

$$\sum_{t=0}^n \frac{R_i}{(1+k)^t} = \sum_{t=0}^n \frac{C_i}{(1+k)^t} \quad (2)$$

In both methods, the sooner the payback period is realized during the economic life of the investment, the better it is for investment profitability and performance. The economic position of a wind turbine basically depends on the electrical energy it generates. The most

basic and important input in electricity production is wind speed. Eq. (3) shows the equation for production output obtained from wind power [27].

$$\text{Power} = kC_p 1/2\rho AV^3 \tag{3}$$

P = Power output, kilowatts

C<sub>p</sub> = Maximum power coefficient, ranging from 0.25 to 0.45, dimension less (theoretical maximum = 0.59)

ρ = Air density, lb/ft<sup>3</sup>

A = Rotor swept area, ft<sup>2</sup> or π D<sup>2</sup>/4 (D is the rotor diameter in ft, π = 3.1416)

V = Wind speed, mph

k = 0.000133 A constant to yield power in kilowatts.

(Multiplying the above kilowatt answer by 1.340 converts it to horse- power [i.e., 1 kW = 1.340 horsepower]).

Wind power is proportional to the cube of wind speed. To explain this with an example, when the wind speed at a location is doubled, energy production increases 8

times. Therefore, the wind speed in the place where the turbine is installed is the most important factor affecting electricity generation, and this situation also reduces the cost associated with electricity generation. This situation also ultimately reduces the payback period of the investment.

$$C_E = \frac{C_A}{8760 C_F P_R} \tag{4}$$

In Equation 4, the cost per unit kWh, “C<sub>E</sub>”, is a good economic indicator. In using electricity generation dependent on wind to determine cost, the characteristics of the wind regime are an important factor. “C<sub>F</sub>” expresses the capacity factor, “C<sub>A</sub>” denotes the annual operating cost, and “P<sub>R</sub>” represents the designed power of the turbine.

Figure 2 shows the relationship between wind speed and power production. Power production begins at wind speeds of 3-4 m/s and stops at 25 m/s according to turbine scale and type.

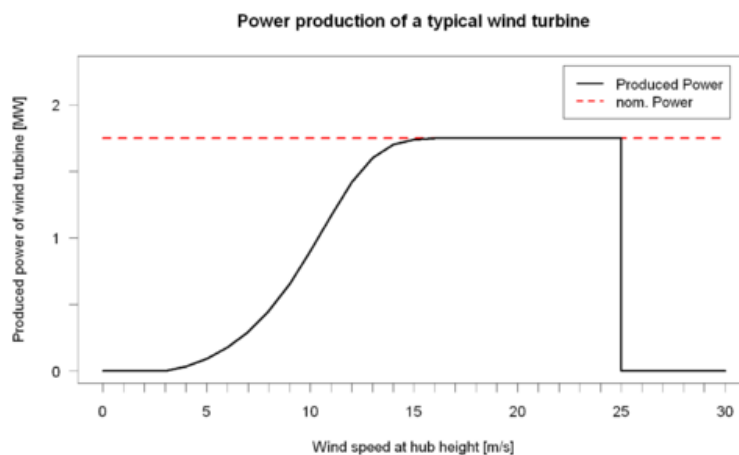


Figure 2. Power curve for wind speed and power production.

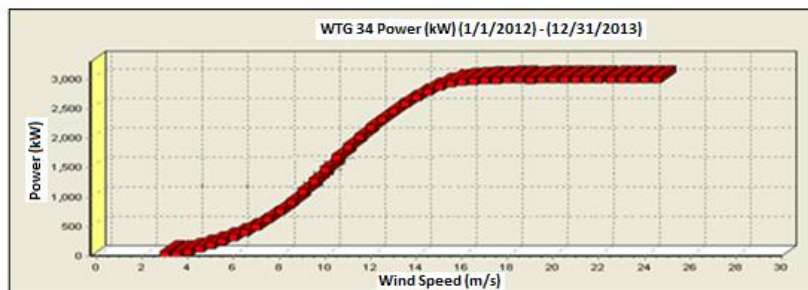


Figure 3. WTG34 power curve.

### 3.1. Input parameters for the research

The average capacity use of the 8 wind turbines that were relocated during the WPP investment was 18%. The wind turbine coded WTG34 is one of the 8 wind

turbines that were relocated during the WPP investment. Considering electricity generation compared with the other wind turbines, the electricity generation of wind turbine WTG34 is a turbine showing the average performance of the 8 turbines for

the previous 2 years. Figure 3 shows the power curve for wind turbine WTG34. The power curve for wind turbine WTG34 was obtained by using the realized wind speeds and the power production values at frequencies of ten-minute periods between the dates 01.01.2012 and 31.12.2013.

In Figure 3, the horizontal axis of the power curve for wind turbine WTG34 shows wind speed in m/s, while the vertical axis shows power in kW. When the wind speed of wind turbine WTG34 reached approximately 2.3 m/s, production commenced, and when the wind speed reached about 16.6 m/s, production reached full capacity, while at a wind speed of 25 m/s, the turbine stopped generating.

### 3.2. Inputs for economic analysis of the turbines

The input variables defined as assumptions to be used in the WPP project are the same for each turbine and are shown in Table 1. The parameters used in wind energy production have been created using sources in the literature [28].

In Table 1, the input variables defined as assumptions for wind turbine WTG34 are grouped under four headings, namely production parameters, operating expenses, investment expenditure and financial variables.

One of the production parameters for wind turbine WTG34 is individual unit capacity, and the individual unit capacity of the turbine is 3 MW. Another input is electricity selling price, and this was set as 7.3 US cents per kWh as a guarantee of purchase for wind power plants by YEKDEM (“Yenilenebilir Enerji Kaynakları Destekleme Mekanizması”, or Support Mechanism for Renewable Energy Sources). As well as electricity purchase price, incentives for unit electricity sales by the use of domestic components in WPP investments are also included. When domestic components are used in WPP investment, incentives are provided as follows: 1.3 US cents per kWh for use of domestic rotors and nacelles, 1 US cent per kWh for use of domestic generators, 0.8 US cents per kWh for use of domestic turbines, and 0.6 US cents per kWh for use of domestic turbine towers.

In the second group of input variables for wind turbine WTG34, operating expenses are included. In operating expenses, annual maintenance expenditure per unit was determined as \$37,000. The number of staff employed in a WPP investment was assumed to be one person for 4 turbines on average. The average monthly cost of each employee was specified as \$1,200. As activity costs of the operation, in WPP investments \$35,000 in system usage costs per unit is paid annually to the public, \$2,900 is paid in electricity quality costs per unit, and \$225 is paid in system operation costs per unit. In addition to activity costs, it was assumed that externally, there were other abnormal operating costs of \$820 per unit related to operation of the turbine. It was also assumed that activity costs would increase at

a rate of 1% per year.

**Table 1:** Input variables defined as assumptions for wind energy investment and assumptions for wind turbine WTG34

| ASSUMPTIONS                               |           |                          |
|---|-----------|--------------------------|
| Production Parameters                     | Value     | Unit                     |
| Unit Number                               | 1         |                          |
| Individual Unit Power                     | 3         | MW                       |
| Electricity Selling Price                 | 0.073     | USD/kWh                  |
| Domestic Incentives (Rotors and Nacelles) | 0.013     | USD/kWh                  |
| Domestic Incentives (Generators)          | 0.01      | USD/kWh                  |
| Domestic Incentives (Turbines)            | 0.008     | USD/kWh                  |
| Domestic Incentives (Turbine Towers)      | 0.006     | USD/kWh                  |
| Operating Costs                           |           |                          |
| Maintenance and Repair Costs              | 37,000    | USD /Unit                |
| Security Costs                            | 1,200     | USD/Employed Staff/Month |
| Number of Security Staff                  | 0.25      | Employed Staff           |
| System Usage Costs                        | 35,000    | USD/Unit/Year            |
| Electricity Quality Cost                  | 2,900     | USD/Unit/Year            |
| System Operating Cost                     | 225       | USD/Unit/Year            |
| Other Operating Costs                     | 820       | USD/Unit/Year            |
| Rate of Increase of Activity Costs        | 1         | %                        |
| Investment Expenditure                    |           |                          |
| Turbine Cost                              | 1,100,000 | USD/MW                   |
| VAT for Turbine Purchase                  | 20        | %                        |
| Turbine Switchyard Cost (*)               | 50,000    | USD/Unit                 |
| Land Requirement (Nationalization) (*)    | 10,000    | m <sup>2</sup> /Unit     |
| Land Use Cost (*)                         | 3,00      | USD/m <sup>2</sup>       |
| Turbine Access Road Cost (*)              | 100,000   | USD/Unit                 |
| Project Development Cost (*)              | 25,000    | USD/MW                   |
| Licence Fee                               | 10,000    | USD/MW                   |
| Maintenance and Repair Equipment Cost     | 30,000    | USD/Unit                 |
| Other Costs                               | 10,000    | USD/Unit                 |
| Financial Variables                       |           |                          |
| Depreciation Rate                         | 0.5       | %                        |
| Interest Rate                             | 7.5       | %                        |
| Capital Ratio (Equity/ Total Sources)     | 50        | %                        |
| Working Capital Requirement               | 100,000   | USD/Unit                 |
| Depreciation Period                       | 25        | Year                     |
| Inflation Rate - US Dollars               | 1.5       | %                        |
| VAT Rate                                  | 18        | %                        |
| Corporation Tax                           | 20        | %                        |
| Equity Expectation Rate                   | 10        | %                        |

The third group of input variables for wind turbine WTG34 is that of investment expenditure. Investment for WPP projects is the total expenditure made for installation of the turbine and completion of the electrical conduction until commencement of production. Within investment expenditure, the cost of the turbine was determined as \$1,100,000 per MW. In the ground works for the turbine installation site, the switchyard cost was assumed to be \$50,000 per unit turbine. The land use per turbine was 10,000 m<sup>2</sup> and \$3 was paid per m<sup>2</sup>. For opening of the turbine access road, the cost was \$100,000 per turbine. In the pre-feasibility and project development period prior to making the WPP investment, \$25,000 was spent per MW production volume. When the project was begun, a \$10,000 licence fee was paid per MW. In addition to these, within the investment expenditure, it was assumed that \$30,000 per unit would be spent related to the purchase of repair and maintenance equipment. Finally, other costs per unit were assumed to be \$10,000.

The fourth group of input variables for wind turbine WTG34 is related to financing. It was assumed that there was an annual loss of capacity in the WPP

investment compared to the previous year. As loss of capacity, the rate of wear and tear was selected as 0.5%. In investment finance, there are choices of financing with debt or with equity. For financing with debt, the central bank's overnight borrowing rate was taken into account. For financing with debt, an annual rate of 7.5% was used as the input variable. Another resource cost is equity cost. Equity cost was taken to be approximately 10% per annum based on the Capital Asset Pricing Model. The working capital of the operation was assumed to be \$100,000 per unit. The depreciation period of the investment was assumed to be 25 years, and the depreciation of the investment was considered to be divided equally throughout its economic life. The annual dollar inflation rate was taken to be 2%. The tax rates for the investment were taken as 18% for VAT and 20% for corporation tax.

The input variables defined as assumptions have been explained above. An input variable is defined as an independent variable that affects an investment at one point.

#### 4. Analysis findings

Following the financial model created in this study, for the relocation of the turbine in the WPP investment to be profitable, the capacity factor of the new installation

site of the turbine was determined. Wind turbine WTG34 was put into use and began production in 2012. In 2012 and 2013, production was carried out with capacity factors of 19% and 17% respectively. Following the year of its installation, if turbine WTG34 operates at a capacity of approximately 24% until the end of its economic life, the WPP investment project will have zero profit. If turbine WTG34 is not relocated, however, the probability of the investment producing a return within the 25-year life of the turbine is low. In this case, the decision by the investor to install the turbine in a location where production can be made at a higher capacity is a logical one. From this viewpoint, even by adding the additional costs marked as (\*) in Table 1 (turbine switchyard cost, land requirement, land use cost, turbine access road cost and project development cost), the turbine operating at a loss can become profitable. What is important here is the question of at least what capacity factor on average the new installation site of the turbine will work at until the end of its economic life.

As a result of the financial model created based on the input parameters included, when considering the investment payback period method, the results of the capacity factors required for the relocation to be significant are shown in Figure 4.

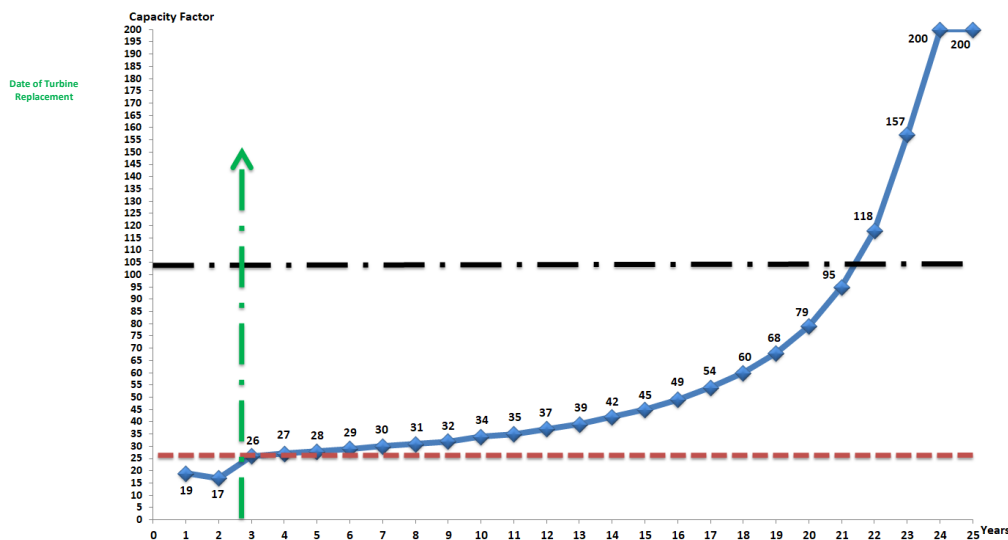


Figure 4. Turbine relocation and capacity factor.

Examining Figure 4, it can be seen that when the relocation of the WPP investment is made during the third year and if the capacity factor of the investment, which has an economic life of up to 25 years, at the new installation site is 26% and over after the third year, the relocation of the investment will be significant. If the capacity factor of the investment, which has an economic life of up to 25 years, at the new installation site is 27% and over after the fourth year, the relocation of the investment will be significant. For relocation in the following years to be significant, the minimum capacity factors are as follows: 28% and over in the 5th year, 29% and over in the 6th year, 30% and over in the

7th year, 31% and over in the 8th year, 32% and over in the 9th year, 34% and over in the 10th year, 35% and over in the 11th year, 37% and over in the 12th year, 39% and over in the 13th year, 42% and over in the 14th year, 45% and over in the 15th year, 49% and over in the 16th year, 54% and over in the 17th year, 60% and over in the 18th year, 68% and over in the 19th year, 79% and over in the 20th year, 95% and over in the 21st year, 118% and over in the 22nd year, 157% and over in the 23rd year, and 200% in the 24th and 25th years. Since there cannot be a capacity factor of over 100%, relocation of the investment in the 22nd year or later is pointless (uneconomic). When the repair and

maintenance of wind turbines is taken into consideration, it is natural for the optimum capacity factor to be below full capacity. The earlier the investment relocation is carried out, the lower the desired mean capacity factor will be until the end of the economic life of the investment. If the decision to relocate the investment is delayed, the desired capacity factor for the investment at its new installation site will increase for every year that it is delayed.

Similar results to those obtained for turbine WTG34 were determined for the other 7 turbines having low capacity factors.

## 5. Conclusion and recommendations

Dependence on energy is increasing day by day all over the world. Turkey, which is one of the developing countries, is the world's 17th largest and Europe's 6th largest economy. Together with its growing economy and increasing population, demand for energy in Turkey is rising rapidly. To meet this increasing energy need and to reduce foreign dependence on energy, the use of domestic and renewable energy sources must be increased. From this perspective, realistic targets for renewable energy sources should be set, and to reach these targets, the barriers preventing investments should be lifted.

When its potential for renewable energy sources is assessed, Turkey is a rich country. Another important matter that needs to be considered when making renewable energy investments is that of carrying out a technical analysis prior to making the investment and of installing the turbine in a location where maximum productivity can be obtained. Before companies make an investment in a renewable energy area, it is important that they undertake technical and economic feasibility studies of the investment. A pre-feasibility study will form a reference for the practicability of the investment. Following the pre-feasibility study, high-productivity renewable energy investments are important for providers of liability in terms of repayment of the credit they are to provide.

Following the financial model created in this study, for the relocation of the WTG34 turbine operating with a low capacity factor to be profitable, the capacity factor of the new installation site of the investment was determined. The results showed that it was important for the relocation decision to be made early for the investment to be more profitable. In the first two years of the turbine investment, the turbine operating at a low capacity of 19% and 17% is profitable if it works at 26% capacity until the end of its economic life when change is made in the third year. It is seen that the capacity factor increases for each year of delay for replacement. In the event of delayed decisions to relocate the turbine, a high capacity factor is expected in the new location. If a high capacity factor is not achieved, the relocation of the turbine will be meaningless and losses will be incurred for the investor.

When its potential for renewable energy sources is evaluated, Turkey is a rich country. When Turkey's future energy targets are examined, it is seen that a target for renewable energy sources to meet 30% of Turkey's energy consumption has been set for the year 2023.

Moreover, to reach the realistic targets determined for renewable energy, significant progress can be made by strengthening the incentive mechanism, making adjustments to periods and amounts in purchase guarantees, activating the operation of the Environmental Impact Assessment (EIA) and supporting technological developments related to renewable energy in domestic industry. Furthermore, informing entrepreneurs that plan to invest in this area about financial sources and access can make a positive contribution to speedier operation of the processes.

## References

- [1] Ministry of Energy and Natural Resources, <https://enerji.gov.tr/>, Accessed Date (11.10.2018).
- [2] Develi, A. & Kaynak, S. (2012). *Energy Economics*, Frankfurt am Main, ISBN 3631633335, DEU:Peter Lang AG.
- [3] Turkish Wind Energy Association (2018), *Turkish Wind Statistic Report*, <https://www.tureb.com.tr/yayinlar/turkiye-ruzgar-enerjisi-istatistik-raporu-temmuz-2018>
- [4] Ministry of Energy and Natural Resources (2014). *2015-2019 Strategy Plan*, [http://sp.enerji.gov.tr/ETKB\\_2015\\_2019\\_Stratejik\\_Planı.pdf](http://sp.enerji.gov.tr/ETKB_2015_2019_Stratejik_Planı.pdf).
- [5] Bahgat, G. (2006). *Europe's Energy Security: Challenges and Opportunities*, International Affairs, 82(5): 961-975.
- [6] Desrochers, G., Blanchard, M. & Sud, S. (1986). *A Monte-Carlo Simulation Method For The Economic Assessment of The Contribution of Wind Energy to Power Systems*, IEEE Transactions on Energy Conversion, (4), 50-56.
- [7] Venetsanos, K., Angelopoulou, P. & Tsoutsos, T. (2002). Renewable Energy Sources Project Appraisal Under Uncertainty: The Case Of Wind Energy Exploitation Within A Changing Energy Market Environment. *Energy Policy*, 30(4), 293-307.
- [8] Liberman, E. J. (2003). *A life cycle assessment and economic analysis of wind turbines using Monte Carlo simulation*. MSc Thesis, Air Force Institute Of Technology, Wright-Patterson Air Force Base, Ohio.
- [9] Özerdem, B., Ozer, S. & Tosun, M. (2006). Feasibility study of wind farms: A case study for Izmir, Turkey, *Journal of Wind Engineering and Industrial Aerodynamics*, 94(10), 725-743.
- [10] Vardar, A. & Çetin, B. (2007). Cost Assessment of The Possibility of Using Three Types of Wind Turbine in Turkey. *Energy Exploration &*

- Exploitation*, 25(1), 71-82.
- [11] Moran, D. & Sherrington, C. (2007). An Economic Assessment of Windfarm Power Generation in Scotland Including Externalities, *Energy Policy*, 35(5), 2811-2825.
- [12] Madlener, R., & Wenk, C. (2008). *Efficient investment portfolios for the Swiss electricity supply sector*.
- [13] Williams, S. K., Acker, T., Goldberg, M. & Greve, M. (2008). Estimating the economic benefits of wind energy projects using Monte Carlo simulation with economic input/output analysis. *Wind Energy*, 11(4), 397-414.
- [14] Vardar, A. & Çetin, B. (2009). Economic Assessment of The Possibility of Using Different Types of Wind Turbine in Turkey, *Energy Sources*, Part B, 4(2), 190-198.
- [15] Ay, A. (2010). *Energy Sources And Investment Project Assessment: A Case Study About Wind Energy In Turkey*, Masters Thesis, Bahçeşehir University, Istanbul.
- [16] Hamamcioğlu, V. (2010). *Rüzgar Enerji Kaynaklı Elektrik Üretiminin Teknik/Ekonomik Analizi ve Yöresel Uygulaması*, Masters Thesis, Yıldız Teknik Üniversitesi, Istanbul.
- [17] Frølund, S. G., & Obling, P. E. (2010). *Valuation models for wind farms under development*. *Graduate Thesis*, <http://studenttheses.cbs.dk/handle/10417/1080>.
- [18] Cardell, J. B. & Anderson, C. L. (2010). *Analysis of The System Costs of Wind Variability Through Monte Carlo Simulation*, In System Sciences (HICSS), 43rd Hawaii International Conference on System Sciences, 1-8.
- [19] Rehman, S., Ahmad, A. & Al-Hadhrami, L. M. (2011). Development and Economic Assessment of a Grid Connected 20 MW Installed Capacity Wind Farm, *Renewable and Sustainable Energy Reviews*, 15(1), 833-838.
- [20] Ertürk, M. (2012). The Evaluation of Feed-In-Tariff Regulation of Turkey For Onshore Wind Energy Based on The Economic Analysis, *Energy Policy*, 45, 359-367.
- [21] Doğan, B. T., Çolakoğlu, A. & Kincay, O. (2012). RETScreen Analiz Programı ile Hatay'da Rüzgar Enerji Santrali Fizibilite Analizi, *Tesisat Mühendisliği*, 131, 22-27.
- [22] Khindanova, I. (2013). A Monte Carlo Model of a Wind Power Generation Investment, *The Journal of Applied Business and Economics*, 15(1), 94.
- [23] Özçelik, B. D. (2016). Türkiye'de Rüzgar Enerjisinin Durumu: Karaburun, Urla, Samandağ ve Hereke Rüzgar Enerjisi Santralleri Fizibilite Analizi, *Maliye Finans Yazıları*, (106), 49-72
- [24] Simoes, M. G. & Farret, F. A. (2008). *Alternative Energy Systems Design and Analysis With Induction Generators*, CRC Press, Second Edition, ISBN: 978-1-4200-5532-0, USA.
- [25] Ross, S, Westerfield, R. W. & Jaffe, J. (2010). *Corporate Finance*, Ninth Edition, McGrawHill.
- [26] Manwell, J.F., MCGowan J.G. & Roger, A.L. (2010). *Wind Energy Explained: Theory, Design and Application*, Second Edition, John Wiley & Sons Ltd.
- [27] Durak, M. & Özer, S. (2008). *Rüzgar Enerjisi Teori ve Uygulama*, Ankara.
- [28] Tansi, B.N. (2012). *An Assessment of Cameroons Wind and Solar Energy Potential – A Guide for A Sustainable Economic Development*, Hamburg, DEU: Diplomica Verlag.

**Hasan Huseyin Yildirim** received his Master's Degree (2011) in Finance from Marmara University and obtained a PhD Degree (2016) from Istanbul University. Mr. Yildirim is Assist. Prof. in the Burhaniye School of Applied Sciences at Balıkesir University. His research interests include the economy, finance and banking sector and renewable energy investments.

**Sakir Sakarya** received his Master's Degree (1994) in Business and obtained a PhD Degree (2002) from Sakarya University in Turkey. Currently, Mr. Sakarya is a Professor in the Faculty of Economics and Administrative Sciences at Balıkesir University. Mr. Sakarya has extensive experience in the finance and investment sector. His main research interest is financial management.



## RESEARCH ARTICLE

## Simulation of glucose regulating mechanism with an agent-based software engineering tool

Sevcan Emek <sup>a\*</sup> , Vedat Evren <sup>b</sup> , Şebnem Bora <sup>c</sup> 

<sup>a</sup> Department of Computer Engineering, Manisa Celal Bayar University, Turkey

<sup>b</sup> Department of Physiology, Ege University, Turkey

<sup>c</sup> Department of Computer Engineering, Ege University, Turkey

[sevcan.emek@cbu.edu.tr](mailto:sevcan.emek@cbu.edu.tr), [vedat.evren@ege.edu.tr](mailto:vedat.evren@ege.edu.tr), [sebnem.bora@ege.edu.tr](mailto:sebnem.bora@ege.edu.tr)

## ARTICLE INFO

## Article history:

Received: 19 August 2018

Accepted: 11 February 2019

Available Online: 20 March 2019

## Keywords:

Agent

Agent-based modeling and simulation

Homeostasis

Negative feedback control

Blood glucose levels

AMS Classification 2010:

68T42, 92C30, 93B52

## ABSTRACT

This study provides a detailed explanation of a regulating mechanism of the blood glucose levels by an agent-based software engineering tool. Repast Symphony which is used in implementation of this study is an agent-based software engineering tool based on the object-oriented programming using Java language. Agent-based modeling and simulation is a computational methodology for simulating and exploring phenomena that includes a large set of active components represented by agents. The agents are main components situated in space and time of agent-based simulation environment. In this study, we present hormonal regulation of blood glucose levels by our improved agent-based control mechanism. Hormonal regulation of blood glucose levels is an important process to maintain homeostasis inside the human body. We offer a negative feedback control mechanism with agent-based modeling approach to regulate the secretion of insulin hormone which is responsible for increasing the blood glucose levels. The negative feedback control mechanism run by three main agents that interact with each other to perform their local actions in the simulation environment. The result of this study shows the local behavior of the agents in the negative feedback loop and illustrates how to balance the blood glucose levels. Finally, this study which is thought a potential implementation of agent-based modeling and simulation may contribute to the exploration of other homeostatic control systems inside the human body.



### 1. Introduction

Human physiology includes fundamental systems that control the vital functions and processes. Each system has its own functional features. For example, the nervous system is considered as a control center that coordinates all bodily actions and activities, and responds to changes both outside and inside the body [1]. The other systems, such as cardiovascular, respiratory, urinary, endocrine, and immune systems, perform their local actions that benefit the internal balance of the body. The internal balance of the body called homeostasis [2] is an important survival process that maintains the keeping of state variables at a constant or stable condition. The endocrine system plays an active role for maintaining homeostasis. It is also known as the hormonal system, which basically regulates metabolic functions such as appetite, mood, sexual, reproduction, growth and development, sleep

cycles, and more [3].

In this study, we modeled and simulated hormonal regulation of blood glucose level using the agent-based modeling and simulation (ABMS) technique. ABMS is a technique of artificial intelligence. It provides a platform to explain systems behavior based on individual actions and interactions. Individual which is a part of system is defined an agent in ABMS. The agents perform specific tasks depending on rules of agents' actions and interactions in agent-based simulation environment [4-6]. Agents in accordance with their characteristics are well suitable to represent the system components which presented in this study. ABMS approach has advantage of creating a model compared to other modeling approach based on mathematical and numerical analysis, control theory, biomechanical techniques, etc. [7]. ABMS is referred to as "individual-based

\*Corresponding author

model” so that some answers need to find in order to describe the model scenario, like what the agents should be in the model, what the agents’ environment is, how to interact with each other and environment, how to define the rules determined the behaviors of agents, what are roles of the agents in the model, and etc. [8, 9].

In this paper, we introduce and visualize the process by which the blood glucose levels are regulated by negative feedback control mechanism [10]. In order to implement negative feedback control mechanism, we offer three main agents; receptor agent, controller agent and effector agent. These agents interact with each other using the messaging service and run the feedback mechanism. We develop this study in Repast Symphony [11] platform based on the object-oriented programming using Java language. Repast Symphony offers the users and researchers a tool which includes graphical user interface, toolbar to control the simulation processes (start, step, pause, stop, exit, and etc.), displaying agents and their environment, monitoring the output data (time chart, histogram bar), scheduling of simulations, parameters management, and etc.

This chapter is organized as follows: Section 2 gives a brief overview of hormonal regulation of blood glucose levels; Section 3 presents the method of this study which offers an agent-based control system; Section 4 provides implementation of case study involving experimental results; Section 5 explains some limitations of this study, and Section 6 concludes with a brief summary of this study.

## 2. Hormonal regulation of blood glucose levels

Endocrine system carries out its actions with the hormones produced by the endocrine glands and transmitted to the target cell by the blood circulation. Endocrine gland includes but not limited to pineal gland, pituitary gland, pancreas, ovaries, testes, thyroid gland, parathyroid gland, hypothalamus and adrenal glands. Pancreas secretes two major hormones, insulin and glucagon, that affect blood glucose level. Insulin is produced by the beta cells of the pancreas and glucagon is produced by the alpha cells of the pancreas. Insulin decreases the concentration of glucose in the blood. When blood glucose levels rise, secretion of insulin is triggered. Insulin causes glucose to be converted into glycogen in the liver which is the target tissue. So, glucose is removed from the blood and the blood glucose levels decrease [3, 12]. All these processes show that hormonal secretions are maintained at optimal levels with negative feedback shown in Figure 1.

Our model scenario is created according to the increasing of blood glucose levels after a meal. Blood glucose/sugar levels are the amount of glucose that varies widely throughout bloodstream according to alternate with periods of fasting. In a healthy person,

ideal blood glucose range for fasting glucose is between 80-90 mg/dL. Two hours after meal blood glucose concentration must be under the 180 (ideal is under 140) mg/dL. If blood glucose concentration is not less than 140 mg/dL, the person’s illness symptoms start to show up [3].

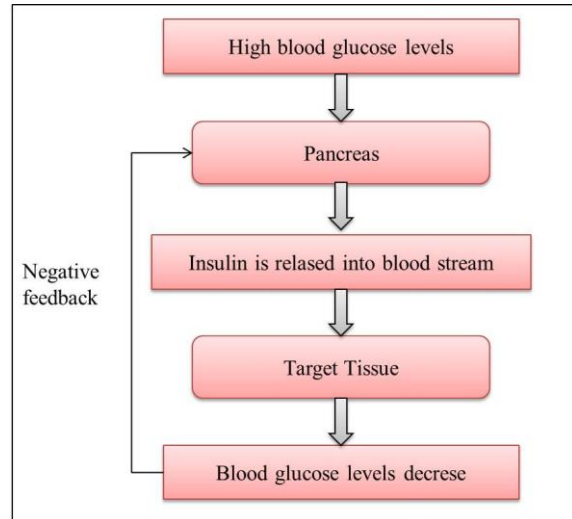


Figure 1. Regulation of blood glucose levels

In Section 3, we introduce our controller model which represents the flow chart shown in Figure 1.

## 3. Method

In this study, we developed an agent-based control mechanism to control the blood glucose levels. In our approach, the agent-based control system is composed of a set of dynamic number of autonomous agents. We defined three important agents: a receptor agent, a controller agent and an effector agent [7, 13]. Figure 2 shows the negative feedback control mechanism that consists of interacting agents.

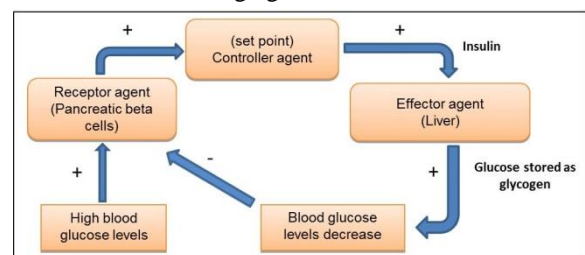


Figure 2. Negative feedback control mechanism of hormonal regulation of blood glucose levels

Receptor agent senses changes in plasma glucose levels and sends its information to controller agent. We represent the receptor agent as pancreas. Controller agent has a set point. If blood glucose levels above the set point, controller agent sends an insulin message to the effector agent. We represent the effector agent as liver which uptakes glucose and stores as glycogen. Effector agent is responsible for the decreasing in blood glucose levels. Once glucose levels drop below a threshold value, there is no longer enough stimulus for sending insulin message.

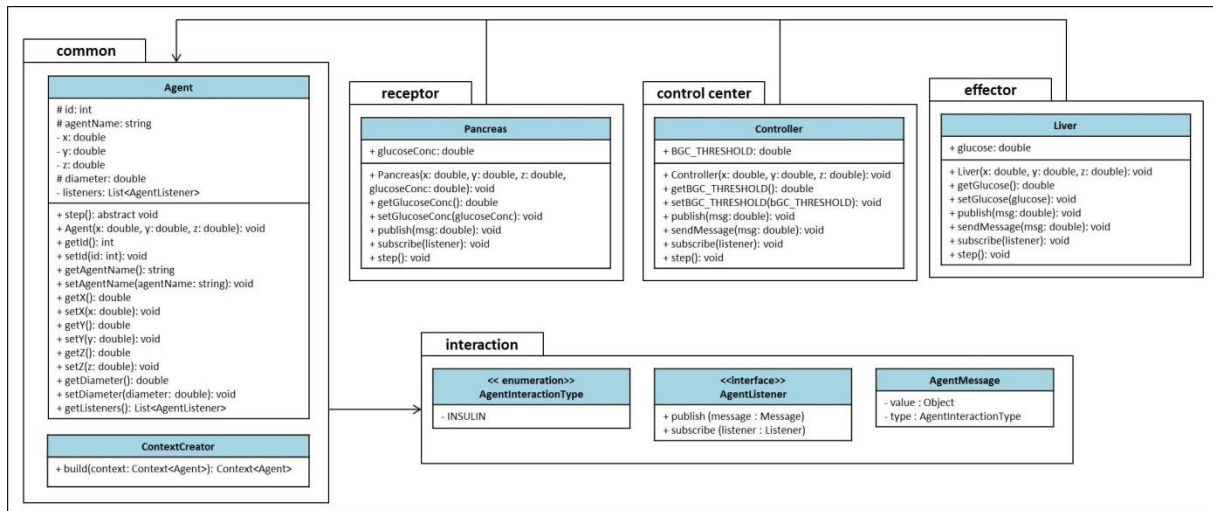


Figure 3. UML class diagram that shown agents and their interactions

The unified modeling language (UML) class diagram that shows the interaction of agents is given in Figure 3.

This study is a Repast Symphony project that uses Eclipse integrated development environment (IDE). The interaction of the agents is provided by the “publish-subscribe” messaging pattern in the interaction package illustrated in Figure 3. Each agent publishes the messages to its listeners and subscribes to the corresponding agent. The listener agent receives

the messages and regulates its behavior according to the current environment situation [7, 13].

#### 4. Experimental study

In this study, we have a scenario that shows increase in blood glucose levels according to breakfast, lunch and dinner. The results of the simulation study are illustrated in Figure 4 and Figure 5.

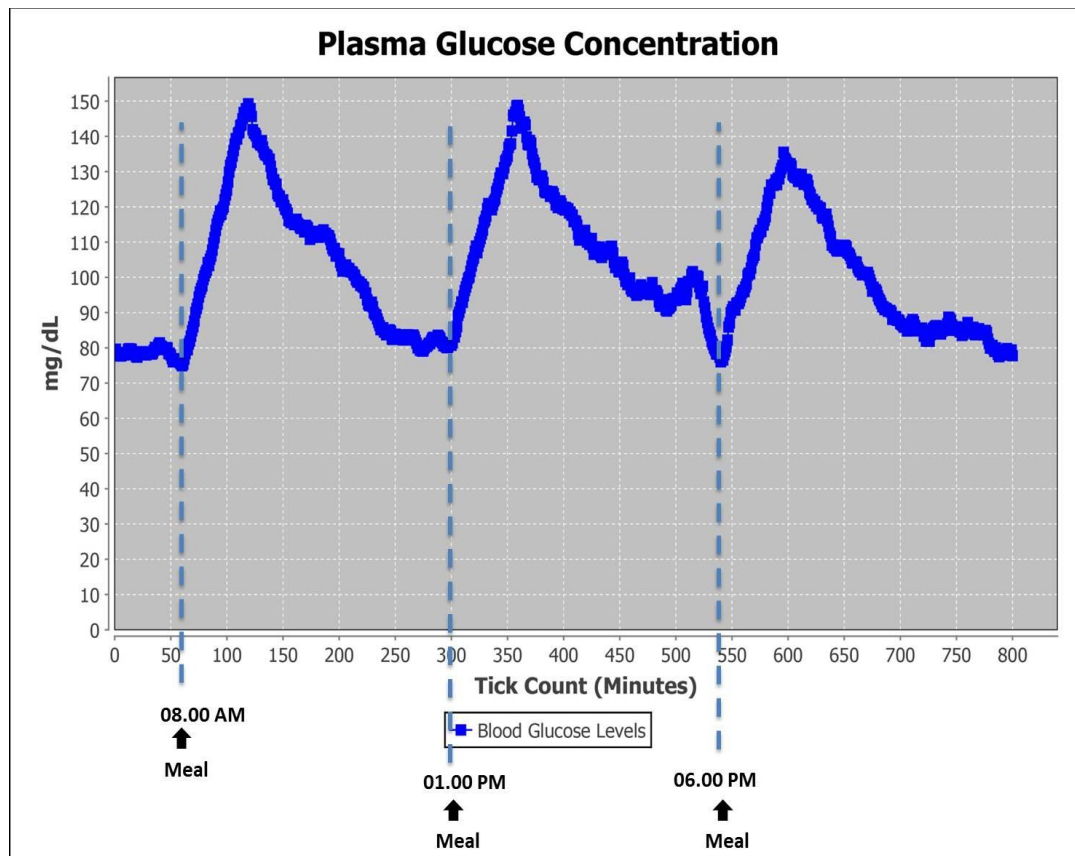


Figure 4. Regulation of blood glucose levels after a meal

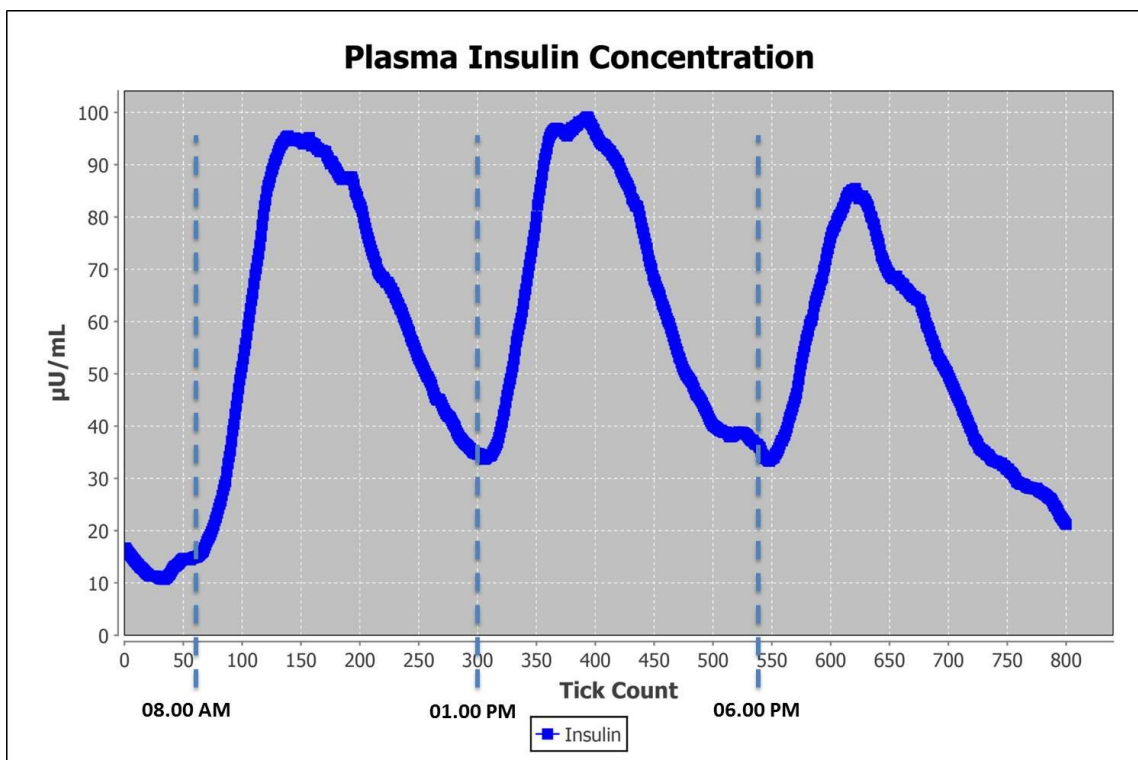


Figure 5. Insulin levels before and after a meal

In Figure 4, 60<sup>th</sup> tick count represents 08.00 am which is time of breakfast. Before breakfast, blood glucose levels fluctuate between 70 and 90 mg/dL. After 60<sup>th</sup> tick count, eating gradually increases the blood glucose levels. Threshold value of blood glucose levels is set to 120 mg/dL. When the blood glucose levels are more than the threshold value, the controller agent sends insulin message to the effector agent. The insulin levels associated with blood glucose levels increase between 100<sup>th</sup> and 150<sup>th</sup> tick counts. Effector agent increases insulin levels shown in Figure 5 and decreases the blood glucose levels. Then, it sends the value of blood glucose to receptor agent. Until the blood glucose levels fall below the threshold value, effector agent keeps on sending message. Two hours after breakfast at 240<sup>th</sup> tick count, blood glucose levels achieve optimal value. 300<sup>th</sup> tick count which is time of lunch at 01.00 pm triggers blood glucose levels. Blood glucose levels decrease on insulin control after two hours. In the simulation, minutes is defined by tick count. At 06.00 pm that is time of the last meal, blood glucose level increases about 130mg/dL. At 700<sup>th</sup> tick count, decrease of blood glucose levels is observed.

## 5. Discussion

This study has some limitations in the creation of the model. We define pancreas as a receptor agent. In the literature [3, 14, 15], pancreatic islets called islets of Langerhans are clusters of cells located in the pancreas. Pancreatic islets contain beta cells that produce insulin. In this study, beta cells of pancreas may be defined as receptor agents. We define liver as

an effector agent. Liver has an important role for glycogen storage. However, skeletal muscle is a major site of glycogen storage [16]. Muscle may be added as target tissue of effector agent.

The results of simulation in respect of the parameters are obtained in reference to normal conditions of a healthy adult. Plasma glucose and insulin are simulated hourly, from 08.00 am to midnight, covering the whole day. We are able to obtain and compare simulation data and results based on references in the literature [3, 17-20].

In this paper, we simulated increase of blood glucose levels and observe insulin levels. In the continuation of this study, we may observe not only the increase in blood glucose level but also the glucagon hormone which is due to the decrease of the blood sugar level.

## 6. Conclusion

This study describes implementation of a glucose regulating mechanism using an agent-based software engineering tool. Interacting agents run the regulating mechanism using the messaging service. While exploiting a feedback loop, agents perform their actions and adapt their behaviors. In the result of this study, we observe that how the agent-based control system adjusts to the blood glucose levels after meal. This study deals only with regulation due to the increase in blood glucose level. In the future of this study, case studies such as diabetes which occur due to increase in blood sugar level can be performed by ABMS.

## References

- [1] Jhonstone, K., & Adam, K. (2012). The Human: As a Biological System. *Core Body of Knowledge for the Generalist OHS Professional*. Safety Institute of Australia Ltd, Tullamarine, Victoria, Australia
- [2] Marieb, E.N., & Hoehn, K. (2010). Human Anatomy and Physiology. 8th ed., San Francisco: Benjamin Cummings, 634-654.
- [3] Guyton, A.C., & Hall J.E. (2006). Textbook of Medical Physiology. Elsevier Inc, 11th ed.
- [4] Klügl, F. & Bazzan, A.L.C. (2012). Agent-Based Modeling and Simulation. *Association for the Advancement of Artificial Intelligence*, 29-40.
- [5] Bandini, S., Manzoni, S.T., & Vizzari, G. (2009). Agent Based Modeling and Simulation: An Informatics Perspective. *Journal of Artificial Societies and Social Simulation*, vol. 12.
- [6] Bonabeau, E. (2002). Agent-based modeling: Methods and techniques for simulating human systems. *Proceedings of the National Academy of Sciences of the United States of America (PNAS)*, 99(3), 7280-7287.
- [7] Bora, Ş., Evren, V., Emek, S., & Çakırlar, I. (2017). Agent-based modeling and simulation of blood vessels in the cardiovascular system. *Simulation: Transactions of the Society for Modeling and Simulation International*, 1-16. Doi: 10.1177/0037549717712602
- [8] DeAngelis, D.L., & Grimm V. (2014). Individual-based models in ecology after four decades. *F1000Prime Reports*; 6:39. DOI: 10.12703/P6-39
- [9] Macal, C.M., & North, M.J. (2010). Tutorial on agent-based modelling and simulation. *Journal of Simulation*, 4:151-162. DOI: 10.1057/jos.2010.3
- [10] Ramaprasad, R. (1983). On the Definition of Feedback. *Behavioral Science*, 28(1):4-13.
- [11] Nikolai, C., & Madey, G. (2009). Tools of the trade: a survey of various agent based modeling platforms. *J. Artif. Soc. Social Simul.*, vol. 12.
- [12] James, P., & McFadden R. (2004). Understanding the processes behind the regulation of blood glucose. *Diabetes Knowledge*, 100(16):56-58.
- [13] Bora, Ş., Emek, S., Evren, V. (2017). An Agent-based Approach in Homeostatic Control Systems: Thermoregulation. *IEEE 9th International Conference on Computational Intelligence and Communication Networks*, 113-116. DOI: 10.1109/CICN.2017.8319367
- [14] Wang, X., Misava, R., Zielinski, M.C., Cowen, P., Jo, J., Periwal, V., Ricordi, C., Khan, A., Szust, J., Shen, J., Millis, J.M., Witkowski, P., & Hara, M. (2013). Regional Differences in Islet Distribution in the Human Pancreas - Preferential Beta-Cell Loss in the Head Region in Patients with Type 2 Diabetes. *PLoS One*, vol. 8(6).
- [15] Krull, D.L., & Peterson, R.A. (2011). Preclinical Applications of Quantitative Imaging, Cytometry to Support Drug Discovery. *Methods in Cell Biology*, Chapter 11, vol. 102, 291-308.
- [16] Berg, J.M., Tymoczko, J.L., & Stryer, L. (2002). Glycogen Metabolism. *Biochemistry*. 5th edition, Chapter 21. Available from: <https://www.ncbi.nlm.nih.gov/books/NBK21190/> Accessed 17 August 2018.
- [17] Buppajarntham, S., & Junpaparp, P. (2014). Insulin, Reference Range. Available from: <https://emedicine.medscape.com/article/2089224-overview>. Accessed 17 August 2018.
- [18] Genuth, S.M. (1973). Plasma Insulin and Glucose Profiles in Normal, Obese, and Diabetic Persons. *Ann Intern Med*. Vol. 79(6), 812-822. doi: 10.7326/0003-4819-79-6-812
- [19] Austin Community College. Glucose Regulation. Available from: [http://www.austincc.edu/apreview/EmphasisItems/Glucose\\_regulation.html](http://www.austincc.edu/apreview/EmphasisItems/Glucose_regulation.html). Accessed 17 August 2018.
- [20] Krinsley, J.S., & Preiser, J-C. (2015). Time in blood glucose range 70 to 140 mg/dl > 80% is strongly associated with increased survival in non-diabetic critically ill adults. *Krinsley and Preiser Critical Care*, 19:179. DOI 10.1186/s13054-015-0908-7

*Sevcan Emek is a PhD candidate and a research assistant in the Computer Engineering Department at Manisa Celal Bayar University, Turkey. She received the B.S. and M.S. degrees in Computer Engineering from Dumlupınar University in 2009 and 2011, respectively. Her research interests include artificial intelligence, control systems and agent-based modeling and simulation.*

*Vedat Evren is an MD-PhD at the Ege University School of Medicine, Department of Physiology, İzmir, Turkey.*

*Şebnem Bora received her PhD degree from Ege University, Turkey in 2006. She is currently an assistant professor in the Computer Engineering Department at Ege University. Her research interests include dependable computing, multiagent systems, self-adaptive systems, complex-adaptive systems, and agent-based modeling and simulation.*



This work is licensed under a Creative Commons Attribution 4.0 International License. The authors retain ownership of the copyright for their article, but they allow anyone to download, reuse, reprint, modify, distribute, and/or copy articles in IJOCTA, so long as the original authors and source are credited. To see the complete license contents, please visit <http://creativecommons.org/licenses/by/4.0/>.

## RESEARCH ARTICLE

## A comparison of some control strategies for a non-integer order tuberculosis model

Tuğba Akman Yıldız 

Department of Logistics Management, University of Turkish Aeronautical Association, Ankara, Turkey  
 tr.tugba.akman@gmail.com

## ARTICLE INFO

## Article History:

Received 30 July 2018

Accepted 19 February 2019

Available 15 April 2019

## Keywords:

*Tuberculosis**Optimal control**Fractional derivative*

## AMS Classification 2010:

49K99; 34A08; 37N25

## ABSTRACT

The aim of this paper is to investigate some optimal control strategies for a generalized tuberculosis model consisting of four compartments. We construct the model with the use of Caputo time fractional derivative. Contribution of distancing control, latent case finding control, case holding control and their combinations are discussed and the optimality system is obtained based on the Hamiltonian principle. Additionally, we prove that the solution is non-negative and bounded from above. We present some illustrative examples to determine the most effective strategy to minimize the number of infected people and maximize the number of susceptible individuals. Moreover, we discuss the contribution of the Caputo derivative and the order of the fractional derivative to efficiency of the control strategies.



### 1. Introduction

Tuberculosis (TB) is a threatening bacterial disease caused by *Mycobacterium tuberculosis*. It is the ninth leading cause of death in the world and about 1.3 million people died due to TB in 2016 according to 2017 TB report of World Health Organization (WHO) [1]. Dynamics of TB is slowly varying when compared to other epidemiological diseases. Additionally, infected people do not show any symptoms of the disease for years and approximately 5 – 10% of the latently infected people become an active TB sufferer [2], while 90 – 95% of people remain latent and they do not infect other people at this stage. For latent individuals to be an active TB sufferer depends on endogenous reactivation or exogenous reinfection [3]. WHO and the United Nations aim to end TB throughout the world, so they set the target as "a 90% reduction in TB deaths and an 80% reduction in TB incidence (new cases per year) by 2030, compared with 2015" [1].

Before setting some goals to end such a disease, the use of mathematical models to understand the

dynamics of the disease has gained a special interest for a while [4]. In the literature, there are different models and optimal intervention strategies that are formulated based on different aspects of the disease. Dynamics of TB was firstly formulated by Waller and his colleagues in 1962 through a system of difference equations [5]. Since then, time evolution of the disease has been investigated. To model the disease, the population has been divided into some groups/classes, for example, representing susceptible, infectious, latent, vaccinated and recovered individuals [6]. A very basic model consisting of susceptible, infectious and recovered individuals has been proposed in [7]. As a different discussion, one-strain and two-strain TB models have been constructed to examine the antibiotic-resistant TB case as a result of incomplete treatment [8]. A long latent period of TB has been formulated with a distributed delay in [9]. A model incorporating seasonal changes has been constructed with the use of periodic coefficients in [10].

Fractional differentiation and integration operators, which are the generalization of classical

integer-order counterparts, capture memory effects due to their nonlocal nature [11]. Recently, it has been observed that the fractional order models with fixed-order may not be capable of expressing some real world phenomena and the need for variable order fractional operators are used [12–14]. It is a useful tool to develop suitable models for describing real-world problems which cannot be expressed by using integer-order differential equations. For example, a model for rubella disease has been formulated with the use of non-local and non-singular fractional derivatives in [15]. A fractional TB model with time delay representing the required time to commencement of treatment and diagnosis has been studied in [16], while uniform asymptotic stability of a TB model with Caputo derivative has been investigated in [17]. These studies mainly concern a single disease. Models for the interaction of two diseases can be mentioned, too. Co-infection of HIV and TB has been discussed in [18], while impact of diabetes to TB has been investigated in [19].

Optimal control problems (OCP) can be used to find an intervention or treatment strategy for real-world problems. For example, new therapy protocols can be found with the use of optimal control strategies for cancerous tumor growth model in [20]. The optimal intervention strategy among vaccination and treatment can be decided by minimizing the transmission of malaria disease [21]. Moreover, spread of Ebola disease can be controlled with vaccination of the susceptible population [22]. On the other hand, the infection level of HIV and the overall treatment cost is minimized and the duration of therapy is optimized in [23]. A fractional optimal control problem (FOCP) has been proposed for two-strain TB model in [24]. Optimal control theory is used to reduce the cost of interventions in case of reinfection and post-exposure interventions, and the sensitivity of the reproduction number has been investigated in [25]. The optimal intervention strategy has been set to minimize the number of infected individuals with the control of exogenous reinfection through the use of chemoprophylaxis [26]. As a case study, the cost of TB treatment in Cameroon has been set as a cost functional and the control functions represent education-diagnosis campaign and chemoprophylaxis treatment [27]. In addition, a two-strain TB model has been taken as a constraint and the latent and infectious groups with the resistant-strain TB have been minimized with two types of treatments [28]. For a review on optimal control of TB models, we refer the reader to the study [29].

In this study, we consider the recent paper of Kim and his colleagues [30] where optimal intervention strategies to reduce the number of infected people in Philippines have been compared and some values for TB incidence for 2035 have been predicted. TB model in that study has been constructed for susceptible, high-risk latent, low-risk latent and infectious individuals using integer-order derivative. We propose a generalized TB model with the use of Caputo time fractional derivative since symptoms of TB may not be observed quickly. On the contrary, latent period of the disease might last for years. In the paper [30], the aim is to minimize the number of high-risk latent and infected people with the cost of applying the controls. In addition to these, we maximize the number of susceptible people and the control strategies are fixed as distancing control, latent case finding control, case holding control and their combination. We record the values of susceptible  $S(t)$  and infected  $I(t)$  individuals for different fractional orders in 2035 and we observe the contribution of the order. In addition, we calculate the reduction and increase in  $I$  and  $S$ , respectively. At the end, we comment on the choice of the optimal intervention strategy for Philippines by underlying the contribution of the fractional derivative.

The rest of the paper is organized as follows: In Section 2, we mention some properties and definitions for Caputo fractional derivative. In Section 3, we describe the generalized TB model, show that the solution is non-negative and bounded from above and propose the FOCP together with the optimality system. In Section 4, we present some numerical results to compare different strategies. Then, the paper ends with summary and conclusion.

## 2. Preliminaries

Fractional differentiation and integration operators, which are the generalization of classical integer-order counterparts, are capable of capturing memory effects due to their nonlocal nature. In the literature, several fractional derivatives have been defined. One of the mostly used fractional differentiation operators is Caputo derivative.

We define the (left) Caputo fractional differentiation operator for  $0 < q < 1$  as [11]

$${}_a^C \mathcal{D}_t^q g(t) = \frac{1}{\Gamma(1-q)} \int_a^t \frac{g'(s)}{(t-s)^q} ds. \quad (1)$$

The corresponding right differentiation operator is given by

$${}^C\mathcal{D}_b^q g(t) = -\frac{1}{\Gamma(1-q)} \int_t^b \frac{g'(s)}{(s-t)^q} ds. \quad (2)$$

To prove that the solution of the model is non-negative, we need the following lemma and corollary related to generalized mean value theorem [31]:

**Lemma 1.** *Let  $g(x) \in C[a, b]$  and  ${}^C\mathcal{D}_t^q g(t) \in C(a, b]$  for  $0 < q \leq 1$ . Then, for  $a \leq s \leq b$  and  $\forall x \in (a, b]$ , the following estimate holds:*

$$g(x) = g(a) + \frac{1}{\Gamma(q)} ({}^C\mathcal{D}_t^q g)(s)(x-a)^q. \quad (3)$$

**Corollary 1.** *Let  $g(x) \in C[a, b]$  and  ${}^C\mathcal{D}_t^q g(t) \in C(a, b]$  for  $0 < q \leq 1$ . If  ${}^C\mathcal{D}_t^q g(t)$  is non-negative  $\forall x \in (a, b)$ , then  $g(x)$  is non-decreasing for each  $x \in [a, b]$ . If  ${}^C\mathcal{D}_t^q g(t)$  is non-positive  $\forall x \in (a, b)$ , then  $g(x)$  is non-increasing for each  $x \in [a, b]$ .*

To show that the solution is bounded from above, we need the Laplace transform. The Laplace transform of the (left) Caputo derivative is obtained as

$$\mathcal{L}\{{}^C\mathcal{D}_t^q g(t)\} = s^q G(s) - g(0)s^{q-1}. \quad (4)$$

Moreover, the Laplace transform of the Mittag-Leffler function is given by

$$\mathcal{L}\{t^{p-1} E_{q,p}(-at^q)\} = \frac{s^{q-p}}{s^q + a}, \quad (5)$$

where  $E_{q,p}(z) = \sum_{i=0}^{\infty} \frac{z^i}{\Gamma(qi+p)}$ .

### 3. Fractional optimal control problem

In this study, we generalize a tuberculosis model given in the study [30] with the use of Caputo time fractional derivative and investigate the contribution of Caputo derivative in terms of a FOCP. The model is composed of four epidemiological classes: susceptible,  $S(t)$ ; high-risk latent,  $H(t)$ ; infectious or active TB,  $I(t)$  and low-risk latent,  $L(t)$ . Indeed, the total population size is represented by  $N(t) = S(t) + H(t) + I(t) + L(t)$ .

The OCP given in the study [30] offers a way to minimize the population of infectious and high-risk latent classes. In this current study, a FOCP is constructed to minimize the population of infectious and high-risk latent classes while maximizing the number of susceptible people together with the cost of implementing three different control strategies as

$$\begin{aligned} & \min_{(u_1, u_2, u_3) \in U_{ad}} J(u_1, u_2, u_3) \\ & = \int_0^{t_f} (H(t) + I(t) - S(t) + \frac{\omega_1}{2} u_1^2(t) \\ & \quad + \frac{\omega_2}{2} u_2^2(t) + \frac{\omega_3}{2} u_3^2(t)) dt \end{aligned} \quad (6)$$

subject to

$$\begin{cases} {}^C\mathcal{D}_t^q S(t) & = b^q N(t) - \beta^q (1 - u_1(t)) \frac{S(t)I(t)}{N(t)} \\ & \quad - \mu^q S(t), \\ {}^C\mathcal{D}_t^q H(t) & = \beta^q (1 - u_1(t)) \frac{S(t)I(t)}{N(t)} \\ & \quad - (\alpha^q (1 + u_2(t)) + \kappa^q + \mu^q) H(t) \\ & \quad + pr^q (1 - u_3(t)) I(t), \\ {}^C\mathcal{D}_t^q I(t) & = \kappa^q H(t) - (r^q + \mu^q + d^q) I(t), \\ {}^C\mathcal{D}_t^q L(t) & = (1 - p(1 - u_3(t))) r^q I(t) \\ & \quad + \alpha^q (1 + u_2(t)) H(t) - \mu^q L(t), \end{cases} \quad (7)$$

with  $S(0) = S_0$ ,  $H(0) = H_0$ ,  $I(0) = I_0$ ,  $L(0) = L_0$  where the admissible space of controls is given by [30]

$$\begin{aligned} U_{ad} & = \{(u_1(t), u_2(t), u_3(t)) \mid u_1(t), u_2(t), u_3(t) \\ & \quad \text{are measurable with} \\ & \quad 0.05 \leq u_1(t), u_2(t), u_3(t) \leq 0.95, t \in [0, t_f]\}. \end{aligned}$$

In other words, the optimal control  $(u_1^*, u_2^*, u_3^*) \in U_{ad}$  is required so that  $J(u_1^*, u_2^*, u_3^*) = \min_{(u_1, u_2, u_3) \in U_{ad}} J(u_1, u_2, u_3)$  is reached.

**Remark 1.** *By adding the equations in the model (7) side by side, the dynamical model for the total population is obtained as*

$${}^C\mathcal{D}_t^q N(t) = (b^q - \mu^q) N(t) - d^q I(t), \quad N(0) = N_0. \quad (8)$$

In Table 1, we mention the values/units of the parameters in the model [30].

**Table 1.** Parameters in the model.

| Parameter | Description (Units)                                  | Value   |
|-----------|--|---------|
| $b$       | Effective birth rate (yr <sup>-1</sup> )             | 0.0442  |
| $\mu$     | Natural death rate (yr <sup>-1</sup> )               | 0.0235  |
| $\beta$   | Transmission rate (yr <sup>-1</sup> )                | 11.7345 |
| $\alpha$  | Progression rate from $H$ to $L$ (yr <sup>-1</sup> ) | 0.2077  |
| $\kappa$  | Progression rate from $H$ to $I$ (yr <sup>-1</sup> ) | 0.0294  |
| $r$       | Treatment rate (yr <sup>-1</sup> )                   | 0.2906  |
| $d$       | TB-induced mortality rate (yr <sup>-1</sup> )        | 0.05    |
| $p$       | Treatment failure probability                        | 0.2     |

**Remark 2.** We follow the study [32] to take  $q^{th}$  powers of the parameters, which have temporal units, to eliminate dimension mismatch.

**3.1. Non-negative and bounded solution**

In this section, we will prove that the solution to (7) is non-negative and bounded from above. To do this, we fix the controls as  $u_1(t) = u_1$ ,  $u_2(t) = u_2$  and  $u_3(t) = u_3$ .

**Theorem 1.** Let  $(S(t), H(t), I(t), L(t))$  be the solution to the model (7). Then, the solution remains in  $\mathbb{R}_+^4$ .

**Proof.** We observe that the the model leads to the following inequalities:

$$\begin{aligned} {}_0^C \mathcal{D}_t^q S(t)|_{S=0} &= b^q N \geq 0, \\ {}_0^C \mathcal{D}_t^q H(t)|_{H=0} &= (1 - u_1(t))\beta^q \frac{SI}{N} \\ &\quad + pr^q(1 - u_3(t))I \geq 0, \\ {}_0^C \mathcal{D}_t^q I(t)|_{I=0} &= \kappa^q H(t) \geq 0, \\ {}_0^C \mathcal{D}_t^q L(t)|_{L=0} &= (1 - (1 - u_3(t))p)r^q I \\ &\quad + (1 + u_2(t))\alpha^q H(t) \geq 0. \end{aligned} \tag{9}$$

By Corollary 1, the solution remains in  $\mathbb{R}_+^4$ .  $\square$

**Theorem 2.** Let  $(S(t), H(t), I(t), L(t))$  be the solution to the model (7). The solution is bounded from above.

**Proof.** Firstly, we add the equations in (7) to reach (8). Then, we observe that the inequality

$${}_0^C \mathcal{D}_t^q N(t) \leq (b^q - \mu^q)N(t), \tag{10}$$

holds. Then, we take the Laplace transform of both sides in (10) to get the relation

$$\lambda^q \mathcal{L}\{N(t)\} - \lambda^{q-1}N(0) \leq (b^q - \mu^q)\mathcal{L}\{N(t)\}. \tag{11}$$

Arranging (11), we reach the inequality

$$\mathcal{L}\{N(t)\} \leq \frac{\lambda^{q-1}}{\lambda^q - b^q + \mu^q}N(0). \tag{12}$$

Using (5) and taking inverse Laplace of both side, we obtain the relation

$$N(t) \leq E_{q,1}(-(\mu^q - b^q)t^q)N(0) \leq CN(0), \tag{13}$$

since  $E_{q,1}(-(\mu^q - b^q)t^q) \leq C$  for some real number  $C$ . Then, we derive that the total population is

bounded from above which leads the solution of (7) to be bounded from above.  $\square$

**3.2. Optimality system**

We proceed with the characterization of the FOCP (6-7). To obtain the optimality system associated to the optimal control  $\mathcal{U}^* = (u_1^*, u_2^*, u_3^*)$ , we use Pontryagin’s maximum principle [33]. We construct the Hamiltonian as

$$\begin{aligned} \mathcal{H}(\mathcal{X}, \mathcal{U}, \mathcal{P}) &= (H(t) + I(t) - S(t) + \frac{\omega_1}{2}u_1^2(t) \\ &\quad + \frac{\omega_2}{2}u_2^2(t) + \frac{\omega_3}{2}u_3^2(t) \\ &\quad + \lambda_1^T(t)({}_0^C \mathcal{D}_t^q S(t)) + \lambda_2^T(t)({}_0^C \mathcal{D}_t^q H(t)) \\ &\quad + \lambda_3^T(t)({}_0^C \mathcal{D}_t^q I(t)) + \lambda_4^T(t)({}_0^C \mathcal{D}_t^q L(t)) \\ &\quad + \lambda_5^T(t)({}_0^C \mathcal{D}_t^q N(t)), \end{aligned} \tag{14}$$

where  $\lambda_i(t)$ ’s are the co-state (adjoint) variables for  $1 \leq i \leq 5$ . Then, the state equation (7) is obtained by the equation

$$\frac{\partial \mathcal{H}}{\partial \mathcal{P}}|_{\mathcal{U}^*} = {}_0 \mathcal{D}_t^q \mathcal{X}(t), \tag{15}$$

where the adjoint equation is derived as

$$\frac{\partial \mathcal{H}}{\partial \mathcal{X}}|_{\mathcal{U}^*} = {}_t \mathcal{D}_{t_f}^q \mathcal{P}, \tag{16}$$

with

$$\frac{\partial J}{\partial \mathcal{X}}|_{t=t_f} = 0 = \mathcal{P}(t_f). \tag{17}$$

Moreover, the optimality condition is given by the equation

$$\frac{\partial \mathcal{H}}{\partial \mathcal{U}}|_{\mathcal{U}^*} = 0. \tag{18}$$

For the optimal control to lie within the admissible space  $U_{ad}$ , we project it onto the interval  $[0.05, 0.95]$ . In the preceding theorem, we state the necessary optimality conditions.

**Theorem 3.** Given an optimal control  $\mathcal{U}^* = (u_1, u_2, u_3)$  and the state solution  $\mathcal{X}^* = (S, H, I, L, N)$  corresponding to

$$\left\{ \begin{array}{l} {}_0^C \mathcal{D}_t^q S(t) = b^q N(t) - \beta^q (1 - u_1(t)) \frac{S(t)I(t)}{N(t)} \\ \quad - \mu^q S(t), \\ {}_0^C \mathcal{D}_t^q H(t) = \beta^q (1 - u_1(t)) \frac{S(t)I(t)}{N(t)} \\ \quad - (\alpha^q (1 + u_2(t)) + \kappa^q + \mu^q) H(t) \\ \quad + pr^q (1 - u_3(t)) I(t), \\ {}_0^C \mathcal{D}_t^q I(t) = \kappa^q H(t) - (r^q + \mu^q + d^q) I(t), \\ {}_0^C \mathcal{D}_t^q L(t) = (1 - p(1 - u_3(t))) r^q I(t) \\ \quad + \alpha^q (1 + u_2(t)) H(t) - \mu^q L(t), \\ {}_0^C \mathcal{D}_t^q N(t) = (b^q - \mu^q) N(t) - d^q I(t), \end{array} \right. \quad (19)$$

with  $S(0) = S_0$ ,  $H(0) = H_0$ ,  $I(0) = I_0$ ,  $L(0) = L_0$  and  $N(0) = N_0$  that minimize the objective functional (6), there exist adjoint variables  $\mathcal{P} = (\lambda_1(t), \lambda_2(t), \lambda_3(t), \lambda_4(t), \lambda_5(t))$  satisfying

$$\left\{ \begin{array}{l} {}_t^C \mathcal{D}_{t_f}^q \lambda_1(t) = -(1 - u_1(t)) \beta^q \frac{I(t)}{N(t)} - \mu^q \lambda_1(t) \\ \quad + (1 - u_1(t)) \beta^q \frac{I(t)}{N(t)} \lambda_2(t) - 1, \\ {}_t^C \mathcal{D}_{t_f}^q \lambda_2(t) = -(\alpha^q (1 + u_2(t)) + \kappa^q + \mu^q) \lambda_2(t) \\ \quad + \kappa^q \lambda_3 + ((1 + u_2(t)) \alpha^q) \lambda_4(t) + 1, \\ {}_t^C \mathcal{D}_{t_f}^q \lambda_3(t) = -(1 - u_1(t)) \beta^q \frac{S(t)}{N(t)} \lambda_1(t) \\ \quad + ((1 - u_1(t)) \beta^q \frac{S(t)}{N(t)} \\ \quad + (1 - u_3(t)) pr^q) \lambda_2 \\ \quad - (r^q + \mu^q + d^q) \lambda_3(t) \\ \quad + (1 - p(1 - u_3(t))) r^q \lambda_4 - d^q \lambda_5(t) + 1, \\ {}_t^C \mathcal{D}_{t_f}^q \lambda_4(t) = -\mu^q \lambda_4(t), \\ {}_t^C \mathcal{D}_{t_f}^q \lambda_5(t) = ((1 - u_1(t)) \beta^q \frac{S(t)I(t)}{N^2(t)} + b^q) \lambda_1(t) \\ \quad - ((1 - u_1(t)) \beta^q \frac{S(t)I(t)}{N^2(t)}) \lambda_2(t) + (b^q - \mu^q) \lambda_5(t), \end{array} \right. \quad (20)$$

with transversality conditions

$$\lambda_i(t_f) = 0, \quad 1 \leq i \leq 5. \quad (21)$$

Moreover, the optimal control  $\mathcal{U}^* = (u_1(t), u_2(t), u_3(t))$  is represented by

$$\left\{ \begin{array}{l} u_1(t) = \min \left( \max \left( (\lambda_2(t) - \lambda_1(t)) \frac{\beta^q S(t)I(t)}{\omega_1 N(t)}, 0.05 \right), 0.95 \right), \\ u_2(t) = \min \left( \max \left( (\lambda_2(t) - \lambda_4(t)) \frac{\alpha^q H(t)}{\omega_2}, 0.05 \right), 0.95 \right), \\ u_3(t) = \min \left( \max \left( (\lambda_2(t) - \lambda_4(t)) \frac{pr^q I(t)}{\omega_3}, 0.05 \right), 0.95 \right). \end{array} \right. \quad (22)$$

## 4. Numerical results

In this section, we present some illustrative examples to observe the contribution of the fractional derivative to the choice of the control strategy. We apply 3 different control intervention approaches and their combinations: The first one (*Case C<sub>1</sub>*) is distancing control  $u_1(t)$ , which is based on eliminating the contact between infectious and susceptible people. The second approach (*Case C<sub>2</sub>*) is latent case finding control  $u_2(t)$  which aims to treat high-risk latent class. The last strategy (*Case C<sub>3</sub>*) is case holding control  $u_3(t)$  which consists of some actions applied to eliminate the failure of the treatment.

We use the parameter values given in Table 1 which lead the reproduction number to be  $\mathcal{R}_0 = \{2.4872, 2.8507, 3.2546\}$  for the fractional orders  $q \in \{0.85, 0.9, 0.95\}$ , respectively. Therefore, the infection will not disappear in the future if the initial conditions are taken close to the disease-free equilibrium point.

We fix the weight parameters as  $\{\omega_1, \omega_2, \omega_3\} = \{10^6, 10^6, 10^5\}$  following the work [30] and they denote the cost of implementing the corresponding control strategy. We solve the FOCP on the time interval [2015, 2035] with a constant step size  $\Delta t = 0.004$ . We discretize the FOCP using L1-method [34] and forward-backward sweep method is used as an optimization algorithm [35]. The initial subpopulations are taken as  $S_0 = 20027781$ ,  $H_0 = 9292101$ ,  $I_0 = 621331$  and  $L_0 = 32006125$  (Aurelio A. de los Reyes V, personal communication, June 26, 2018). We investigate the contribution of three intervention strategies and their combinations by measuring the reduction/increase in  $I$  and  $S$  compared to uncontrolled case in Table 3. All simulations are performed on a Windows 10 machine with Intel Core i7, 2.5 GHz and 16 GB using MATLAB R2016a. With the discretization mentioned above, the FOCP is solved for 430 seconds in case of triple controls, while the uncontrolled problem is solved in almost 25 seconds. Here, rather than the computational time, we will focus on the influence of the fractional order.

Before discussing an optimal control strategy, we obtain the numerical solution of TB model (7) without control, that is,  $u_1 = u_2 = u_3 = 0$ . We measure the values of  $H(t) + I(t)$ ,  $I(t)$  and  $S(t)$  in 2035 and we present these results in Table 2. We observe an increasing risk of the disease due to a large number of infected people.

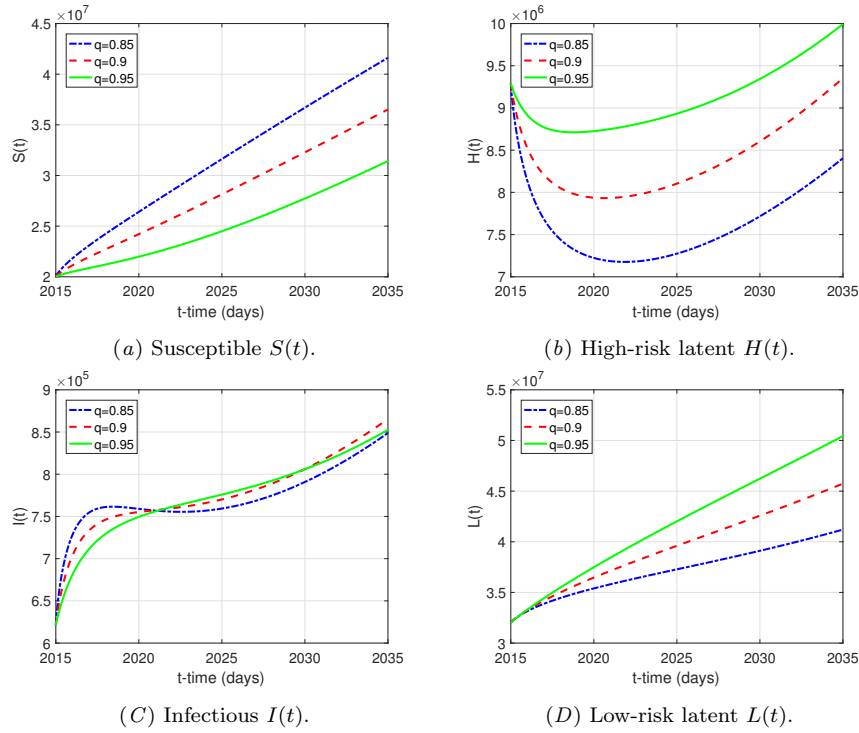


Figure 1. No control: Epidemiological classes.

Table 2. Uncontrolled case: Estimates for  $H + I$ ,  $I$  and  $S$  in 2035.

| $\alpha$ | $H(2035) + I(2035)$ | $I(2035)$  | $S(2035)$  |
|----------|---------------------|------------|------------|
| 0.85     | 9.2539e+06          | 8.4889e+05 | 4.1626e+07 |
| 0.9      | 1.0218e+07          | 8.6547e+05 | 3.6519e+07 |
| 0.95     | 1.0846e+07          | 8.5268e+05 | 3.1422e+07 |

Moreover, four epidemiological classes are shown in Fig. 1. We observe that infectious  $I(t)$  and high-risk latent  $H(t)$  populations increase over time which underlines the requirement of an efficient control strategy to eliminate the disease.

Therefore, we set the optimal control strategy to minimize the difference between uninfected and infected individuals with the following the cost functional:

$$\min_{(u_1, u_2, u_3) \in U_{ad}} J(u_1, u_2, u_3) = \int_0^{t_f} (H(t) + I(t) - S(t) + \frac{\omega_1}{2} u_1^2(t) + \frac{\omega_2}{2} u_2^2(t) + \frac{\omega_3}{2} u_3^2(t)) dt$$

We immediately observe that cases  $C_1$ ,  $C_{12}$  and  $C_{123}$  lead to the highest reduction in  $I$  and increase in  $S$ . In other words, distancing control is the most efficient choice to reduce the number of infected people which leads to an increase in the susceptible individuals. Additionally, the case  $C_3$ , namely case holding control, is the least efficient choice. It means that some efforts to eliminate the failure of the treatment cannot be successful

without any supportive strategy. Moreover, case  $C_2$  denoting latent case finding control is the second most effective approach. However, its contribution can be boosted with distancing control. Since the contribution of case holding control is limited, there is not a big difference between  $C_{12}$  and  $C_{123}$  in the reduction of  $I$ , while increase in  $S$  is almost the same for the cases  $C_1$ ,  $C_{12}$  and  $C_{123}$ . On the other hand, as we increase the order of the fractional derivative  $q$ , we observe a positive change in both reduction in  $I$  and increase in  $S$ . It can be thought as the contribution of the memory effect. If we add more information about the history to the model, which corresponds to a higher value of  $q$ , then the success of the treatment will be more visible.

As some illustrative results, we depict the epidemiological classes for Case  $C_{123}$ , namely the combination of three control strategies, in Fig. 2. We observe that the number of susceptible individuals is higher than one for the uncontrolled case, while there is a decline in the number of infected people. It means that the control strategy works well and the figures are compatible with the aim behind the FOCP.

In addition, we present the optimal controls  $u_1$ ,  $u_2$  and  $u_3$  in Fig. 3. We see that the control lies between the predefined box constraints. As time passes, a smaller control (compared to initial time) is needed. Among these three different control strategies, distancing control is the most effective one to eliminate the disease.

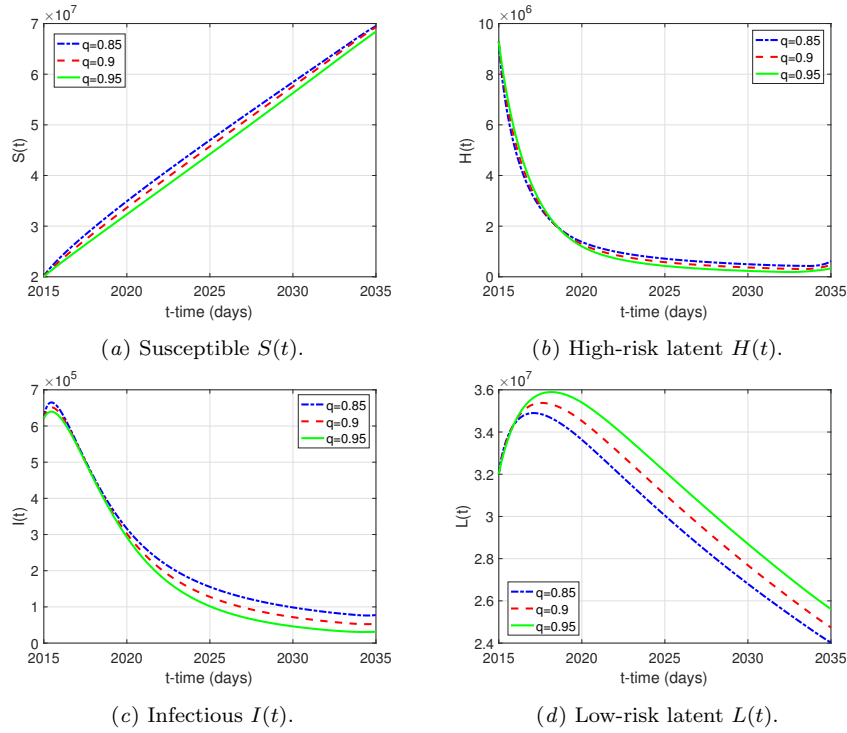


Figure 2. Case  $C_{123}$ : Epidemiological classes.

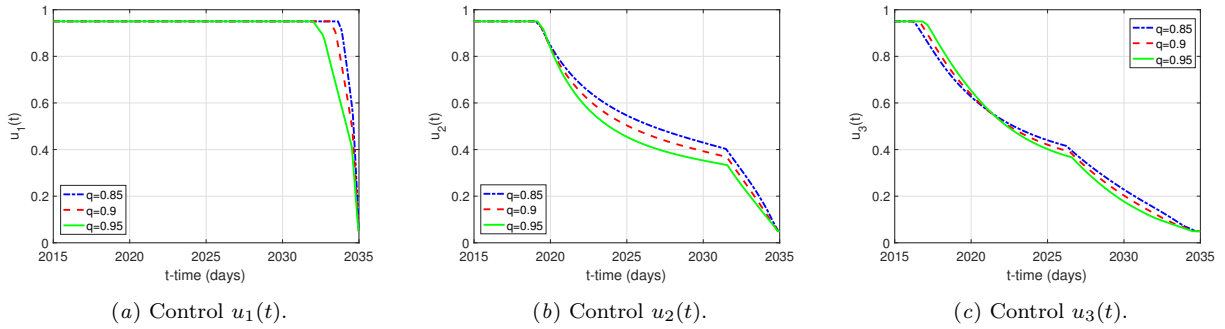


Figure 3. Case  $C_{123}$ : Optimal controls  $u_1(t)$ ,  $u_2(t)$  and  $u_3(t)$ .

### 5. Summary and conclusion

In this study, we investigate an OCP governed by a TB model with Caputo time fractional derivative. We justify that the solution is non-negativity and bounded from above and the optimality system is derived based on the Hamiltonian. We compare three different control strategies and their combinations, namely, distancing control, latent case finding and case holding control. We presented some numerical results to underline the contribution of the fractional order and the choice of the intervention strategy. We observe that the cases  $C_1$ ,  $C_{12}$  and  $C_{123}$  lead to the most reduction in the number of infected people and increase in the susceptible individuals. Moreover, as we increase the order of the fractional derivative, optimal control strategies become more effective.

### Acknowledgments

The author thanks the anonymous referees for their helpful suggestions.

### References

- [1] World Health Organization. (2017). *Tuberculosis fact sheet*. Geneva, Switzerland. Available from [https://www.who.int/tb/publications/global\\_report/gtbr2017\\_main\\_text.pdf](https://www.who.int/tb/publications/global_report/gtbr2017_main_text.pdf). [Accessed 6 July 2018].
- [2] Feng, Z., Castillo-Chavez, C., & Capurro, A.F. (2000). A model for tuberculosis with exogenous reinfection. *Theoretical Population Biology*, 57 (3), 235–247.
- [3] Small, P.M., & Fujiwara, P.I. (2001). Management of tuberculosis in the United States,

**Table 3.** Estimates for  $I(t)$  and  $S(t)$  in 2035 and the corresponding reduction/increase.

| Case $C_1$     |            |               |            |              |
|----------------|------------|---------------|------------|--------------|
| $\alpha$       | $I(2035)$  | (Reduction %) | $S(2035)$  | (Increase %) |
| 0.85           | 1.0862e+05 | %87.20        | 6.9310e+07 | %66.51       |
| 0.9            | 7.9264e+04 | %90.84        | 6.9068e+07 | %89.13       |
| 0.95           | 5.2400e+04 | %93.85        | 6.8138e+07 | %116.85      |
| Case $C_2$     |            |               |            |              |
| $\alpha$       | $I(2035)$  | (Reduction %) | $S(2035)$  | (Increase %) |
| 0.85           | 2.9670e+05 | %65.05        | 5.4971e+07 | %32.06       |
| 0.9            | 2.8429e+05 | %67.15        | 5.1607e+07 | %41.32       |
| 0.95           | 2.6649e+05 | %68.75        | 4.7425e+07 | %50.93       |
| Case $C_3$     |            |               |            |              |
| $\alpha$       | (2035) $I$ | (Reduction %) | $S(2035)$  | (Increase %) |
| 0.85           | 8.3356e+05 | %1.81         | 4.2935e+07 | %3.14        |
| 0.9            | 8.4981e+05 | %1.81         | 3.7681e+07 | %3.18        |
| 0.95           | 8.3386e+05 | %2.21         | 3.2304e+07 | %2.81        |
| Case $C_{12}$  |            |               |            |              |
| $\alpha$       | $I(2035)$  | (Reduction %) | $S(2035)$  | (Increase %) |
| 0.85           | 7.8062e+04 | %90.80        | 6.9499e+07 | %66.96       |
| 0.9            | 5.3686e+04 | %93.80        | 6.9293e+07 | %89.75       |
| 0.95           | 3.1645e+04 | %96.29        | 6.8405e+07 | %117.70      |
| Case $C_{13}$  |            |               |            |              |
| $\alpha$       | $I(2035)$  | (Reduction %) | $S(2035)$  | (Increase %) |
| 0.85           | 1.0653e+05 | %87.45        | 6.9317e+07 | %66.52       |
| 0.9            | 7.7363e+04 | %91.06        | 6.9080e+07 | %89.16       |
| 0.95           | 5.0710e+04 | %94.05        | 6.8151e+07 | %116.89      |
| Case $C_{23}$  |            |               |            |              |
| $\alpha$       | $I(2035)$  | (Reduction %) | $S(2035)$  | (Increase %) |
| 0.85           | 2.9065e+05 | %65.76        | 5.5203e+07 | %32.62       |
| 0.9            | 2.7810e+05 | %67.87        | 5.1875e+07 | %42.05       |
| 0.95           | 2.6041e+05 | %69.46        | 4.7717e+07 | %51.86       |
| Case $C_{123}$ |            |               |            |              |
| $\alpha$       | $I(2035)$  | (Reduction %) | $S(2035)$  | (Increase %) |
| 0.85           | 7.7656e+04 | %90.85        | 6.9502e+07 | %66.97       |
| 0.9            | 5.3334e+04 | %93.84        | 6.9297e+07 | %89.76       |
| 0.95           | 3.1380e+04 | %96.32        | 6.8410e+07 | %117.71      |

*New England Journal of Medicine*, 345 (3), 189–200.

- [4] Bailey, N.T., et al., (1975). *The mathematical theory of infectious diseases and its applications*. Charles Griffin & Company Ltd, 5a Crendon Street, High Wycombe, Bucks HP13 6LE.
- [5] Waaler, H., Geser, A., & Andersen, S. (1962). The use of mathematical models in the study of the epidemiology of tuberculosis. *American Journal of Public Health and the Nations Health*, 52 (6), 1002–1013.
- [6] Hethcote, H.W. (2000). The mathematics of infectious diseases. *SIAM Review*, 42 (4), 599–653.
- [7] Choisy, M., Guégan, J.F., & Rohani, P. (2007). Mathematical modeling of infectious diseases dynamics. *Encyclopedia of infectious diseases: Modern methodologies*, 379–404.
- [8] Castillo-Chavez, C., & Feng, Z. (1997) To treat or not to treat: the case of tuberculosis. *Journal of Mathematical Biology*, 35 (6), 629–656.
- [9] Castillo-Chávez, C., Feng, Z., et al. (1998). Mathematical models for the disease dynamics of tuberculosis. in: G. S. Mary Ann Horn, G. Webb (Eds.), *Advances in Mathematical Population Dynamics-Molecules, Cells and Man*, Vanderbilt University Press, 117–128.
- [10] Liu, L., Zhao, X.Q., & Zhou, Y., (2010). A tuberculosis model with seasonality. *Bulletin of Mathematical Biology*, 72 (4), 931–952.

- [11] Podlubny, I. (1999). *Fractional differential equations*, Vol. 198 of Mathematics in Science and Engineering, Academic Press, Inc., San Diego, CA, An introduction to fractional derivatives, fractional differential equations, to methods of their solution and some of their applications.
- [12] Yang, X.J., & Machado, J.A.T. (2017). A new fractional operator of variable order: application in the description of anomalous diffusion. *Physica A: Statistical Mechanics and its Applications*, 481, 276–283.
- [13] Moghaddam, B.P., & Machado, J.A.T. (2017). Extended algorithms for approximating variable order fractional derivatives with applications. *Journal of Scientific Computing*, 71 (3), 1351–1374.
- [14] Moghaddam, B.P., & Machado, J.A.T. (2017). SM-algorithms for approximating the variable-order fractional derivative of high order. *Fundamenta Informaticae*, 151 (1-4), 293–311.
- [15] Koca, I. (2018). Analysis of rubella disease model with non-local and non-singular fractional derivatives. *An International Journal of Optimization and Control: Theories and Applications*, 8 (1), 17–25.
- [16] Sweilam, N.H., Al-Mekhlafi, S.M., & Assiri, T.A.R. (2017). Numerical study for time delay multistrain tuberculosis model of fractional order. *Complexity*, 2017, Article ID 1047381, 14 pages.
- [17] Wojtak, W., Silva, C.J., & Torres, D.F. (2018). Uniform asymptotic stability of a fractional tuberculosis model. *Mathematical Modelling of Natural Phenomena*, 13 (1), 9.
- [18] Pinto, C.M.A., & Carvalho, A.R.M. (2017). The HIV/TB coinfection severity in the presence of TB multi-drug resistant strains. *Ecological complexity*, 32, 1–20.
- [19] Carvalho, A.R.M., & Pinto, C.M.A. (2018). Non-integer order analysis of the impact of diabetes and resistant strains in a model for TB infection. *Communications in Nonlinear Science and Numerical Simulation*, 61, 104–126.
- [20] De Pillis, L.G., & Radunskaya, A. (2001). A mathematical tumor model with immune resistance and drug therapy: An optimal control approach. *Computational and Mathematical Methods in Medicine*, 3 (2), 79–100.
- [21] Okosun, K.O., Oufiki, R., & Marcus, N. (2011). Optimal control analysis of a malaria disease transmission model that includes treatment and vaccination with waning immunity. *Biosystems*, 106 (2-3), 136–145.
- [22] Area, I, Ndaïrou, F., Nieto, J.J., Silva, C.J., & Torres, D.F.M. (2018). Ebola model and optimal control with vaccination constraints. *Journal of Industrial & Management Optimization*, 14 (2), 427–446.
- [23] Hamdache, A., Saadi, S., & Elmouki, I. (2016). Free terminal time optimal control problem for the treatment of HIV infection. *An International Journal of Optimization and Control: Theories & Applications*, 6 (1), 33–51.
- [24] Sweilam, N.H., & Al-Mekhlafi, S.M. (2016). On the optimal control for fractional multi-strain TB model. *Optimal Control Applications and Methods*, 37 (6), 1355–1374.
- [25] Silva, C.J., & Torres, D.F.M. (2013). Optimal control for a tuberculosis model with reinfection and post-exposure interventions. *Mathematical Biosciences*, 244 (2), (2013) 154–164.
- [26] Bowong, S. (2010). Optimal control of the transmission dynamics of tuberculosis. *Nonlinear Dynamics*, 61 (4), 729–748.
- [27] Moualeu, D.P., Weiser, M., Ehrig, R., & Deuffhard, P. (2015). Optimal control for a tuberculosis model with undetected cases in Cameroon. *Communications in Nonlinear Science and Numerical Simulation*, 20 (3), 986–1003.
- [28] Jung, E., Lenhart, S., & Feng, Z. (2002). Optimal control of treatments in a two-strain tuberculosis model. *Discrete and Continuous Dynamical Systems Series B*, 2 (4), 473–482.
- [29] Silva, C.J., & Torres, D.F.M. (2015). Optimal control of tuberculosis: A review, in: *Dynamics, Games and Science*, Springer, 701–722.
- [30] Kim, S., Aurelio, A. de Los Reyes V., & Jung, E. (2018). Mathematical model and intervention strategies for mitigating tuberculosis in the Philippines. *Journal of Theoretical Biology*, 443, 100–112.
- [31] Odibat, Z.M., & Shawagfeh, N.T. (2007). Generalized Taylor’s formula. *Applied Mathematics and Computation*, 186 (1), 286–293.
- [32] Diethelm, K. (2013). A fractional calculus based model for the simulation of an outbreak of dengue fever. *Nonlinear Dynamics*, 71 (4), 613–619.
- [33] Pontryagin, L., Boltyanskii, V., Gamkrelidze, R., & Mishchenko, E. (1962). *The Mathematical Theory of Optimal Processes*. John Wiley & Sons, New York.

- [34] Lin, Y., & Xu, C. (2007). Finite difference/spectral approximations for the time-fractional diffusion equation. *Journal of Computational Physics*, 225 (2), 1533–1552.
- [35] Lenhart, S., Workman, J.T. (2007). *Optimal Control Applied to Biological Models*. Chapman & Hall, CRC Press.
- Tuğba Akman Yıldız** achieved her PhD degree in Scientific Computing Program at Institute of Applied Mathematics, Middle East Technical University in 2015. She has been working as an assistant professor at UTAA since 2016. Her research interests are numerical solutions of differential equations, optimal control problems and model order reduction methods.

An International Journal of Optimization and Control: Theories & Applications (<http://ijocta.balikesir.edu.tr>)



This work is licensed under a Creative Commons Attribution 4.0 International License. The authors retain ownership of the copyright for their article, but they allow anyone to download, reuse, reprint, modify, distribute, and/or copy articles in IJOCTA, so long as the original authors and source are credited. To see the complete license contents, please visit <http://creativecommons.org/licenses/by/4.0/>.



## RESEARCH ARTICLE

# A new auxiliary function approach for inequality constrained global optimization problems

Nurullah Yilmaz  and Ahmet Sahiner 

Department of Mathematics, Suleyman Demirel University, Isparta, Turkey  
 nurullahyilmaz@sdu.edu.tr, ahmetsahiner@sdu.edu.tr

## ARTICLE INFO

## Article History:

Received 14 August 2018

Accepted 26 January 2019

Available 15 April 2019

## Keywords:

Constrained optimization

Global optimization

Smoothing approach

Penalty function

## AMS Classification 2010:

90C26; 90C30; 65D10; 65K10

## ABSTRACT

In this study, we deal with the nonlinear constrained global optimization problems. First, we introduce a new smooth exact penalty function for solving constrained optimization problems. We combine the exact penalty function with the auxiliary function in regard to constrained global optimization. We present a new auxiliary function approach and the adapted algorithm in order to solve non-linear inequality constrained global optimization problems. Finally, we illustrate the efficiency of the algorithm on some numerical examples.



## 1. Introduction

We consider the following continuous constrained optimization problem

$$(P) \quad \begin{aligned} & \min_{x \in \mathbb{R}^n} f(x) \\ & \text{s.t. } g_j(x) \leq 0, \quad j = 1, 2, \dots, m, \end{aligned}$$

where  $f : \mathbb{R}^n \rightarrow \mathbb{R}$  and  $g_j(x) : \mathbb{R}^n \rightarrow \mathbb{R}$ ,  $j \in J = \{1, 2, \dots, m\}$  are continuously differentiable functions. The problem (P) is considered in many problems of engineering and natural sciences [1–4] and it is studied in many papers [6, 7].

There exists a very rich theory for the solution of the problem (P) [5]. One of the traditional but effective method to solve the problem (P) is the penalty function method [8]. The penalty function method has been proposed in order to transform a constrained optimization problem to an unconstrained optimization problem. The method offers constructing a barrier on the boundary of the set of feasible solutions which is defined as  $D_0 := \{x \in \mathbb{R}^n : g_j(x) \leq 0, j = 1, 2, \dots, m\}$  and it is assumed that  $D_0$  is not empty. In order to construct a barrier the “ $b(t) = -\log(-t)$ ”, “ $b(t) = \max(t, 0)$ ” functions

are used. The penalized objective function is defined as

$$F(x, \rho) = f(x) + \rho \sum_{j=1}^m b(g_j(x)), \quad (1)$$

and problem (P) re-stated as

$$(P_\rho) \quad \min_{x \in \mathbb{R}^n} F(x, \rho),$$

where  $\rho > 0$  is a penalty parameter. If  $b(t) = \max(t, 0)$  is in the formula (1), the penalty function is called as exact penalty function according to Zangwill [9]. It can be observed that the exact penalty function may be non-smooth. When the penalty function approach is non-smooth, one of the conventional approaches is constructing a smoothing approach. The smoothing approach is based on modifying the objective function or approximating the objective function by smooth functions [10]. In order to improve the smoothing approaches, different types of valuable techniques and algorithms are developed [11–14]. In recent years, the smoothing approaches have been used for many non-smooth problems such as min-max [15, 16], exact penalty [17–20] and etc. [21].

If the problem  $(P)$  or  $(P_\rho)$  has just one minimizer, then many local optimization methods can be used to solve with penalty method, but if it has multiple local minimizers, most of the well-known methods are not available to solve [22]. The studies on global optimization have become extensively increase among the other research areas of optimization [23, 24]. There are many valuable studies on global optimization depending on deterministic, stochastic and heuristic approaches [25, 26]. Most of the global optimization techniques are proposed to solve unconstrained problems, but by combining the penalty function method with a global optimization algorithm the global solution of the problem  $(P)$  can be obtained. One of the important global optimization approaches is the auxiliary function approach which includes the Tunneling Method (Algorithm) [27], Filled Function Method [28, 29], Global Descent Method [30] and Cut-Peak Function Method [31]. These methods are established on finding the lower minimizer than the current one by making a suitable modification on the objective function. The modified function is generally called as auxiliary function (Filled Function, Tunneling Function and etc.) [33].

In the next section, we give some preliminary definitions. In section 3, we introduce a new penalty function in order to transform the problem  $(P)$  into an unconstrained problem. In Section 4, we present a minimization algorithm and convergence results. In Section 5, we apply the algorithms on the important test problems. In the last section, we give some concluding remarks.

## 2. Preliminaries

We assume that the set  $D_0$  is closed and bounded and the function  $f$  has a finite number of local minimizers in  $D_0$ . Throughout the paper, we use  $x_k^*$  to denote the  $k$ -th local minimizer of  $f$  whereas by  $x^*$  we mean the global minimizer.  $\|x\| = \sqrt{\sum_{k=1}^n x_k^2}$  denotes the Euclidean norm in  $\mathbb{R}^n$ .

**Definition 1.** [13] Let  $f : \mathbb{R}^n \rightarrow \mathbb{R}$  be a continuous function. The function  $\tilde{f} : \mathbb{R}^n \times \mathbb{R}_+ \rightarrow \mathbb{R}$  is called a smoothing function of  $f(x)$ , if  $\tilde{f}(\cdot, \beta)$  is continuously differentiable in  $\mathbb{R}^n$  for any fixed  $\beta$ , and for any  $x \in \mathbb{R}^n$ ,

$$\lim_{z \rightarrow x, \beta \rightarrow 0} \tilde{f}(z, \beta) = f(x).$$

**Definition 2.** [19] Let  $\varepsilon > 0$ , a point  $x_\varepsilon$  is called  $\varepsilon$ -feasible solution for the problem  $(P)$ , if

$$g_j(x) \leq \varepsilon, \quad j = 1, 2, \dots, m.$$

## 3. A New Penalty Function

In this section, we present a new penalty approach for the problem  $(P)$ . Let us define the sets  $D_j = \{x \in \mathbb{R}^n : g_j(x) \leq 0\}$  for  $j = 1, 2, \dots, m$ . It can be observed that  $\cap_{j=1}^m D_j = D_0$ . The main idea in exact penalty function approach is to construct a barrier at the boundary of  $D_0$  such that any local (global) solver can not find a point outside the set  $D_0$ . Based on this idea, we define a new penalty function as

$$F(x, \rho) = f(x) + \rho \left( \sum_{j=1}^m \chi_{D_j^c}(x) \right) \|x - x_0\|^2,$$

where  $\rho > 0$ ,  $x_0 \in D_0$  and

$$\chi_{D_j^c}(x) = \begin{cases} 0, & x \in D_j, \\ 1, & x \notin D_j, \end{cases}$$

for  $j = 1, 2, \dots, m$ . Since the function  $\chi_{D_j^c}(x)$  is non-smooth, we apply the smoothing approach to this function in order to make it smooth. We design the following function

$$\tilde{\chi}_{D_j^c}(x, \varepsilon) = \begin{cases} 0, & t \leq 0, \\ R_1(t), & 0 \leq t \leq \varepsilon, \\ 1, & t \geq \varepsilon, \end{cases} \quad (2)$$

where  $\varepsilon > 0$  and

$$R_1(t) = \frac{-2}{\varepsilon^3} t^3 + \frac{3}{\varepsilon^2} t^2,$$

for  $t = g_j(x)$ ,  $j = 1, 2, \dots, m$ . By using  $R_1$  in formula (2), the obtained smoothing function is continuously differentiable. If the following function

$$R_2(t) = \frac{6}{\varepsilon^5} t^5 - \frac{15}{\varepsilon^4} t^4 + \frac{10}{\varepsilon^3} t^3,$$

is used in formula (2) instead of  $R_1$ , the obtained smoothing function is second order continuously differentiable. The function  $R_i$ , ( $i = 1, 2, \dots, k$ ) is called the smooth transition function. Now, we obtain surrogate problem  $(\tilde{P}_\rho)$  as follows:

$$(\tilde{P}_\rho) \quad \min_{x \in \mathbb{R}^n} F(x, \rho, \varepsilon), \quad (3)$$

where

$$F(x, \rho, \varepsilon) = f(x) + \rho \left( \sum_{j=1}^m \tilde{\chi}_{D_j^c}(x, \varepsilon) \right) \|x - x_0\|^2.$$

**Theorem 1.** Let  $x^*$  be a solution for  $(\tilde{P}_\rho)$  for sufficiently large  $\rho > 0$  then  $x^* \in D_0$ .

**Proof.** Suppose that  $x^* \notin D_0$ . Then, there exists  $j$  such that  $t = g_j(x^*) > 0$ . We have two cases:

**Case 1.** Let  $t \geq \varepsilon$  then, we have

$$F(x^*, \rho, \varepsilon) = f(x^*) + \rho \|x^* - x_0\|^2,$$

and

$$\nabla F(x^*, \rho, \varepsilon) = \nabla f(x^*) + 2\rho(x^* - x_0) = 0.$$

Therefore, we obtain

$$\rho = -\nabla f(x^*)(2(x^* - x_0))^{-1}.$$

Since  $f(x)$  continuous differentiable  $\|f(x)\| < \infty$  and  $x^* \neq x_0$ , it can be concluded that  $\rho$  is finite. If anyone chooses  $\rho_1 > \rho$ , the  $\nabla F(x^*, \rho_1, \varepsilon) \neq 0$ .

**Case 2.** Let  $0 < t \leq \varepsilon$  then, we have

$$F(x^*, \rho, \varepsilon) = f(x^*) + \rho \left( \frac{-2}{\varepsilon^3} t^3 + \frac{3}{\varepsilon^2} t^2 \right) \times \|x^* - x_0\|^2,$$

and

$$\nabla F(x^*, \rho, \varepsilon) = \nabla f(x^*) + \rho A(x^*, \varepsilon),$$

where

$$A(x^*, \varepsilon) = \left( \left( \frac{-2}{\varepsilon^3} t^3 + \frac{3}{\varepsilon^2} t^2 \right) \|x^* - x_0\|^2 + \left( \frac{-2}{\varepsilon^3} t^3 + \frac{3}{\varepsilon^2} t^2 \right) (2(x^* - x_0)) \right).$$

Thus, we obtain

$$\rho = -\nabla f(x^*) A(x^*, \varepsilon)^{-1}.$$

It can be seen that  $\rho$  is finite. If anyone chooses  $\rho_2 > \rho$ , the  $\nabla F(x^*, \rho_2, \varepsilon) \neq 0$ .

As a consequence, if anyone chose the parameter  $\rho$  in (1) as  $\rho > \max\{\rho_1, \rho_2\}$ , the point  $x^*$  cannot be outside of  $D_0$ .  $\square$

**Corollary 1.** Let  $x^*$  be a solution for  $(\tilde{P}_\rho)$  for sufficiently large  $\rho$  then  $x^*$  is a solution for  $(P)$ .

**Proof.** From Theorem 1, we have  $x^* \in D_0$ . Then, we obtain

$$\begin{aligned} f(x^*) &= F(x^*, \rho, \varepsilon) \\ &= F(x^*, \rho, 0) \\ &\leq F(x, \rho, 0) \\ &= f(x). \end{aligned}$$

This completes the proof.  $\square$

#### 4. Algorithms for Minimization Procedure

In this section, we propose our new algorithm to find the global optimal point by considering the problem  $(\tilde{P}_\rho)$ .

##### Algorithm

Step 1 Determine  $x^0$ ,  $\rho_0 = 10$ ,  $\varepsilon_0 > 0$ ,  $N > 1$ ,  $0 < \eta < 1$  and let  $j = 1$  and go to Step 2.

Step 2 Use  $x^{j-1}$  as an initial point and apply one of the global optimization algorithms to solve the problem  $(\tilde{P}_\rho)$ . Let  $x_j$  is the solution.

Step 3 If  $x_j \in \text{int}D_0$  then stop the algorithm and  $x^j$  is the optimal solution else go to Step 4.

Step 4 If  $x^j$  is  $\varepsilon$ -feasible for  $(P)$ , then stop and  $x^j$  is the optimal solution. Otherwise, take  $\rho_j = N\rho_{j-1}$ ,  $\varepsilon_j = \eta\varepsilon_{j-1}$  and  $j = j + 1$ , then go to Step 2.

In Step 2 of algorithm  $x_j$  is the global optimal solution of the problem  $(\tilde{P}_\rho)$  depending on the parameter  $\varepsilon$ . In order to obtain the global solution, any of the global optimization methods can be used. We use the auxiliary function based global optimization method studied in [21,33]. The Auxiliary Function Method (AFM) is very effective in terms of numerical results which is illustrated in [21]. Our auxiliary function is defined as follows:

$$\begin{aligned} \tilde{\phi}(x, x_k^*, \beta, \alpha) &= f_k^* + (f(x) - f_k^*) \tilde{\chi}_{A_k}(t, \beta) \\ &\quad + \alpha H(\|x - x_k^*\|^2), \end{aligned}$$

where  $\alpha$  and  $\beta$  are real parameters. The function  $\tilde{\chi}_{A_k}(t, \beta)$  is defined by

$$\tilde{\chi}_{A_k}(t, \beta) = \begin{cases} 0, & t > \beta, \\ q(t, \beta), & -\beta \leq t \leq \beta, \\ 1, & t < -\beta, \end{cases}$$

where

$$q(t, \beta) = \frac{1}{4\beta^3} t^3 - \frac{3}{4\beta} t + \frac{1}{2},$$

and the function  $H$  is defined on  $\mathbb{R}_+$  and it satisfies the following properties:

- i.  $H(u) > 0$ ,
- ii.  $H'(u) < 0$ ,
- iii.  $\lim_{u \rightarrow \infty} H(u) = 0$ .

At Step 3 and 4, the feasibility of the solution is checked and the stopping conditions are declared.

In order to guarantee that the algorithm is worked straightly, we prove the following theorems.

**Theorem 2.** Assume that the sequence  $\{x^j\}$  is produced by the Algorithm has a limit point  $x^*$ , then  $x^* \in D_0$ .

**Proof.** Assume  $x^*$  is a limit point of  $\{x^j\}$ . Then there exists set  $J \subset \mathbb{N}$ , such that  $x^j \rightarrow \bar{x}$  for  $j \in J$ . Let us consider the contrary that  $x^* \notin D_0$ , i.e. for sufficiently large  $j \in J$ , there exist  $\delta_0 > 0$  and  $i_0 \in \{1, 2, \dots, m\}$  such that:

**Case 1.**  $g_{i_0}(x^j) \geq \delta_0 \geq \varepsilon > 0$ . Since  $x^j$  is the global minimum according  $j$ -th values of the parameters  $\rho_j, \varepsilon_j$ , for any  $x \in D_0$  we have

$$F(x^j, \rho_j, \varepsilon_j) = f(x^j) + \rho_j \|x^j - x_0\|.$$

If  $j \rightarrow \infty$  then,  $\rho_j \rightarrow \infty$  and  $\rho_j \|x^j - x_0\| \rightarrow \infty$  (since  $x^j \notin D_0$  and  $\|x^j - x_0\| > 0$ ). Thus,  $f(x)$  takes infinite values on  $D_0$  and it contradicts with the boundedness of  $f$  on  $D_0$ .

**Case 2.**  $t = g_{i_0}(x^j) \geq \varepsilon \geq \delta_0 > 0$ . Since  $x^j$  is the global minimum according to  $j$ -th values of the

parameters  $\rho_j, \varepsilon_j$ , for any  $x \in D_0$  we have

$$F(x^j, \rho_j, \varepsilon_j) = f(x^j) + \rho_j \left( \frac{-2}{\varepsilon^3} t^3 + \frac{3}{\varepsilon^2} t^2 \right) \|x^j - x_0\|$$

$$\geq f(x^j) + \rho_j \|x^j - x_0\|.$$

If  $j \rightarrow \infty$  then,  $\rho_j \rightarrow \infty$  and  $\rho_j \|x^j - x_0\| \rightarrow \infty$  (since  $x^j \notin D_0$  and  $\|x^j - x_0\| > 0$ ). Thus,  $f(x)$  takes infinite values on  $D_0$  and it contradicts with the boundedness of  $f$  on  $D_0$ . From the Cases 1 and 2, we obtain the result.  $\square$

**Theorem 3.** Assume that for  $\varepsilon \in (0, \varepsilon_0]$  the set

$$\operatorname{argmin}_{x \in \mathbb{R}^n} F(x, \rho, \varepsilon) \neq \emptyset.$$

Let  $x^j$  is generated by Algorithm when  $\eta N < 1$ . If  $\{x^j\}$  has a limit point, then the limit point of  $x^j$  is the solution for (P).

**Proof.** Let  $x^*$  be a limit point of  $\{x^j\}$ . From Theorem 2, we have  $x^* \in D_0$ . Then, we obtain

$$f(x^*) = F(x^*, \rho, \varepsilon)$$

$$= F(x^*, \rho, 0)$$

$$\leq F(x, \rho, 0)$$

$$= f(x).$$

This completes the proof.  $\square$

### 5. Numerical Examples

In this section, we apply our algorithm to test problems. The proposed algorithm is programmed in Matlab. Numerical results show the efficiency of this method. The detailed results are presented in the tables for all problems. For these tables, we use some symbols in order to abbreviate the expressions. The meanings of these symbols are as follows:

$j$  :The number of iterations,

$x^j$  :the local minimum point of the  $j$ th iteration,

$\varepsilon_j$  :smoothing parameter of the  $j$ th iteration,

$g(x^j)$  :the value of the point  $x^j$  under the constraint functions,

$F(x^j, \rho_j, \varepsilon_j)$  :the value of the point  $x^j$  under  $F$ ,

$f(x^j)$  :the value of the point  $x^j$  under  $f$ .

**Problem 1.** Let us consider the Example in [34]

$$\min f(x) = x_1^2 + x_2^2 - \cos(17x_1) - \cos(17x_2) + 3,$$

s.t.

$$g_1(x) = (x_1 - 2)^2 + x_2^2 \leq 1.6^2,$$

$$g_2(x) = x_1^2 + (x_2 - 3)^2 \leq 2.7^2,$$

$$0 \leq x_1 \leq 2, \quad 0 \leq x_2 \leq 2.$$

We choose  $x^0 = (1, 1)$  as a starting point  $\rho_0 = 10$ ,  $\varepsilon_0 = 0.01$ ,  $\eta_0 = 0.1$  and  $N = 3$ . The results are shown in the Table 1. Considering ( $\hat{P}_\rho$ ) the global minimum is obtained at a point  $x^* = (0.7254, 0.3993)$  with the corresponding value 1.8376. In the paper [34], the obtained global minimum point is  $x^* = (0.72540669, 0.3992805)$  with the corresponding value 1.837623. Our algorithm finds the correct point as in [34].

**Problem 2.** Let us consider the Example in [35]

$$\min f(x) = -x_1 - x_2,$$

s.t.

$$x_2 - 2x_1^4 + 8x_1^3 - 6x_1^2 \leq 2,$$

$$x_2 - 4x_1^4 + 32x_1^3 - 88x_1^2 + 96x_1 \leq 36,$$

$$0 \leq x_1 \leq 3, \quad 0 \leq x_2 \leq 4.$$

We choose  $x^0 = (0, 0)$  as a starting point  $\rho_0 = 10$ ,  $\varepsilon_0 = 0.01$ ,  $\eta_0 = 0.1$  and  $N = 3$ . The results are shown in the Table 2. The global minimum is obtained at a point  $x^* = (2.3295, 3.1783)$  with the corresponding value  $-5.5079$ . In the papers [35, 36], the obtained global minimum point is  $x^* = (2.3289, 3.1883)$  with the corresponding value  $-5.5091$ . Our algorithm find the correct point as in [35, 36].

**Problem 3.** Let us consider the example in [34],

$$\min f(x) = 1000 - x_1^2 - 2x_2^2 - x_3^2 - x_1x_2 - x_1x_3,$$

s.t.

$$g_1(x) = \sum_{i=1}^3 x_i^2 = 25,$$

$$g_2(x) = (x_1 - 5)^2 + \sum_{i=2}^3 x_i^2 = 25,$$

$$g_3(x) = \sum_{i=1}^3 (x_i - 5)^2 \leq 25.$$

We choose  $x^0 = (2, 2, 2)$  as a starting point  $\rho_0 = 10$ ,  $\varepsilon_0 = 0.01$ ,  $\eta_0 = 0.1$  and  $N = 3$ . The results are shown in the Table 3. The global minimum is obtained at a points  $x^* = (2.5000, 4.2196, 0.9721)$  with the corresponding value 944.2157. In the papers [34], the obtained global minimum point is  $x^* = (2.500000, 4.221305, 0.964666)$  with the corresponding value 944.2157. Our algorithm finds the correct solution with the lower iteration numbers in comparison with the algorithm in [34].

**Problem 4.** Consider the example in [36],

$$\min f(x) = -x_1^2 + x_2^2 + x_3^2 - x_1,$$

s.t.

$$g_1(x) = x_1^2 + x_2^2 + x_3^2 \leq 4,$$

$$g_2(x) = \min\{x_2 - x_3, x_3\} \leq 0.$$

We choose  $x^0 = (-1.6, -1, 0.2)$  as a starting point  $\rho_0 = 10$ ,  $\varepsilon_0 = 0.01$ ,  $\eta_0 = 0.1$  and

**Table 1.** Table of minimization process of the Problem 1.

| $j$ | $x^j$            | $\rho_j$ | $\varepsilon_j$ | $g_1(x^j)$ | $g_2(x^j)$    | $F(x^j, \rho_j, \varepsilon_j)$ | $f(x^j)$ |
|-----|------------------|----------|-----------------|------------|---------------|---------------------------------|----------|
| 1   | (0.7249, 0.4007) | 10       | 0.01            | -0.7737    | -0.0083       | 1.8774                          | 1.8522   |
| 2   | (0.7252, 0.3996) | 30       | 0.001           | -0.7753    | -0.0018       | 1.8446                          | 1.8408   |
| 3   | (0.7253, 0.3993) | 90       | 0.0001          | -0.7758    | -0.0003       | 1.8388                          | 1.8382   |
| 4   | (0.7253, 0.3992) | 270      | $1e-05$         | -0.7758    | $-6.2645e-05$ | 1.8378                          | 1.8377   |
| 5   | (0.7253, 0.3992) | 810      | $1e-06$         | -0.7758    | $-1.0667e-05$ | 1.8376                          | 1.8376   |

**Table 2.** Table of minimization process of the Problem 2.

| $j$ | $x^j$            | $\rho_j$ | $\varepsilon_j$ | $g_1(x^j)$ | $g_2(x^j)$ | $F(x^j, \rho_j, \varepsilon_j)$ | $f(x^j)$ |
|-----|------------------|----------|-----------------|------------|------------|---------------------------------|----------|
| 1   | (2.3307, 3.1477) | 10       | 0.01            | 3.9592     | 508.57     | -5.4454                         | -5.4784  |
| 2   | (2.3297, 3.173)  | 30       | 0.001           | 3.9928     | 507.95     | -5.4973                         | -5.5027  |
| 3   | (2.3296, 3.1775) | 90       | 0.0001          | 3.9988     | 507.85     | -5.5062                         | -5.5071  |
| 4   | (2.3295, 3.1783) | 270      | $1e-05$         | 3.9998     | 507.83     | -5.5079                         | -5.5079  |

**Table 3.** Table of minimization process of the Problem 3.

| $j$ | $x^j$                    | $\rho_j$ | $\varepsilon_j$ | $g_1(x^j)$ | $g_2(x^j)$  | $g_3(x^j)$ | $F_p(x^j, \rho_j, \varepsilon_j)$ | $f(x^j)$ |
|-----|--------------------------|----------|-----------------|------------|-------------|------------|-----------------------------------|----------|
| 1   | (2.5002, 4.2214, 0.9650) | 10       | 0.01            | 0.0022     | 0.0001      | -1.864     | 944.4134                          | 944.2108 |
| 2   | (2.5000, 4.2212, 0.9650) | 30       | 0.001           | $7.17e-05$ | $3.26e-06$  | -1.8625    | 944.2756                          | 944.2155 |
| 3   | (2.5000, 4.2212, 0.9650) | 90       | 0.0001          | $1.73e-05$ | $-2.62e-05$ | -1.8625    | 944.2341                          | 944.2156 |
| 4   | (2.5000, 4.2212, 0.9650) | 270      | $1e-05$         | $3.92e-06$ | $-4.27e-06$ | -1.8625    | 944.2157                          | 944.2157 |

**Table 4.** Table of minimization process of the Problem 4.

| $j$ | $x^j$                     | $\rho_j$ | $\varepsilon_j$ | $g_1(x^j)$ | $g_2(x^j)$ | $F(x^j, \rho_j, \varepsilon_j)$ | $f(x^j)$ |
|-----|---------------------------|----------|-----------------|------------|------------|---------------------------------|----------|
| 1   | (1.995, -0.0300, 0.0300)  | 10       | 0.01            | -0.0180    | -0.0601    | -5.9393                         | -5.9733  |
| 2   | (1.9991, -0.0094, 0.0094) | 30       | 0.001           | -0.0033    | -0.0188    | -5.9902                         | -5.9954  |
| 3   | (1.9998, -0.0029, 0.0029) | 90       | 0.0001          | -0.0005    | -0.0058    | -5.9984                         | -5.9992  |
| 4   | (2.0000, -0.0009, 0.0009) | 270      | $1e-05$         | -0.0001    | -0.0018    | -5.9997                         | -5.9999  |
| 5   | (2.0000, -0.0009, 0.0009) | 810      | $1e-06$         | $-1.6e-05$ | -0.0018    | -6.0000                         | -6.0000  |

$N = 3$ . The results are shown in the Table 4. The global minimum is obtained at a point  $x^* = (2, -0.0009, 0.0009)$  with the corresponding value  $-6.0000$ . In the papers [35, 36], the obtained global minimum point is  $x^* = (1.9889, -0.0001, -0.0111)$  with the corresponding value  $-5.9446$ . Our algorithm finds the correct point as in [35, 36].

**Problem 5.** The Rosen-Suzuki problem in [34]

$$\min f(x) = \sum_{i=1}^4 x_i^2 - 5x_1 - 21x_3 + 7x_4,$$

$$\text{s.t. } g_1(x) = 2x_1^2 + \sum_{i=2}^3 x_i^2 + 2x_1 + x_2 + x_4 \leq 5,$$

$$g_2(x) = \sum_{i=1}^4 x_i^2 + x_1 - x_2 + x_3 - x_4 \leq 8,$$

$$g_3(x) = \sum_{i=1}^2 (x_{2i-1}^2 + 2x_{2i}^2) - x_1 - x_4 \leq 10.$$

First, we choose  $x^0 = (0, 0, 0, 0)$ ,  $\rho_0 = 10$ ,  $\varepsilon_0 = 0.01$ ,  $\eta_0 = 0.1$  and  $N = 3$ . The results are shown in the Tables 5. The global minimum is obtained at a point  $x^* = (0.1697, 0.8358, 2.0084, -0.9651)$  with the corresponding value  $-44.2338$ . In the paper [19], the obtained global minimum point is  $x^* = (0.1684621, 0.8539065, 2.000167, -0.9755604)$  with the corresponding value  $-44.23040$ . In [34], the obtained global minimum point is  $x^* = (0.170189, 0.835628, 2.008242, -0.95245)$  with the corresponding value  $-44.2338$ . It can be seen that our algorithm present numerically better result than the algorithm in [34].

**Table 5.** Table of minimization process of the Problem 5.

| $j$ | $x^j$                             | $\rho_j$ | $\varepsilon_j$ | $g_1(x^j)$  | $g_2(x^j)$  | $g_3(x^j)$ | $F(x^j, \rho_j, \varepsilon_j)$ | $f(x^j)$ |
|-----|-----------------------------------|----------|-----------------|-------------|-------------|------------|---------------------------------|----------|
| 1   | (0.1682, 0.8338, 2.0070, -0.9661) | 10       | 0.01            | -0.0161     | -0.0075     | -1.8886    | -44.1675                        | -44.2068 |
| 2   | (0.1694, 0.8351, 2.0083, -0.9651) | 30       | 0.001           | -0.0030     | -0.0017     | -1.885     | -44.2217                        | -44.2281 |
| 3   | (0.1697, 0.8354, 2.0085, -0.9649) | 90       | 0.0001          | -0.0005     | -0.0003     | -1.8839    | -44.2317                        | -44.2328 |
| 4   | (0.1697, 0.8354, 2.0086, -0.9649) | 270      | $1e-05$         | $-9.36e-05$ | $-5.85e-05$ | -1.8837    | -44.2335                        | -44.2337 |
| 5   | (0.1697, 0.8354, 2.0086, -0.9649) | 810      | $1e-06$         | $-5.60e-05$ | $-1.20e-05$ | -1.8837    | -44.2338                        | -44.2338 |

**Problem 6.** Consider the example in [35],

$$\min f(x) = \frac{\pi}{n} [10 \sin^2 \pi x_1 + h(x) + (x_n - 1)^2],$$

$$\text{s.t. } -10 \leq x_i \leq 10 \quad i = 1, 2, \dots, n,$$

where  $h(x) = \sum_{i=1}^{n-1} [(x_i - 1)^2(1 + 10 \sin^2 \pi x_{i+1})]$ . For  $n = 3, 5, 7$  we choose  $x^0 = (6, 6, \dots, 6)$  as a starting point  $\rho_0 = 10$ ,  $\varepsilon_0 = 0.01$ ,  $\eta_0 = 0.1$  and  $N = 3$ . The results are shown in the Table 6. The global minimum is obtained at a point  $x^* = (1, 1, \dots, 1)$  with the corresponding value 0. In the paper [35], the obtained global minimum point is  $x^* = (1, 1, \dots, 1)$  with the corresponding value 0. Our algorithm finds the correct point as in [35].

**Problem 7.** Let us consider the Example in [34]

$$\min f(x) = 10x_2 + 2x_3 + x_4 + 3x_3 + 4x_6,$$

$$\text{s.t. } g_1(x) = x_1 + x_2 = 10,$$

$$g_2(x) = -x_1 + x_3 + x_4 + x_5 = 0,$$

$$g_3(x) = -x_2 - x_3 + x_5 + x_6 = 0,$$

$$g_4(x) = 10x_1 - 2x_3 + 3x_4 - 2x_5 \leq 16,$$

$$g_5(x) = x_1 + 4x_3 + x_5 \leq 10,$$

$$0 \leq x_1 \leq 12, \quad 0 \leq x_2 \leq 18,$$

$$0 \leq x_3 \leq 5, \quad 0 \leq x_4 \leq 12,$$

$$0 \leq x_5 \leq 1, \quad 0 \leq x_6 \leq 16.$$

We choose  $x^0 = (0, 0, \dots, 0)$  as a starting point  $\rho_0 = 10$ ,  $\varepsilon_0 = 0.01$ ,  $\eta_0 = 0.1$  and  $N = 4$  for the Algorithm. The results are shown in the Table 7. In [34], in which three algorithms are offered for a new smoothing technique, approximate solution is found with 4, 3 and 13 iterations in the Algorithms I, II and III, respectively. Note that the solution is not found in Algorithm II of [34]. Whereas, an approximate solution is found with 4 iterations in our Algorithm.

## 6. Conclusion

In this study, we propose a new exact penalty function and a new algorithm for continuous constrained optimization. By considering this new penalty function approach, we construct a new minimization algorithm. We apply the algorithm on test problems and obtain satisfactory results.

We also propose a new smoothing approach for non-smooth penalty functions and it provides good approximations to the non-smooth penalty functions. Moreover, it is easy applicable and has easy formulation.

The results convince that the Algorithm can be used for large scale optimization problems. By applying the minimization algorithm, the optimum value is found rapidly and the algorithm presents high accuracy in finding the optimum point. We use the auxiliary function method in the algorithm as a global optimization method but anyone can use any other algorithms such as DIRECT [38], Kriging-based techniques [39] or heuristic algorithms [40, 41].

## References

- [1] Ling, B.W.K., Wu, C.Z., Teo, K.L. & Rehbock, V. (2013). Global optimal design of IIR filters via constraint transcription and filled function methods. *Circuits, Systems, and Signal Processing*, 32, 1313–1334.
- [2] Evirgen, F. (2016). Analyze the optimal solutions of optimization problems by means of fractional gradient based system using VIM. *An International Journal of Optimization and Control: Theories & Applications (IJOCTA)*. 6(2), 75–83.
- [3] Akteke-Ozkurt, B., Weber, G.W. and Koksal, G. (2017). Optimization of generalized desirability functions under model uncertainty. *Optimization*, 66(12), 2157–2169.
- [4] Ozmen, A., Kropat, E. & Weber, G.W. (2017). Robust optimization in spline regression models for multi-model regulatory networks under polyhedral uncertainty. *Optimization*, 66 (12), 2135–2155.
- [5] Nocedal, J. and Wright, S.J. (2006). *Numerical Optimization*. 2nd Edition, Springer, New York.
- [6] Di Pillo, G. & Grippo, L. (1989). Exact penalty functions in constrained optimization, *SIAM Journal on Control and Optimization*, 27(6), 1333–1360.
- [7] Zheng, F.Y. & Zhang, L.S. (2012). New simple exact penalty function for constrained

**Table 6.** Table of minimization process of the Problem 6.

| $n$ | $j$ | $x^j$                         | $\rho_j$ | $\varepsilon_j$ | $F(x^j, \rho_j, \varepsilon_j)$ | $f(x^j)$       |
|-----|-----|-------------------------------|----------|-----------------|---------------------------------|----------------|
| 3   | 1   | (1.0000, 1.0000, 1.0000)      | 10       | 0.01            | $5.8448e - 13$                  | $5.8448e - 13$ |
|     | 2   | (1.0000, 1.0000, 1.0000)      | 30       | 0.001           | $5.7929e - 13$                  | $5.7929e - 13$ |
| 5   | 1   | (1.0000, 1.0000, ..., 1.0000) | 10       | 0.01            | $1.6646e - 12$                  | $1.6646e - 12$ |
|     | 2   | (1.0000, 1.0000, ..., 1.0000) | 30       | 0.001           | $1.4643e - 12$                  | $1.4643e - 12$ |
| 7   | 1   | (1.0000, 1.0000, ..., 1.0000) | 10       | 0.01            | $2.5965e - 14$                  | $2.5965e - 14$ |
|     | 2   | (1.0000, 1.0000, ..., 1.0000) | 30       | 0.001           | $1.1379e - 15$                  | $1.1379e - 15$ |

**Table 7.** Table of minimization process of the Problem 7.

| $j$ | $x^j$  | $\rho_j$ | $\varepsilon_j$ | $g_1(x^j)$    | $g_2(x^j)$    | $g_3(x^j)$    | $g_4(x^j)$ | $g_5(x^j)$ | $F(x^j, \rho_j, \varepsilon_j)$ | $f(x^j)$ |
|-----|--|----------|-----------------|---------------|---------------|---------------|------------|------------|---------------------------------|----------|
| 1   | (1.9216, 8.0745, 0.7949, 0.1248, 1.0020, 7.8680) | 40       | 0.001           | -0.0039       | $-5.33e - 07$ | 0.0006        | -0.0032    | -3.8969    | 117.2736                        | 116.9372 |
| 2   | (1.9208, 8.0792, 0.7945, 0.1265, 0.9998, 7.8739) | 160      | 0.0001          | $-8.99e - 06$ | $-2.56e - 06$ | $-2.57e - 06$ | -0.0007    | -3.9015    | 117.0525                        | 117.0021 |
| 3   | (1.9208, 8.0792, 0.7945, 0.1265, 0.9998, 7.8739) | 640      | $1e - 05$       | $-3.71e - 07$ | $-2.49e - 07$ | $-1.76e - 07$ | -0.0006    | -3.9015    | 117.0215                        | 117.0022 |
| 4   | (1.9208, 8.0792, 0.7945, 0.1265, 0.9998, 7.8739) | 2560     | $1e - 06$       | $-3.05e - 07$ | $2.79e - 08$  | $5.72e - 09$  | -0.0006    | -3.9015    | 117.0100                        | 117.0022 |

optimization. *Applied Mathematics and Mechanics*, 33(7), 951–962.

- [8] Rao, S.S. (2009). *Engineering Optimization: Theory and Practice*. 4th Edition, John Wiley & Sons, New Jersey.
- [9] Zangwill, W.I. (1967). Nonlinear programming via penalty functions. *Management Science*, 13, 344–358.
- [10] Bertsekas, D. (1975). Nondifferentiable optimization via approximation. *Mathematical Programming Study*, 3, 1–25.
- [11] Chen, C., & Mangasarian, O.L. (1996). A class of smoothing functions for nonlinear and mixed complementarity problem. *Computational Optimization and Applications*, 5, 97–138.
- [12] Xavier, A.E. (2010). The hyperbolic smoothing clustering method. *Pattern Recognition*, 43, 731–737.
- [13] Chen, X. (2012). Smoothing methods for nonsmooth, nonconvex minimization. *Mathematical Programming Ser. B*, 134 71–99.
- [14] Grossmann, C. (2016). Smoothing techniques for exact penalty function methods. *Contemporary Mathematics*, 658, 249–265.
- [15] Zang, I. (1980). A smoothing out technique for min-max optimization. *Mathematical Programming*, 19, 61–77.
- [16] Bagirov, A.M., Nuamiat, A. Al & Sultanova, N. (2013). Hyperbolic smoothing functions for non-smooth minimization. *Optimization*, 62(6), 759–782.
- [17] Pinar, M.C. & Zenios, S. (1994). On smoothing exact penalty functions for convex constrained optimization. *SIAM Journal of Optimization*, 4, 468–511.
- [18] Meng, Z., Dang, C., Jiang, M. & Shen R. (2011). A smoothing objective penalty function algorithm for inequality constrained optimization problems. *Journal Numerical Functional Analysis and Optimization*, 32, 806–820.
- [19] Lian, S.J. (2012). Smoothing approximation to  $l_1$  exact penalty for inequality constrained optimization. *Applied Mathematics and Computation*, 219, 3113–3121 (2012).
- [20] Sahiner, A., Kapusuz, G. & Yilmaz, N. (2016). A new smoothing approach to exact penalty functions for inequality constrained optimization problems. *Numerical Algebra, Control and Optimization*, 6(2), 161–173.
- [21] Sahiner, A., Yilmaz, N. & Kapusuz, G. (2019). A novel modeling and smoothing technique in global optimization. *Journal of Industrial and Management Optimization*, 15 (1), 113–139.
- [22] Lin, H., Wang, Y., Gao, Y. & Wang, X. (2018). A filled function method for global optimization with inequality constraints. *Computational and Applied Mathematics*, 37(2), 1524–1536.
- [23] Horst, R. & Pardalos, P.M. (eds.). (1995). *Handbook of Global Optimization*. Kluwer Academic Publishers, Dordrecht.
- [24] Locatelli, M. & Schoen, F. (2013). *Global Optimization: Theory, Algorithms, and Applications*. SIAM, Philadelphia.
- [25] Sergeyev, Y.D., Strongin, R.G. & Lera, D. (2013). *Introduction to Global Optimization Exploiting Space-Filling Curves*. Springer, New York.
- [26] Zhigljavsky, A. & Zilinskas, A. (2008). *Stochastic Global Optimization*, Springer, New York.
- [27] Levy, A.V. & Montalvo, A. (1985). The tunneling algorithm for the global minimization

- of functions. *SIAM Journal on Scientific and Statistical Computing*, 6 (2), 15–29.
- [28] Ge, R.P. (1990). A filled function method for finding global minimizer of a function of several variables. *Mathematical Programming*, 46, 191–204.
- [29] Zhang, L.-S., Ng, C.-K., Li, D. & Tian, W.-W. (2004). A new filled function method for global optimization. *Journal of Global Optimization*, 28, 17–43.
- [30] Ng, C.K., Li, D. & Zhang, L.S. (2010). Global descent method for global optimization. *SIAM Journal of Optimization*, 20(6), 3161–3184.
- [31] Wang, Y., Fang, W. & Wu, T. (2009). A cut-peak function method for global optimization. *Journal of Computational and Applied Mathematics*, 230, 135–142.
- [32] Liu, J., Zhang, S., Wu, C., Liang, J., Wang, X. & Teo, K.L. (2016). A hybrid approach to constrained global optimization. *Applied Soft Computing*, 47, 281–294.
- [33] Sahiner, A., Yilmaz, N. & Kapusuz, G. (2017). A descent global optimization method based on smoothing techniques via Bezier curves. *Carpathian Journal of Mathematics*, 33(3), 373–380.
- [34] Xu, X., Meng, Z., Sun, J. & Shen, R. (2011). A penalty function method based on smoothing lower order penalty function. *Journal of Computational and Applied Mathematics*, 235, 4047–4058.
- [35] Zhang, Y., Xu, Y. & Zhang, L. (2009). A filled function method applied to nonsmooth constrained global optimization. *Journal of Computational and Applied Mathematics*, 232, 415–426.
- [36] Wu, Z.Y., Bai, F.S., Lee, H.W.J. & Yang, Y.J. (2007). A filled function method for constrained global optimization. *Journal of Global Optimization*, 39, 495–507.
- [37] Gao, Y., Yang, Y. & You, M. (2015). A new filled function method for global optimization. *Applied Mathematics and Computation*, 268, 685–695.
- [38] Jones, D.R., Perttunen, C.D. & Stuckman, B.E. (1993). Lipschitzian optimization without the Lipschitz constant. *Journal of Optimization Theory and Applications*, 79, 157–181.
- [39] Jones, D.R., Schonlau, M. & Welch, W.J. (1998). Efficient global optimization of expensive black-box functions. *Journal of Global Optimization*, 13, 455–492.
- [40] Kirkpatrick, S., Gelatt, C.D. & Vecchi, P.M. (1983). Optimization by simulated annealing. *Science*, 220, 671–680.
- [41] Kennedy, J. & Eberhart, R. (1997). Particle swarm optimization. *IEEE International Conference on Neural Networks*, 1, 1942–1948.

**Nurullah Yilmaz** is worked as Dr. Research Assistant at Suleyman Demirel University, Isparta. His research interests are functional analysis and non-linear optimization.

**Ahmet Sahiner** is presently employed as Full Professor at Suleyman Demirel University, Isparta. His research interests are functional analysis, global optimization and approximation theory.



## RESEARCH ARTICLE

## Analysis of boride layer thickness of borided AISI 430 by response surface methodology

Turker Turkoglu\*  and Irfan Ay 

<sup>a</sup> Department of Mechanical Engineering, Balikesir University, Turkey  
 turker.turkoglu@balikesir.edu.tr, ay@balikesir.edu.tr

## ARTICLE INFO

## Article history:

Received: 7 August 2018

Accepted: 2 April 2019

Available Online: 23 April 2019

## Keywords:

Boriding process

Optimization

Response surface methodology

Stainless Steel

AMS Classification 2010:

62Kxx, 62K20, 74N15

## ABSTRACT

The boriding process is a thermochemical surface treatment which can be applied to many iron and non-ferrous materials and improves the properties of the material such as hardness, wear resistance. In the present study, the layer thickness values of the boronized AISI 430 material were optimized using the Response Surface Methodology. Mathematical model was constructed using parameters such as temperature and time and the results were analyzed comparatively. As a result of the analysis, the optimum layer thickness value for AISI 430 material was obtained as 39.0183  $\mu\text{m}$  for 1000  $^{\circ}\text{C}$  and 5.9h and it was determined that the boriding temperature and time are effective on the boride layer formation process of AISI 430 material. Finally, the Response Surface Methodology and Face Centered Central Composite Design have been effectively applied to the boriding process.



### 1. Introduction

Surface treatments are applied to overcome the problems of exposed materials such as corrosion, abrasion, oxidation [1-2]. The surface properties of machine elements and tools can be improved by diffusing the atoms of various materials. Carbonization, nitriding, chroming and boriding processes are diffusion methods used to improve the surface properties of materials [3].

Boriding is one of the most well-known thermochemical surface hardening processes that provide features such as high surface hardness, corrosion and abrasion resistance [4-6]. Approximately in 800 – 1100  $^{\circ}\text{C}$ , process is applied for 2 - 8 hours [7]. Boriding can be applied to materials using various methods, such as solid, liquid, and gas [8]. The solid boronizing method used in the study is a simple and economical method compared to other methods. AISI 430 Stainless Steel materials are used in a variety of industries. AISI 430 is especially used in the automotive industry for machine parts such as exhaust manifolds, turbochargers and catalytic converters [9]. Optimization studies of the boriding process are limited in the literature [10-13].

Genel et al. [10] studied that the boride layer properties of the boronized AISI W1 material by solid boronizing method were modeled mathematically by Artificial Neural Networks (ANN) and the boride layer thickness was estimated to be approximately 95%. They concluded that borided layer thickness increases with boriding time for each process temperature. Besides, they found that surface hardness of layer increased approximately 6 times compared to non-borided material.

Arguellas - Ojeda et al. [11] investigated the hardness of ASTM F-75 alloy, which borided by paste method. They performed process optimization through Response Surface Methodology (RSM) and determined the model effects of process factors. They developed response surface equation to analyze the effect of values on borided layer hardness. Developed model showed that processing temperature has significant whereas processing time has no significant effect on the boride surface hardness. Under these conditions, they determined that maximum hardness value can be obtained by RSM.

Chen et al. [12] reported that they optimized boride layer depths of the boronized Cr12MoV material by Response Surface Methodology. As a result of obtained values, they determined that the depth of the boride layer increased with the increasing temperature in the process and applied heat treatment processes such as quenching and tempering to investigate their impact on wear resistance.

Kayalı et al. [13] applied boriding process in three different temperature and time parameters using box boriding method to AISI 52100 material. Afterward, they analyzed the wear behaviors of the boronized AISI 52100 material by the Taguchi Method and determined the optimum parameters. According to Taguchi Analysis, the most effective parameter was boriding temperature and wear resistance of AISI 52100 increased as the boriding temperature and time increases. Besides, they found wear load and sliding rate effect on surface wear resistance as the second and third effective parameter.

In order to obtain boride layer thickness, the process parameters must be selected appropriately. In this study; the layer thicknesses of the boronized AISI 430 material were optimized through the Face Centered Central Composite Design (FCCD) using the Response Surface Method. Due to the fact that it is difficult to apply the AISI 430 containing high alloy elements, the thickness of boride layer has been maximized by using RSM. In the RSM model, temperature and time were determined as input, and layer thicknesses were determined as output. The parameters affecting the model and the results are given comparatively. In light of this study, appropriate technique can be determined and used in industrial applications in comparison with other optimization techniques for boriding heat treatment. Besides, the effect of heat treatment such as boriding, chromizing and nitriding on the mechanical properties of material can be optimized by using RSM. Due to the high cost of heat treatment applications, the importance of process optimization is high. The high temperature and process materials required for the boriding process make the optimization work inevitable



**Figure 1.** Heat treatment furnace where boriding process is performed.

## 2. Experimental work

### 2.1. Boriding process conditions

The AISI 430 test specimens to be used in the work were cut to a diameter of 20 x 20 mm and made ready for boriding. The method chosen for the boriding process is the box boriding method. After filling the supplied  $B_4C + SiC + KBF_4$  powders into the stainless steel box, the metallographically prepared samples were embedded in the  $(B_4C + SiC + KBF_4)$  powders.

The boriding process was carried out in the electric controlled furnace by increasing gradually to the temperatures determined in 2-4-6 hours at 850-925-1000°C temperatures.

Subsequently, the samples removed from the furnace were left to cool down in the air. Finally, AISI 430 samples were ground to the 1200 grid level by SiC paper and polished, then made ready for optical microstructural examination using (100ml ethanol + 5ml HCl + 1g picric acid) etching. Layer thicknesses of boronized AISI 430 materials were measured with a Leica Optical Microscope by the aid of a microscope-assembled tool.

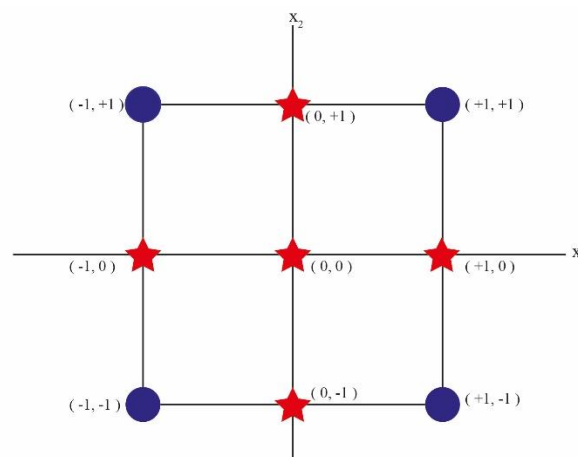


**Figure 2.** Central composite design for Face Centered Central Composite Model (FCCD).

**Table 1.** Coded and uncoded level of factors.

| Factors            | Coded and Uncoded Levels |            |           |
|--------------------|--------------------------|------------|-----------|
|                    | -1 (Low)                 | 0 (Medium) | +1 (High) |
| Temperature ( °C ) | 850 °C                   | 925°C      | 1000°C    |
| Time ( Hour )      | 2h                       | 4h         | 6h        |

## 2.2. Statistical design of borided AISI 430 by response surface methodology

In this study, the layer thicknesses of boronized AISI 430 were statistically examined by using FCCD. The FCCD consists of axial points located on the cube five-sided surface. Central Composite Design (CCD) is used to develop experimental design in RSM [14-17]. The interaction between the inputs and the experimental variables were examined and the statistical results were presented comparatively. Compared to other optimization techniques such as Taguchi Method, the RSM gives optimum results with decimal system of factor levels, while in Taguchi analysis, the best combination can be obtained for given factors [18].

In the work, three levels were chosen for the factors used as input when creating the experimental design. These values were coded as -1, 0, +1. The factors used in the experimental design and the coded levels are shown in Table 1. The MINITAB 16 package program was used to determine the results of the mathematical models of the experimental design. Graphs of the results obtained from the program were also obtained through the MINITAB 16 package software.

## 3. Results and discussion

Layer thicknesses of boronized AISI 430 stainless steel were modeled mathematically using the FCCD method at three different temperatures and at three different time durations.

Equation 1 describes the mathematical model on the results (Y) of the relevant factors used in the design of the experiment.

$$Y = \beta_0 + \sum_{i=1}^n \beta_i X_i + \sum_{i=1}^n \beta_{ii} X_i^2 + \sum_{i=1}^n \beta_{ij} X_i X_j + e \quad (1)$$

According to Eq. (1); Y value is defined as the response value, and  $x_i$  and  $x_j$  are the coded values of the factors.

$\beta_0$ ,  $\beta_i$ ,  $\beta_{ii}$ ,  $\beta_{ij}$ , represent the regression coefficient, i and j are the linear and quadratic coefficients, respectively. e is the residual experimental error.

ANOVA (Analysis of Variance) was performed to show the significance and interaction of the factors used in the mathematical model.

The statistical analysis results are shown in Table 2 and Table 3.

**Table 2.** Face centered composite design of two factors for coded, uncoded and response ( boride layer thickness ).

| No. | Coded Values |    | Uncoded Values     |               | Boride Thickness |
|-----|--------------|----|--------------------|---------------|------------------|
|     | T            | t  | Temperature ( °C ) | Time ( Hour ) | Y ( μm )         |
| 1   | -1           | -1 | 850                | 2             | 10               |
| 2   | 1            | -1 | 1000               | 2             | 21               |
| 3   | -1           | +1 | 850                | 6             | 17               |
| 4   | +1           | +1 | 1000               | 6             | 38               |
| 5   | -1           | 0  | 850                | 4             | 12               |
| 6   | +1           | 0  | 1000               | 4             | 32               |
| 7   | 0            | -1 | 925                | 2             | 19               |
| 8   | 0            | +1 | 925                | 6             | 33               |
| 9   | 0            | 0  | 925                | 4             | 25               |
| 10  | 0            | 0  | 925                | 4             | 26               |
| 11  | 0            | 0  | 925                | 4             | 26               |
| 12  | 0            | 0  | 925                | 4             | 25               |
| 13  | 0            | 0  | 925                | 4             | 27               |

$$Y, \text{ Response (Boride Layer Thickness)} = 25.2069 + 8.6667T + 6.3333t - 4.1379T^2 - 0.1379t^2 + 2.500Tt \quad (2)$$

**Table 3.** Analysis of variance for boride layer thickness.

| Source         | Sum of Squares | Degrees of Freedom | Mean Square | F      | p - value |
|----------------|----------------|--------------------|-------------|--------|-----------|
| Regression     | 773.118        | 5                  | 154.624     | 110.39 | 0.000     |
| Linear         | 691.333        | 2                  | 345.667     | 246.79 | 0.000     |
| T              | 450.667        | 1                  | 450.667     | 321.75 | 0.000     |
| t              | 240.667        | 1                  | 240.667     | 171.82 | 0.000     |
| Square         | 56.785         | 2                  | 56.785      | 20.27  | 0.001     |
| T x T          | 56.733         | 1                  | 47.291      | 33.76  | 0.001     |
| t x t          | 0.053          | 1                  | 0.053       | 0.04   | 0.852     |
| Interaction    | 25.000         | 1                  | 25.000      | 17.85  | 0.004     |
| T x t          | 25.000         | 1                  | 25.000      | 17.85  | 0.004     |
| Residual Error | 9.805          | 7                  | 1.401       |        |           |
| Lack of Fit    | 7.005          | 3                  | 2.335       | 3.34   | 0.137     |
| Total          | 782.923        | 12                 |             |        |           |

R-Sq = 98.75%, R-Sq (pred.) = 90.51%, R-Sq (adj.)= 97.85

As a result of statistical analyzes;  $R^2$  (coefficient of determinant) and  $R^2$ -adj (adjusted  $R^2$  value) were found to be 98.75 and 97.85, respectively.  $R^2$  (coefficient of determination) indicates that 98.75% of the model is affected from mathematical model whereas,  $R^2$ -adj (adjusted  $R^2$  value) is the value that is calculated after subtracting insignificant values from the mathematical model. If the p value obtained from the ANOVA is less than 0.05, the model for that parameter is significant.

When Table 3 is examined, the p values are important for the main factors. In other words, all the main factors are important for the layer thickness of the boronized AISI 430 material.

In mathematical model, Temperature (T), Time (t), [Temperature (T) x Temperature (T)], [Temperature (T) x Time (t)] is significant, while [Time (t) x Time (t)] is insignificant.

Equation 2 represents the mathematical model which was developed for the boride layer thickness (Y) of boronized AISI 430 material.

In order to reveal the effect of the factors on the results, 3D and 2D interaction graphs were created using the MINITAB 16 package software.

Contour plots for the interaction effects of factors (time and temperature) as 2D and 3D are given in Figure 3.a. and Figure 3.b. Figure 3.a. and Figure 3.b. show that the temperature (T) and time (t) factors have a positive effect on the boride layer. It is also reported in the previous boriding studies that the temperature and time parameters are effective on the formation of the boride layer and the increase in the layer thickness is generally accompanied by increasing temperature and time [1,5].

The correlation graph of the experimental and predicted results is shown in Figure 5. In Figure 5, it is clearly shown that experimental values and predicted values are close to line. This case indicates high correlation between the values.

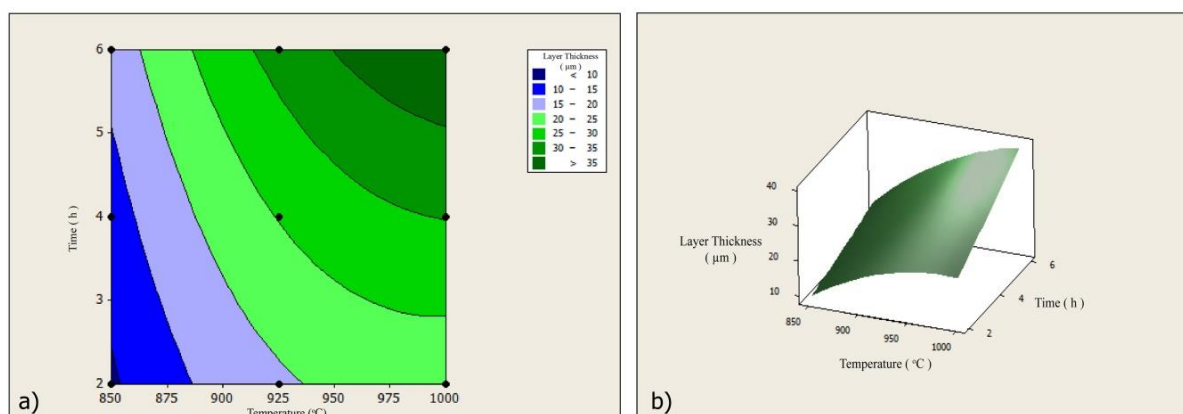


**Figure 3.** a) Contour plot for borided layer thickness. b) Response surface plot for borided layer thickness.

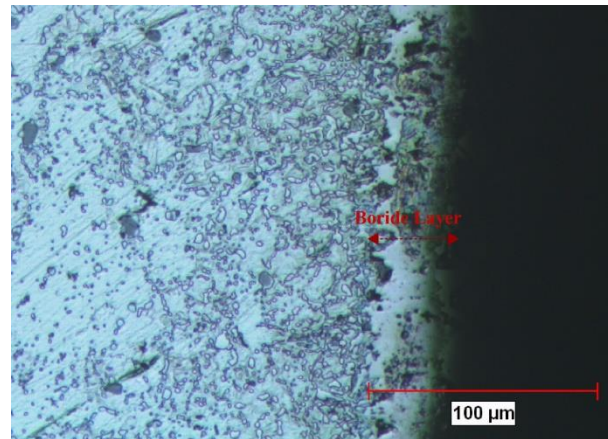


**Figure 4.** Optical microstructure image of borided AISI 430 material.

Furthermore, it has been stated in literature [19-21] that the boride layer thickness value of the target material during the boronizing process may vary according to the boron source content and the alloy content of the target material as well as the temperature and time.

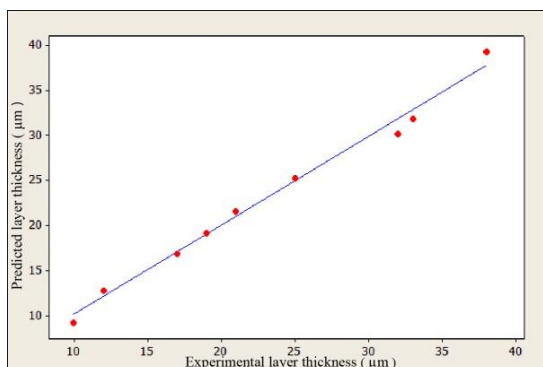


**Figure 5.** The correlation graph of the experimental and predicted results.

Optical microstructure images of boronized AISI 430 are given in Figure 4. According to Figure 4; the boride layer of the boronized AISI 430 material was found to be a planar structure. As seen in Figure 4, there is no porosity or discontinuity in the boride layer morphology. The cause of this condition is considered to be made of properly the boriding process. When the values of layer thicknesses of boronized AISI 430 were examined, it was determined that the layer thickness values increased parabolically as the temperature and time increased.

#### 4. Conclusion

In this study, it has been showed that the RSM Method can be effectively applied to the boriding process of AISI 430 material.

Layer thickness values of boronized AISI 430 material

using box boriding method have been experimentally successfully designed using temperature and time parameters by FCCD.

As the result of ANOVA analysis;  $R^2$  and  $R^2$  (adj) values of 98.75 and 97.85 were found.

Except for the factor (t x t) (p value: 0.852), all the main factors in the mathematical model for the layer thickness of the boronized AISI 430 are significant.

According to analysis results; optimum conditions for the boride layer thickness of AISI 430 were obtained at 1000 °C and 5.9 hours, respectively.

According to the results of this input, the optimum value of the boride layer thickness is 39.0183 μm.

Consequently, the generated mathematical model has proven to be able to explain the boriding process at a high rate.

Because of the costly surface treatment methods such as the boriding process, successful implementation of the optimization operation is thought to be a significant contribution to cost and time.

#### References

- [1] Campos, I., Ramirez, G., Figueroa, U., Martinez, J., & Morales, O. (2007). Evaluation of boron mobility on the phases FeB, Fe<sub>2</sub>B, and diffusion zone in AISI 1045 and M2 steels. *Applied Surface Science*, 253, 3469-3475.
- [2] Lee, S.Y., Kim, G.S., & Kim, B.S. (2004). Mechanical properties of duplex layer formed on AISI 403 stainless steel by chromizing and boronizing treatment. *Surface & Coatings Technology*, 177, 178-184.
- [3] Krelling, A.P., da Costa, C.E., Milan, J.C.G., & Almeida, E.A.S. (2017). Micro-abrasive wear mechanisms of borided AISI 1020 steel. *Tribology International*, 111, 234-242.
- [4] ASM Handbook. (1995). *Heat Treating*. ASM International Handbook Committee, Ohio.

- [5] Angkurarach, L., & Juijerm, P. (2012). Effects of direct current field on powder-packet boriding process on martensitic stainless steel AISI 420. *Archives of Metallurgy and Materials*, 57(3), 799-804.
- [6] Balusamy, T., Narayanan, T.S.N.S., Ravichandran K., Song Park, Il., & Lee, M.H. (2013). Effect of surface mechanical attrition treatment (SMAT) on pack boronizing of AISI 304 stainless steel. *Surface & Coating Technology*, 232, 60-67.
- [7] Carrera-Espinoza, R., Figueroa-Lopez, U., Martinez-Trinidad, J., Campos-Silva, I., Hernandez-Sanchez, E., & Motallebzadeh, A. (2016). Tribological behavior of borided AISI 1018 steel under linear reciprocating sliding conditions. *Wear*, 362-363, 1-7.
- [8] Gunen, A. (2017). Characterization of borided Inconel 625 alloy with different boron chemicals. *Pamukkale University Journal of Engineering Sciences*, 23(4), 411-416.
- [9] Turkoglu, T. (2017). *Investigation of properties hardness, corrosion resistance and microstructure on the boronized AISI 304, AISI 420 and AISI 430 stainless steels*. MSc Thesis. Balikesir University.
- [10] Genel, K., Ozbek, I., Kurt, A., & Bindal, C. (2002). Boriding response of AISI W1 steel and use of artificial neural network for prediction of borided layer properties. *Surface & Coatings Technology*, 160, 38-43.
- [11] Arguellas – Ojeda, J.L., Marquez – Herrera, A., Robles, A.S., & Angel, C.R.M. (2017). Hardness optimization of boride diffusion layer on ASTM F-75 alloy using response surface methodology. *Revista Mexicana de Fisica*, 63, 76-81.
- [12] Chen J., Yang A., & Hao, S. (2011). Optimization of Cr12MoV steel boronizing technology. *Advanced Materials Research*, 216, 687-691.
- [13] Kayali, Y., Gokce, B., & Colak, F. (2013). Analysis of wear behavior of borided AISI 52100 steel with the Taguchi method. *Journal of the Balkan Tribological Association*, 19(3), 365-376.
- [14] Diler, E.A., & Ipek, R. (2012). An experimental and statistical study of interaction effects of matrix particle size, reinforcement particle size and volume fraction on the flexural strength of Al-SiC<sub>p</sub> composites by P/M using central composite design. *Materials Science and Engineering A*, 548, 43-55.
- [15] Montgomery, D.C. (2012). *Design and Analysis of Experiments*. Wiley, U.S.A.
- [16] Eriksson, L., Johansson, E., Kettenah-Wold, N., Wikström, C., & Wold, S. (2008). *Design of Experiments*. Umetrics, Sweden.
- [17] Myers, R.H., Montgomery, D.C., & Cook, C.M.A. (2009). *Response Surface Methodology Process and Product Optimization Using Designed Experiments*. Wiley, USA.
- [18] Celik, S., Karaoglan, A.D., & Ersozlu, I. (2015). An effective approach based on response surface methodology for predicting friction welding parameters. *High Temperature Materials and Processes*, 35(3), 235-242.
- [19] Carbuicchio, M. (1987). Effects of alloying elements on the growth of iron boride coatings. *Journal of Materials Science Letters*, 6, 1147-1149.
- [20] Kayali, Y. (2015). Investigation of diffusion kinetics of borided AISI P20 steel in micro-wave furnace. *Vacuum*, 121, 129-134.
- [21] Mathew, M., & Rajendrakumar, P.K. (2014). Effect of precarburation on growth kinetics and mechanical properties of borided low-carbon steel. *Materials and Manufacturing Processes*, 29(9), 1073-1084.

**Turker Turkoglu** received the Bachelor Degree from Kocaeli University, Turkey in 2014. He obtained MSc Degree in Mechanical Engineering from Balikesir University, Turkey in 2017. Since 2017, he has pursued PhD education in Mechanical Engineering from Balikesir University, Turkey. He is working as Research Assistant at Mechanical Engineering Department, Balikesir University, Turkey. His main research interest is Material Science, Manufacturing Processes, Surface Treatments.

**Irfan Ay** is a professor at the Department of Mechanical Engineering in Balikesir University, Balikesir, Turkey. He received his PhD degree in Mechanical Engineering, Dokuz Eylul University, Izmir, Turkey. He has many research papers about Welding, Composite Materials, Fracture and Failure of Materials.



## RESEARCH ARTICLE

## An application of fuzzy linear modeling: prediction of uncertainty for beta-glucan content

Özlem Türkşen<sup>a</sup> , Suna Ertunç<sup>b\*</sup> 

<sup>a</sup> Department of Statistics, Ankara University, Turkey

<sup>b</sup> Department of Chemical Engineering, Ankara University, Turkey

[turksen@ankara.edu.tr](mailto:turksen@ankara.edu.tr), [ertunc@eng.ankara.edu.tr](mailto:ertunc@eng.ankara.edu.tr)

## ARTICLE INFO

## Article history:

Received: 5 August 2018

Accepted: 4 April 2019

Available Online: 2 May 2019

## Keywords:

Beta-Glucan

Yeast

Fuzzy Least Squares

Triangular Type-1 Fuzzy Numbers

Interval Estimation

AMS Classification 2010:

90C29, 90C70, 92E99

## ABSTRACT

Beta-glucan (BG) has positive health effects for the mammals. However, the BG sources have limited content of it. Besides, the production of the BG has stringent procedures with low productivity. Economical production of the BG needs the improvement of the BG production steps. In this study, it is aimed to improve the BG content during the first step of the BG production, microorganism growth step, by obtaining the optimal values of additive materials (EDTA, CaCl<sub>2</sub> and Sorbitol). For this purpose, the experimental data sets with replicated response measures (RRM) are obtained at specific levels of EDTA, CaCl<sub>2</sub> and Sorbitol. Fuzzy modeling, a flexible modeling approach, is applied on the experimental data set because of the small sized data set and difficulty of satisfying probabilistic modeling assumptions. The predicted fuzzy function is obtained according to the fuzzy least squares approach. In order to get the optimal values of EDTA, CaCl<sub>2</sub> and Sorbitol, the predicted fuzzy function is maximized based on multi-objective optimization (MOO) approach. By using the optimal values of EDTA, CaCl<sub>2</sub> and Sorbitol, the uncertainty for predicted BG content is evaluated from the economic perspective.



### 1. Introduction

Beta glucan (BG) is an active ingredient which was approved by FDA (Food Drug Administration) in USA and EFSA in Europe (European Food Safety Administration) due to its positive effects on health. The BG has potential application in medicine and pharmacy, food, cosmetic and chemical industries, in feed production and veterinary medicine [1-4]. Production of the BG from different sources such as yeast, fungi, bacteria, and cereals is possible by extraction, isolation and purification technologies. Among these sources yeasts are the most used in industrial production because they have plentiful of BG about 8-16 %. Yeast cell wall contains the glucans, mannoproteins and chitin. Economically production of the BG from the yeast cell wall is depend on both the microbial growth and the extraction conditions. Growth conditions influence the morphology and composition of the cell wall during growth process.

Major factors, which affect the yeast cell wall composition, include yeast strain [5], growth conditions [6, 7] and the time of harvesting [8, 9]. Extraction of BG from yeast generally consists of two main steps: (i) yeast cell lysis (separation of cell wall from

cytoplasm) and, (ii) BG extraction (extraction from insoluble cell wall) [10]. Several studies reported about chemical [11-13], physical [14, 15] and enzymatic lysis [16] of yeast cells. There are lots of medicinal studies about the health effects of the BG however there is still necessity of researches to enhance the BG content.

In many real life problems, e.g. engineering, health, business, economics, the researchers aim to obtain mathematical models of the problems. For this purpose, functional relationship between input (factor, independent) variable/variables and response (output, dependent) variable/variables is wanted to be defined. Generally, statistical regression analysis is considered as a basic modeling tool to define the analytical relationship between the variables [17, 18]. This procedure needs some assumptions to apply, e.g. adequate number of observations, certain relationship between variables, zero mean and uncorrelated errors, and normally distributed errors to make statistical inferences. However, there are some cases where the statistical modeling assumptions can not be satisfied. Modeling of the replicated response measured small sized data set can be one of the examples for this situation.

\*Corresponding author

When the data set has replicated response measures (RRM), the qualification of the response has uncertainty different than randomness. In this case, the uncertainty of the RRM can be defined as fuzzy number, firstly introduced by Zadeh [19] since it will be hard to define replicated values as a single numerical quantity. In this study, Triangular Type-1 Fuzzy Numbers (TT1FNs) are used to present the RRM due to sake of simplicity. In order to transform RRM to TT1FNs, some descriptive statistics of replicates, e.g. minimum, median, maximum, are used. Then, it is aimed to obtain fuzzy linear model with fuzzy model parameters for fuzzy response valued data set. It is assumed here that the input variables are crisp. In order to estimate the unknown fuzzy linear model parameters, fuzzy least squares (FLS) approach is used. The FLS is based on minimizing the sum of squared fuzzy errors.

In the literature, there have been several studies about modeling of the replicated response measured data sets through FLS approach. In the studies of Bashiri and Hosseinezhad [20], Bashiri and Hosseinezhad [21], Türkşen and Apaydın [22], Türkşen and Güler [23], Türkşen [24, 25], the RRM are transformed to TT1FNs for each observation unit. Therefore, the natural structure of replicated measures are taken into account to represent the uncertainty of replicated values.

The main aim of the study is to propose a flexible way of modeling, using FLS approach, for the small sized data set with RRM to obtain maximum amount of BG content from the yeast cell wall. Thus, the uncertainty of BG content should be predicted without using any strong modeling assumptions. In order to optimize predicted fuzzy response function, weighted optimization is applied. By maximizing the predicted fuzzy function, optimal values of additive materials are defined.

The paper is organized as follows: In Section 2, detailed information about BG production is given. Section 3 gives a brief information about data set with RRM and fuzzy linear regression modeling. And also, optimization methodology of predicted fuzzy response function is presented in Section 3. In Section 4, a real data set about BG content is used for application purpose of the fuzzy modeling approach with comparison results. Finally, conclusion is given in Section 5.

## 2. Beta-glucan production

Beta glucans (BGs) are polysaccharides that are composed of glucose units. The BGs exist together with the mannoproteins and chitin in the cell wall. In order to produce the BG, three steps process be followed; (1) microorganism growth, (2) cell wall lysis and, (3) extraction of BG from the cell wall components. For these three steps process, each step can be accomplished by various type of procedures. In the microorganism growth step, growth conditions (microorganism type, temperature, pH, aeration level,

growth medium, operation mode etc.) are the most important factors. These growth factors must be determined according to selected microorganism strain to enhance the BG content. In general, yeast strains of *Saccharomyces cerevisiae* which is known as baker's yeast due to higher BG content. The *S. cerevisiae* has advantageous for producing high quality BG.

The usage of some additive materials in the growth medium results the enhancement of yeast BG content [6]. EDTA, Sorbitol and  $\text{CaCl}_2$  are considered as additive materials in the growth medium. Determining the optimal values of these additive materials has importance to obtain maximum amount of BG content from the yeast cell wall. For this purpose, the experimental studies should be done at specifically defined conditions which are the growth factors (e.g. pH, T), the cell wall lysis and the extraction procedures of BG. These conditions were explained in detail from the previous studies [7].

## 3. Fuzzy modeling and optimization

### 3.1. Design of experimental data set with fuzzy response

A basic and fundamental step of an experiment is the experimental design which enables researchers to find the most valuable information about the problem. The design of the experimental data can be composed of replicated response measured data set as given in Table 1.

**Table 1.** Experimental design with RRM.

| No  | Input levels |          |     |          | Response    |          |     |          |
|-----|--------------|----------|-----|----------|-------------|----------|-----|----------|
|     | $X_1$        | $X_2$    | ... | $X_p$    | $\tilde{Y}$ |          |     |          |
| 1   | $x_{11}$     | $x_{12}$ | ... | $x_{1p}$ | $y_{11}$    | $y_{12}$ | ... | $y_{1r}$ |
| 2   | $x_{21}$     | $x_{22}$ | ... | $x_{2p}$ | $y_{21}$    | $y_{22}$ | ... | $y_{2r}$ |
| .   | .            | .        | ... | .        | .           | .        | ... | .        |
| .   | .            | .        | ... | .        | .           | .        | ... | .        |
| .   | .            | .        | ... | .        | .           | .        | ... | .        |
| $n$ | $x_{n1}$     | $x_{n2}$ | ... | $x_{np}$ | $y_{n1}$    | $y_{n2}$ | ... | $y_{nr}$ |

**Table 2.** Experimental design with fuzzy response.

| No  | Input levels |          |     |          | Response      |
|-----|--------------|----------|-----|----------|---------------|
|     | $X_1$        | $X_2$    | ... | $X_p$    | $\tilde{Y}$   |
| 1   | $x_{11}$     | $x_{12}$ | ... | $x_{1p}$ | $\tilde{y}_1$ |
| 2   | $x_{21}$     | $x_{22}$ | ... | $x_{2p}$ | $\tilde{y}_2$ |
| .   | .            | .        | ... | .        | .             |
| .   | .            | .        | ... | .        | .             |
| .   | .            | .        | ... | .        | .             |
| $n$ | $x_{n1}$     | $x_{n2}$ | ... | $x_{np}$ | $\tilde{y}_n$ |

In Table 1,  $n$  denotes the number of experimental units and  $r$  is the number of replications for the response. The replicated values of the response are obtained for each setting of a group of  $p$  input variables. It is clear here that the RRM have uncertainty different than randomness for each unit. The uncertainty of the nature of the RRM should be taken into account to model the replicated response measured data set properly. For this

purpose, the RRM are transformed to TT1FNs instead of using a single numerical quantity for RRM. The design of the experimental data with fuzzy observed response is presented in Table 2.

### 3.2. Triangular type-1 fuzzy numbers

A type-1 fuzzy set  $A$  is a set function on universe  $D_A$  into  $[0,1]$ , e.g.  $\mu_A : X \rightarrow [0,1]$ . The membership function (MF) of  $A$  is denoted and is called a type-1 MF, e.g.  $A = \{(x, \mu_A(x)) : x \in X\}$  in which  $0 \leq \mu_A(x) \leq 1$ . When the uncertainty is modeled using a type-1 fuzzy set it is called a type-1 fuzzy number (TT1FNs). Let  $A$  be a fuzzy set in  $R$ .  $A$  is called a type-1 fuzzy number if: (i)  $A$  is normal, (ii)  $A$  is convex, and (iii)  $A$  has a bounded support [26].

A TT1FN is a fuzzy number represented with three points  $(a_1, a_2, a_3) \in A$ . A presentation of a TT1FN can be seen in Figure 1.

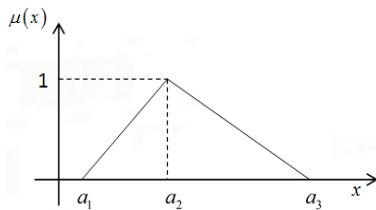


Figure 1. A presentation of TT1FN  $x = (a_1, a_2, a_3)$

The MF formula for TT1FN is given below

$$\mu_A(x) = \begin{cases} (x-a_1)/(a_2-a_1) & , a_1 \leq x < a_2 \\ (a_3-x)/(a_3-a_2) & , a_2 \leq x \leq a_3 \\ 0 & , x > a_3 \text{ or } x < a_1 \end{cases} \quad (1)$$

where the  $A$  can be denoted as  $\tilde{A} = (a_1, a_2, a_3)$ . Suppose that  $\tilde{A} = (a_1, a_2, a_3)$  and  $\tilde{B} = (b_1, b_2, b_3)$  be two TT1FNs. Some elementary arithmetic operations for TT1FNs can be given basically as follows:

- $\tilde{A} + \tilde{B} = (a_1 + b_1, a_2 + b_2, a_3 + b_3)$
- $\tilde{A} - \tilde{B} = (a_1 - b_3, a_2 - b_2, a_3 - b_1)$
- $\tilde{A} \times \tilde{B} = (a_1 b_1, a_2 b_2, a_3 b_3)$
- Let  $\lambda$  be a scalar.

$$\lambda \tilde{A} = \begin{cases} (\lambda a_1, \lambda a_2, \lambda a_3) & , \lambda > 0 \\ (-\lambda a_3, -\lambda a_2, -\lambda a_1) & , \lambda < 0 \end{cases}$$

Detailed information about TT1FNs can be seen in the study of [27].

### 3.3. Transforming the RRM to TT1FNs

The observed replicated response measures can be represented in matrix form as below

$$\mathbf{Y} = \begin{bmatrix} y_{11} & y_{12} & \dots & y_{1r} \\ y_{21} & y_{22} & \dots & y_{2r} \\ \vdots & \vdots & \dots & \vdots \\ \vdots & \vdots & \dots & \vdots \\ y_{n1} & y_{n2} & \dots & y_{nr} \end{bmatrix} \quad (2)$$

and the fuzzy presentation of the response for each unit can be given as

$$\mathbf{Y} = \begin{bmatrix} \tilde{y}_1 \\ \tilde{y}_2 \\ \vdots \\ \tilde{y}_n \end{bmatrix} = \begin{bmatrix} (y_1^l, y_1^c, y_1^u) \\ (y_2^l, y_2^c, y_2^u) \\ \vdots \\ (y_n^l, y_n^c, y_n^u) \end{bmatrix} \quad (3)$$

where  $\tilde{y}_i = (y_i^l, y_i^c, y_i^u)$ ,  $i = 1, 2, \dots, n$  are obtained by using the following fuzzification rule:

$$\begin{aligned} y_i^l &= y_{i(1)} \\ y_i^c &= \text{med}(y_{ij}), \quad i = 1, 2, \dots, n, \quad j = 1, 2, \dots, r \\ y_i^u &= y_{i(r)} \end{aligned} \quad (4)$$

in which  $y_{i(1)}$  and  $y_{i(r)}$  are the smallest and the largest order statistics, respectively, and the  $\text{med}(y_{ij})$  is the median of the RRM for each unit.

### 3.4. Fuzzy linear regression model

The general form of the fuzzy linear regression model can be given as

$$\tilde{\mathbf{Y}} = \mathbf{X}\tilde{\boldsymbol{\beta}} + \tilde{\boldsymbol{\varepsilon}} \quad (5)$$

in which observed fuzzy response values ( $\tilde{\mathbf{Y}}$ ), fuzzy model coefficients ( $\tilde{\boldsymbol{\beta}}$ ), and fuzzy errors ( $\tilde{\boldsymbol{\varepsilon}}$ ) are assumed as TT1FNs whereas the input variables are considered as crisp values. In this study, it is assumed that the predicted fuzzy response function has second order polynomial form given as

$$\tilde{\mathbf{Y}} = \hat{\boldsymbol{\beta}}_0 + \sum_{j=1}^p \hat{\boldsymbol{\beta}}_j \mathbf{X}_j + \sum_{j=1}^p \sum_{j < w} \hat{\boldsymbol{\beta}}_{jw} \mathbf{X}_j \mathbf{X}_w + \sum_{j=1}^p \hat{\boldsymbol{\beta}}_{jj} \mathbf{X}_j^2. \quad (6)$$

It is clear from the Eq. (6) that the predicted fuzzy response model is linear according to the fuzzy model parameters,  $\tilde{\boldsymbol{\beta}}$ .

### 3.5. Fuzzy least squares approach

The estimates of triangular fuzzy model coefficient vector,  $\hat{\boldsymbol{\beta}}$ , is calculated by minimizing the following sum of squared error function, called fuzzy least squares (FLS), with respect to Diamond's distance metric

$$\min_{\tilde{\boldsymbol{\beta}}} \phi(\tilde{\boldsymbol{\beta}}) = \min_{\tilde{\boldsymbol{\beta}}} (\tilde{\boldsymbol{\varepsilon}}' \tilde{\boldsymbol{\varepsilon}}) = \min_{\tilde{\boldsymbol{\beta}}} \left( d^2(\tilde{\mathbf{Y}}, \hat{\mathbf{Y}}) \right) \quad (7)$$

where

$$d^2(\hat{Y}, \hat{Y}) = \frac{1}{3} \left( (\hat{Y}^l - \hat{Y}^l)^2 + (\hat{Y}^c - \hat{Y}^c)^2 + (\hat{Y}^u - \hat{Y}^u)^2 \right). \quad (8)$$

The root mean of sum of squared error (RMSE) is preferred to use as a criteria to evaluate the prediction performances of the fuzzy predicted regression model. In order to minimize the objective function given in Eq. (7), derivative-based optimization approach is applied as follows:

$$\begin{aligned} \phi(\tilde{\beta}) &= \tilde{\epsilon}'\tilde{\epsilon} \\ &= (\tilde{Y} - \tilde{X}\tilde{\beta})'(\tilde{Y} - \tilde{X}\tilde{\beta}) \\ &= \tilde{Y}'\tilde{Y} - \tilde{Y}'\tilde{X}\tilde{\beta} - \tilde{\beta}'\tilde{X}'\tilde{Y} + \tilde{\beta}'\tilde{X}'\tilde{X}\tilde{\beta}. \end{aligned}$$

By using derivative calculation

$$\frac{\partial \phi}{\partial \tilde{\beta}} = 0$$

the fuzzy model coefficients are obtained as

$$\hat{\tilde{\beta}} = (\tilde{X}'\tilde{X})^{-1} \tilde{X}'\tilde{Y}.$$

where  $\tilde{X}$  is design matrix composed with crisp input values and  $\tilde{Y}$  is fuzzy observed response vector.

### 3.6. Optimization of the predicted fuzzy response function

The main goal of the study is to obtain the optimal additive material values which maximize the BG content of the yeast. For this purpose, it is aimed to maximize the predicted fuzzy response function. The optimization can be achieved by solving the following problem:

$$\max_{x \in R} \hat{Y} = \max_{x \in R} (\hat{Y}^l, \hat{Y}^c, \hat{Y}^u). \quad (9)$$

In order to optimize the problem given in Eq. (9), it is possible to consider the problem as multi-objective optimization (MOO) problem since each element of the triplet should be maximized simultaneously. The MOO problem can be presented as

$$\begin{aligned} \max_{x \in R} \hat{Y}^l \\ \max_{x \in R} \hat{Y}^c \\ \max_{x \in R} \hat{Y}^u \end{aligned} \quad (10)$$

It is clear that the MOO problem, given in Eq. (10), is hard to solve. To make the calculations easier, the objective functions are aggregated in a single objective function with weighted approach as below

$$\max_{x \in R} \frac{1}{3} (\hat{Y}^l + \hat{Y}^c + \hat{Y}^u). \quad (11)$$

It should be noted here that the weighted values are chosen equal since each member of fuzzy predicted response triplet, denoted as  $\hat{Y} = (\hat{Y}^l, \hat{Y}^c, \hat{Y}^u)$ , has equal importance. The solution of the weighted objective function, given in Eq. (11), will give optimal values of additive materials for maximization of the BG content.

## 4. Application

In this section, a real RRM data set is used to illustrate

the flexible modeling procedure to obtain optimal additive material values for maximizing the BG content which is considered as response variable. Here, EDTA ( $X_1$ ),  $CaCl_2$  ( $X_2$ ) and Sorbitol ( $X_3$ ) are considered as crisp input variables. The individual experiments are done for  $X_1$ ,  $X_2$  and  $X_3$  by using optimal values of temperature (T) and pH which are dealt with growth factors. The optimal values of T and pH are considered as 34.7 °C and 4.8, respectively, from the previous studies. The levels of  $X_1$ ,  $X_2$  and  $X_3$  are defined according to literature knowledge. And also, the second and third steps of the BG production process are done by following of the study [7].

The experimental results are presented as in Tables 3-5. It can be seen from the Tables 3-5 that the BG content is obtained with three replicates for each additive material value.

**Table 3.** Data set for EDTA and BG.

| No | EDTA<br>(µg/ml) | Beta-glucan (µg/ml) |       |       |
|----|-----------------|---------------------|-------|-------|
|    |                 | Rep-1               | Rep-2 | Rep-3 |
| 1  | 0               | 17.4                | 17.8  | 17.7  |
| 2  | 10.1367         | 23.3                | 24.4  | 24.8  |
| 3  | 25              | 27.3                | 26.8  | 27.5  |
| 4  | 39.8633         | 16.7                | 16.3  | 16.8  |
| 5  | 50              | 15.5                | 15.2  | 15.8  |

**Table 4.** Data set for  $CaCl_2$  and BG.

| No | $CaCl_2$<br>(mmol/L) | Beta-glucan (µg/ml) |       |       |
|----|----------------------|---------------------|-------|-------|
|    |                      | Rep-1               | Rep-2 | Rep-3 |
| 1  | 0.15                 | 20.3                | 20.2  | 20.2  |
| 2  | 0.3223               | 16.2                | 16.3  | 16.3  |
| 3  | 0.575                | 17.1                | 17.1  | 17.1  |
| 4  | 0.8277               | 17.4                | 17.2  | 17.4  |
| 5  | 1.00                 | 16.1                | 16.2  | 16.3  |

**Table 5.** Data set for Sorbitol and BG.

| No | Sorbitol<br>(mmol/L) | Beta-glucan (µg/ml) |       |       |
|----|----------------------|---------------------|-------|-------|
|    |                      | Rep-1               | Rep-2 | Rep-3 |
| 1  | 0                    | 14.3                | 14.8  | 15.2  |
| 2  | 4.0547               | 20.1                | 21.1  | 20.8  |
| 3  | 10                   | 23.2                | 23.7  | 23.7  |
| 4  | 15.9453              | 17.9                | 17.8  | 17.4  |
| 5  | 20                   | 17.4                | 17.3  | 17.2  |

In this study, fuzzy linear modeling approach is preferred to use to obtain functional relationship between BG and individual additive material since each data set has small sized and composed of RRM. In order to transform the replicated BG measures to TT1FNs, the fuzzification rule given in Eq. (4) is used. The data sets with fuzzy response values are given in Tables 6-8 for additive materials.

The predicted fuzzy regression models are obtained as following:

**Table 6.** Fuzzy data set for EDTA and BG.

| No | EDTA<br>( $\mu\text{g/ml}$ ) | Beta-glucan<br>( $\mu\text{g/ml}$ ) |
|----|------------------------------|-------------------------------------|
| 1  | 0                            | (17.4, 17.7, 17.8)                  |
| 2  | 10.1367                      | (23.3, 24.4, 24.8)                  |
| 3  | 25                           | (26.8, 27.3, 27.5)                  |
| 4  | 39.8633                      | (16.3, 16.7, 16.8)                  |
| 5  | 50                           | (15.2, 15.5, 15.8)                  |

**Table 7.** Fuzzy data set for CaCl<sub>2</sub> and BG.

| No | CaCl <sub>2</sub><br>(mmol/L) | Beta-glucan<br>( $\mu\text{g/ml}$ ) |
|----|-------------------------------|-------------------------------------|
| 1  | 0.15                          | (20.2, 20.2, 20.3)                  |
| 2  | 0.3223                        | (16.2, 16.3, 16.3)                  |
| 3  | 0.575                         | (17.1, 17.1, 17.1)                  |
| 4  | 0.8277                        | (17.2, 17.4, 17.4)                  |
| 5  | 1                             | (16.1, 16.2, 16.3)                  |

**Table 8.** Fuzzy data set for Sorbitol and BG.

| No | Sorbitol<br>(mmol/L) | Beta-glucan<br>( $\mu\text{g/ml}$ ) |
|----|----------------------|-------------------------------------|
| 1  | 0                    | (14.3, 14.8, 15.2)                  |
| 2  | 4.0547               | (20.1, 20.8, 21.1)                  |
| 3  | 10                   | (23.2, 23.7, 23.7)                  |
| 4  | 15.9453              | (17.4, 17.8, 17.9)                  |
| 5  | 20                   | (17.2, 17.3, 17.4)                  |

$$\hat{Y}_{EDTA} = (17.911, 18.5689, 18.9163) + (0.5761, 0.6421, 0.6881)X_1 + (-0.0158, -0.0148, -0.0133)X_1^2 \quad (12)$$

$$\hat{Y}_{CaCl_2} = (20.8605, 20.9247, 21.1967) + (-13.1142, -11.8605, -11.5751)X_2 + (7.4608, 7.7845, 8.8298)X_2^2 \quad (13)$$

$$\hat{Y}_{Sorbitol} = (14.8212, 15.4796, 16.0275) + (1.2092, 1.3939, 1.4936)X_3 + (-0.0728, -0.0684, -0.0594)X_3^2 \quad (14)$$

In Tables 9-11, the predicted fuzzy response values of the BG content are presented for EDTA, CaCl<sub>2</sub> and Sorbitol, respectively. The deviations between observed and predicted response values are calculated, denoted with **e**, as follows:

$$\mathbf{e} = \frac{1}{6} (|\mathbf{Y}^l - \hat{\mathbf{Y}}^l| + 4 * |\mathbf{Y}^c - \hat{\mathbf{Y}}^c| + |\mathbf{Y}^u - \hat{\mathbf{Y}}^u|) \quad (15)$$

**Table 9.** Predicted BG content and deviations for EDTA

| EDTA<br>( $\mu\text{g/ml}$ ) | Observed BG<br>( $\mu\text{g/ml}$ ) | Predicted BG<br>( $\mu\text{g/ml}$ ) | Deviation<br>(e) |
|------------------------------|-------------------------------------|--------------------------------------|------------------|
| 0                            | (17.4, 17.7, 17.8)                  | (17.9, 18.6, 18.9)                   | 0.8667           |
| 10.1367                      | (23.3, 24.4, 24.8)                  | (22.1, 23.6, 24.5)                   | 0.7833           |
| 25                           | (26.8, 27.3, 27.5)                  | (22.4, 25.4, 27.8)                   | 2.05             |
| 39.8633                      | (16.3, 16.7, 16.8)                  | (15.8, 20.6, 25.2)                   | 4.0833           |
| 50                           | (15.2, 15.5, 15.8)                  | (7.2, 13.7, 20)                      | 3.2333           |

It can be said from the Table 10 that the deviations for CaCl<sub>2</sub> are considerably small. Besides, it is seen from Table 9 and Table 11 that the deviations are getting larger for the larger values of EDTA and Sorbitol, respectively.

**Table 10.** Predicted BG content and deviations for CaCl<sub>2</sub>

| CaCl <sub>2</sub><br>(mmol/L) | Observed BG<br>( $\mu\text{g/ml}$ ) | Predicted BG<br>( $\mu\text{g/ml}$ ) | Deviation<br>(e) |
|-------------------------------|-------------------------------------|--------------------------------------|------------------|
| 0.15                          | (20.2, 20.2, 20.3)                  | (19.1, 19.3, 19.7)                   | 0.8833           |
| 0.3223                        | (16.2, 16.3, 16.3)                  | (17.4, 17.9, 18.4)                   | 1.6167           |
| 0.575                         | (17.1, 17.1, 17.1)                  | (15.8, 16.7, 17.5)                   | 0.55             |
| 0.8277                        | (17.2, 17.4, 17.4)                  | (15.1, 16.4, 17.7)                   | 1.0667           |
| 1.00                          | (16.1, 16.2, 16.3)                  | (15.2, 16.8, 18.4)                   | 0.9              |

**Table 11.** Predicted BG content and deviations for Sorbitol

| Sorbitol<br>(mmol/L) | Observed BG<br>( $\mu\text{g/ml}$ ) | Predicted BG<br>( $\mu\text{g/ml}$ ) | Deviation<br>(e) |
|----------------------|-------------------------------------|--------------------------------------|------------------|
| 0                    | (14.3, 14.8, 15.2)                  | (14.8, 15.5, 16)                     | 0.6833           |
| 4.0547               | (20.1, 20.8, 21.1)                  | (18.5, 20, 21.1)                     | 0.8              |
| 10                   | (23.2, 23.7, 23.7)                  | (19.6, 22.6, 25)                     | 1.55             |
| 15.9453              | (17.4, 17.8, 17.9)                  | (15.6, 20.3, 24.7)                   | 3.1              |
| 20                   | (17.2, 17.3, 17.4)                  | (9.9, 16.9, 22.1)                    | 2.2667           |

After flexible modeling, the optimal value of each additive material is to be obtained. For this purpose, each predicted fuzzy response functions given in Eq. (12)-(14) are maximized by the way of given in subsection 3.6. The calculations are performed by using Matlab programme.

The optimal values of additive materials are  $X_1^* = 21.71 \mu\text{g/mL}$ ,  $X_2^* = 0.7591 \text{ mmol/L}$ , and  $X_3^* = 10.2111 \text{ mmol/L}$ . The predicted fuzzy BG values for these optimal values are calculated as

$$\hat{Y}_{EDTA}(21.71) = (22.9712, 25.5333, 27.5863) \mu\text{g/ml}$$

$$\hat{Y}_{CaCl_2}(0.7591) = (15.2047, 16.4071, 17.4981) \mu\text{g/ml}$$

$$\hat{Y}_{Sorbitol}(10.2111) = (19.5779, 22.581, 25.0854) \mu\text{g/ml}.$$

If the minimum values of these additive materials are used then the predicted fuzzy BG values are obtained as

$$\hat{Y}_{EDTA}(0) = (17.911, 18.5689, 18.9163) \mu\text{g/ml}$$

$$\hat{Y}_{CaCl_2}(0.15) = (19.0612, 19.3208, 19.6591) \mu\text{g/ml}$$

$$\hat{Y}_{Sorbitol}(0) = (14.8212, 15.4796, 16.0275) \mu\text{g/ml}.$$

The fuzzy intervals of the BG content can be determined as [22.9712, 27.5863], [15.2047, 17.4981] and [19.5779, 25.0854] for optimal values of the EDTA, CaCl<sub>2</sub> and Sorbitol, respectively. According to the obtained results, if the researcher does not use any EDTA for the yeast growth, it is possible to get BG content approximately between [18-19]  $\mu\text{g/ml}$ . It is clear from the results that CaCl<sub>2</sub> may not be considered as an additive material whereas optimal value of Sorbitol can be used as an additive material for maximizing BG content. Besides, it seems from the results that the EDTA and the Sorbitol are

interchangeable. However, economically, it will be proper to prefer to use the EDTA for the yeast growth since the BG has high added value.

## 5. Conclusion

In this study, with the aim of enhancing the BG content of *S. cerevisiae*, concentration of each additive material (EDTA, CaCl<sub>2</sub> and Sorbitol) in the growth medium was optimized. This investigation is important due to the BG has incremental value in so many industries. It is clear that the BG content of the yeast cell wall increased when the yeast was cultured in the growth medium containing the EDTA and Sorbitol. Conversely usage of CaCl<sub>2</sub> more than the minimum concentration in the growth medium resulted with decrease the BG content of the yeast. Results show that the optimal concentration of EDTA (21.71 mg/mL) and Sorbitol (10.211 mmol/mL), cause to an increment in the BG content about 28-46 % and 32-56 %, respectively. In point of the economical aspects usage of optimal amount of EDTA has more profitable. It was proposed a flexible modeling way using the FLS approach for the production process of BG, which inherently have uncertainties. By considering this problem as MOO one, predicted fuzzy response functions were maximized simultaneously to determine the optimal values of additive materials. Thus, modeling and optimization procedures for a real engineering problem which have small sized and contain RRM data, were presented and applied successfully.

## Acknowledgments

Authors are thankful to Ankara University Research Fund (Project Number: 13L4343005) for the encouragement and support to carry out the research.

## References

- [1] Mantovani, M.S., Bellini, M.F., Angeli, J.P.F., Oliveira, R.J., Silva, A.F. & Ribeiro, L.R. (2008).  $\beta$ -Glucans in promoting health: Prevention against mutation and cancer. *Mutation Research* 658, 154–161.
- [2] Chen, J. & Raymond, K. (2008). Beta-glucans in the treatment of diabetes and associated cardiovascular risks. *Vasc. Health Risk Manag.* 4(6): 1265–1272.
- [3] Magnani, M., Gomez, R.J.H.C, Mori M.P., Kuasne, H., Gregorio, E.P., Libos, F.Jr. & Colus, I.M.S. (2011). Protective effect of carboxymethyl-glucan (CM-G) against DNA damage in patients with advanced prostate cancer. *Genet. Mol. Biol.* 34(1), 131–135.
- [4] Satrapai, S. & Suphantharika, M. (2007). Influence of spent brewer's yeast  $\beta$ -glucan on gelatinization and retrogradation of rice starch. *Carbohydr. Polym.* 67:500-510.
- [5] Hahn-Hägerdal, B., Karhumaa, K., Larsson, C.U., Gorwa-Grauslund, M., Görgens, J. & van Zyl, W.H. (2005). Role of cultivation media in the development of yeast strains for large scale industrial use. *Microbial Cell Factories*, 4:31, 1-16.
- [6] Naruemon, M., Romanee, S., Cheunjit, P., Xiao, H., Mclandsborough, L.A. & Pawadee, M., (2013). Influence of additives on *Saccharomyces cerevisiae*  $\beta$ -Glucan production, *International Food Research Journal*, 20, 1953-1959.
- [7] Sabuncu, N. (2016).  $\beta$ -glukan içeriğinin artırılması için *S.cerevisiae* üretilen bir biyoreaktörde çoğalma koşullarının incelenmesi ve pH kontrolü. Master Thesis. Ankara University.
- [8] Aguilar-Uscanga, B. & François, J.M. (2003). A study of the yeast cell wall composition and structure in response to growth conditions and mode of cultivation, *Letters in Applied Microbiology*, 37, 268–274.
- [9] Klis, F.M., Boorsma, A. & De Groot, P.W.J. (2006). Cell wall construction in *Saccharomyces cerevisiae*. *Yeast*, 23, 185–202.
- [10] Javmen, A., Grigiskis, S. & Gliebute, R. (2012).  $\beta$ -glucan extraction from *Saccharomyces cerevisiae* yeast using *Actinomyces rutgersensis* 88 yeast lyzing enzymatic complex. *Biologija*. 58(2), 51–59.
- [11] Lee, J.N., Lee, D.Y., Ji, I.H., Kim, G.E., Kim, H.N., Shon, J., Kim, S. & Kim, C.W. (2001) Purification of Soluble  $\beta$ -Glucan with Immune-enhancing Activity from the Cell Wall of Yeast. *Bioscience, Biotechnology, and Biochemistry*. 65(4), 837-841.
- [12] Hunter, K. W. Jr., Gault, R. A. & Berner, M. D. (2002). Preparation of microparticulate  $\beta$ -glucan from *Saccharomyces cerevisiae* for use in immune potentiation. *Letters in Applied Microbiology*, 35(4), 267-271.
- [13] Pelizon, A. C., Kaneno, R., Soares, A. M. V. C., Meira, D. A. & Sartori, A. (2005). Immunomodulatory activities associated with  $\beta$ -glucan derived from *Saccharomyces cerevisiae*. *Physiological Research*, 54(5), 557-564.
- [14] Shokri, H., Asadi, F. & Khosravi, A. R. (2008). Isolation of  $\beta$ -glucan from the cell wall of *Saccharomyces cerevisiae*. *Natural Product Research*, 22(5), 414-421.
- [15] Wenger, M. D., DePhillips, P. & Bracewell, D. G. (2008). A microscale yeast cell disruption technique for integrated process development strategies. *Biotechnology Progress*, 24(3), 606-614.
- [16] Freimund, S., Sauter, M., Kappeli, O. & Dutler, H. (2003). A new non-degrading isolation process for 1,3-  $\beta$ -D-glucan of high purity from baker's yeast *Saccharomyces cerevisiae*. *Carbohydrate Polymers*. 54, 159–171.
- [17] Box, G.E.P. & Draper, N.R. (2007). *Response Surface Mixtures and Ridge Analysis*. John Wiley and Sons, New Jersey.
- [18] Khuri, A.I. & Cornell, J.A. (1996). *Response Surfaces: Designs and Analysis*, Marcel Dekker, New York.

- [19] Zadeh, L.A. (1965). Fuzzy sets. *Information Control*, 338-353.
- [20] Bashiri, M. & Hosseini-zhad, S.J. (2009). A Fuzzy Programming for Optimizing Multi Response Surface in Robust Designs. *Journal of Uncertain Systems*, 3(3), 163-173.
- [21] Bashiri, M. & Hosseini-zhad, S.J. (2012). Fuzzy Development of Multiple Response Optimization. *Group Decision and Negotiation*, 21(3), 417-438.
- [22] Türkşen, Ö. & Apaydın, A. (2014). A Modeling Approach Based on Fuzzy Least Squares Method for Multi-Response Experiments with Replicated Measures. *Chaos, Complexity and Leadership 2012 Springer Proceedings in Complexity*, Springer Netherlands, 153-158.
- [23] Türkşen, Ö. & Güler, N. (2015). Comparison of fuzzy logic based models for the multi-response surface problems with replicated response measures. *Applied Soft Computing*, 37, 887-896.
- [24] Türkşen, Ö. (2016). Analysis of Response Surface Model Parameters with Bayesian Approach and Fuzzy Approach. *International Journal of Uncertainty, Fuzziness and Knowledge-Based Systems*, 24(1), 109-122.
- [25] Türkşen, Ö. (2018). A Fuzzy Modeling Approach for Replicated Response Measures Based on Fuzzification of Replications with Descriptive Statistics and Golden Ratio. Süleyman Demirel University Journal of Natural and Applied Sciences, 22(1), 153-159.
- [26] Mendel, J.M. (2017). Type-1 Fuzzy Sets and Fuzzy Logic. *Uncertain Rule-Based Fuzzy Systems*, Springer International Publishing AG, 25-99.
- [27] Lai, Y.J. Hwang, C.L. (1992). *Fuzzy Mathematical Programming*. Springer Verlag, Berlin.
- Özlem Türkşen** received MSc degree in 2005 from Statistics, Ankara University, Turkey. She was awarded PhD in 2011 from Statistics, Ankara University, Turkey. She has worked as Research Assistant and Assistant Professor at the Department of Statistics, Ankara University during 2004-2014 and 2014-2017, respectively. She has been working as Associated Professor at the Department of Statistics, Ankara University since 2017. Her research interests include response surface methodology, computational statistics, soft computing methods, heuristic algorithms, multi-objective optimization.
- Suna ERTUNÇ** received MSc degree in 1997 from Chemical Engineering, Ankara University, Turkey. She was awarded PhD in 2003 from Chemical Engineering, Ankara University, Turkey. She worked as Research Assistant during 1995-2010. She has been working as Assistant Professor since 2010. Her research areas are unit operations, biotechnology, modeling and optimization, system identification and process control.



## RESEARCH ARTICLE

## On the explicit solutions of fractional Bagley-Torvik equation arises in engineering

Zehra Pinar 

Department of Mathematics, Tekirdağ Namık Kemal University, Turkey  
 zpinar@nku.edu.tr

## ARTICLE INFO

Article history:  
 Received: 19 July 2018  
 Accepted: 10 December 2018  
 Available Online: 2 May 2019

Keywords:  
 Bagley-Torvik equation  
 Explicit solutions  
 Conformable derivative

AMS Classification 2010:  
 35A20, 35CXX, 34K37

## ABSTRACT

In this work, Bagley-Torvik equation is considered with conformable derivatives. The analytical solutions will be obtained via Sine-Gordon expansion method and Bernoulli equation method for the two cases of Bagley-Torvik equation. We will illustrate and discuss about the methodology and solutions therefore the proposed equation has meaning in different areas of science and engineering.



### 1. Introduction

For engineering and science, fractional calculus has become the important theory including both conservative and nonconservative phenomena [1] and to model realistic processes such as diffusion wave, electromagnetic waves, heat conduction, electro-electrolyte polarization [2, 3].

In this paper, the Bagley-Torvik equation, the specific type of fractional hyperbolic partial differential equation, is considered

$$u_t^2 - u_{xx} + u_t^\alpha = f(x, t) \quad (1)$$

where  $f(x, t)$  is continuous for  $t > 0, x < 1$  and  $m - 1 < \alpha < m$  is the order fractional derivative.

Generally, the 1/2-order derivative and 3/2-order derivative is common to determine the frequency-dependent damping materials [4,5]. Therefore, Eq. (1) with 1/2-order derivative or 3/2-order derivative is used to model the motion of real physical systems. The most known examples for each derivative are an immersed plate in a Newtonian fluid and a gas in a fluid, respectively [6, 7]. When  $\alpha$  is between 0 and 2, it describes damping force. We will consider Eq. (1) for  $\alpha = 1/2$ .

The papers on the modelling physical phenomena via fractional Bagley-Torvik equation, the numeric [8-12] or analytical solutions [6, 13, 14] of Eq. (1) are seen in the literature commonly. A fractional mathematical model for a micro-electro-mechanical system

(MEMS) device has been developed to measure the viscosity of fluids during oil well exploration by Fitt et al. [15]. There are many numerical methods based on Bernoulli polynomials [11], generalized form of the Bessel functions of the first kind [9], wavelet [10], the generalized Taylor series [8], spline methods [17, 18], finite difference scheme [12, 16] etc. to solve the fractional Bagley-Torvik equation. In addition, the approximations and analytical methods are proposed to solve the fractional Bagley-Torvik equation such as quadratic polynomial spline function [18], homogenous balanced principle [13], Adomian decomposition method [20, 21], first integral method [22], homotopy analysis method [19, 23], Lie group theory method [24, 25], invariant subspace method [14, 26, 27, 36], Fractional variational method [28- 30, 56],  $G'/G$ -expansion method [31], sub-equation method [32-35], transformed rational function method [37], multiple exp-function method [38].

Besides different approaches to solve fractional partial differential equation, the other most important tool is definition of the fractional derivative. So there are many approaches/definitions for fractional derivative such as Riemann-Liouville definition, Grünwald-Letnikov definition, Caputo definition, Riesz-Feller definition, Miller-Ross sequential definition, Weyl definition, Jumarie's modified Riemann-Liouville definition [3, 39, 40]. Among them, the most knowns are Riemann-Liouville definition and Caputo

\*Corresponding author

definition whereas in the recent times, the most popular ones are conformable derivative [41, 42]. The most known definitions of fractional derivatives, Riemann–Liouville definition and Caputo definition, depend on Gamma function. Therefore, Gamma function can be defined as a definite integral and also it is seen as in the definitions whose behavior is asymptotic. Because of this reason, we consider the conformable derivative.

In the work, the fractional Bagley-Torvik equation with the one of the popular derivative definitions, conformable derivative is considered. The analytical solutions will be obtained via Sine-Gordon expansion method and Bernoulli approximation method. The obtained solutions will be compared with the exact solutions.

## 2. Definitions and methodologies

### 2.1. Basic definitions

As we mentioned in the introduction, various definitions for fractional derivative are seen and the most known and used ones are the Riemann–Liouville and the Caputo fractional derivative, there is a relation between the two. Generally, Caputo fractional derivative is preferred so it is not depended on initial conditions to give the physical meaning, but generally it can be said that it has advantages for fractional differential equations with initial conditions. These definitions are useful for modelling but they have lack of main properties for the computation as the product rule, quotient rule and the chain rules and etc. Because their definitions include the Gamma function which is a special function and has an asymptotic behavior. The transition between fractional derivative and Newton derivative is not exact. To overcome these problems, Abdeljawad [43] proposed the conformable derivative and its most properties correspond to classical derivative and with this definition the equations can be solved more easily.

**Definition 1.**  $f : [0, \infty) \rightarrow R$  is a function, the conformable derivative of order  $\alpha$  is given by

$$T_\alpha(f)(t) = \lim_{\varepsilon \rightarrow 0} \frac{f(t + \varepsilon t^{1-\alpha}) - f(t)}{\varepsilon}, \forall t > 0, \alpha \in (0, 1).$$

Therefore, if  $f$  is  $\alpha$ -differentiable in some  $(0, a), a > 0$  and  $\lim_{t \rightarrow 0^+} f^\alpha(t)$  exists, then define  $f^\alpha(0) = \lim_{t \rightarrow 0^+} f^\alpha(t)$ .

**Properties.** All properties of the classical derivatives are same as the conformable derivative such as linearity, sum, product, division, etc. In addition to these properties, assume that  $\alpha \in (0, 1)$  and  $f$  is differentiable  $t > 0$ , the following property of the conformable derivative is given:

$$T_\alpha(f)(t) = t^{1-\alpha} \frac{df}{dt}, \text{ if } f \text{ is differentiable.}$$

### 2.2. Methodologies

There are various analytical methods to obtain the analytical/exact solutions of partial differential equations and also these methods can be applied to fractional partial differential equations with some modifications. The popular methods in the last decade are to obtain the exact solutions of NPDEs such as tanh-method [44, 45],  $G'/G$ -expansion method [46, 47], simplest equation method [48], auxiliary equation method [49, 50], sub-equation method [51], and so on. With the same view, the methods can also be applied to the fractional partial differential equations with the modification of the transformation [42, 52, 53, 57].

For the general case, the conformable fractional partial differential equation is considered

$$F\left(u, \frac{\partial^\alpha u}{\partial t^\alpha}, \frac{\partial u}{\partial x}, \frac{\partial^{2\alpha} u}{\partial t^{2\alpha}}, \frac{\partial^2 u}{\partial x^2}, \dots\right) = 0. \tag{2}$$

To reduce Eq. (2) into nonlinear ODE, instead of  $\zeta = \mu x + \beta t$  the classical wave transformation, the

new transformation  $\zeta = x + \beta \frac{t^\alpha}{\alpha}$  is used by many authors in the literature.

**Proposition 1.** Using the wave transformation  $\zeta = \mu x + \beta t$  and properties of the conformable

derivative especially  $T_\alpha(u)(t) = t^{1-\alpha} \frac{du}{dt}$ , if  $u$  is differentiable are used to reduce into nonlinear ODE respect to  $\zeta$

$$F(u, u', u'', u''', \dots) = 0. \tag{3}$$

**Remark 1.** As a result, the obtained nonlinear ODE is generally variable coefficient nonlinear differential equation.

In the view of auxiliary equation method, the solution of Eq. (3) is considered as the finite sum of the solution of the proposed auxiliary equation

$$u(\zeta) = \sum_{i=1}^N a_i z^i(\zeta) \tag{4}$$

where  $z(\zeta)$  is the solution of the proposed auxiliary equation,  $a_i$  are the parameters will be determined via obtained algebraic system,  $N$  is determined by the balancing principle [54]. The procedure is the same, substituting the proposed auxiliary equation and solution (Eq. 4) into the reduced equation (Eq. 3), then classify the obtained equation respect to the powers of  $z(\zeta)$  Each coefficient of the power of  $z(\zeta)$  is equal

to zero, so the algebraic system is obtained and the solutions of system are parameters in Eq. (4). Substituting results and transformation in Eq. (4), the analytical solution of Eq. (2) is obtained.

In this work, two types of auxiliary equations which are different from the literature are considered. The first one is the case of the Sine-Gordon equation and the second one is the variable coefficient Bernoulli type differential equation [50, 55].

**3. Results and discussion**

The Bagley-Torvik equation with the conformable derivative of order  $\alpha = 1/2$  is considered

$$u_t^2 - u_{xx} + u_t^{1/2} = f(x, t) \tag{5}$$

where  $f(x, t) = \left( 2 - \frac{8t^{3/2}}{3\sqrt{\pi}} + (\pi t)^2 \right) \sin(\pi x)$ . Its

exact solution  $u(x, t) = t^2 \sin(\pi x)$  is given via separation of variables by [12, 16].

Now we try to obtain analytical solutions by suggested methods with the proposed transformation  $\zeta = \mu x + \beta t$  for  $\alpha = 1/2$ . With the proposed transformation, Eq. (5) is reduced into

$$\beta^2 (u')^2 - u'' + \beta t^{1-\alpha} u' = \left( 2 - \frac{8t^{3/2}}{3\sqrt{\pi}} + (\pi t)^2 \right) \sin(\pi x).$$

**Case 1.** The Sine-Gordon equation  $u_{xx} - u_u = m^2 \sin(u)$  is considered and its solution is obtained via the wave transformation as  $\sin(w) = \sec h(\xi), \cos(w) = \tanh(\xi)$ . Therefore, the ansatz is

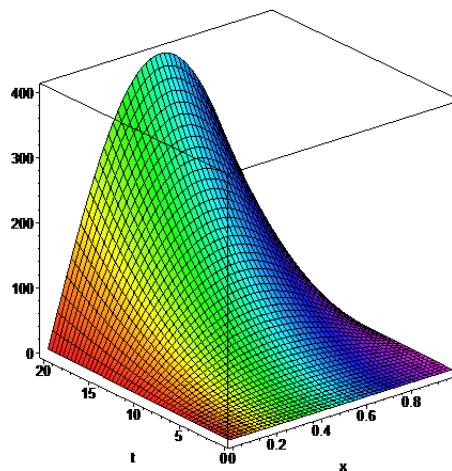
$$u(\xi) = a_0 + \sum_{i=1}^N \tanh^{i-1}(\xi) (b_i \sec h(\xi) + a_i \tanh(\xi)), \xi = \mu x + \beta t$$

When the given procedure is applied, as a solution of algebraic system, the parameters are obtained;

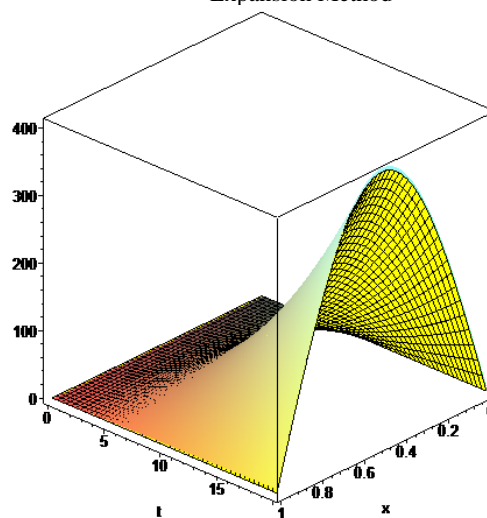
$$b_1 = \frac{1\mu^2}{2\beta^2}, a_2 = b_2 = -\frac{\mu^2}{2\beta^2}, a_1 = -b_1 - 2b_2 \tanh(\xi), a_0 = t^2 \sin(\pi x)$$

As a result, substituting the parameters and the solution of Sine-Gordon equation into Eq. (4), the analytical solution is given by Figure 1 for the special parameters

$$\beta = \frac{-144 + 42I}{((-5760 + 1680I)t)^{1/2}}, \mu = \left( -\frac{3}{10} + \frac{I}{10} \right) (-9 - 13I)^{1/2}.$$



i) The solution of Eq. (5) via Sine-Gordon Expansion Method



ii) the comparison between analytical solution (surface) with the exact solution (surface wireframe)

**Figure 1.** The solutions obtained via Sine-Gordon Expansion Method

In the following figures are obtained for  $\alpha \in (0, 1)$  and  $x = 0.6$ , the comparison of  $\alpha$  values, comparison of approximate and exact solutions (see Figure 2).

**Case 2.** For the second we will consider the variable coefficient Bernoulli equation instead of the classical auxiliary equation

$$z'(\zeta) = P(\zeta)z(\zeta) + Q(\zeta)z^n(\zeta), n \neq 0, 1 \tag{6}$$

The solutions of Eq. (6) depends upon the coefficient functions  $P(\zeta), Q(\zeta)$  and the degree of Eq. (6)  $n$ .

When the classical procedure is applied to Eq. (5), the coefficient functions and parameters are obtained

$$P(\zeta) = \frac{\beta}{1 + c_1 \beta e^{-\beta \zeta}}, Q(\zeta) = \frac{8\beta^2 g_2}{3 + 3c_1 \beta e^{-\beta \zeta}},$$

$$g_2 = \frac{5}{19} \beta^2 g_1^2, g_0 = \left( 2 - \frac{8t^{3/2}}{3\sqrt{\pi}} + (\pi t)^2 \right) \sin(\pi x)$$

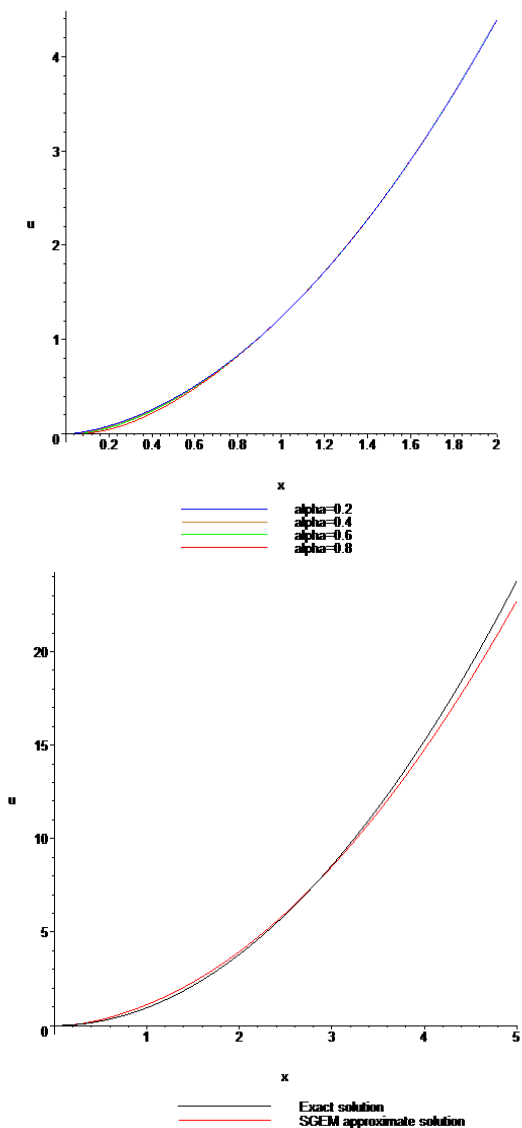
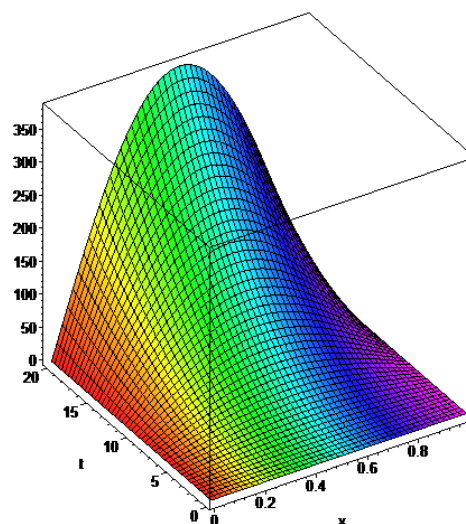


**Figure 2.** First one is the comparison of  $\alpha$  values for the obtained solution; the second one is the comparison of exact solution with the analytical solution obtained via SGEM

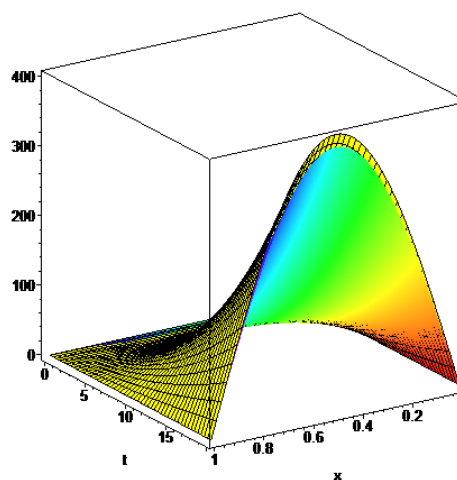
As a result, the solution of Eq. (6) with the obtained functions is

$$z(\zeta) = \pm \frac{3(e^{\beta\zeta} + c_1\beta)}{\sqrt{-24g_2\beta^2 e^{2\beta\zeta} - 48g_2c_1\beta^3 e^{\beta\zeta} + 9c_2}}$$

Hence the solution of Eq. (5) is given by Figure 3 for the parameter values  $c_1 = -1.1, c_2 = 10^{-5}, \beta = 0.8, g_1 = 10^{-4}$ . In the following figures are obtained for  $\alpha \in (0,1)$  and  $x = 0.6$ , the comparison of  $\alpha$  values, comparison of approximate and exact solutions.



i) The solution via Bernoulli approximation method



ii) the comparison between analytical solution (surface) with the exact solution (surface wireframe)  
**Figure 3.** The solutions obtained via Bernoulli approximation Method

#### 4. Conclusion

In this work the Bagley-Torvik equation with the conformable derivative is considered and the solutions are obtained expected behavior via the Sine-Gordon expansion method and Bernoulli approximation method. Also the exact solution comparisons and the obtained analytical solutions are given by Figure 1 and Figure 3. These solutions are not have any sense in physics but in the future they will be useful for developing technology.

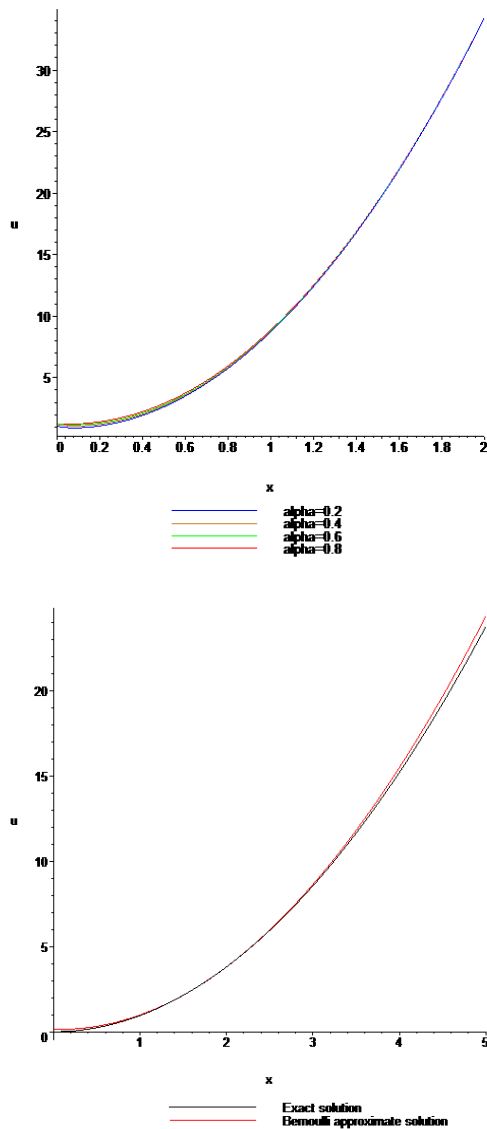


**Figure 4.** First one is the comparison of  $\alpha$  values for the obtained solution; the second one is the comparison of exact solution with the analytical solution obtained via Bernoulli approximation method.

## References

- [1] Baleanu, D. (2009). About fractional quantization and fractional variational principles. *Communications in Nonlinear Science and Numerical Simulation*, 14(6), 2520–2523.
- [2] Gülsu, M., Öztürk, Y. & Anapali, A. (2017). Numerical solution the fractional Bagley–Torvik equation arising in fluid mechanics. *International Journal of Computer Mathematics*, 94(1), 173–184.
- [3] Podlubny, I. (1999). *Fractional differential equations*. Academic Press, San Diego.
- [4] Bagley, R.L. & Torvik, P.J. (1984). On the appearance of the fractional derivative in the behavior of real materials. *Journal of Applied Mechanics*, 51(2), 294–302.
- [5] Bagley, R.L. & Torvik, P.J. (1983). Fractional calculus – a different approach to the analysis of viscoelastically damped structures. *AIAA Journal*, 21(5), 741–749.
- [6] Ray, S.S. & Bera, R.K. (2005). Analytical solution of the Bagley–Torvik equation by Adomian decomposition method. *Applied Mathematics and Computation*, 168(1), 398–410.
- [7] Wang, Z.H. & Wang, X. (2010). General solution of the Bagley–Torvik equation with fractional-order derivative. *Communications in Nonlinear Science and Numerical Simulation*, 15, 1279–1285.
- [8] Gülsu, M., Öztürk, Y. & Anapali, A. (2017). Numerical solution of the fractional Bagley–Torvik equation arising in fluid mechanics. *International Journal of Computer Mathematics*, 94(1), 173–184.
- [9] Yüzbaşı, S. (2013). Numerical solution of the Bagley–Torvik equation by the Bessel collocation method. *Mathematical Methods in the Applied Sciences*, 36, 300–312.
- [10] Mohammadi, F. (2014). Numerical solution of Bagley–Torvik equation using Chebyshev wavelet operational matrix of fractional derivative. *International Journal of Advances in Applied Mathematics and Mechanics*, 2, 83–91.
- [11] Mashayekhi, S. & Razzaghi, M. (2016). Numerical solution of the fractional Bagley–Torvik equation by using hybrid functions approximation. *Mathematical Methods in the Applied Sciences*, 39, 353–365.
- [12] Ashyralyev, A., Dal, F. & Pinar, Z. (2011). A note on the fractional hyperbolic differential and difference equations. *Applied Mathematics and Computation*, 217(9), 4654–4664.
- [13] Rui, W. (2017). Applications of homogenous balanced principle on investigating exact solutions to a series of time fractional nonlinear PDEs. *Communications in Nonlinear Science and Numerical Simulation*, 47, 253–266.
- [14] Sahadevan, R. & Prakash, P. (2016). Exact solution of certain time fractional nonlinear partial differential equations. *Nonlinear Dynamics*, 1–15.
- [15] Fitt, A.D., Goodwin, A.R.H., Ronaldson, K.A. & Wakeham, W.A. (2009). A fractional differential equation for a MEMS viscometer used in the oil industry. *Journal of Computational and Applied Mathematics*, 229, 373–381.
- [16] Ashyralyev, A., Dal, F. & Pinar, Z. (2009). On the Numerical Solution of Fractional Hyperbolic Partial Differential Equations. *Mathematical Problems in Engineering*, 1–11.
- [17] Zahra, W.K. & Van Daele, M. (2017). Discrete spline methods for solving two point fractional Bagley–Torvik equation. *Applied Mathematics and Computation*, 296, 42–56.
- [18] Zahra, W.K. & Elkholy, S.M. (2012). Quadratic

- spline solution for boundary value problem of fractional order. *Numerical Algorithms*, 59, 373–391.
- [19] Bakkyaraj, T. & Sahadevan, R. (2016). Approximate analytical solution of two coupled time fractional nonlinear schrodinger equations. *International Journal of Applied and Computational Mathematics*, 2(1), 113–35.
- [20] Daftardar-Gejji, V. & Jafari H. (2005). Adomian decomposition: a tool for solving a system of fractional differential equations. *Journal of Mathematical Analysis and Applications*, 301(2), 508–18 .
- [21] Bakkyaraj, T. & Sahadevan, R. (2014). An approximate solution to some classes of fractional nonlinear partial differential difference equation using adomian decomposition method. *Journal of Fractional Calculus and Applications*, 5(1), 37–52 .
- [22] Eslami, M., Vajargah, B.F., Mirzazadeh, M. & Biswas, A. (2014). Applications of first integral method to fractional partial differential equations. *Indian Journal of Physics*, 88(2), 177–84 .
- [23] Bakkyaraj, T. & Sahadevan, R. (2014). On solutions of two coupled fractional time derivative hirota equations. *Nonlinear Dynamics*, 77(4), 1309–1331 .
- [24] Sahadevan, R., Bakkyaraj, T. (2012). Invariant analysis of time fractional generalized burgers and korteweg-de vries equations. *Journal of Mathematical Analysis and Applications*, 393(2), 341–348 .
- [25] Bakkyaraj, T. & Sahadevan, R. (2015). Invariant analysis of nonlinear fractional ordinary differential equations with Riemann–Liouville derivative. *Nonlinear Dynamics*, 80(1), 447–55 .
- [26] Sahadevan, R. & Bakkyaraj, T . (2015). Invariant subspace method and exact solutions of certain nonlinear time fractional partial differential equations. *Fractional Calculus and Applied Analysis*, 18(1), 146–62 .
- [27] Harris, P.A. & Garra, R. (2013). Analytic solution of nonlinear fractional burgers-type equation by invariant subspace method. *Nonlinear Studies*, 20(4), 471–81 .
- [28] Odibat, Z.M. & Shaher, M. (2009) . The variational iteration method: an efficient scheme for handling fractional partial differential equations in fluid mechanics. *Computers & Mathematics with Applications*, 58, 2199–208 .
- [29] Wu, G. & Lee, E.W.M. (2010). Fractional variational iteration method and its application. *Physics Letters A*, 374(25), 2506–9 .
- [30] Momani, S., & Zaid, O. (2007). Comparison between the homotopy perturbation method and the variational iteration method for linear fractional partial differential equations. *Computers & Mathematics with Applications*, 54(7), 910–19 .
- [31] Eslami, M. (2017). Solutions for space-time fractional (2+1)-dimensional dispersive long wave equations. *Iranian Journal of Science and Technology, Transactions A: Science*, 41, 1027–1032.
- [32] Neirameh, A. (2016). New soliton solutions to the fractional perturbed nonlinear Schrodinger equation with power law nonlinearity. *SeMA Journal*, 73(4), 309-323.
- [33] Neirameh, A. (2015). Topological soliton solutions to the coupled Schrodinger–Boussinesq equation by the SEM. *Optik - International Journal for Light and Electron Optics*, 126, 4179–4183.
- [34] Neirameh, A. (2015). Binary simplest equation method to the generalized Sinh–Gordon equation. *Optik - International Journal for Light and Electron Optics*, 126, 4763–4770.
- [35] Neirameh, A. (2016). New analytical solutions for the coupled nonlinear Maccari’s system. *Alexandria Engineering Journal*, 55, 2839–2847.
- [36] Ma, W.X. (2012). A refined invariant subspace method and applications to evolution equations. *Science China Mathematics*, 55(9), 1–10.
- [37] Ma, W.X. & Lee, J.H. (2009). A transformed rational function method and exact solutions to the 3+1 dimensional Jimbo–Miwa equation. *Chaos, Solitons Fractals*, 42(3), 1356–1363.
- [38] Ma, W.X., Huang, T. & Zhang, Y. (2010). A multiple exp-function method for nonlinear differential equations and its application. *Physica Scripta*, 82(6), 065003.
- [39] Kilbas, A.A., Srivastava, H.M. & Trujillo, J.J. (2006). *Theory and application of fractional differential equations*. First ed., Elsevier Science (North-Holland), Amsterdam.
- [40] Miller, K.S. & Ross, B. (1993). *An Introduction to the Fractional Calculus and Differential Equations*. John Wiley, New York.
- [41] Khalil, R., Al Horani, M., Yousef, A. & Sababheh, M. (2014). A new definition of fractional derivative. *Journal of Computational and Applied Mathematics*, 264, 65–70.
- [42] Atangana, A., Baleanu, D. & Alsaedi, A. (2015). New properties of conformable derivative. *Open Mathematics*, 13 (1), 1–10.
- [43] Abdeljawad, T. (2015). On conformable fractional calculus. *Journal of Computational and Applied Mathematics*, 279, 57–66.
- [44] Wazwaz, A. M. (2002). *Partial Differential Equations: Methods and Applications*. Balkema, Leiden.
- [45] Wazwaz, A. M. (2009). *Partial Differential Equations and Solitary Wave Theory*. Higher Education Press, Berlin Heidelberg.
- [46] Younis, M. & Rizvi, S. T. R. (2015). Dispersive

- dark optical soliton in (2+1)-dimensions by (G'/G)-expansion with dual-power law nonlinearity. *Optik-International Journal for Light and Electron Optics*, 126(24), 5812-5814.
- [47] Parkes, E.J. (2010). Observations on the basic G/G'-expansion method for finding solutions to nonlinear evolution equations. *Applied Mathematics and Computation*, 217, 1759-1763.
- [48] Vitanov, N. K. (2011). Modified method of simplest equation: Powerful tool for obtaining exact and approximate traveling-wave solutions of nonlinear PDEs. *Communications in Nonlinear Science and Numerical Simulation*, 16, 1176-1185.
- [49] Pinar, Z. & Öziş, T. (2013). An Observation on the Periodic Solutions to Nonlinear Physical models by means of the auxiliary equation with a sixth-degree nonlinear term. *Communications in Nonlinear Science and Numerical Simulation*, 18, 2177-2187.
- [50] Pinar, Z. & Ozis, T. (2015). A remark on a variable-coefficient Bernoulli equation based on auxiliary equation method for nonlinear physical systems. arXiv:1511.02154 [math.AP]
- [51] Yomba, E. (2005). The extended Fan's sub-equation method and its application to KdV-MKdV, BKK and variant Boussinesq equations. *Physics Letters A*, 336, 463-476.
- [52] Kurt, A., Tasbozan, O. & Baleanu, D. (2017). New solutions for conformable fractional Nizhnik–Novikov–Veselov system via G'/G expansion method and homotopy analysis methods. *Optical and Quantum Electronics*, 49, 333-384.
- [53] Yépez-Martínez, H., Gómez-Aguilar, J.F. & Baleanu, D. (2018). Beta-derivative and sub-equation method applied to the optical solitons in medium with parabolic law nonlinearity and higher order dispersion. *Optik*, 155, 357-365.
- [54] Pinar, Z. & Öziş, T. (2015). Observations on the class of 'Balancing Principle' for nonlinear PDEs that can be treated by the auxiliary equation method. *Nonlinear Analysis: Real World Applications*, 23, 9-16.
- [55] Pinar, Z. & Kocak, H. (2018). Exact solutions for the third-order dispersive-Fisher equations. *Nonlinear Dynamics*, 91, 421-426.
- [56] Evirgen, F. (2016). Analyze the optimal solutions of optimization problems by means of fractional gradient based system using VIM. *An International Journal of Optimization and Control: Theories & Applications*, 6(2), 75-83.
- [57] Yavuz, M. (2018). Novel solution methods for initial boundary value problems of fractional order with conformable differentiation. *An International Journal of Optimization and Control: Theories & Applications*, 8(1), 1-7.

**Zehra Pinar** received her B.S. degree in Applied Mathematics from Ege University, İzmir, Turkey in 2007 and her M.S. and PhD degrees also from the same university in 2009 and 2013, respectively. In January 2014, she joined Tekirdağ Namık Kemal University, Turkey as an Assistant Professor. Current research interests include analytically-approximate and numerical methods for nonlinear problems in physics and engineering.



RESEARCH ARTICLE

## Application of precedence constrained travelling salesman problem model for tool path optimization in CNC milling machines

Ilker Kucukoglu , Tulin Gunduz\* , Fatma Balkancioglu , Emine Chousein Topal   
Oznur Sayim 

Department of Industrial Engineering, Bursa Uludag University, Turkey  
[ikucukoglu@uludag.edu.tr](mailto:ikucukoglu@uludag.edu.tr), [tg@uludag.edu.tr](mailto:tg@uludag.edu.tr), [fatmabalkancioglu@gmail.com](mailto:fatmabalkancioglu@gmail.com), [emine.c.topal@gmail.com](mailto:emine.c.topal@gmail.com),  
[ssayim16@gmail.com](mailto:ssayim16@gmail.com)

### ARTICLE INFO

Article history:  
*Received: 3 August 2018*  
*Accepted: 28 March 2019*  
*Available Online: 28 May 2019*

Keywords:  
*Tool path optimization*  
*Mathematical modelling*  
*Travelling salesman problem*  
*Combinatorial optimization*  
*Satin Bowerbird Optimizer*

AMS Classification 2010:  
*90B23, 90B56, 90C27, 90C90*

### ABSTRACT

In this study, a tool path optimization problem in Computer Numerical Control (CNC) milling machines is considered to increase the operational efficiency rates of a company. In this context, tool path optimization problem of the company is formulated based on the precedence constrained travelling salesman problem (PCTSP), where the general form of the TSP model is extended by taking the precedence of the tool operations into account. The objective of the model is to minimize total idle and unnecessary times of the tools for internal operations. To solve the considered problem, a recent optimization algorithm, called Satin Bowerbird Optimizer (SBO), is used. Since the SBO is first introduced for the global optimization problems, the original version of the SBO is modified for the PCTSP with discretization and local search procedures. In computational studies, first, the performance of the proposed algorithm is tested on a well-known PCTSP benchmark problems by comparing the proposed algorithm against two recently proposed meta-heuristic approaches. Results of the comparisons show that the proposed algorithm outperforms the other two competitive algorithms by finding better results. Then, the proposed algorithm is carried out to optimize the hole drilling processes of three different products produced by the company. For this case, with up to 4.05% improvement on the operational times was provided for the real-life problem of the company. As a consequence, it should be noted that the proposed solution approach for the tool path optimization is capable of providing considerable time reductions on the CNC internal operations for the company.



### 1. Introduction

Nowadays, to achieve an effective and efficient production system for a company is very important due to the tough competition conditions. In this context, one of the most important factors that provide efficient production is increasing capacity utilization in operations, which directly affects factory production efficiency. With regards to the innovations in the field of mechanical engineering, Computer Numerical Control (CNC) machines are mostly employed in the various manufacturing process to increase production efficiency [1-3].

The total production time for a part in CNC machines basically consists of two components: The machining time when the tool is actually cutting material and the non-productive time when the tool is travelling in the air or the tool is switched in the magazine [4].

Regarding the machining time, it should be noted that there exist many researches have been studied in the literature to reduce total production time by optimizing the machining parameters [5, 6]. On the other hand, fewer studies are introduced in the field of optimization to reduce non-productive times in CNC machines [4]. One of the critical issues in process planning of CNC machines to reduce non-productive times is tool path planning for machining since the tool path generation in current CAM technology is still based on the only geometric computations and away from being an optimum manufacturing process, which may lead a considerable increase on total production time [7]. The tool path planning is simply named in the literature as tool path optimization problem (TPOP) and results in travelling salesman problem (TSP) as each tool-path contour can be considered as a city coordinate to be visited [8]. Since the TSP is known as an NP-Hard

combinatorial problem, the TPOP can also be considered as a complicated problem to solve.

The TPOP can be investigated as the extension of the hole drilling path optimization problem (HDPOP). The HDPOP simply considers the routing a single bit over a workpiece in such a way that all holes are visited in the fastest manner [9]. The HDPOP is classified into two versions concerning the number of tools required for the machining operations on the workpieces:

- Single tool hole drilling path optimization problem (STHDPOP)
- Multi-tool hole drilling path optimization problem (MTHDPOP)

The STHDPOP is the most basic version, where every hole has to be drilled by a single specific tool. Due to only one type of tool is used, a tool switch is not required for the operations. However, the processing time of each hole can be different with respect to hole depth [9].

In case the holes on a workpiece require different diameter or different type of finishing, the STHDPOP shade into the MTHDPOP. As a result of multiple tool usage, tool switch and tool travel times have to be taken into account [10, 11].

A detailed literature review on HDPOP is presented by Dewil et al. [9] and Abidin et al. [10], in which various heuristic approaches proposed to solve HDPOP are listed. Considering both single and multi-tool hole drilling path optimization problems, well-known simulated annealing algorithm [12], tabu search algorithm [13] ant colony optimization algorithm [11, 14, 15], particle swarm optimization algorithm [16-18], genetic algorithm [19-23] are proposed. In addition to these algorithms, various recent algorithms are also implemented to HDPOP, such as biogeography based optimization [24], charged system search algorithm [25], hybrid cuckoo search-genetic algorithm [26], shuffled frog leaping algorithm [18], optimal foraging algorithm [27], etc.

According to the review study of Abidin et al. [10], in which 41 papers are taken into account, the modelling approaches of HDPOP can be classified into three main groups: TSP based models, precedence constrained travelling salesman problem (PCTSP) based models, and travelling cutting tool problem (TCP) based models. From the reviewed papers, the TSP concept is the most widely used in modeling the HDPOP about 92%, while 5% of them consider the PCTSP and 3% of them consider the TCP. A similar result is reported by Dewil et al. [9] that only 7 of 53 reviewed papers consider the PCTSP based model.

In this study, TPOP in CNC milling machines of a company is taken into account to increase the internal operational efficiency of the machines. The mathematical model of the problem is formulated based on PCTSP. To solve the TPOP efficiently, a newly developed bio-inspired optimization algorithm called Satin Bowerbird Optimizer (SBO) is used. SBO is first

introduced by Moosavi and Bardsiri [28] to efficiently estimate software development effort. Since the original version of the SBO is introduced for the global optimization problems, the SBO is modified with two components: Discretization procedure for representing a solution for TPOP, and local search procedure. In this context, the main contributions of the proposed study are as follows:

- The TPOP is formulated based on the PCTSP.
- To the author' knowledge, this is the first application of the SBO in a combinatorial optimization problem.
- The original version of the SBO is modified with discretization and local search procedures.
- Detailed comparisons are presented for the proposed SBO with statistical significance tests.
- A real-life application of the SBO to the TPOP is carried out by considering hole drilling processes of three different products produced by the company.

The rest of the paper is organized as follows. In Section 2, the TPOP is described with the considered assumptions. Mathematical formulation of the TPOP is presented in Section 3 as a mixed integer mathematical model. Details of the proposed algorithm are given in Section 4. Section 5 presents the computational results of the proposed algorithm. Finally, conclusions are given in Section 6.

## 2. Problem definition

The TPOP addressed in this study is the extension of the MTHDPOP in which precedences of the operations are taken into account. In literature, this problem is called a multi-tool hole drilling path optimization problem with precedence constraints (MTHDPOP-PC). In MTHDPOP-PC, a specific sequence of drilling operations is defined for each hole [24]. Figure 1 shows an illustrative tool operation for the MTHDPOP-PC, where operation  $i$  has to be completed before operation  $j$ . In this case, the operation  $i$  can be defined as the precedence of operation  $j$ .

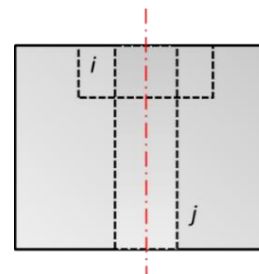
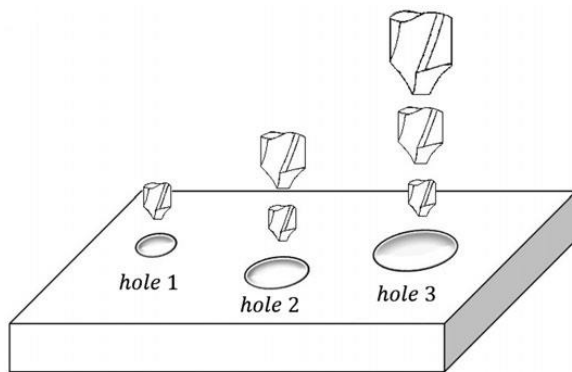


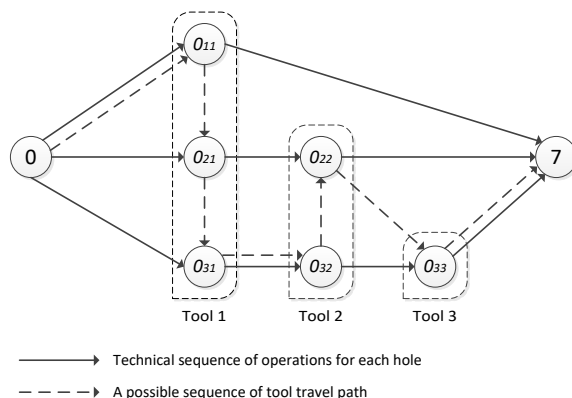
**Figure 1.** Illustrative representation of precedence drilling operations.

With regards to the precedence constraints, Figure 2a presents an example part of tool sequence for multi-tool hole drilling, where the sequence of operations for the holes are given in Table 1. According to the given

operational sequences, hole 1 ( $o_{11}$ ) needs to be drilled by only tool 1, hole 2 ( $o_{21}$  and  $o_{22}$ ) needs to be drilled by tools 1 and 2, respectively, and hole 3 ( $o_{31}$ ,  $o_{32}$  and  $o_{33}$ ) needs to be drilled by tools 1, 2, and 3 in that order. For better visualization, Figure 2b shows an operational precedence graph of the example, where 0 and 7 present the start and end of the hole drilling process. As a consequence of the example, it can be specified that the multi-tool hole drilling path optimization problem with precedence is identical to the well-known PCTSP since both of the problems shows the same characteristics.



(a) Example part of multi-tool hole drilling.



(b) Technical sequence of operations.

Figure 2. Example for the MTHDPOP-PC [24].

Table 1. Sequence of operations for illustrative example.

| Hole   | Tool Sequence | Sequence of operation ( $o_{ij}$ ) |
|--------|---------------|------------------------------------|
| Hole 1 | 1             | $o_{11}$                           |
| Hole 2 | 1, 2          | $o_{21} - o_{22}$                  |
| Hole 3 | 1, 2, 3       | $o_{31} - o_{32} - o_{33}$         |

Based on the MTHDPOP-PC, the TPOP can be described as finding the best operational plan for the CNC milling machines that minimizes total idle and unnecessary times of the tools for internal operations regarding the following assumptions:

- In addition to the hole making, different type of milling operations in CNC milling machines (such as reaming, boring, counterboring, tapping, etc.) are considered on the workpiece.
- The production process of a workpiece starts and ends at the magazine.

- Each milling operation may need a pre-process before it starts. In other words, a milling operation cannot be processed until its precedence operations are completed.
- Each milling operation can be processed by only one type of tool and can be completed in one pass.
- Tools can be used for multiple milling operations.
- In case a tool switch operation is required between two milling operations, the spindle has to visit the magazine.

### 3. Model formulation

Since the MTHDPOP-PC is identical to the PCTSP, which is shown in the previous section, the mathematical model formulation of the TPOP is proposed based on the PCTSP model introduced by Kubo and Kasugai [29]. The proposed model is the extension of the well-known TSP model, where the general form of the TSP model is modified by taking the precedence of the tool operations into account. In this context, the proposed mathematical model of the TPOP is formulated as follows:

#### Notations

0 Tool magazine point in CNC machine

$N$  Number of points on the product to be processed in CNC machine. This can also be assumed as the number of milling operations operated in the CNC machine.

$t_{ij}$  Travelling time from operation  $i$  to operation  $j$  including processing time of operation  $i$  and tool switch time at the magazine if the tool is switched;  $i, j = 0, \dots, N$

$p_{ij}$  Binary data and 1 if milling operation  $i$  is precedence of milling operation  $j$ ;  $i, j = 1, \dots, N$

#### Decision Variables

$x_{ij}$  Binary variable and equals to 1 if the tool travels from operation  $i$  to operation  $j$ , 0 otherwise;  $i, j = 0, \dots, N$

$u_i$  Positive variable to avoid sub-tours;  $i = 0, \dots, N$ .

#### Model

$$\text{Min } Z = \sum_{i=0}^N \sum_{j=0}^N t_{ij} x_{ij} \quad (1)$$

s.t.

$$\sum_{\substack{j=0 \\ i \neq j}}^N x_{ij} = 1 \quad i = 0, \dots, N \quad (2)$$

$$\sum_{\substack{j=0 \\ i \neq j}}^N x_{ji} = 1 \quad i = 0, \dots, N \quad (3)$$

$$u_i - u_j + Nx_{ij} \leq N - 1 \quad i \neq j \quad i, j = 1, \dots, N \quad (4)$$

$$u_j - u_i \geq 1 \quad i, j = 1, \dots, N \quad p_{ij} = 1 \quad (5)$$

$$x_{ij} \in \{0,1\} \quad i, j = 0, \dots, N \quad (6)$$

$$u_i \geq 0 \text{ and integer} \quad i = 0, \dots, N \quad (7)$$

Eq. (1) defines the objective function of the model which aims to minimize total operational times in CNC milling machine. Eq. (2) and Eq. (3) ensure that each operation is operated once in the CNC milling machine. Eq. (4) eliminates the sub-tour for the tool path. These constraints assign an auxiliary non-repetitive variable to each node for a Hamilton tour [30, 31]. Operational precedence for the tool is guaranteed by Eq. (5). Finally, the decision variables of the proposed model are defined in Eq. (6) and Eq. (7).

#### 4. Proposed algorithm

The SBO is a recently proposed bio-inspired meta-heuristic algorithm introduced by Moosavi and Bardsiri [28] to efficiently estimate software development effort. The SBO is inspired by the attraction of the male bowerbirds to the female bowerbirds for mating by constructing a bower, a structure built from sticks and twigs, and decorating the surrounding area. Based on the behavior of the bowerbirds, the SBO is structured as follows.

Similar to other meta-heuristic algorithms, the SBO starts with a randomly generated population consists of  $NB$  bowers. Let  $\mathbf{X}_i = \{x_{i,1}, x_{i,2}, \dots, x_{i,D}\}$  represents the  $i^{th}$  bower, where  $D$  is the problem size. Each bower is generated by using the following equation

$$x_{i,k} = x_k^L + rand(x_k^U - x_k^L) \quad (8)$$

where  $i = 1, \dots, NB$  and  $k = 1, \dots, D$ . Here  $x_k^L$  and  $x_k^U$  are the lower and upper bounds of parameter  $k$ , respectively. Finally,  $rand$  is a uniformly distributed random number.

After the initialization step, the fitness of each bower is calculated by using equation (9), where  $f(\mathbf{X}_i)$  is the cost function of bower  $i$ . Then the bowers are sorted based on their fitness value in descending order. To prevent the experience of best bowerbird in population, elitism is applied for the population. To do this, the position of the best bower built by birds is identified as elite.

$$fit_i = \begin{cases} \frac{1}{1 + f(\mathbf{X}_i)}, & f(\mathbf{X}_i) \geq 0 \\ \frac{1}{1 + |f(\mathbf{X}_i)|}, & f(\mathbf{X}_i) < 0 \end{cases} \quad (9)$$

In each iteration, SBO starts to generate a new population by calculating the probability of the bowers to identify their attractiveness. The probabilities of the bowers are calculated as shown in Equation (10).

$$Prob_i = \frac{fit_i}{\sum_{n=1}^{NB} fit_n} \quad (10)$$

Following the probability calculation step, new changes at any bower are calculated by using the Equations (11) and (12). In Equation (11),  $\mathbf{X}_{elite}$  is the elite bower of the current population, and  $\mathbf{X}_j$  is the target bower, which is calculated by the roulette wheel selection procedure. Finally,  $\lambda_k$  is the attraction power in the goal bower, which is controlled by greatest step size parameter  $\alpha$ .

$$x_{i,k}^{new} = x_{i,k}^{old} + \lambda_k \left( \left( \frac{x_{j,k} + x_{elite,k}}{2} \right) - x_{i,k}^{old} \right) \quad (11)$$

$$\lambda_k = \frac{\alpha}{1 + Prob_j} \quad (12)$$

At the end of each cycle, a mutation procedure is carried out by applying random changes to the bowers with a certain probability, which is described as  $P\_mutation$  in this study. The random changes on the bower are determined by

$$x_{i,k}^{new} = x_{i,k}^{old} + (\sigma \times N(0,1)) \quad (13)$$

where  $N(0,1)$  is a standard normal distributed random number and  $\sigma$  is a proportion of space width which is calculated by using Equation 14. The  $\sigma$  in Equation 14 is controlled by parameter  $z$ , which is the percent of the difference between the  $x_k^L$  and  $x_k^U$ .

$$\sigma = z \times (x_k^U - x_k^L) \quad (14)$$

At the end of each iteration, the fitness values of newly generated bowers are evaluated. Then, the bowers from the old population and newly generated bowers are combined and re-sorted with respect to their fitness. The new population is formed by removing the last  $NB$  bowers from the sorted population. Finally, the elite is updated if the first bower in the new population is fitter than the existing elite.

According to the procedures of the SBO described above, Algorithm 1 presents the main steps of the algorithm. For more details for the SBO, readers can refer to [28] and access to the source code of the algorithm given by the authors.

Since the original version of the SBOs introduced to optimize global optimization problems, this paper introduces a modified version of the SBO for the TPOP, which is called modified satin bowerbird optimizer (MSBO). The MSBO integrates two main procedures to SBO: Discretization and local search. The discretization procedure converts the continuous solution vector of the algorithm to the discrete solution vector considering the precedence constraints. In the local search procedure, two simple movement

operators are carried out to improve the solution quality of the newly generated solution vectors. The details of both discretization and local search procedures are given in the following sub-sections.

**Algorithm 1.** Main steps of the SBO

|    |   |
|----|---|
| 1  | : Initialization                                      |
| 2  | : Fitness evaluation and sorting                      |
| 3  | : Identify the best bower as the elite                |
| 4  | : <b>Repeat</b>                                       |
| 5  | : Probability calculation                             |
| 6  | : <b>For Each</b> Bower                               |
| 7  | : Determination of new changes                        |
| 8  | : Mutation  |
| 9  | : <b>End For</b>                                      |
| 10 | : Evaluation of bowers                                |
| 11 | : Re-sorting and selection                            |
| 12 | : Update elite bower                                  |
| 13 | : <b>Until</b> the termination criterion is satisfied |

#### 4.1. Discretization procedure

One of the critical issue for the continuous meta-heuristic algorithms while solving the combinatorial problems is discretization procedure to represent a solution for the considered problem. Since many problems require discrete search spaces, there exist several techniques to convert continuous solution to discrete solution, which can be classified into three main groups [32]: (i) rounding off generic technique, (ii) priority position techniques, (iii) specific techniques associated with meta-heuristic discretizations. In this study, the *smallest position value* rule, which is one of the priority position techniques introduced by [33], is used in the MSBO to convert a continuous solution vector to discrete solution vector. The *smallest position value* method converts the continuous values to a permutation order of the position values by sorting the positions with respect to ascending order of the position values.

The *smallest position value* method provides a permutation order for a continuous solution vector. However, a feasible solution cannot always be produced for the TPOP by this method because of the precedences of some operations in the CNC machine. Therefore, the *smallest position value* is adapted to the TPOP with the following insertion rule. According to the position values in ascending order, a candidate position with the smallest position value can be inserted into the permutation order if and only if its precedence operations are inserted to the order previously. An example of the modified *smallest position value* rule for the TPOP is shown in Table 2, where the permutation order of the positions with respect to operational precedence is 4 – 5 – 2 – 3 – 1.

**Table 2.** Example of the modified *smallest position value* rule.

| Position Index         | 1      | 2    | 3      | 4    | 5    |
|------------------------|--------|------|--------|------|------|
| Position Value         | 0.75   | 0.29 | 0.95   | 0.12 | 0.36 |
| Precedence of Position | (2, 3) | (5)  | (4, 2) | (-)  | (4)  |

#### 4.2. Local search

After a permutation ordered solution is obtained in the discretization step for each bower, a local search procedure is carried out by consecutively applying two simple operators: *Insertion(x, y)*, and *Swap(x, y)*. In *Insertion(x, y)* operator, a specific position (x) in permutation order is inserted into another specific location (y). In swap operation, locations of two specific positions (x, y) are replaced. Figure 3 shows an illustrative example of both insertion and swap operations. For both the operators, the best improvement strategy is taken into account and each operator is repeated if any improvement is provided at the end of the search.

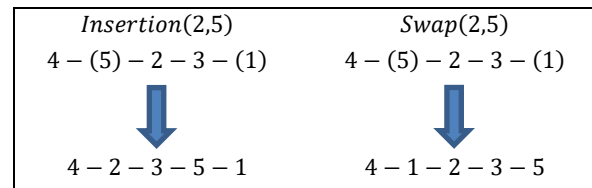


**Figure 3.** Example of insertion and swap operators.

### 5. Computational results and discussion

Computational studies for the MSBO are formed into two parts. In the first part, the performance of the MSBO is tested by comparing the proposed algorithm with SBO and also two recent meta-heuristic algorithms. In the second part, the MSBO is carried out for the real-life problem of the company. Moreover, managerial insights of the results are discussed in the last sub-section.

All experiments are performed on a workstation equipped with a 3.4GHz Xeon E5-2643v3 and 64 GB RAM. However, a single thread is used for the algorithm runs. According to preliminary experiments, the parameter values of the MSBO are identified as follows:  $\alpha = 0.25$ ,  $z = 0.50$  and,  $P_{mutation} = 0.05$ .

#### 5.1. Performance analyses of the MSBO

Since the PCTSP is also known as the sequential ordering problem (SOP), a well-known SOP dataset from the TSPLIB repository is used in order to test the performance of the proposed MSBO. The SOP dataset includes 41 different sized instances, where the number of nodes to be visited varies between 9-380. Each instance consists of a number of nodes and distances for each pair of nodes. The aim of the problem is to find a minimum Hamiltonian path from the first node to the last node with minimum length by considering the precedence constraints. Regarding the maximum TPOP size of the company, 27 of 41 instances from the dataset (up to 100 nodes) are used for the performance analyses.

In this subsection, the MBSO is first compared with the SBO and two variants of the MBSO. To point out the effect of local search procedure on the solution quality,

the first variant of the MBSO considers only insertion operation in the local search part, which is named MSBO<sup>I</sup>. Similarly, the second variant considers only swap operation, which is named MSBO<sup>S</sup>. The algorithms are repeated 30 times for each instance, and the results of each instance are identified via the average result of 30 runs (mean), and the standard deviation of the results (std). Table 3 presents the results of the SBO, MSBO<sup>I</sup>, MSBO<sup>S</sup>, and MSBO. Furthermore Table 3 shows a statistical comparison of the algorithms based on paired *t*-test with a significance

level of 0.05. For each pair of algorithms, the successful one is shown if there is a significant difference between the algorithm results. In this perspective, it should be clearly seen from Table 3 that the MSBO<sup>I</sup> and MSBO show better performance for all instances with respect to the SBO and MSBO<sup>S</sup>. On the other hand, the MSBO outperforms the MSBO<sup>I</sup> for three instances. However, the average results of the MBSO are mostly better than the average results of MSBO<sup>I</sup>. Thus, it should be concluded from Table 3 that the proposed MBSO outperforms the SBO, MSBO<sup>I</sup>, and MSBO<sup>S</sup>.

**Table 3.** Comparisons of SBO and MSBO variants

| Instance | SBO (A)  |         | MSBO <sup>I</sup> (B) |        | MSBO <sup>S</sup> (C) |       | MSBO (D) |       | Statistical Comparisons |     |     |     |     |     |
|----------|----------|---------|-----------------------|--------|-----------------------|-------|----------|-------|-------------------------|-----|-----|-----|-----|-----|
|          | Mean     | Std     | Mean                  | Std    | Mean                  | Std   | Mean     | Std   | A-B                     | A-C | A-D | B-C | B-D | C-D |
| br17.10  | 58.1     | 1.6     | 55.0                  | 0.0    | 55.0                  | 0.0   | 55.0     | 0.0   | B                       | C   | D   | -   | -   | -   |
| br17.12  | 58.9     | 3.8     | 55.0                  | 0.0    | 55.0                  | 0.0   | 55.0     | 0.0   | B                       | C   | D   | -   | -   | -   |
| ESC07    | 2125.0   | 0.0     | 2125.0                | 0.0    | 2125.0                | 0.0   | 2125.0   | 0.0   | -                       | -   | -   | -   | -   | -   |
| ESC12    | 1722.6   | 49.2    | 1675.0                | 0.0    | 1675.0                | 0.0   | 1675.0   | 0.0   | B                       | C   | D   | -   | -   | -   |
| ESC25    | 3286.9   | 423.6   | 1723.9                | 38.9   | 1986.2                | 138.3 | 1711.6   | 28.2  | B                       | C   | D   | B   | -   | D   |
| ESC47    | 6626.3   | 815.3   | 2264.8                | 76.1   | 3104.9                | 143.8 | 2197.7   | 84.8  | B                       | C   | D   | B   | D   | D   |
| ESC63    | 123.8    | 16.5    | 62.0                  | 0.0    | 64.2                  | 0.7   | 62.0     | 0.0   | B                       | C   | D   | B   | -   | D   |
| ESC78    | 207887.0 | 497.9   | 18230.0               | 0.0    | 18347.8               | 79.9  | 18230.0  | 0.0   | B                       | C   | D   | B   | -   | D   |
| ft53.1   | 12527.4  | 1011.2  | 7621.1                | 66.3   | 8350.7                | 196.8 | 7619.1   | 71.5  | B                       | C   | D   | B   | -   | D   |
| ft53.2   | 12984.8  | 1129.9  | 8083.3                | 25.7   | 8843.5                | 219.5 | 8084.5   | 32.1  | B                       | C   | D   | B   | -   | D   |
| ft53.3   | 14796.0  | 420.6   | 10284.8               | 36.8   | 10960.9               | 145.8 | 10273.1  | 23.3  | B                       | C   | D   | B   | -   | D   |
| ft53.4   | 16700.8  | 526.4   | 14425.0               | 0.0    | 14643.3               | 112.7 | 14425.0  | 0.0   | B                       | C   | D   | B   | -   | D   |
| ft70.1   | 54076.0  | 1692.7  | 40344.1               | 190.90 | 42326.9               | 326.6 | 40386.9  | 229.3 | B                       | C   | D   | B   | -   | D   |
| ft70.2   | 54550.0  | 2196.0  | 41528.3               | 314.1  | 43778.0               | 317.1 | 41486.3  | 406.9 | B                       | C   | D   | B   | -   | D   |
| ft70.3   | 55101.6  | 1653.8  | 42889.6               | 194.7  | 46078.3               | 501.6 | 42822.4  | 201.7 | B                       | C   | D   | B   | -   | D   |
| ft70.4   | 58985.0  | 709.5   | 53606.1               | 64.7   | 54790.2               | 349.1 | 53616.8  | 66.3  | B                       | C   | D   | B   | -   | D   |
| p43.1    | 28794.5  | 238.7   | 28144.5               | 13.7   | 28163.7               | 21.5  | 28140.0  | 0.0   | B                       | C   | D   | B   | -   | D   |
| p43.2    | 40474.5  | 13476.9 | 28482.2               | 3.1    | 28487.5               | 6.5   | 28480.7  | 1.7   | B                       | C   | D   | B   | D   | D   |
| p43.3    | 47183.0  | 12728.0 | 28838.0               | 5.4    | 28851.3               | 18.3  | 28836.7  | 3.8   | B                       | C   | D   | B   | -   | D   |
| p43.4    | 87072.7  | 9200.6  | 83005.0               | 0.0    | 83040.7               | 42.5  | 83005.0  | 0.0   | B                       | C   | D   | B   | -   | D   |
| prob.42  | 623.5    | 55.3    | 302.8                 | 17.4   | 357.1                 | 15.0  | 259.7    | 5.4   | B                       | C   | D   | B   | D   | D   |
| rbg048a  | 431.0    | 21.3    | 351.0                 | 0.0    | 353.2                 | 1.7   | 351.0    | 0.0   | B                       | C   | D   | B   | -   | D   |
| rbg050c  | 533.2    | 20.1    | 467.1                 | 0.3    | 472.5                 | 3.2   | 467.1    | 0.3   | B                       | C   | D   | B   | -   | D   |
| ry48p.1  | 23246.1  | 2575.0  | 15861.4               | 100.3  | 16271.4               | 246.4 | 15829.7  | 75.4  | B                       | C   | D   | B   | -   | D   |
| ry48p.2  | 24065.5  | 1590.0  | 16686.4               | 44.5   | 17079.9               | 215.2 | 16705.4  | 51.3  | B                       | C   | D   | B   | -   | D   |
| ry48p.3  | 27496.1  | 1384.1  | 19894.0               | 0.0    | 20618.8               | 305.2 | 19894.0  | 0.0   | B                       | C   | D   | B   | -   | D   |
| ry48p.4  | 34109.2  | 899.2   | 31446.1               | 0.4    | 31605.0               | 136.3 | 31446.0  | 0.0   | B                       | C   | D   | B   | -   | D   |

Another performance analysis for the MBSO is made by comparing the proposed algorithm with two recent meta-heuristic algorithms proposed for the PCTSP and SOP, which are Adaptive Evolutionary Algorithm (AEA) introduced by Sung and Jeong [34] and an improved Ant Colony System (ACS) introduced by Skinderowics [35]. Table 4 shows the available results of the AEA and ACS and comparisons between MBSO and other two algorithms, where “best” and “time” represent the best results and average computational time of the runs for a specified instance. To identify the better results for the comparisons, the smallest values in a row are written in bold. Table 4 additionally presents the best-known solutions of the instances, which are also known as optimal solution excepting “prob.100”, “ry48p.2”, and “ry48p.3”. Here, it should

be noted that the two results of AEA given by the authors are less than the optimum solutions. Therefore, it is not notable to compare the MBSO with AEA for these instances. For the other instances, it can be seen from Table 4 that proposed MBSO outperforms the AEA for each instance. With regards to the ACS solutions, better results are obtained for most of the instances by the MBSO.

For the computational times, it is reported by the Sung and Jeong [34] that the computational time of the AEA varies between 0.01-290.93 seconds for the considered problems. For the ACS, the authors report that the results are obtained with 60 seconds time limitation [35]. Regarding both the algorithm times, the CPU times of the MBSO, which are shown in Table 4, are acceptable for the real-life applications.

**Table 4.** Comparison of MSBO with AEA and ACS

| Instance | Best-Known | AEA    |         | ACS          |              | MSBO         |                |          |              |
|----------|------------|--------|---------|--------------|--------------|--------------|----------------|----------|--------------|
|          |            | Best   | Mean    | Mean         | Std          | Best         | Mean           | Time (s) | Std          |
| br17.10  | 55         | 55     | 55.9    | NA           | NA           | 55           | <b>55.0</b>    | 1.82     | 0.0          |
| br17.12  | 55         | 55     | 55.0    | NA           | NA           | 55           | 55.0           | 1.82     | 0.0          |
| ESC07    | 2125       | 2125   | 2125.0  | NA           | NA           | 2125         | 2125.0         | 0.51     | 0.0          |
| ESC12    | 1675       | 1675   | 1720.6  | NA           | NA           | 1675         | <b>1675.0</b>  | 1.05     | 0.0          |
| ESC25    | 1681       | 2354   | 3378.4  | NA           | NA           | <b>1681</b>  | <b>1711.6</b>  | 4.44     | 28.2         |
| ESC47    | 1288       | 4160   | 5648.3  | NA           | NA           | <b>2026</b>  | <b>2197.7</b>  | 21.27    | 84.8         |
| ESC63    | 62         | 73     | 80.9    | NA           | NA           | <b>62</b>    | <b>62.0</b>    | 46.38    | 0.0          |
| ESC78    | 18230      | NA     | NA      | NA           | NA           | 18230        | 18230.0        | 89.23    | 0.0          |
| ft53.1   | 7531       | 10619  | 11537.4 | 7702         | <b>46.1</b>  | <b>7568</b>  | <b>7619.1</b>  | 27.98    | 71.5         |
| ft53.2   | 8026       | 11000  | 12092.1 | 8348         | 156.6        | <b>8026</b>  | <b>8084.5</b>  | 29.02    | <b>32.1</b>  |
| ft53.3   | 10262      | 13231  | 13797.0 | 11271        | 605.5        | <b>10262</b> | <b>10273.1</b> | 29.45    | <b>23.3</b>  |
| ft53.4   | 14425      | 15579  | 16263.3 | 14639        | 101.1        | <b>14425</b> | <b>14425.0</b> | 35.96    | <b>0.0</b>   |
| ft70.1   | 39313      | 46390  | 48696.2 | <b>40054</b> | <b>223.6</b> | <b>39930</b> | 40386.9        | 79.03    | 229.3        |
| ft70.2   | 40419      | 46485  | 49162.1 | 41629        | 409          | <b>40587</b> | <b>41486.3</b> | 73.40    | <b>406.9</b> |
| ft70.3   | 42535      | NA     | NA      | 43946        | 436.6        | 42535        | <b>42822.4</b> | 65.90    | <b>201.7</b> |
| ft70.4   | 53530      | NA     | NA      | 55305        | 362.9        | 53530        | <b>53616.8</b> | 68.07    | <b>66.3</b>  |
| p43.1    | 28140      | 28830  | 29107.0 | NA           | NA           | <b>28140</b> | <b>28140.0</b> | 17.30    | 0.0          |
| p43.2    | 28480      | 28896  | 47979.5 | NA           | NA           | <b>28480</b> | <b>28480.7</b> | 17.69    | 1.7          |
| p43.3    | 28835      | 28680* | 29362.5 | NA           | NA           | <b>28835</b> | <b>28836.7</b> | 17.20    | 3.8          |
| p43.4    | 83005      | 82960* | 83393.5 | NA           | NA           | <b>83005</b> | <b>83005.0</b> | 18.07    | 0.0          |
| prob.42  | 243        | 443    | 530.7   | NA           | NA           | <b>248</b>   | <b>259.7</b>   | 15.67    | 5.4          |
| rbg048a  | 351        | 376    | 412.6   | NA           | NA           | <b>351</b>   | <b>351.0</b>   | 25.46    | 0.0          |
| rbg050c  | 467        | 505    | 528.7   | NA           | NA           | <b>467</b>   | <b>467.1</b>   | 28.26    | 0.3          |
| ry48p.1  | 15805      | 18650  | 21732.2 | NA           | NA           | <b>15805</b> | <b>15829.7</b> | 24.95    | 75.4         |
| ry48p.2  | 16666      | 18499  | 22210.8 | NA           | NA           | <b>16666</b> | <b>16705.4</b> | 24.45    | 51.3         |
| ry48p.3  | 19894      | 22480  | 25029.2 | NA           | NA           | <b>19894</b> | <b>19894.0</b> | 23.60    | 0.0          |
| ry48p.4  | 31446      | 33961  | 34944.7 | NA           | NA           | <b>31446</b> | <b>31446.0</b> | 24.80    | 0.0          |

NA: Not available

\*Solution given in the related study is less than the optimal solution

**5.2. Application of the MSBO to real-life TPOP problem**

In the second part of the computational studies, the proposed MSBO is carried out for the real-life TPOP problem of the company. In this context, three different products produced over than thousands in a year by the company are taken into account. Solid models of the products 1, 2, and 3 are presented in Figure 4a, 4b, and 4c respectively. Table 5 shows the number of milling operations and tools required to produce these products in CNC milling machines.

**Table 5.** Operational requirements of the products.

| Product   | # of milling operations | # of tools |
|-----------|-------------------------|------------|
| Product 1 | 22                      | 9          |
| Product 2 | 58                      | 6          |
| Product 3 | 37                      | 11         |

To compare the performance of the MSBO, first, the mathematical model of the problem is solved for each product by using Gurobi 7.5.1 solver on MPL 5.0 software with 10 hours time limitation. The input data of the models are determined by using SolidCAM software, which is also used by the company for their production process.

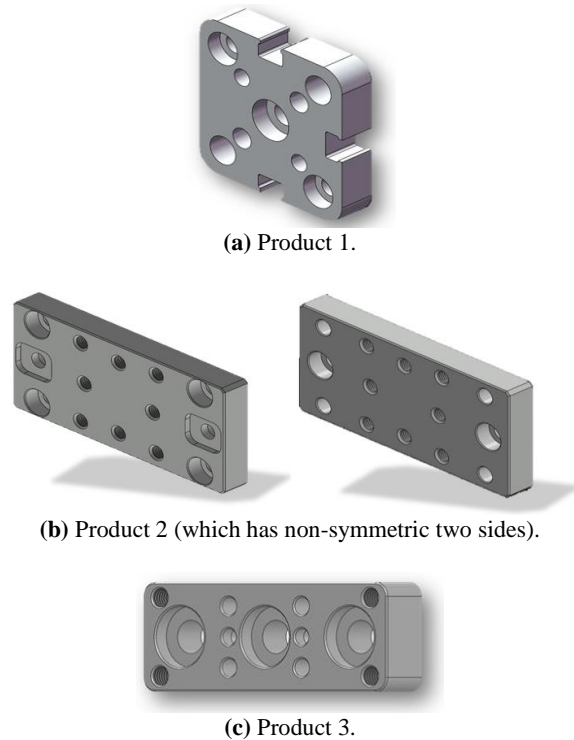


**Figure 4.** Solid models of the products considered for computational studies.

Following the Gurobi computations, the MSBO is performed for the TPOP problems of the company. Results of the Gurobi solver and MBSO are shown in Table 6. Additionally, operational times of the

productions carried out by the company are presented in Table 6, and percentage improvements provided by the Gurobi and MBSO are pointed out in the columns named "Imp%".

**Table 6.** Gurobi and MBSO results for three products.

| Product   | Operational time<br>of company | Gurobi Solution         |      |                 | MBSO   |      |        |          |      |
|-----------|--------------------------------|-------------------------|------|-----------------|--------|------|--------|----------|------|
|           |                                | Result<br>(Upper Bound) | Imp% | CPU<br>Time (s) | Best   | Imp% | Mean   | Time (s) | Std  |
| Product 1 | 108.92                         | 108.48                  | 0.40 | 108.52          | 108.48 | 0.40 | 108.48 | 6.34     | 0.0  |
| Product 2 | 78.78                          | 77.03                   | 2.22 | 36 000.00       | 75.59  | 4.05 | 75.61  | 56.07    | ~0.0 |
| Product 3 | 110.71                         | 109.69                  | 0.92 | 36 000.00       | 109.69 | 0.92 | 109.7  | 35.03    | ~0.0 |

It should be concluded from Table 6 that an optimum solution is found by Gurobi for only product 1. For the other two problems, the computations are terminated at the end of the time limit and, upper bounds of the solution are taken into account for the comparisons. According to the Gurobi results, an improvement with up to 2.22% is provided for the drilling operations of the company. On the other hand, MBSO could find the optimum solution for product 1 and better result than the upper bound of the Gurobi solutions for product 2 (with 4.05% improvement). Regarding the average computational times of the MBSO, it should be noted that better results can be obtained by the proposed algorithm in shorter CPU times with respect to the Gurobi solver. As a result of the computational studies for these parts, it should be noted that considerable variable cost savings are provided for the company since these products are produced over than thousands in a year.

### 5.3. Managerial insights

The computational results of the MBSO show the efficiency and the robustness of the proposed solution methodology. Similar to most of the meta-heuristic algorithm, the tuned parameter set directly affects the performance of the algorithm. Therefore, a preliminary study is made in order to find the best parameter values for the MBSO. On the other hand, computational studies on the SOP dataset show that the local search procedure significantly affects the performance of the MBSO. Particularly, MBSO with the insertion move, and the combination of insertion-swap move show superior performance. Although, these procedures increase the computational times of the algorithm, with reasonable time limits better results can be obtained by using both local searches.

Another interesting observation of the results is the stability of the MBSO solutions. It can be clearly seen from the computations that the standard deviations of most of the results are 0. Comparing with the ACS results, a less standard deviation is observed by MBSO for 6 of 8 instances.

When the results of the case-stud are analyzed, an improvement is provided by the MBSO for each case

even though the number of problems is limited with three product types. For these experiments, the most significant saving is provided on the largest problem. Furthermore, the MBSO outperforms the Gurobi regarding both the results and CPU times.

As a consequence, the MBSO can be efficiently used in the optimization of CNC operations at the tactical and operational decision-making level. In particular, the proposed MBSO is capable of finding the optimal or near-optimal solution for the real-life TPOPs for the CNC machines. Since an improvement on a process in mass production system provides considerable cost savings for the companies, the proposed study has a potential to take forward the researches on this field. In practice, considering that such production parts consist of numerous CNC operations, operational times and machining costs can be significantly reduced by the MBSO.

### 6. Conclusion

This paper addresses the TPOP in CNC milling machines to improve the internal operational efficiency of a company. To find the best tool path in the CNC machines, the mathematical model of the problem is formulated based on the assumptions of PCTSP. With this assumption, tool movement between two operational points is allowed if the successor operation is not the precedence of the predecessor operations. To efficiently solve the considered problem, a newly developed SBO is taken into account and modified its original version with discretization and local search procedures. The computational studies for the proposed MSBO are formed into two parts. In the first part, the MSBO is carried out on a well-known benchmark problem set introduced for the PCTSP, and compared with two recent meta-heuristic algorithms. Results of these computations show that the proposed MSBO is capable of finding efficient solution for the TPOP by finding better results with respect to the other two algorithms. Then, the proposed MSBO is applied for real-life drilling operations of three products. For this case, with up to 4.05% improvement on the operational times is achieved by the MSBO.

As a future work, this study can be extended by

considering the following issues. In this study, MBSO is carried out for a set of PCTSP instances, in which the largest problem consists of 100 nodes. Thereupon, the proposed MBSO can be carried out for the larger PCTSPs, and its efficiency can be analyzed. On the other hand, the MBSO can be improved with additional search strategies since only insertion and swap operations are used in the MBSO. Finally, other bio-inspired algorithms can be modified for the PCTSP, and detailed comparative analysis can be reported.

### Acknowledgments

The authors thank to company consultants Mr. Mustafa Karataş who have shared their experiences and knowledge, and also to the employees of HID-TEK for their support.

### References

- [1] Bohez, E., Makhanov, S.S., Sonthipaumpoon, K. (2000). Adaptive nonlinear tool path optimization for five-axis machining. *International Journal of Production Research*, 38(17), 4329-4343.
- [2] Makhanov, S.S., Batanov, D., Bohez, E., Sonthipaumpoon, K., Anotai, W. (2002). On the tool-path optimization of a milling robot. *Computers and Industrial Engineering*, 43(3), 455-472.
- [3] Chandrasekaran, M., Muralidhar, M., Murali Krishna, C., Dixit, U.S. (2010). Application of soft computing techniques in machining performance prediction and optimization: A literature review. *The International Journal of Advanced Manufacturing Technology*, 46(5-8), 445-464.
- [4] D'Souza, K., Castelino, R., Wright, P.K. (2003). Tool-path optimization for minimizing airtime during machining. *Journal of Manufacturing Systems*, 22, 173-180.
- [5] Park, K.S., Kim, S.H. (1998). Artificial intelligence approaches to determination of CNC machining parameters in manufacturing: A review. *Artificial Intelligence in Engineering*, 12(1-2), 127-134.
- [6] Lasemi, A., Xue, D., Gu, P. (2010). Recent development in CNC machining of freeform surfaces: A state-of-the-art review. *Computer-Aided Design*, 42(7), 641-654.
- [7] Lazoglu, I., Manav, C., Murtezaoglu, Y. (2009). Tool path optimization for free form surface machining. *CIRP Annals*, 58(1), 101-104.
- [8] Oysu, C., Bingul, Z. (2009). Application of heuristic and hybrid-GASA algorithms to tool-path optimization problem for minimizing airtime during machining. *Engineering Applications of Artificial Intelligence*, 22(3), 389-396.
- [9] Dewil, R., Küçükoğlu, İ., Luteyn, C., Cattrysse, D. (2018). A critical review of multi-hole drilling path optimization. *Achieves of Computational Methods in Engineering*, In Press, 1-11.
- [10] Abidin, N.W.Z., Ab Rashid, M.F.F., Mohamed, N.M.Z.N. (2017). A review of multi-holes drilling path optimization using soft computing approaches. *Achieves of Computational Methods in Engineering*, In Press, 1-12.
- [11] Narooei, K.D., Ramli, R., Nizam, M., Rahman, A., Ibrahım, F., Qudeiri, J.A. (2014). Tool routing path optimization for multi-hole drilling based on ant colony optimization. *World Applied Sciences Journal*, 32(9), 1894-1898.
- [12] Linn, R.J., Liu, J., Kowe, P.S.H (1999). Efficient heuristics for drilling route optimization in printed circuit board manufacturing. *Journal of Electronics Manufacturing*, 8(2), 127-138.
- [13] Kolahan, F., Liang, M. (2000). Optimization of hole-making operations: A tabu search approach. *International Journal of Machine Tools and Manufacture*, 40(12), 1735-1753.
- [14] Abbas, A.T., Aly, M.F., Hamza, K. (2011). Optimum drilling path planning for a rectangular matrix of holes using ant colony optimization. *International Journal of Production Research*, 49(19), 5877-5891.
- [15] Montiel-Ross, O., Medina-Rodríguez, N., Sepúlveda, R., Melin, P. (2012). Methodology to optimize manufacturing time for a CNC using a high performance implementation of ACO. *International Journal of Advanced Robotic Systems*, 9, 1-10.
- [16] Zhu, G.-Y., Zhang, W.-B. (2008). Drilling path optimization by the particle swarm optimization algorithm with global convergence characteristics. *International Journal of Production Research*, 46(8), 2299-2311.
- [17] Onwubolu, G.C., Clerc, M. (2004). Optimal path for automated drilling operations by a new heuristic approach using particle swarm optimization. *International Journal of Production Research*, 42(3), 473-491.
- [18] Dalavi, A.M., Pawar, P.J., Singh T.P. (2016). Optimal sequence of hole-making operations using particle swarm optimisation and shuffled frog leaping algorithm. *Engineering Review*, 36(2), 187-196.
- [19] Kumar, A., Pachauri, P.P. (2012). Optimization drilling sequence by genetic algorithm. *International Journal of Scientific Research Publications*, 2(9), 1-7.
- [20] Nabeel, P., Abid, K., Abdulrazzaq, H.F. (2014). Tool path optimization of drilling sequence in CNC machine using genetic algorithm. *Innovation System Design and Engineering*, 5(1), 15-26.
- [21] Khalkar, S., Yadav, D., Singh, A. (2015). Optimization of hole making operations for sequence precedence constraint. *International Journal of Innovative and Emerging Research in Engineering*, 2(7), 26-31.
- [22] Pezer, D. (2016). Efficiency of tool path optimization using genetic algorithm in relation to the optimization achieved with the CAM software.

- Procedia Engineering*, 149, 374-379.
- [23] Raja, C.K.B., Saravanan, M. (2017). Genetic algorithm for TSP in optimizing CNC tool path. *International Journal of Engineering Technology, Management and Applied Sciences*, 5(2), 139-146.
- [24] Tamjidy, M. (2015). Biogeography based optimization (BBO) algorithm to minimize non-productive time during hole-making process. *International Journal of Production Research*, 53(6), 1880-1894.
- [25] Kanagaraj, G., Ponnambalam, S.G., Loo, C.K. (2015). Charged system search algorithm for robotic drill path optimization. *Proceedings of the 2015 International Conference on Advanced Mechatronic Systems, Beijing, China*, 125-130.
- [26] Lim, W.C.E., Kanagaraj, G., Ponnambalam, S.G. (2016). A hybrid cuckoo search-genetic algorithm for hole-making sequence optimization, *Journal of Intelligent Manufacturing*, 27, 417-429.
- [27] Zhang, W.-B., Zhu, G.-Y. (2018). Drilling path optimization by optimal foraging algorithm. *IEEE Transactions on Industrial Informatics*, 14(7), 2847-2856.
- [28] Moosavi, S.H.S., Bardsiri, V.K. (2017). Satin bowerbird optimizer: A new optimization algorithm to optimize ANFIS for software development effort estimation. *Engineering Applications of Artificial Intelligence*, 60, 1-15.
- [29] Kubo, M., Kasugai, H. (1991). The precedence constrained traveling salesman problem. *Journal of the Operations Research*, 34(2), 152-172.
- [30] Miller, C.E., Tucker, A.W., Zemlin, R.A. (1960). Integer programming formulation of traveling salesman problems. *Journal of the ACM*, 7(4), 326-329.
- [31] Bellmore, M., Nemhauser, G.L. (1968). The traveling salesman problem: A Survey. *Operations Research*, 16(3), 538-558.
- [32] Crawford, B., Soto, R., Astorga, G., Garcia, J., Castro, C., Paredes, F. (2017). Putting continuous metaheuristics to work in binary search spaces. *Hindawi-Complexity*, 2017, 1-17.
- [33] Tasgetiren, M.F., Liang, Y.-C., Sevkli, M., Gencyilmaz, G. (2007). A particle swarm optimization algorithm for makespan and total flowtime minimization in the permutation flowshop sequencing problem. *European Journal of Operational Research*, 177, 1930-1947.
- [34] Sung, J., Jeong, B. (2014). An adaptive evolutionary algorithm for travelling salesman problem with precedence constraints. *Hindawi-The Scientific World Journal*, 2014, 1-11.
- [35] Skinderowicz, E. (2017). An improved ant colony system for the sequential ordering problem. *Computers and Operations Research*, 86, 1-17.
- Ilker Kucukoglu** is a Research Assistant in the Industrial Engineering Department of Bursa Uludag University, Turkey. He received his BS from Gazi University (2008), his MS from Bursa Uludag University (2010) and his Ph.D. from Bursa Uludag University (2015) – all in Department of Industrial Engineering. His research interests include supply chain management, vehicle routing, green logistics, heuristic methods, optimization, and mathematical modelling.
- Tulin Gunduz** is currently an Associate Professor in the Department of Industrial Engineering at the Bursa Uludag University. She completed her undergraduate, master's and Ph.D. degrees in 1995, 1998 and 2005, respectively, at Bursa Uludag University, Department of Mechanical Engineering. Her Ph.D. was on Ergonomics. Her research interests are ergonomics, driver comfort, anthropometry, cognitive science and Industry 4.0
- Fatma Balkancioglu** is an Industrial Engineer and received her BS degree from Bursa Uludag University (2018).
- Emine Chousein Topal** is a BS student in Bursa Uludag University Industrial Engineering department.
- Oznur Sayim** is a BS student in Bursa Uludag University Industrial Engineering department.



## RESEARCH ARTICLE

## Maintenance of the latent reservoir by pyroptosis and superinfection in a fractional order HIV transmission model

Ana R.M. Carvalho <sup>a</sup> , Carla M.A. Pinto <sup>\*b</sup>  and João Nuno Tavares <sup>c</sup> 

<sup>a</sup>Faculty of Sciences, University of Porto, Rua do Campo Alegre s/n, 4440-452 Porto, Portugal

<sup>b</sup>School of Engineering, Polytechnic of Porto, Center for Mathematics of the University of Porto, Rua Dr António Bernardino de Almeida 431, 4249-015 Porto, Portugal

<sup>c</sup>Faculty of Sciences, University of Porto, Rua do Campo Alegre s/n, 4440-452 Porto, Portugal  
[up200802541@fc.up.pt](mailto:up200802541@fc.up.pt), [cap@isep.ipp.pt](mailto:cap@isep.ipp.pt), [jntavar@fc.up.pt](mailto:jntavar@fc.up.pt)

## ARTICLE INFO

## Article History:

Received 25 July 2018

Accepted 19 November 2018

Available 27 July 2019

## Keywords:

Latent reservoir

Pyroptosis

Superinfection

HIV

Fractional model

AMS Classification 2010:

26A33; 92D30; 34A08; 34K20

## ABSTRACT

We focus on the importance of pyroptosis and superinfection on the maintenance of the human immunodeficiency virus (HIV) latent reservoir on infected patients. The latent reservoir has been found to be crucial to the persistence of low levels of viral loads found in HIV-infected patients, after many years of successfully suppressive anti-retroviral therapy (ART). This reservoir seems to act as an archive for strains of HIV no longer dominant in the blood, such as wild-type virus. When a patient decides to quit therapy there is a rapid turnover and the wild-type virus re-emerges. Thus, it is extremely important to understand the mechanisms behind the maintenance of this reservoir. For that, we propose a fractional order model for the dynamics of HIV, where pyroptosis and superinfection are considered. The model is simulated for biological meaningful parameters and interesting patterns are found. Our results are interpreted for clinical appreciation.



### 1. Introduction

HIV is associated with impairment and destruction of the immune system's response, mostly by depletion of CD4<sup>+</sup> T cells. HIV infects several types of these cells, but its primary targets are the CD4<sup>+</sup> T helper cells. The depletion of these cells may have destructive effects in immune regulation [1]. These include reduced antibody development capacity for new attackers, abnormal function of macrophages and decrease in production of chemical messengers.

A fraction of HIV infected CD4<sup>+</sup> T cells enter a latency state. In this state, the cells do not produce new virus. HIV can remain inside these cells for years, forming reservoirs, which constitute major obstacles for the eradication of HIV. Cells in the latent state escape treatment for HIV. Current anti-retroviral drugs can suppress HIV to

undetectable levels, but cannot completely eradicate it [2]. Latently infected cells may be infected by HIV, although with slower kinetics than activated T cells. Productive superinfection of these latent cells would eliminate virus genome through cell death. A similar effect may be obtained from the induction of pyroptosis of latent cells, in cell-to-cell transmission. Pyroptosis is a process which leads to the destruction of latent T cells, by causing an intensely inflammatory form of programmed cell death, where cytoplasmic contents and pro-inflammatory cytokines are released [3].

Mathematical models have largely been used to predict the dynamics of infections. In 2006, Kim *et al* [4] study the factors influencing the persistence of the latent reservoir and of low viral load in HIV infected patients, under anti-retroviral therapy (ART). They consider that T

\*Corresponding Author

cells can undergo bystander proliferation, without producing active virus, and assume that the latent cells' activation rate decreases with time on ART. The results of the model point to a combined contribution of intrinsic physiological patients' parameters, such as the minimum activation rate or the net regeneration rate of latently infected cells, to explain the persistence of the latent reservoir and of low viral loads. In 2009, Rong *et al* [5] review several mathematical models for HIV dynamics proposed in the literature. They focus on the quantitative events underlying HIV latency, on the reservoir stability, on the low-level viremia persistence and on the emergence of intermittent viral blips. The authors also distinguish treatment options for each case. In 2015, Wang *et al* [6] develop a mathematical model to study the pyroptosis mechanism, a programmed cell death, and show how pyroptosis explains the slow time scale of CD4<sup>+</sup> T cells depletion and its contribution to the persistence of latently infected cells. Conway *et al* [7] describe a mathematical model for the dynamics of HIV to capture the interactions between target cells, productively infected cells, latently infected cells, virus, and cytotoxic T lymphocytes (CTLs). The model provides a CTL response interval for which patients either present viral rebound or post-treatment control, depending on the size of the latent reservoir when treatment finishes. Outside this interval, for lower values, the patients always rebound and for higher values the patients behave as elite controllers. In 2017, Wodarz *et al* [8] use mathematical models to explain the fundamental mechanisms of the size and of the composition of the latent reservoir in HIV infection. The analysis of the model suggests that though pyroptosis/superinfection are significant factors that influence the dynamics of latency, additional mechanisms might also play a significant role. In particular, abortative infections, higher activation status of cells due to high virus load, the carrying capacity of the latent reservoir.

### 1.1. Fractional calculus

Many mathematical models have a close proximity to reality, however, they are not able to describe it perfectly. Therefore, there is a need to build more accurate models, with the aim of providing better fittings to real data. As such, the Fractional Calculus is one of the most precise tools to refine the description of a series of phenomena present in the most diverse areas of knowledge, namely in engineering, physics, biology, and others [9–14].

There are several and important definitions for a fractional order derivative. The most well-studied are the Riemann-Liouville (RL), the Grünwald-Letnikov (GL), and the Caputo formula (C). We consider the interval  $(0, t)$  instead of  $(a, t)$ , for simplification. Now, let  $y(\tau)$  be a smooth function in every interval  $(0, t)$ ,  $t \leq T$ . The RL definition reads:

$$D_{RL}^{\alpha}y(t) = \begin{cases} \frac{1}{\Gamma(m-\alpha)} \frac{d^m}{dt^m} \int_0^t \frac{y(\tau)}{(t-\tau)^{\alpha+1-m}}, & m-1 \leq \alpha < m \\ \frac{d^m y(t)}{dt^m}, & \alpha = m \end{cases}$$

The Caputo definition is written as:

$$D_C^{\alpha}y(t) = \begin{cases} \frac{1}{\Gamma(m-\alpha)} \int_0^t \frac{y^m(\tau)}{(t-\tau)^{\alpha+1-m}}, & m-1 \leq \alpha < m \\ \frac{d^m y(t)}{dt^m}, & \alpha = m \end{cases}$$

The GL definition is equivalent to the RL formula and is based on finite differences. It is given by:

$$D_{GL}^{\alpha}y(t) = \lim_{h \rightarrow 0} h^{-\alpha} \sum_{k=0}^n (-1)^k \frac{\Gamma(\alpha+1)}{k! \Gamma(\alpha-k+1)} y(x-kh), \quad nh = x.$$

Diethelm [10] demonstrates that a non-integer order model simulates the dynamics of data from the 2009 outbreak of dengue fever, on the Cape Verde islands, more accurately than an integer first order model. The author also shows that the dynamics of the human and of the mosquito populations are modeled by different orders of the fractional derivative. In 2017, Pinto *et al* [11] study a fractional order model for HIV infection where the dynamics of the latent CD4<sup>+</sup> T cells, macrophages and cytotoxic T lymphocytes (CTLs) are considered. The simulations of the model suggest that the order of the fractional derivative is associated to a decrease in the severity of the disease. Namely, are observed decreased values of infected CD4<sup>+</sup> T cells and virus with  $\alpha$ . Moreover, the results of the simulations of the model for relevant parameters, such as the fraction of uninfected CD4<sup>+</sup> T cells that become latently infected, and the CTLs proliferation rate due to infected CD4<sup>+</sup> T cells, are biologically acceptable, for all values of  $\alpha$ . Arshad *et al* [13] present a non-integer order mathematical model for HIV infection, to study the degree of T cell depletion caused by viral cytopathology. The results of the model point to the use of the fractional derivative as a parameter to vary to provide better fits to the data of each HIV infected individual. Each individual has its own specificities which are better captured by a non-integer model. Moreover, these models can help doctors choosing the optimal dosage and verify its effects for each individual.

With the aforesaid ideas in mind, in this paper, we propose a fractional order model for HIV dynamics, where latency, pyroptosis and superinfection are considered. The model is given in Section 2. Its reproduction number and the stability of the disease-free equilibrium are done in Section 3. In Section 4, we analyze the global stability of the disease free equilibrium, and the sensitivity analysis is done in Section 5. In Section 6, we simulate the model for epidemiologically relevant parameters and discuss the results. Finally in Section 7, we state the main conclusions of this work.

## 2. The model

The uninfected CD4<sup>+</sup> T cells,  $T(t)$ , are produced at rate  $s$  and die at rate  $d$ . These cells proliferate exponentially at a rate  $r$ , until reaching the carrying capacity  $K$ . They are infected by HIV or by infected CD4<sup>+</sup> T cells at rates  $\beta$  and  $\beta_1$ , respectively. A fraction,  $(1-q)$ , of infected CD4<sup>+</sup> T cells becomes latently infected,  $L(t)$ , and the other fraction,  $q$ , is actively infected,  $I(t)$ . The latently infected CD4<sup>+</sup> T cells become productively infected at a rate  $g$  and die at a rate  $a_L$ . The latently infected cells can be successfully superinfected by productive virus at rate  $f q \beta$ . As the productive infection rate of latently CD4<sup>+</sup> T cells is lower than that of infected CD4<sup>+</sup> T cells, we considered the parameter  $f < 1$ . When infected by CD4<sup>+</sup> T cells, the latently CD4<sup>+</sup> T cells die by pyroptosis, which is a form of cell death. Thus, cell-to-cell transmission contributes for cells' death at rate  $\beta_1$ . The infected CD4<sup>+</sup> T cells,  $I(t)$ , die at a rate  $a_I$ . HIV,  $V(t)$ , is produced by the infected CD4<sup>+</sup> T cells at a rate  $p$  and is cleared at a rate  $c$ . The nonlinear system of fractional-order differential equations describing the dynamics of the model is given by:

$$\begin{aligned} \frac{d^\alpha T}{dt^\alpha} &= s^\alpha - d^\alpha T + r^\alpha T \left(1 - \frac{T}{K}\right) - \beta^\alpha TV - \beta_1^\alpha TI \\ \frac{d^\alpha L}{dt^\alpha} &= (1-q)(\beta^\alpha TV + \beta_1^\alpha TI) - a_L^\alpha L - f q \beta^\alpha LV - \beta_1^\alpha LI - g^\alpha L \\ \frac{d^\alpha I}{dt^\alpha} &= q(\beta^\alpha TV + \beta_1^\alpha TI) - a_I^\alpha I + f q \beta^\alpha LV + g^\alpha L \\ \frac{d^\alpha V}{dt^\alpha} &= p^\alpha I - c^\alpha V \end{aligned} \quad (1)$$

where  $\alpha \in (0, 1]$  is the order of the fractional derivative, and  $\cdot^\alpha$  represents the  $\cdot$  to the power of  $\alpha$ . When  $\alpha = 1$ , then the model is the integer order counterpart. The fractional derivative of the proposed model is used in the Caputo sense.

## 3. Reproduction number

In this section, we compute the reproduction number of model (1),  $R_0$ , and the local stability of its disease-free equilibrium. The basic reproduction number is defined as the number of CD4<sup>+</sup> T cells which are infected by one single cell entering a completely susceptible population. We begin by computing the reproduction number of system (1),  $R_0$ . We use the next generation method [15]. The disease-free equilibrium of model (1) is given by:

$$\begin{aligned} P_0 &= (T_0, L_0, I_0, V_0) \\ &= \left( \frac{K^\alpha \left[ r^\alpha - d^\alpha + \sqrt{(r^\alpha - d^\alpha)^2 + \frac{4r^\alpha s^\alpha}{K}} \right]}{2r^\alpha}, 0, 0, 0 \right) \end{aligned} \quad (2)$$

Using the notation in [15] on system (1), matrices for the new infection terms,  $F$ , and the other terms,  $V$ , are given by:

$$\begin{aligned} F &= \begin{pmatrix} 0 & (1-q)\beta_1^\alpha T_0 & (1-q)\beta^\alpha T_0 \\ 0 & q\beta_1^\alpha T_0 & q\beta^\alpha T_0 \\ 0 & 0 & 0 \end{pmatrix} \\ V &= \begin{pmatrix} g^\alpha + a_L^\alpha & 0 & 0 \\ -g^\alpha & a_I^\alpha & 0 \\ 0 & -p^\alpha & c^\alpha \end{pmatrix} \end{aligned}$$

The associative basic reproduction number is written as:

$$R_0 = \rho(FV^{-1}) = \frac{T_0(p^\alpha \beta^\alpha + c^\alpha \beta_1^\alpha)(q a_L^\alpha + g^\alpha)}{c^\alpha a_I^\alpha (g^\alpha + a_L^\alpha)} \quad (3)$$

where  $\rho$  indicates the spectral radius of  $FV^{-1}$ .

The linearization matrix of model (1) around the disease-free equilibrium,  $P_0$ , is:

$$M_1 = \begin{pmatrix} -\sqrt{(r^\alpha - d^\alpha) + \frac{4r^\alpha s^\alpha}{K}} & 0 & -\beta_1^\alpha T_0 & -\beta^\alpha T_0 \\ 0 & -a_L^\alpha - g^\alpha & (1-q)\beta_1^\alpha T_0 & (1-q)\beta^\alpha T_0 \\ 0 & g^\alpha & q\beta_1^\alpha T_0 - a_I^\alpha & q\beta^\alpha T_0 \\ 0 & 0 & p^\alpha & -c^\alpha \end{pmatrix}$$

Stability of  $P_0$  can be determined using the following lemmas:

**Lemma 1.** (Theorem 2, [16])

Let  $\alpha \left( = \frac{p}{q} \right)$  where  $p, q \in \mathbb{Z}^+$  and  $\gcd(p, q) = 1$ . Define  $M = q$ , then the disease-free equilibrium  $P_0$  of the system (1) is asymptotically stable if  $|\arg(\lambda)| > \frac{\pi}{2M}$  for all roots  $\lambda$  of the following equation

$$\det(\text{diag}[\lambda^{M\alpha} \lambda^{M\alpha} \lambda^{M\alpha} \lambda^{M\alpha}] - M_1) = 0$$

**Lemma 2.** The disease-free equilibrium  $P_0$  of the system (1) is unstable if  $R_0 < 1$ .

**Proof.** Expanding,

$$\det (\text{diag} [\lambda^{M\alpha} \lambda^{M\alpha} \lambda^{M\alpha} \lambda^{M\alpha}] - M_1) = 0$$

we have the following equation in terms of  $\lambda$ :

$$\begin{aligned} & [\lambda^{M\alpha} + \sqrt{(r^\alpha - d^\alpha) + \frac{4r^\alpha s^\alpha}{K}}] [\lambda^{3M\alpha} + (a_L^\alpha + g^\alpha + a_I^\alpha + c^\alpha - q\beta_1^\alpha T_0) \lambda^{2M\alpha} \\ & + (c^\alpha(a_L^\alpha + g^\alpha + a_I^\alpha) + (a_L^\alpha + g^\alpha)a_I^\alpha - T_0(\beta_1^\alpha(qc^\alpha + qa_L^\alpha + g^\alpha) + \beta^\alpha qp^\alpha)) \lambda^{M\alpha} \\ & + (a_L^\alpha + g^\alpha)a_I^\alpha c^\alpha(1 - R_0)] = 0 \end{aligned} \tag{4}$$

Now arguments of the roots of the equation,  $\lambda^{M\alpha} + \sqrt{(r^\alpha - d^\alpha) + \frac{4r^\alpha s^\alpha}{K}} = 0$ , are given by:

$$\arg(\lambda_k) = \frac{\pi}{M\alpha} + k \frac{2\pi}{M\alpha} > \frac{\pi}{M} > \frac{\pi}{2M}$$

where  $k = 0, 1, \dots, (M\alpha - 1)$ .

Thus, using Lemma 1, we show that the disease-free equilibrium,  $P_0$ , of system (1) is stable if all roots of the polynomial:

$$\begin{aligned} & \lambda^{3M\alpha} + (a_L^\alpha + g^\alpha + a_I^\alpha + c^\alpha - q\beta_1^\alpha T_0) \lambda^{2M\alpha} + (c^\alpha(a_L^\alpha + g^\alpha + a_I^\alpha) + (a_L^\alpha + g^\alpha)a_I^\alpha \\ & - T_0(\beta_1^\alpha(qc^\alpha + qa_L^\alpha + g^\alpha) + \beta^\alpha qp^\alpha)) \lambda^{M\alpha} + (a_L^\alpha + g^\alpha)a_I^\alpha c^\alpha(1 - R_0) = 0 \end{aligned} \tag{5}$$

have argument greater than  $\frac{\pi}{2M}$ , for  $R_0 < 1$ .

Finally, using Descartes' rule of signs in equation (5), we find that there is exactly one sign change for  $R_0 > 1$ . Thus there is exactly one positive real root of the aforesaid equation for which the argument is less than  $\frac{\pi}{2M}$ . We concluded that, if  $R_0 < 1$ , the disease-free equilibrium  $P_0$  of the system (1) is stable.  $\square$

#### 4. Global stability of the disease-free equilibria

In this section, we compute the global stability of the disease-free equilibrium of the model (1). We rewrite model (1) as:

$$\begin{aligned} \frac{d^\alpha X}{dt^\alpha} &= F(X, Z) \\ \frac{d^\alpha Z}{dt^\alpha} &= G(X, Z), \quad G(X, 0) = 0 \end{aligned} \tag{6}$$

where  $X = T$  and  $Z = (L, I, V)$ , with  $X \in \mathbf{R}_+$  being the number of uninfected  $CD4^+$  T cells and  $Z \in \mathbf{R}_+^3$  denoting the number of latent and infected  $CD4^+$  T cells, and virus.

The disease-free equilibrium is written as  $U = (X^*, 0)$ , where  $X^* = \left( \frac{K^\alpha \left[ r^\alpha - d^\alpha + \sqrt{(r^\alpha - d^\alpha)^2 + \frac{4r^\alpha s^\alpha}{K}} \right]}{2r^\alpha}, 0 \right)$ .

The conditions  $(H_1)$  and  $(H_2)$  must be met to guarantee the global asymptotic stability of the disease-free equilibrium of the model (1):

$$\begin{aligned} (H_1) : & \text{ For } \frac{d^\alpha X}{dt^\alpha} = F(X, 0), \\ & X^* \text{ is globally asymptotically stable} \end{aligned} \tag{7}$$

$$\begin{aligned} (H_2) : & G(X, Z) = AZ - \hat{G}(X, Z), \quad \hat{G} \geq 0, \\ & \text{ for } (X, Z) \in \Upsilon_1 \end{aligned}$$

where  $A = D_Z G(X^*, 0)$  is a M-matrix (the off-diagonal elements of  $A$  are non-negative) and  $\Upsilon_1$  is the region where the model makes biological sense. If the system (6) satisfies the conditions in (7) the following theorem holds.

**Theorem 1.** *The fixed point  $U = (X^*, 0)$  is a globally asymptotically stable equilibrium of the system (6) provided that  $R_0 < 1$  and that the assumptions in (7) are satisfied.*

**Proof.** Let

$$F(X, 0) = \left( s^\alpha - d^\alpha T + r^\alpha T \left( 1 - \frac{T}{K} \right) \right) \tag{8}$$

and

$$A = \begin{pmatrix} -g^\alpha - a_L^\alpha & (1 - q)\beta_1^\alpha T_0 & (1 - q)\beta^\alpha T_0 \\ g^\alpha & q\beta_1^\alpha T_0 - a_I^\alpha & q\beta^\alpha T_0 \\ 0 & p^\alpha & -c^\alpha \end{pmatrix} \tag{9}$$

and

$$\begin{aligned} \hat{G}(X, Z) &= \begin{pmatrix} \hat{G}_1(X, Z) \\ \hat{G}_2(X, Z) \\ \hat{G}_3(X, Z) \end{pmatrix} \\ &= \begin{pmatrix} (1 - q)T_0 \left( 1 - \frac{T}{T_0} \right) (\beta_1^\alpha I + \beta^\alpha V) + fq\beta^\alpha LV + \beta_1^\alpha LI \\ qT_0 \left( 1 - \frac{T}{T_0} \right) (\beta_1^\alpha I + \beta^\alpha V) - fq\beta^\alpha LV \\ 0 \end{pmatrix} \end{aligned} \tag{10}$$

Thus  $\hat{G}_1(X, Z), \hat{G}_2(X, Z) \geq 0$  and  $\hat{G}_3(X, Z) = 0 \Rightarrow \hat{G}(X, Z) \geq 0$ . Conditions in (7) are satisfied, thus the disease-free equilibrium of the model (1) is globally asymptotically stable for  $R_0 < 1$ .  $\square$

#### 5. Sensitivity analysis

In this section we compute the sensitivity indexes of the reproduction number,  $R_0$  (1). Sensitivity indexes are given in Table 1 and provide information on the variation of the value of  $R_0$  as a function of each parameter. We follow the procedure proposed in [17]. Generically, when  $R_0 > 1$ , the epidemics spreads, on the other hand, for  $R_0 < 1$  the epidemics halts.

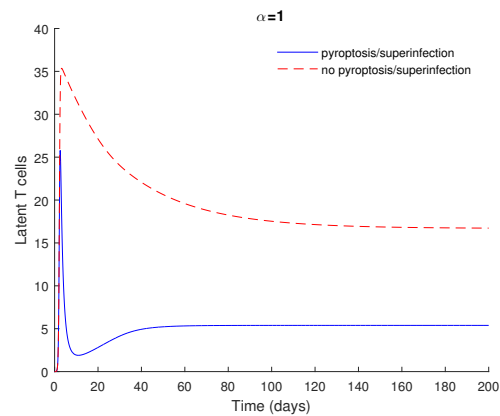
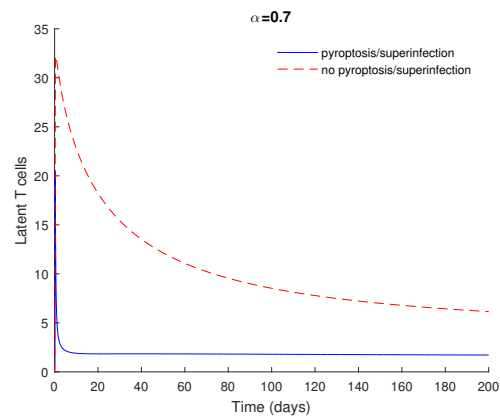
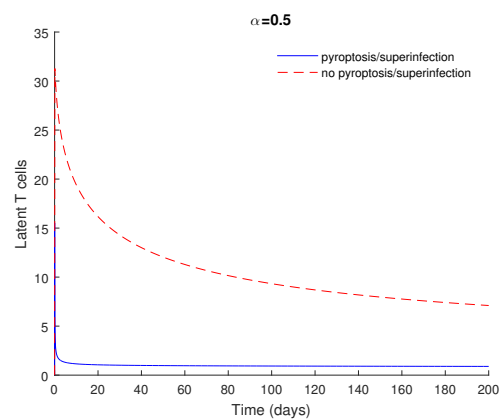
**Table 1.** Sensitivity indexes for relevant parameters of model (1).

| Parameter | Sensitivity index sign |
|-----------|------------------------|
| $\beta$   | +                      |
| $\beta_1$ | +                      |
| $p$       | +                      |
| $q$       | +                      |
| $g$       | +                      |
| $c$       | -                      |
| $a_L$     | -                      |
| $a_I$     | -                      |

## 6. Numerical results

We simulate the model (1) for different values of the order of the fractional derivative,  $\alpha$  and for epidemiologically valid parameters. The parameters used in the simulations, based on [7, 8], are:  $s = 10 \text{ day}^{-1}$ ,  $d = 0.015 \text{ day}^{-1}$ ,  $r = 0.03 \text{ day}^{-1}$ ,  $K = 1500 \text{ mm}^{-3}$ ,  $\beta = 0.0001 \text{ mm}^3 \text{ day}^{-1}$ ,  $\beta_1 = 0.0001 \text{ mm}^3 \text{ day}^{-1}$ ,  $q = 0.95$ ,  $g = 0.001 \text{ day}^{-1}$ ,  $a_L = 0.03 \text{ day}^{-1}$ ,  $f = 1/7$ ,  $a_I = 0.45 \text{ day}^{-1}$ ,  $p = 2000 \text{ day}^{-1}$ ,  $c = 23 \text{ day}^{-1}$ , and the initial conditions are:  $T(0) = 700$ ,  $L(0) = I(0) = 0$  and  $V(0) = 10$ .

Figures 1-3 depict the number of latently infected cells in the cases of existence and absence of pyroptosis/superinfection. It is observed a higher number of latent cells when there is no pyroptosis/superinfection, for the three values of the order of the fractional derivative,  $\alpha$ . In both cases, with and without pyroptosis, there is a first increase in the number of latent cells towards a peak and then a convergence to an asymptotic state. Moreover, the behaviour with pyroptosis/superinfection at  $\alpha = 1$  shows a minimum after the peak and then a rise to the equilibrium state. This may be due to the variation of the HIV viral load, which is related with the phenomenon of pyroptosis/superinfection, as follows. The HIV viral load increase from lower levels is followed by the rise of the latent cells. When the HIV load reaches its peak value, the number of latent cell decreases due to cell death by pyroptosis or by superinfection. As the viral load declines and tends asymptotically to its equilibrium, the latent pool rebounds and increases to some value. Lower viral loads are associated with less pyroptosis and less superinfection, which translates in the perseverance of the latent cells' pool. This rebound feature is rapidly forgotten for smaller values of the order of the fractional derivative  $\alpha$ , probably due to the memory property, which causes transients to be faster in these systems than in integer order ones.

**Figure 1.** Number of latent cells with and without pyroptosis/superinfection, for  $\alpha = 1$ . Parameter values and initial conditions in the text.**Figure 2.** Number of latent cells with and without pyroptosis/superinfection, for  $\alpha = 0.7$ . Parameter values and initial conditions in the text.**Figure 3.** Number of latent cells with and without pyroptosis/superinfection, for  $\alpha = 0.5$ . Parameter values and initial conditions in the text.

## 7. Conclusion

We proposed a non-integer order mathematical model for HIV infection to study the influence of pyroptosis and superinfection on the maintenance of the latent reservoir. We computed the basic reproduction number and the stability of the disease-free equilibrium. The simulations of the model provide good agreement with experimental data available in the literature concerning the maintenance of the latent reservoir. It is observed that as HIV load increases from lower levels, the latent cells' population also rises. When the viral load reaches its peak, the number of latent cells decreases, due to cell death by pyroptosis and superinfection. As the viral load declines and tends asymptotically to its equilibrium, the latent pool rebounds and increases to some threshold. Thus, pyroptosis and superinfection, are important players in the perseverance of the latent cells' pool in HIV infection.

## Acknowledgment

The authors were partially funded by the European Regional Development Fund through the program COMPETE and by the Portuguese Government through the FCT - Fundação para a Ciência e a Tecnologia under the project PEst-C/MAT/UI0144/2013. The research of AC was partially supported by a FCT grant with reference SFRH/BD/96816/2013.

## References

- [1] Perelson, A.S., Kirschner, D.E & De Boer, R. (1993). Dynamic of HIV infection of CD4+ T cells. *Mathematical Biosciences*, 112, 81-125.
- [2] Chavez, L., Calvanese, V & Verdin, E. (2015). HIV latency is established directly and early in both resting and activated primary CD4 T cells. *PLOS Pathogens*, 11(6), e1004955.
- [3] Doitsh, G., Galloway, N.L.K., Geng, X., Yang, Z., Monroe, K.M., Zepeda, O., Hunt, P.W., Hatano, H., Sowinski, S., Muoz-Arias, I. & Greene, W.C. (2014). Pyroptosis drives CD4 T-cell depletion in HIV-1 infection. *Nature*, 505(7484), 509–514.
- [4] Kim, H. & Perelson, A.S. (2006). Viral and latent reservoir persistence in HIV-1-infected patients on therapy. *PLOS Computational Biology*, 2(10), e135.
- [5] Rong, L. & Perelson, A.S. (2009). Modeling HIV persistence, the latent reservoir, and viral blips. *Journal of Theoretical Biology*, 260, 308–331.
- [6] Wang, S., Hottz, P., Schechter, M. & Rong, L. (2015). Modeling the slow CD4+ T cell decline in HIV-infected individuals. *PLOS Computational Biology*, 11(12), e1004665.
- [7] Conway, J.M. & Perelson, A.S. (2015). Post-treatment control of HIV infection. *Proceedings of the National Academy of Sciences*, 112(17), 5467–5472.
- [8] Wodarz, D., Levy, D.N., Pyroptosis, superinfection, and the maintenance of the latent reservoir in HIV-1 infection. *Nature - Scientific Reports*, 7(1), 1-10 (2017).
- [9] Samko, S., Kilbas, A. & Marichev, O. (1993). *Fractional Integrals and Derivatives: Theory and Applications*. London: Gordon and Breach Science Publishers.
- [10] Diethelm, K. (2013). A fractional calculus based model for the simulation of an outbreak of dengue fever. *Nonlinear Dynamics*, 71, 613–619.
- [11] Pinto, C.M.A. & Carvalho, A.R.M. (2017). A latency fractional order model for HIV dynamics. *Journal of Computational and Applied Mathematics*, 312, 240–256.
- [12] Téjado, I., Valério, D., Pérez, E. & Valério, N. (2017). Fractional calculus in economic growth modelling: the Spanish and Portuguese cases. *International Journal of Dynamics and Control*, 5(1), 208–222.
- [13] Arshad, S., Baleanu, D., Bu, W., Tang, Y., Effects of HIV infection on CD4+ T-cell population based on a fractional-order model. *Advances in Difference Equations*, 2017(92), 1–14 (2017).
- [14] Carvalho, A.R.M., Pinto, C.M.A. & Baleanu, D. (2018). HIV/HCV coinfection model: a fractional-order perspective for the effect of the HIV viral load. *Advances in Difference Equations*, 2018(1), 1–22.
- [15] Driessche, P. & Watmough, P. (2002). Reproduction numbers and sub-threshold endemic equilibria for compartmental models of disease transmission. *Mathematical Biosciences*, 180, 29-48.
- [16] Tavazoei, M.S. & Haeri, M. (2008). Chaotic attractors in incommensurate fractional order systems. *Physica D*, 237, 2628–2637.
- [17] Chitnis, N., Hyman, J.M. & Cushing, J.M. (2008). Determining important parameters in the spread of malaria through the sensitivity analysis of a mathematical model. *Bulletin of Mathematical Biology*, 70, 1272–1296.

**Ana R.M. Carvalho** is a Doctor in Mathematics since May 2018. Her current research interests comprise the development of mathematical models for epidemiology. She has more than 20 papers published in international journals and conferences. Her *h*-index is 9 and the *i*-index is 8.

**Carla M.A. Pinto** is an Adjunct Professor of the School of Engineering of the Polytechnic of Porto. She is a Doctor in Mathematics since 2004. Her research interests involve: the study of integer-order and fractional order models, using bifurcation theory, stability theory, numerical simulations. Applications: epidemiology, robotics, engineering. She has published original research in several high impact international journals and international conferences. She is Associate Editor of International Journals, has been member of the Scientific Committee and of the International Program Committee of several international conferences, chair

of sessions at international conferences. She has more than 799 citations. Her *h*-index is 15 and the *i*-index is 20.

**João Nuno Tavares** is an Associate Professor at the Faculty of Sciences of the University of Porto (FCUP). He is a Doctor in Physics since 1993. His research interests include recreational mathematics, optimization, computational mathematics, mathematical models in cancer therapy. He is a member of the Scientific Committee of the Department of Mathematics of FCUP since July 2017. He is the Director of the Department of Mathematics since November 2017. He was a member of the Executive Commission of the Department of Mathematics in October 2013, and a member of the Council of Representatives since July 2014. He is the Director of GEMAC - Gabinete de Estatística, Modelação e Aplicações Computacionais. He has organized several international conferences. He publishes papers in international high impact journals.

An International Journal of Optimization and Control: Theories & Applications (<http://ijocta.balikesir.edu.tr>)



This work is licensed under a Creative Commons Attribution 4.0 International License. The authors retain ownership of the copyright for their article, but they allow anyone to download, reuse, reprint, modify, distribute, and/or copy articles in IJOCTA, so long as the original authors and source are credited. To see the complete license contents, please visit <http://creativecommons.org/licenses/by/4.0/>.



## RESEARCH ARTICLE

# The DRBEM solution of Cauchy MHD duct flow with a slipping and variably conducting wall using the well-posed iterations

Cemre Aydin\*  and Munevver Tezer-Sezgin 

Department of Mathematics, Middle East Technical University, Turkey  
 e171938@metu.edu.tr, munt@metu.edu.tr

## ARTICLE INFO

## Article History:

Received 15 August 2018

Accepted 01 February 2019

Available 27 July 2019

## Keywords:

DRBEM

Cauchy problem

MHD duct flow

Slip velocity

Variable conductivity

## AMS Classification 2010:

65N20; 65N21; 65N38

## ABSTRACT

The present study focuses on the numerical investigation of the Cauchy Magneto-hydrodynamic (MHD) duct flow in the presence of an externally applied oblique magnetic field, with a slipping and variably conducting wall portion of the duct walls. The underspecified and overspecified boundary informations for the velocity of the fluid and the induced magnetic field on both slipping and variably conducting duct wall and its opposite part, respectively, constitutes the Cauchy MHD duct flow problem. This study aims to recompute the velocity of the fluid and induced magnetic field with specified slip length and conductivity constant, respectively, on the underspecified wall which is both slipping and variably conducting. The governing coupled convection-diffusion type MHD equations for the direct and inverse formulations are solved in one stroke using the dual reciprocity boundary element method (DRBEM). Both the velocity and induced magnetic field and their normal derivatives to be used as overspecified boundary conditions for the construction of Cauchy problem are obtained through the direct formulation of the problem. The well-posed iterations are used in the regularization of the ill-conditioned systems of linear algebraic equations resulting from the DRBEM discretization of Cauchy problem (inverse problem). Numerical solutions for the slip velocity and induced magnetic field are obtained for Hartmann number values  $M=5, 10, 50$ . The main advantages of the DRBEM are its boundary only nature and the capability of providing both the unknowns and their normal derivatives on the underspecified walls so that the conductivity constant and the slip length between them can be recovered at a low computational expense.



## 1. Introduction

The effects of magnetic field through the electrically conducting fluids, such as electrolytes, blood plasmas, salt waters, liquid metals etc. are concerned by the magneto-hydrodynamics (MHD). The combination of the Navier-Stokes equations of fluid dynamics with the Maxwell's equations of electromagnetism through Ohm's law describes the conducting fluid motion under the impact of externally applied magnetic field. The industrial

and biological applications of the magneto-hydrodynamic fluid flow in channels are generally encountered in the MHD generators, MHD pumps, accelerators, nuclear reactors, and the blood flow pressure measurements [1].

The distance from the fluid to the channel walls within the solid stage where the velocity of the flow diminished is described as the slip length. It is stated that the slip in the MHD flow will likely occur in fusion reactors with liquid metal flows in contact with ceramics as some current experimental data shows. The presence of Dirichlet/Neumann or mixed type boundary conditions

\*Corresponding Author

for the velocity  $V$  and the induced magnetic field  $B$  on the complete channel walls results in direct problems. The slipping velocity is defined with mixed boundary condition as  $V + \alpha \frac{\partial V}{\partial n} = 0$  where  $\alpha$  is the slip length and the variably conducting duct wall is defined with  $B + c \frac{\partial B}{\partial n} = 0$  where  $c$  is the conductivity constant. Exact solutions of the MHD equations exist for some particular duct geometries with no-slip and insulated or perfectly conducting duct walls [1, 2]. Analytical solutions in terms of asymptotic expansions are given by Ligere et. al [3, 4] for MHD duct flow with perfectly conducting Hartmann walls and slipping side walls. The MHD equations are commonly solved using numerical methods in no-slip and most general form of the wall conductivity conditions [5–8]. In some engineering applications some parts of the boundary may allow both the velocity slip and conductivity change depending on the material it is made of. Slip length and conductivity constant on these parts of the boundary can be determined when the MHD flow problem is designed as a Cauchy problem. In this case, the boundary conditions for the velocity of the fluid can be incomplete either in the form of under-specified or over-specified on different parts of the boundary. These are called inverse problems or Cauchy problems and it is well-known that they are generally ill-posed [9]. Therefore, to solve such kind of problems, a regularization technique must be used.

The DRBEM transforms the differential equations defined in the problem region into integral equations defined on the boundary, approximating also the inhomogeneities of the equations using radial basis functions which are related to differential operator with particular solutions. By this way, a system of discretized equations for the boundary nodes and at some selected interior points is solved [10]. One main advantage of BEM or DRBEM is to provide both the unknown and its normal derivative on the boundaries. There are quite a number of BEM or DRBEM solutions of MHD duct flow problems with no-slip velocity condition and different combinations of wall conductivities [5, 6, 8, 11, 12]. In the studies carried by S. Smolentsev and E. Ligere [4, 13], MHD flow problems with slip velocity conditions and with a known slip length in a channel are solved analytically on various parts of the duct walls. The DRBEM solution of Cauchy MHD duct flow equations with a perturbed slipping upper boundary is given in [14] by solving the MHD equations as a whole.

In this paper, the numerical solutions of the direct and Cauchy MHD flow problems are accomplished when one of the channel walls contains both the slip and variably conducting conditions. The slip length and the conductivity constant are assumed to be unknown in the inverse or Cauchy problem and thus, both the velocity, the induced magnetic field and their normal derivatives are going to be determined which are under-specified boundary conditions on that part of the duct walls. When the direct problem is solved for a specified slip length and conductivity constant with Dirichlet type velocity and induced magnetic field conditions, the opposite side of the duct wall contains over-specified conditions (both the velocity, induced magnetic field and their normal derivatives obtained from the direct DRBEM solution). The well-posed iterations are employed to regularize the discretized ill-posed problem resulting from the discretization of Cauchy MHD problem. The numerical results are performed for direct and inverse problems for Hartmann number values  $M = 5, 10, 50$ , and the regularization method is examined in terms of convergence to the solution of direct problem obtained with an estimated slip length and conductivity constant. Also, the slip length and the conductivity constant are regained through the Cauchy MHD flow problem solution on the slipping and variably conducting wall. The DRBEM has the advantage of discretizing only the boundary and providing both the unknowns and their normal derivatives on the boundary which form overdetermined boundary information for the Cauchy MHD flow problem. Thus, it enables us to obtain the solution of Cauchy MHD flow problem at a small computational expense.

## 2. Mathematical formulation of the problem

An electrically conducting fluid is flowing in a long pipe of rectangular cross-section (duct) with a pressure gradient  $\frac{\partial p}{\partial z}$ , and an external uniform magnetic field is applied by forming an angle  $\beta$  with the y-axis. The flow becomes fully developed in the direction of pipe-axis and the problem reduces to two-dimension in the duct. Thus, the two-dimensional, steady and fully developed MHD flow in a rectangular duct under the effect of an externally applied oblique magnetic field is considered [6].

The left vertical wall allows the slip of the fluid and also variable conductivity. The non-dimensional governing equations for the velocity

$V(x, y)$  of the fluid and the induced magnetic field  $B(x, y)$  are [1]

$$\begin{aligned} \nabla^2 V + M_x \frac{\partial B}{\partial x} + M_y \frac{\partial B}{\partial y} &= -1 \\ &\text{in } -1 < x, y < 1 \\ \nabla^2 B + M_x \frac{\partial V}{\partial x} + M_y \frac{\partial V}{\partial y} &= 0 \end{aligned} \tag{1}$$

where  $M_x = M \sin(\beta)$ ,  $M_y = M \cos(\beta)$  and  $M = LB_0 \sqrt{\sigma/\nu\rho} = \sqrt{(M_x)^2 + (M_y)^2}$  is the Hartmann number resulted during the non-dimensionalization of the equations, and  $L$ ,  $B_0$ ,  $\sigma$ ,  $\nu$  and  $\rho$  are the characteristic length, the external magnetic field intensity, electrical conductivity, kinematic viscosity, and the density of the fluid, respectively. The magnetic field applies in the direction obtained with an angle  $\beta$  from the  $y$ -axis.

The physical configuration of the MHD duct flow problem with a slipping and variably conducting left wall leads to the boundary conditions as

$$\begin{aligned} V = 0, B = 0 &\quad \text{on } y = \mp 1, \quad -1 < x < 1 \\ V = 0, B = 0 &\quad \text{on } x = 1, \quad -1 < y < 1 \\ V + \alpha \frac{\partial V}{\partial n} = 0 &\quad \text{on } x = -1, \quad -1 < y < 1 \\ B + c \frac{\partial B}{\partial n} = 0 &\quad \text{on } x = -1, \quad -1 < y < 1. \end{aligned} \tag{2}$$

The main purpose of the study is to regain the slip length and conductivity constant on the slipping and variably conducting portion (left wall) of the duct walls. Hence, the MHD duct flow problem is constructed as a Cauchy problem in terms of the velocity  $V(x, y)$  and the induced magnetic field  $B(x, y)$  as direct and inverse problems configured in Figure 1.

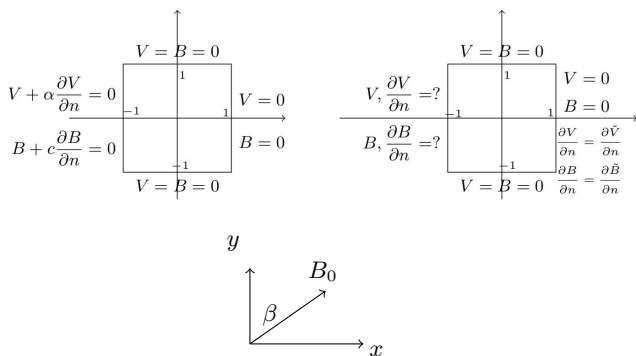


**Figure 1.** Boundary conditions for the direct (left) and the Cauchy (right) problems.  $\tilde{V}$ ,  $\tilde{B}$  denote direct problem solution.

$\alpha$  is the dimensionless slip length and  $c$  is the conductivity constant which are going to be gained from the inverse formulation of the problem. First the MHD problem (1)-(2) is going to be solved for specific values of  $\alpha$  and  $c$ . Then, with the obtained normal derivative values of the velocity and the induced magnetic field on the left wall, the Cauchy problem is constructed.

### 3. The DRBEM application

The DRBEM is applied to the MHD differential equations (1) by using the fundamental solution of the Laplace equation which is  $u^* = \ln(\frac{1}{r})/2\pi$ , [10]. Therefore, the terms other than Laplacian are considered as inhomogeneity and by weighting the equations (1) by  $u^*$  and applying Green's second identity two times, we obtain the following equations

$$\begin{aligned} c_i V_i + \int_{\Gamma} q^* V d\Gamma - \int_{\Gamma} u^* \frac{\partial V}{\partial n} d\Gamma &= \\ \int_{\Omega} (-1 - M \frac{\partial B}{\partial x} - M_y \frac{\partial B}{\partial y}) u^* d\Omega &= \int_{\Omega} b_1 u^* d\Omega \end{aligned} \tag{3}$$

$$\begin{aligned} c_i B_i + \int_{\Gamma} q^* B d\Gamma - \int_{\Gamma} u^* \frac{\partial B}{\partial n} d\Gamma &= \\ \int_{\Omega} (-M_x \frac{\partial V}{\partial x} - M_y \frac{\partial V}{\partial y}) u^* d\Omega &= \int_{\Omega} b_2 u^* d\Omega \end{aligned} \tag{4}$$

where  $q^* = \frac{\partial u^*}{\partial n}$ ,  $\Gamma$  is the boundary  $x = \mp 1, y = \mp 1$ , and the index  $i$  denotes the source point. The constant  $c_i$  is 1/2 and 1 when the source point is on the boundary and in the interior of the domain, respectively.

The right hand side domain integrals contain the inhomogeneities of equations (1) which can be approximated by radial basis functions, e.g,  $f(r) = 1 + r$  which are connected to particular solutions  $\hat{u}_j$ 's with the equation  $\nabla^2 \hat{u}_j = f_j$ . The approximations of the integrands in the domain integrals are given by  $\sum_{j=1}^{N+L} \alpha_j f_j$  and  $\sum_{j=1}^{N+L} \beta_j f_j$  for the equations (3) and (4), respectively, where  $\alpha_j$ 's and  $\beta_j$ 's are undetermined coefficients. The radial basis functions are collocated at the discretized points as  $f_{ij} = 1 + r_{ij}$  giving the coordinate matrix  $F = (f_{ij})$  where  $r_{ij}$  is the distance between the nodes  $i$  and  $j$ ,  $N$  and  $L$  denote the number of boundary and interior nodes, respectively, when the boundary  $\Gamma$  is discretized using  $N$  constant boundary elements. The collocation of the inhomogeneities at  $N + L$  points results in the systems  $F\alpha = b_1$ ,  $F\beta = b_2$ .

Then, the right hand sides of the equations (3)-(4) are rewritten as

$$c_i V_i + \int_{\Gamma} q^* V d\Gamma - \int_{\Gamma} u^* \frac{\partial V}{\partial n} d\Gamma = \sum_{j=1}^{N+L} \alpha_j (c_i \hat{u}_{ij} + \int_{\Gamma} q^* \hat{u}_j d\Gamma - \int_{\Gamma} u^* \frac{\partial \hat{u}_j}{\partial n} d\Gamma) \quad (5)$$

$$c_i B_i + \int_{\Gamma} q^* B d\Gamma - \int_{\Gamma} u^* \frac{\partial B}{\partial n} d\Gamma = \sum_{j=1}^{N+L} \beta_j (c_i \hat{u}_{ij} + \int_{\Gamma} q^* \hat{u}_j d\Gamma - \int_{\Gamma} u^* \frac{\partial \hat{u}_j}{\partial n} d\Gamma) \quad (6)$$

by applying the BEM also to the inhomogeneities connected to the same Laplace operator as  $\nabla^2 \hat{u}_j = f_j$ . The discretization of the boundary results in a system of matrix vector equations

$$HV - G \frac{\partial V}{\partial n} = (H\hat{U} - G\hat{Q})F^{-1} \left\{ -1 - M_x \frac{\partial B}{\partial x} - M_y \frac{\partial B}{\partial y} \right\} \quad (7)$$

$$HB - G \frac{\partial B}{\partial n} = (H\hat{U} - G\hat{Q})F^{-1} \left\{ -M_x \frac{\partial V}{\partial x} - M_y \frac{\partial V}{\partial y} \right\}. \quad (8)$$

The matrices  $\hat{U}$ ,  $\hat{Q}$  and  $F$  are constructed by taking each of the vectors  $\hat{u}_j$ ,  $\hat{q}_j$  and  $f_{ij} = f_j(r_i)$  as columns, respectively. The components of the  $H$  and  $G$  matrices are given for constant elements as

$$\begin{aligned} H_{ij} &= c_i \delta_{ij} + \frac{1}{2\pi} \int_{\Gamma_j} \frac{\partial}{\partial n} \left( \ln\left(\frac{1}{r}\right) \right) d\Gamma_j \\ H_{ii} &= - \sum_{j=1, j \neq i}^N H_{ij} \\ G_{ij} &= \frac{1}{2\pi} \int_{\Gamma_j} \ln\left(\frac{1}{r}\right) d\Gamma_j \\ G_{ii} &= \frac{l}{2\pi} \left( \ln\left(\frac{2}{l}\right) + 1 \right) \end{aligned} \quad (9)$$

where  $l$  is the length of the elements and  $\delta_{ij}$  is the Kronecker delta function.

The space derivatives for  $V$  and  $B$  are computed by using the coordinate matrix as

$$\begin{aligned} \frac{\partial V}{\partial x} &= \frac{\partial F}{\partial x} F^{-1} V, \\ \frac{\partial B}{\partial x} &= \frac{\partial F}{\partial x} F^{-1} B, \\ \frac{\partial V}{\partial y} &= \frac{\partial F}{\partial y} F^{-1} V, \end{aligned}$$

$$\frac{\partial B}{\partial y} = \frac{\partial F}{\partial y} F^{-1} B$$

where the coordinate matrix  $F$  is invertible since the leading diagonal of  $F$  is nonzero [10]. The coupled matrix-vector equations (7) and (8) can be solved together by constructing the whole system as

$$\begin{bmatrix} H_{N+L \times N+L} & K_{N+L \times N+L} \\ K_{N+L \times N+L} & H_{N+L \times N+L} \end{bmatrix} \begin{bmatrix} V_{N+L \times 1} \\ B_{N+L \times 1} \end{bmatrix} = \begin{bmatrix} G_{N+L \times N+L} & 0_{N+L \times N+L} \\ 0_{N+L \times N+L} & G_{N+L \times N+L} \end{bmatrix} \begin{bmatrix} \frac{\partial V}{\partial n}_{N+L \times 1} \\ \frac{\partial B}{\partial n}_{N+L \times 1} \end{bmatrix} + \begin{bmatrix} b_{N+L \times 1} \\ 0_{N+L \times 1} \end{bmatrix}$$

where  $K = (H\hat{U} - G\hat{Q})F^{-1} (M_x \frac{\partial F}{\partial x} F^{-1} + M_y \frac{\partial F}{\partial y} F^{-1})$  and  $b = -(H\hat{U} - G\hat{Q})F^{-1}$ .

The solution of the above matrix-vector equation gives the unknown vectors  $V$ ,  $B$ ,  $\frac{\partial V}{\partial n}$  and  $\frac{\partial B}{\partial n}$  which are  $(N+L) \times 1$  vectors on each part of the boundary.

#### 4. The well-posed iterations

For the inverse MHD problem, the  $\frac{\partial \tilde{V}}{\partial n}$  and  $\frac{\partial \tilde{B}}{\partial n}$  values obtained from the direct formulation corresponding to a specified slip length and conductivity constant are taken as overspecified boundary conditions in addition to  $V = 0$  and  $B = 0$  on the right wall. The DRBEM discretization of the Cauchy MHD duct flow problem leads to an ill-conditioned system of equations in the form of  $Ax = b$  due to overspecified conditions on the right wall and underspecified conditions on the left wall. The iterative algorithm developed by Kozlov et al. [15] is used to regularize the ill-posed Cauchy problem including the following steps

**Step 1.** Solve the matrix-vector equations (7)-(8) in one stroke as a direct problem with the specified  $\alpha$  and  $c$  values given as in Figure 1 to get the unknown values for  $V$ ,  $B$  on  $x = -1$  and their normal derivatives on  $x = \mp 1$ . Now, the Cauchy MHD problem is constructed with the assumption that the underspecified conditions on  $x = -1$

(neither  $V, B$  nor  $\frac{\partial V}{\partial n}, \frac{\partial B}{\partial n}$  are known) and over-specified conditions on  $x = 1$  ( $V, B$  and their normal derivatives are known).

**Step 2.** Solve the coupled discretized equation (7)-(8) as a direct problem using the Dirichlet type boundary conditions for  $V$  and  $B$  on  $x = \mp 1$  part of the boundary. The solution gives normal derivatives of  $V$  and  $B$  everywhere on the boundary.

**Step 3.** Use  $\frac{\partial V}{\partial n}$  and  $\frac{\partial B}{\partial n}$  on  $x = -1$  and  $x = 1$  obtained from **Step 2** for solving the direct problem to find the new  $V, B$  values.

**Step 4.** Update the values of  $V$  and  $B$  with the values obtained from step 3 on  $x = -1$ .

**Step 5.** Repeat steps 2-4 until the velocity and the induced magnetic field values converge to the solution of the direct problem corresponding to the specified slip length  $\alpha$  and the conductivity constant  $c$ .

## 5. Numerical results

In the application of the DRBEM,  $N = 80, 100, 160$  constant boundary elements and  $L = 400, 625, 1600$  interior nodes are taken for  $M = 5, 10, 50$ , respectively. In the well-posed iterations, the convergence criteria is taken as  $10^{-4}$  as the maximum absolute error in the values of  $V$  and  $B$ , separately, between the consecutive iterations.

Although there are discontinuities at the corners of the rectangular duct due to the different boundary conditions for  $V$  and  $B$  on each part of the duct, since the constant boundary elements are used in the numerical solution through the DRBEM, the nodes are not lying on the corners. Hence there is no discontinuity at the corner points numerically (nodes are located at the centers of the constant boundary elements).

**Table 1.** Velocity and induced magnetic field values from the inverse solution at the point  $(-1, 0)$ ,  $M = 10, \beta = \frac{\pi}{2}, \alpha = 0.2, c = 0.3$ .

| $N$ | $V$    | $B$    |
|-----|--------|--------|
| 44  | 0.0630 | 0.0618 |
| 60  | 0.0623 | 0.0616 |
| 68  | 0.0621 | 0.0616 |
| 76  | 0.0620 | 0.0616 |
| 84  | 0.0619 | 0.0616 |
| 92  | 0.0619 | 0.0616 |
| 100 | 0.0618 | 0.0616 |
| 108 | 0.0618 | 0.0616 |
| 116 | 0.0618 | 0.0616 |

The mesh independence is shown in Table 1 for Hartmann number  $M = 10$ . The velocity and induced magnetic field values at the point  $x = -1, y = 0$  which is on the slipping and variably conducting part of the duct are given for several numbers of constant boundary elements. It is seen that when  $N$  is taken as larger than  $N = 100$ , the values of  $V$  and  $B$  are the same up to the order  $10^{-4}$ . Hence,  $N = 100$  can be taken as the optimal number of boundary elements for that Hartmann number.

The integrals in the off-diagonal entries of the matrices  $H$  and  $G$  in (9) are calculated by using Gauss-Legendre integration with 16 points. The diagonal entries  $G_{ii}$  are evaluated theoretically taking care of the singularities and given in equation (9).  $H_{ii}$  are computed implicitly with the assumption of a constant potential over the whole boundary giving zero flux and  $HI = 0$ .

The direct problem is solved when the left wall is taken as slipping and variably conducting by taking the slip length  $\alpha = 0.2$  and the conductivity constant  $c = 0.3$ . In addition, the external magnetic field is applied with an angle  $\beta = 0, \frac{\pi}{4}, \frac{\pi}{3}, \frac{\pi}{2}$  formed with the  $y$ -axis.

The direct solutions for  $V$  and  $B$  are obtained by using the radial basis functions as  $f = 1 + r, f = 1 + r + r^2, f = r^2 \ln r$  for the angle  $\beta = \frac{\pi}{2}$  and the Hartmann number  $M = 10$ . The Figure 2 indicates that there is no significant difference between the solutions, hence because of the simplicity and computational effort, the rest of the calculations are carried by using  $f = 1 + r$ .

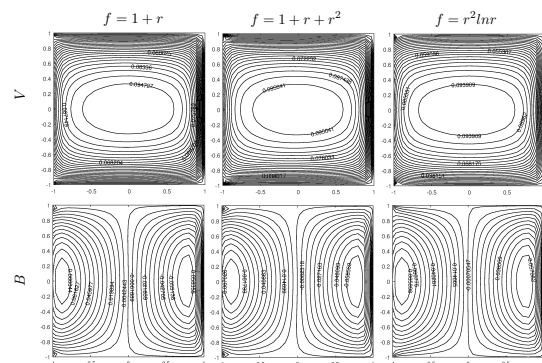


**Figure 2.** Velocity and induced magnetic field from direct solution,  $\beta = \frac{\pi}{2}, \alpha = 0.2, c = 0.3, M = 10$ .

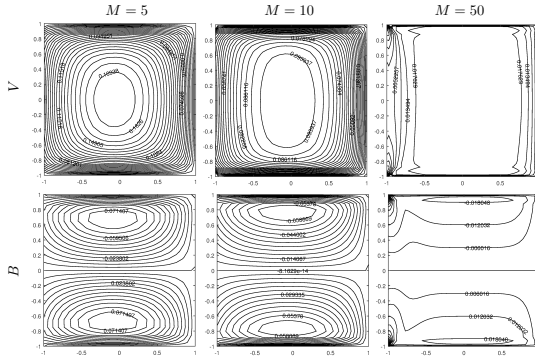


**Figure 3.** Velocity and induced magnetic field from direct problem,  $\beta = 0, \alpha = 0.2, c = 0.3$ .

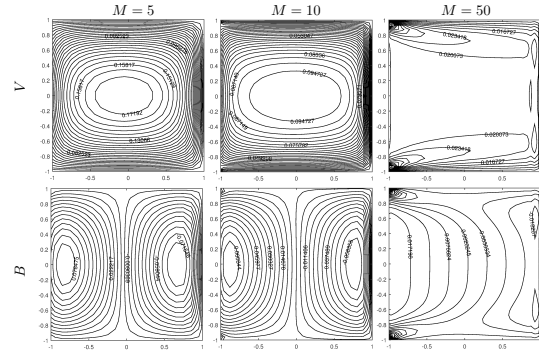


**Figure 5.** Velocity and induced magnetic field from direct problem,  $\beta = \frac{\pi}{2}, \alpha = 0.2, c = 0.3$ .

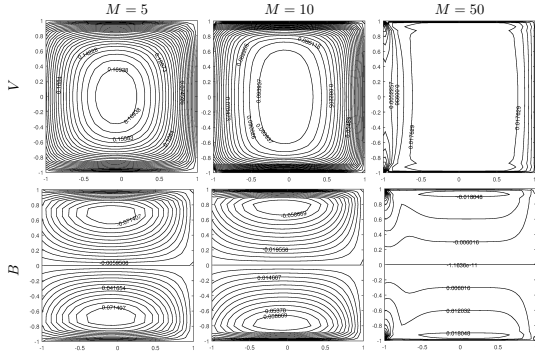


**Figure 4.** Velocity and induced magnetic field from inverse solution,  $\beta = 0$ .

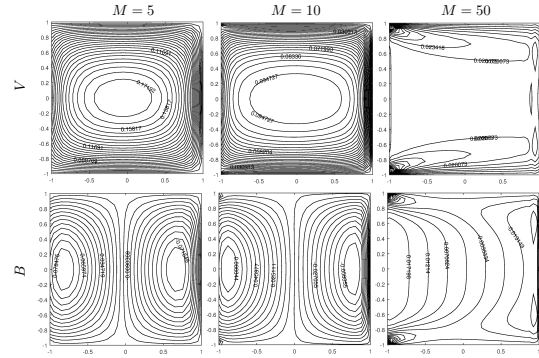


**Figure 6.** Velocity and induced magnetic field from inverse solution,  $\beta = \frac{\pi}{2}$ .

The direct solutions of MHD flow equations (1) for  $V$  and  $B$  with the boundary conditions (2) and the slip length  $\alpha = 0.2$ , conductivity constant  $c = 0.3$  on the left wall are presented for Hartmann number values  $Ha = 5, 10, 50$  for the angle  $\beta = 0$  in Figure 3. It is noted that when  $\beta = 0$ , the external magnetic field  $B_0$  applies in the  $y$ -direction. It is observed that as  $Ha$  number increases, Hartmann layers near the top and bottom walls are developed for both  $V$  and  $B$  which is a well-known behaviour of the MHD duct flow. Also, on the left wall the slip effect is observed which is weakened when  $M$  increases. In addition, as  $M$  increases, the core region of the fluid enlarges and flow becomes flattened. The induced current separates into two bunches. Due to the variable conductivity, current lines cross the left walls.

Figure 4 shows the velocity behaviours for the Cauchy MHD flow problem resulted from the well-posed iterations for  $M = 5, 10, 50$  and  $\beta = 0$ . It can be seen that the velocity contours obtained from the inverse formulation are in a very well agreement with the ones in the direct problem obtained for  $\alpha = 0.2$  and  $c = 0.3$ .

In Figures 5-6, the angle  $\beta$  is taken as  $\beta = \frac{\pi}{2}$ , i.e, the external magnetic field applies in the  $x$ -direction. It is clearly seen that the slip and variable conductivity effect weakens the Hartmann layer near the left wall. A further increase in Hartmann number separates the flow through the top and bottom walls and diminishes the slip phenomenon on the left wall. In addition, the solutions of the direct and inverse problems are in a very well agreement in the sense of fluid movement and the induced current behavior.

Due to the variable conductivity, current lines cross the left walls. An increase in  $M$  results in squeezing the right bunch of the induced current through the right wall.

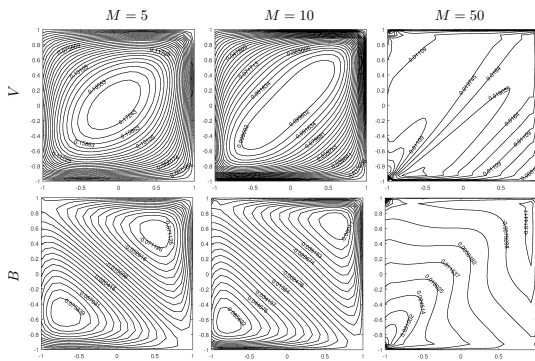


**Figure 7.** Velocity and induced magnetic field from direct problem,  $\beta = \frac{\pi}{4}, \alpha = 0.2, c = 0.3$ .

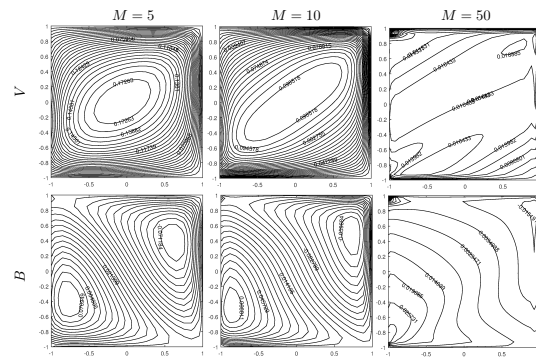


**Figure 10.** Velocity and induced magnetic field from inverse solution,  $\beta = \frac{\pi}{3}$ .

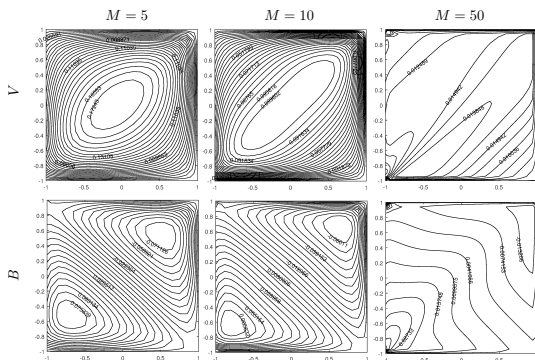


**Figure 8.** Velocity and induced magnetic field from inverse solution,  $\beta = \frac{\pi}{4}$ .

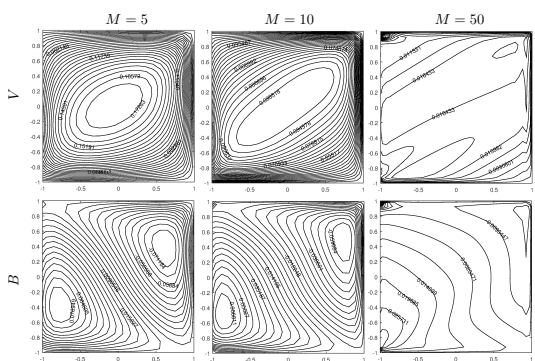


**Figure 9.** Velocity and induced magnetic field from direct problem,  $\beta = \frac{\pi}{3}, \alpha = 0.2, c = 0.3$ .

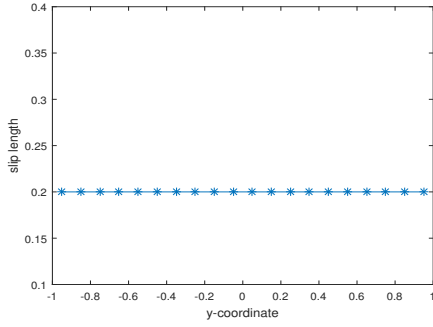
When the angle  $\beta = \frac{\pi}{4}, \frac{\pi}{3}$  are taken, the direct and inverse solutions for the velocity  $V$  and the induced magnetic field  $B$  are given in the Figures 6-9. It is depicted that the core region of the fluid rotates in accordance with the angle  $\beta$  with the y-axis showing the slip near the left wall. The boundary layers are directed near the corners of the duct in the external applied magnetic field direction showing the well-known behavior of the MHD duct flow. It is observed that the Cauchy MHD flow problem solutions through the well-posed iterations show the very well agreement with the ones in the direct problem solutions for each angle considered.

### 5.1. Reconstruction of the slip length and the conductivity constant

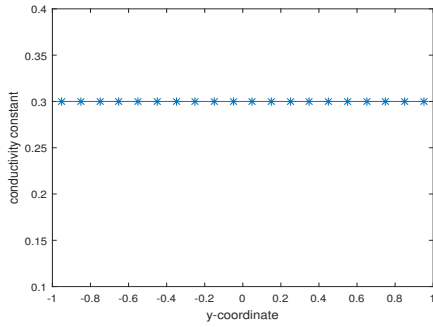
In this study, the main purpose of the Cauchy formulation of MHD duct flow problem is to regain the slip length  $\alpha$  and the conductivity constant  $c$  on both the slipping and variably conducting part of the boundary. Since the slip condition and variable conductivity condition contain both the velocity, the induced magnetic field and their normal derivative values on the left part of the boundary, one need both of these computed values to extract  $\alpha$  from the equation  $V + \alpha \frac{\partial V}{\partial n} = 0$  and also  $c$  from  $B + c \frac{\partial B}{\partial n} = 0$ . The boundary element method is the unique numerical procedure which provides the normal derivative if the solution itself is known or vice versa. Thus, we made use of the knowledge of direct solutions to obtain normal derivative values of the velocity and the induced magnetic field through the Cauchy MHD flow problem solution.

Resized slip length and the conductivity constant on the left wall from the inverse formulations are computed through the relation

$\alpha = -V/\frac{\partial V}{\partial n}$  and  $c = -B/\frac{\partial B}{\partial n}$  where  $V$ ,  $B$  and their normal derivatives are obtained by DRBEM.

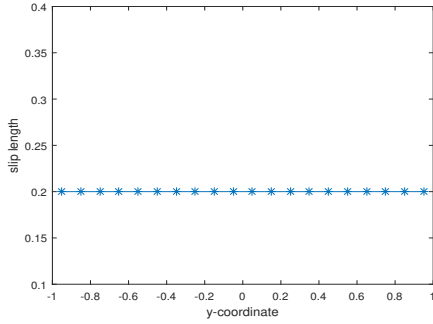


(a) slip length,  $\alpha$ .

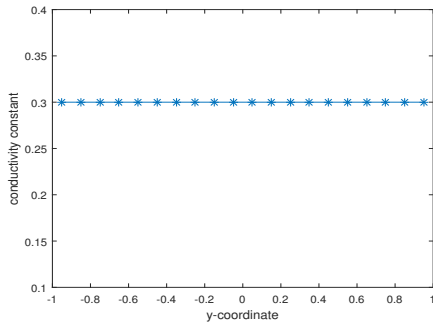


(b) conductivity constant,  $c$ .

**Figure 11.**  $\beta = \frac{\pi}{4}$ ,  $x = -1$ .

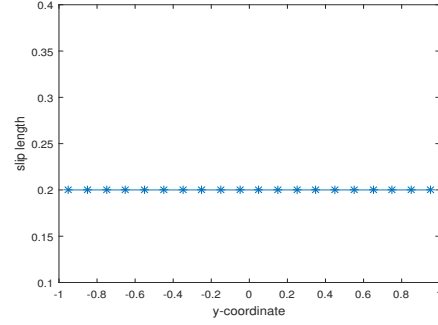


(a) slip length,  $\alpha$ .

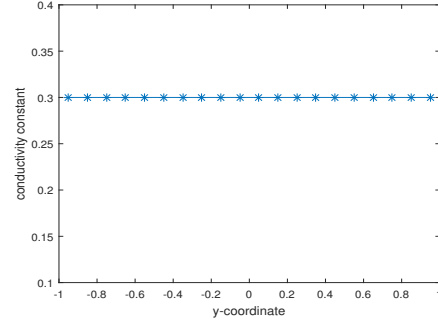


(b) conductivity constant,  $c$ .

**Figure 12.**  $\beta = \frac{\pi}{3}$ ,  $x = -1$ .



(a) slip length,  $\alpha$ .



(b) conductivity constant,  $c$ .

**Figure 13.**  $\beta = \frac{\pi}{2}$ ,  $x = -1$ .

Figures 10-13 show that the slip length  $\alpha = 0.2$  and the conductivity constant  $c = 0.3$  are very well approached from the Cauchy MHD flow problem for all of the points on the slipping and variably conducting left wall for  $\beta = 0, \frac{\pi}{4}, \frac{\pi}{3}, \frac{\pi}{2}$ , and  $M = 5, 10, 50$  when the well-posed iterations technique is used.

## 6. Conclusion

The direct and Cauchy formulations are constructed for the MHD rectangular duct flow problems in terms of the slip velocity and induced magnetic field on the left wall, and they are solved by using the DRBEM. The Cauchy problems are considered with the normal derivatives of the velocity and induced magnetic field on the right wall obtained from the direct solution to determine the underspecified velocity informations on the left part of the boundary. The well-posed iterations are used to regularize the Cauchy MHD flow problem and the inverse solutions for the velocity and induced magnetic field on the slipping and variably conducting duct wall are obtained for several orientations of the external magnetic field. The Cauchy problems resized the slip velocities and the varying induced magnetic fields using the solution of corresponding direct problem with a preassigned slip length and conductivity constant for  $M = 5, 10, 50$ . When reconstructing slip

length and conductivity constant from the well-posed iterations, it is clearly seen that it gives the same estimated slip length and conductivity constant value used in the direct problem. Providing both the velocity, the induced magnetic field and their normal derivative values on the underspecified wall, extracting the slip length  $\alpha$  and conductivity constant  $c$  between them and discretizing only the boundary of the problem region, the DRBEM is the most appropriate numerical technique for the solution of Cauchy MHD duct flow problems.

## References

- [1] Dragoş, L. (1975). *Magnetofluid Dynamics*. Abacus Press, England.
- [2] Shercliff, J.A. (1953). Steady motion of conducting fluids in pipes under transverse fields. *Proc. Cambridge Philos. Soc.*, 49, 136-144.
- [3] Ligere, E., Dzenite, I., Matvejevs, A. (2017). Analytical solution of the problem on MHD flow in duct with perfectly conducting Hartmann walls and slip condition on conducting side walls. *Proc. of the Engineering for Rural Development*. Jelgava.
- [4] Ligere, E., Dzenite, I., Matvejevs, A. (2016). MHD Flow in the duct with perfectly conducting Hartmann walls and slip condition on side walls. *Proc. of the 10th Pamir International Conference- Fundamental and Applied MHD*. Cagliari-Italy.
- [5] Aydin, S.H., Tezer-Sezgi, M. (2014). DRBEM solution of MHD pipe flow in a conducting Medium. *Journal of Computational and Applied Mathematics*, 259, 720–729.
- [6] Bozkaya, C., Tezer-Sezgin, M. (2007). Fundamental solution for coupled magnetohydrodynamic flow equations. *Journal of Computational and Applied Mathematics*, 203, 125–144.
- [7] Nesliturk, A.I., Tezer-Sezgin, M. (2006). Finite element method solution of electrically driven magnetohydrodynamic flow. *Journal of Computational and Applied Mathematics*, 192, 339–352.
- [8] Tezer-Sezgin, M., Aydin, S.H. (2006). Solution of MHD flow problems using the boundary element method. *Engineering Analysis with Boundary Elements*, 30(5), 411–418.
- [9] Marin, L., Elliott, L., Heggs, P.J., Ingham, D.B., Lesnic, D., Wen, X. (2006). Dual reciprocity boundary element method solution of the Cauchy problem for Helmholtz-type equations with variable coefficients. *Journal of Sound and Vibration*, 297, 89–105.
- [10] Partridge, P.W., Brebbia, C.A., Wrobel, L.C. (1992). *The Dual Reciprocity Boundary Element Method*. Computational Mechanics Publications, Southampton, Boston.
- [11] Hosseinzadeh, H., Dehghan, M., Mirzaei, D., Aydin, S.H. (2013). The boundary elements method for magneto-hydrodynamic (MHD) channel flows at high Hartmann numbers. *Applied Mathematical Modelling*, 37(4), 2337–2351.
- [12] Pekmen, B., Tezer-Sezgin, M. (2013). DRBEM solution of incompressible MHD flow with magnetic potential. *Computer Modeling in Engineering and Sciences*, 96(4), 275-292.
- [13] Smolentsev, S. (2009). MHD duct flows under hydrodynamic slip condition. *Theoretical and Computational Fluid Dynamics*, 23, 557–570.
- [14] Aydin, C., Tezer-Sezgin, M. (2018). DRBEM solution of the Cauchy MHD duct flow with a slipping perturbed boundary. *Engineering Analysis with Boundary Elements*, 93, 94-104.
- [15] Kozlov, V.A., Maz'ya, V.G., Fomin, A.F. (1991). An iterative method for solving the Cauchy problem for elliptic equations. *Computational Mathematics and Mathematical Physics*, 31, 45–52.

**Cemre Aydin** She received her B.Sc. degree in mathematics from the Middle East Technical University, Turkey in 2014. She is currently a Ph.D student in the Department of Mathematics, Middle East Technical University. Her research is in applied mathematics and numerical analysis focusing especially on the numerical solutions of the Cauchy magnetohydrodynamic flow problems.

**Munever Tezer-Sezgin** She holds B.Sc. and M.Sc. degrees in mathematics from the Middle East Technical University, Turkey, M.Sc. and Ph.D degrees in Applied Mathematics from the University of Saskatchewan and the University of Calgary, Canada. Currently, she is a professor in the Department of Mathematics and an affiliated member of the Institute of Applied Mathematics, Middle East Technical University. She has held visiting positions at the University of Victoria, Canada, and Technical University of Darmstadt. Her research is mainly in numerical analysis applied to fluid dynamics and magnetohydrodynamics. She has published over 130 research articles in specialized international journals and the international conference proceedings. She is the recipient of the "Mustafa Parlar Foundation 1990 Research Prize" and "Mustafa Parlar Foundation 2014 Science Prize" in applied mathematics and engineering.



This work is licensed under a Creative Commons Attribution 4.0 International License. The authors retain ownership of the copyright for their article, but they allow anyone to download, reuse, reprint, modify, distribute, and/or copy articles in IJOCTA, so long as the original authors and source are credited. To see the complete license contents, please visit <http://creativecommons.org/licenses/by/4.0/>.

## RESEARCH ARTICLE

## Approximate controllability of nonlocal non-autonomous Sobolev type evolution equations

Arshi Meraj\*  and Dwijendra Narain Pandey 

Department of Mathematics, Indian Institute of Technology Roorkee, Uttarakhand, India, PIN - 247667  
 arshimeraj@gmail.com, dwij.iitk@gmail.com

## ARTICLE INFO

## Article History:

Received 26 July 2018

Accepted 16 May 2019

Available 30 July 2019

## Keywords:

Krasnoselskii fixed point theorem

Evolution system

Approximate controllability

Sobolev type differential equations

## AMS Classification 2010:

93B05; 34G20; 34K30

## ABSTRACT

The aim of this article is to investigate the existence of mild solutions as well as approximate controllability of non-autonomous Sobolev type differential equations with the nonlocal condition. To prove our results, we will take the help of Krasnoselskii fixed point technique, evolution system and controllability of the corresponding linear system.



### 1. Introduction

In this article, we discuss the approximate controllability of nonlocal Sobolev type non-autonomous evolution equations in a separable Hilbert space  $X$ :

$$\begin{aligned} \frac{d}{dt}[\mathbb{E}x(t)] + \mathbf{A}(t)x(t) &= \mathcal{F}(t, x(t)) + \mathbb{B}u(t), \\ t &\in (0, b), \\ x(0) + \mathcal{G}(x) &= x_0, \quad x_0 \in D(\mathbb{E}), \end{aligned} \quad (1)$$

where  $\mathbf{A}(t)$ ,  $\mathbb{E}$  are  $X$ -valued linear operators with domains are subsets of  $X$ , and  $\mathcal{F}$  is  $X$ -valued function defined over  $J \times X$ ,  $\mathcal{G}$  is  $D(\mathbb{E})$ -valued function defined over  $\mathcal{C}(J, X)$ ,  $J = [0, b]$ . The control function  $u \in \mathcal{L}^2(J, \mathbb{U})$ ,  $\mathbb{U}$  is a Hilbert space and  $\mathbb{B}$  is  $X$ -valued linear and bounded operator defined over  $\mathbb{U}$ .

The Sobolev type differential equations appears in several fields such as thermodynamics [1], fluid flow via fissured rocks [2], and mechanics of soil

[3]. Brill [4] first established the existence of solution for a semilinear Sobolev differential equation in a Banach space. Lightbourne et al. [5] studied a partial differential equation of Sobolev type.

Generalization of classical initial condition which is known as nonlocal condition is more effective to obtain better results. Nonlocal Cauchy problem was first considered by Byszewski [6].

Controllability is an important issue in engineering and mathematical control theory. The problem of exact controllability is to show that there exists a control function, that steers the solution of the system from its initial state to the given final state. However in approximate controllability, it is possible to steer the solution of the system from its initial state to arbitrary small neighbourhood of the the final state. Mostly the problem of controllability for various kinds of differential, integro-differential equations and impulsive differential equations are studied for autonomous systems. For more details, we refer to [7] - [13].

The existence of mild solutions for a non-autonomous nonlocal integro-differential equation

\*Corresponding Author

is investigated by Yan [14] via Banach contraction principle, Schauder's fixed point theorem and the theory of evolution families. Haloi et al. [15] generalized the above results for non-autonomous differential equations with deviated arguments by the use of theory of analytic semigroup and Banach fixed point theorem. Alka et al. [16] generalized the results of [15] for instantaneous impulsive non-autonomous differential equations with iterated deviating arguments. Hamdy [17] studied sufficient conditions for controllability of autonomous Sobolev type fractional integro-differential equations with the help of Schauder's fixed point theorem and the theory of compact semigroup. Mahmudov [18] discussed the approximate controllability of autonomous fractional Sobolev type differential system in Banach space with the help of Schauder's fixed point theorem. Recently, Haloi [19] established sufficient conditions for approximate controllability of non-autonomous nonlocal delay differential systems with deviating arguments by using theory of compact semigroup and Krasnoselskii fixed point theorem.

To the best of our knowledge, no work yet available on approximate controllability of non-autonomous Sobolev type differential systems, inspired by this, we consider the system (1) to find the sufficient conditions for the approximate controllability.

The remaining part of the article is organized as following. Section 2 is concerned with some basic notations and definitions, also we will introduce the expression for mild solutions of the system (1). In section 3, we will study our main results. In section 4, we will present an example to illustrate our results. In last section 5, we will discuss the conclusions.

## 2. Preliminaries

This section is concerned with some basic assumptions, definitions and theorems required to prove our objectives. For more details, we refer [7], [20] and [21]. Let us denote  $\mathcal{C}(J, X)$  for the complete norm space of all continuous maps from  $J$  to  $X$ , for a finite constant  $r > 0$ , let  $\Omega_r = \{x \in \mathcal{C}(J, X) : \|x(t)\| \leq r, t \in J\}$ .  $\mathcal{L}^p(J, X)$  ( $1 \leq p < \infty$ ) is the Banach space of all Bochner integrable functions from  $J$  to  $X$  with norm  $\|x\|_{\mathcal{L}^p(J, X)} = (\int_0^b \|x(t)\|^p dt)^{\frac{1}{p}}$ .

Now, we impose the following restrictions (see [4], [20], [21]).

- (A1) The operator  $\mathbf{A}(t)$  is closed, domain of  $\mathbf{A}(t)$  is dense in  $X$  and independent of  $t$ .

- (A2) For  $Re(\vartheta) \leq 0$ ,  $t \in J$ , the resolvent operator of  $\mathbf{A}(t)$  exists and satisfies  $\|\mathcal{R}(\vartheta; t)\| \leq \frac{\varsigma}{|\vartheta|^{|\alpha|+1}}$ , for some positive constant  $\varsigma$ .
- (A3) For each fixed  $\tau_3 \in J$ , there are constants  $\mathcal{K} \geq 0, \rho \in (0, 1]$  such that  $\|[\mathbf{A}(\tau_1) - \mathbf{A}(\tau_2)]\mathbf{A}^{-1}(\tau_3)\| \leq \mathcal{K}|\tau_1 - \tau_2|^\rho$  for any  $\tau_1, \tau_2 \in J$ .
- (S1)  $\mathbb{E}$  is closed, bijective operator, and  $D(\mathbb{E}) \subset D(\mathbf{A})$ .
- (S2)  $\mathbb{E}^{-1} : X \rightarrow D(\mathbb{E})$  is compact.

The assumptions (A1), (A2) imply that  $-\mathbf{A}(t)$  generates an analytic semigroup in  $B(X)$ , where the symbol  $B(X)$  stands for Banach space of all bounded linear operators on  $X$ . The closed graph theorem with the above assumptions imply that the linear operator  $-\mathbf{A}(t)\mathbb{E}^{-1} : X \rightarrow X$  is bounded, and so for each  $t \in J$ ,  $-\mathbf{A}(t)\mathbb{E}^{-1}$  generates a semigroup of bounded linear operators and hence a unique evolution system  $\{\mathcal{S}(t_1, t_2) : 0 \leq t_2 \leq t_1 \leq b\}$  on  $X$ , which satisfies (see [14], [20], [21]):

- (i)  $\mathcal{S}(t_1, t_2) \in B(X)$  and is continuous strongly in  $t_1, t_2$  for  $0 \leq t_2 \leq t_1 \leq b$ .
- (ii)  $\mathcal{S}(t_1, t_2)x \in D(\mathbf{A})$ ,  $x \in X$ ,  $0 \leq t_2 \leq t_1 \leq b$ .
- (iii)  $\mathcal{S}(t_1, t_2)\mathcal{S}(t_2, t_3) = \mathcal{S}(t_1, t_3)$ ,  $0 \leq t_3 \leq t_2 \leq t_1 \leq b$ .
- (iv)  $\mathcal{S}(\eta, \eta)$  is identity operator, for  $\eta \in J$ .
- (v)  $\|\mathcal{S}(t_1, t_2)\| \leq \mathcal{M}$ ,  $0 \leq t_2 \leq t_1 \leq b$ , for some positive constant  $\mathcal{M}$ .
- (vi) For each fixed  $t_2$ ,  $\{\mathcal{S}(t_1, t_2), t_2 < t_1\}$  is uniformly continuous in uniform operator norm.
- (vii) For  $0 \leq t_2 < t_1 \leq b$ , the derivative  $\frac{\partial \mathcal{S}(t_1, t_2)}{\partial t_1}$  exists in strong operator topology, is strongly continuous in  $t_1$ . Moreover,

$$\frac{\partial \mathcal{S}(t_1, t_2)}{\partial t_1} + \mathbf{A}(t_1)\mathcal{S}(t_1, t_2) = 0, \quad 0 \leq t_2 < t_1 \leq b.$$

**Theorem 1.** ([4, 20]) *Let  $\mathcal{F}$  is a uniformly Hölder continuous function on  $J$  with exponent  $\beta \in (0, 1]$ , and the assumptions (A1)-(A3), (S1)-(S2) hold, then the unique solution for the linear Cauchy problem*

$$\begin{aligned} \frac{d}{dt}[\mathbb{E}x(t)] + \mathbf{A}(t)x(t) &= \mathcal{F}(t), \quad t \in J, \\ x(0) &= x_0 \in D(\mathbb{E}), \end{aligned} \quad (2)$$

is given by

$$x(t) = \mathbb{E}^{-1}\mathcal{S}(t,0)\mathbb{E}x_0 + \int_0^t \mathbb{E}^{-1}\mathcal{S}(t,s)\mathcal{F}(s)ds. \quad (3)$$

**Definition 1.** A mild solution of (1) is a function  $x \in \mathcal{C}(J, X)$  satisfying the following integral equation

$$x(\varrho) = \mathbb{E}^{-1}\mathcal{S}(\varrho,0)\mathbb{E}(x_0 - \mathcal{G}(x)) + \int_0^\varrho \mathbb{E}^{-1}\mathcal{S}(\varrho,\eta)[\mathcal{F}(\eta,x(\eta)) + \mathbb{B}u(\eta)]d\eta, \quad \varrho \in J.$$

For the control  $u$  and initial data  $x_0$ , use  $x^b(x_0, u)$  to denote the state value at time  $b$ . The set  $\mathcal{R}(b, x_0) = \{x^b(x_0, u) : u \in \mathcal{L}^2(J, \mathbb{U})\}$ , is called the reachable set at time  $b$ .

**Definition 2.** ([8]) If  $\mathcal{R}(b, x_0)$  is dense in  $X$ , the system (1) is called approximately controllable on  $J$ .

Consider the linear control system:

$$\begin{aligned} \frac{d}{dt}[\mathbb{E}x(t)] + \mathbf{A}(t)x(t) &= \mathbb{B}u(t), \quad t \in J, \\ x(0) &= x_0. \end{aligned} \quad (4)$$

Corresponding to (4), the controllability operator is given as

$$\Gamma_0^b = \int_0^b \mathcal{V}(b,\eta)\mathbb{B}\mathbb{B}^*\mathcal{V}^*(b,\eta)d\eta, \quad (5)$$

where  $\mathcal{V}(t, s) := \mathbb{E}^{-1}\mathcal{S}(t, s)$ ,  $*$  denotes the adjoint of the operator. Notice that  $\Gamma_0^b$  is a bounded linear operator.

**Theorem 2.** ([8]) The necessary and sufficient conditions for the linear system (4) to be approximately controllable on  $J$  is that,  $\delta R(\delta, \Gamma_0^b) \rightarrow 0$  as  $\delta \rightarrow 0^+$  in the strong operator topology, where  $R(\delta, \Gamma_0^b) := (\delta I + \Gamma_0^b)^{-1}$ ,  $\delta > 0$ .

Now, we recall the Krasnoselskii fixed point technique.

**Theorem 3.** ([22]) Let  $S$  is a convex bounded closed subset of a Banach space  $X$ . Suppose that  $F_1, F_2$  be two  $X$ -valued operators defined on  $S$  such that  $F_1x + F_2y \in S$  whenever  $x, y \in S$ ,  $F_1$  is continuous and compact, and  $F_2$  is contraction map. Then  $F_1 + F_2$  has a fixed point in  $S$ .

### 3. Main results

In this section, we prove the existence of mild solutions and approximate controllability of (1). For

$x \in \mathcal{C}(J, X)$ , consider the control function for the system (1) as following :

$$u(t) = u_\lambda(t, x) = \mathbb{B}^*\mathcal{V}^*(b, t)R(\lambda, \Gamma_0^b)p(x), \quad (6)$$

with

$$p(x) = x^b - \mathcal{V}(b,0)\mathbb{E}(x_0 - \mathcal{G}(x)) - \int_0^b \mathcal{V}(b,\eta)\mathcal{F}(\eta,x(\eta))d\eta. \quad (7)$$

For any  $\lambda > 0$ , define  $F_\lambda$  on  $\mathcal{C}(J, X)$  as following:

$$(F_\lambda x)(\varrho) = (\Phi_\lambda x)(\varrho) + (\Psi_\lambda x)(\varrho), \quad \varrho \in J, \quad (8)$$

where

$$\begin{aligned} (\Phi_\lambda x)(\varrho) &= \mathcal{V}(\varrho,0)\mathbb{E}(x_0 - \mathcal{G}(x)) \\ &\quad + \int_0^\varrho \mathcal{V}(\varrho,\eta)\mathcal{F}(\eta,x(\eta))d\eta, \\ (\Psi_\lambda x)(\varrho) &= \int_0^\varrho \mathcal{V}(\varrho,\eta)\mathbb{B}u_\lambda(\eta)d\eta. \end{aligned} \quad (9)$$

Now, we state the assumptions that are useful to prove our objective.

(H1)  $\mathcal{S}(t, s)$ , is a compact evolution system whenever  $t - s > 0$  ( $0 \leq s < t \leq b$ ).

(H2) The function  $\mathcal{F}(\cdot, x)$  from  $J$  to  $X$  is Lebesgue measurable for every fixed  $x \in X$ , and the function  $\mathcal{F}(t, \cdot)$  from  $X$  to  $X$  is continuous for every fixed  $t \in J$ , and for all  $\varrho \in J, \eta_1, \eta_2 \in X$ , we have

$$\|\mathcal{F}(\varrho, \eta_1) - \mathcal{F}(\varrho, \eta_2)\| \leq L_1\|\eta_1 - \eta_2\|,$$

for some constant  $L_1 > 0$ .

(H3) The function  $\mathcal{G}$  from  $\mathcal{C}(J, X)$  to  $D(\mathbb{E})$  is continuous and there is a constant  $L_2 > 0$  such that

$$\begin{aligned} \|\mathbb{E}(\mathcal{G}(x_1) - \mathcal{G}(x_2))\| &\leq L_2\|x_1 - x_2\|, \\ &\forall x_1, x_2 \in \mathcal{C}(J, X). \end{aligned}$$

(H4)  $(A_1)$ - $(A_3)$  and  $(S_1)$ ,  $(S_2)$  hold.

For convenience, we use the following notations:

$$\begin{aligned} N_1 &= \sup_{t \in J} \|\mathcal{F}(t,0)\|, \quad K_1 = (L_1r + N_1)b, \\ \mathcal{M}_1 &= \|\mathbb{B}\|, \quad \mathcal{M}_2 = \|\mathbb{E}^{-1}\|. \end{aligned}$$

**Lemma 1.** If the assumption (H2) holds, then for  $x \in \Omega_r$  and  $\varrho \in J$  we have  $\int_0^\varrho \|\mathcal{F}(\eta, x(\eta))\|d\eta \leq K_1$ .

**Proof.** By assumption (H2), we get

$$\begin{aligned}
 \int_0^e \|\mathcal{F}(\eta, x(\eta))\| d\eta &\leq \int_0^e \left( \|\mathcal{F}(\eta, x(\eta))\right. \\
 &\quad \left. - \mathcal{F}(\eta, 0)\| + \|\mathcal{F}(\eta, 0)\| \right) d\eta \\
 &\leq \int_0^e (L_1\|x\| + N_1) d\eta \\
 &\leq (L_1r + N_1)b = K_1.
 \end{aligned}$$

$$\begin{aligned}
 \|(F_\lambda x)(t)\| &\leq \|\mathcal{V}(t, 0)\|(\|\mathbb{E}(x_0)\| + \|\mathbb{E}\mathcal{G}(x)\|) \\
 &\quad + \int_0^t \|\mathcal{V}(t, \eta)\| \|\mathcal{F}(\eta, x(\eta))\| d\eta \\
 &\quad + \int_0^t \|\mathcal{V}(t, \eta)\| \|\mathbb{B}\| \|u_\lambda(\eta, x)\| d\eta \\
 &\leq \mathcal{M}_2\mathcal{M}(\|\mathbb{E}x_0\| + L_2r + \|\mathbb{E}\mathcal{G}(0)\|) \\
 &\quad + \mathcal{M}_2\mathcal{M}K_1 \\
 &\quad + \mathcal{M}_2\mathcal{M}\mathcal{M}_1K_2b.
 \end{aligned} \tag{12}$$

□

This implies, for large enough  $r > 0$ ,  $F_\lambda(\Omega_r) \subset \Omega_r$  holds.

**Theorem 4.** *Let the assumptions (H1)-(H4) hold and the functions  $\mathbb{E}(\mathcal{G}(0))$  is bounded, then a mild solution to the system (1) exists, provided that*

$$\Lambda := \mathcal{M}_2\mathcal{M}(L_2 + L_1b) < 1. \tag{10}$$

**Proof.** The proof is divided into the following steps :

**Step I:** For  $\lambda > 0$ , we have a constant  $R$  (depends on  $\lambda$ ), satisfying  $F_\lambda(\Omega_R) \subset \Omega_R$ .

For any positive constant  $r$  and  $x \in \Omega_r$ , if  $t \in J$ , then by using (6), (H3) and Lemma (1), we have

$$\begin{aligned}
 u_\lambda(t, x) &= \mathbb{B}^*\mathcal{V}^*(b, t)R(\lambda, \Gamma_0^b) \left[ x^b \right. \\
 &\quad \left. - \mathcal{V}(b, 0)\mathbb{E}(x_0 - \mathcal{G}(x)) \right. \\
 &\quad \left. - \int_0^b \mathcal{V}(b, \eta)\mathcal{F}(\eta, x(\eta))d\eta \right] \\
 \|u_\lambda(t, x)\| &\leq \frac{\mathcal{M}_1\mathcal{M}_2\mathcal{M}}{\lambda} \left[ \|x^b\| + \mathcal{M}_2\mathcal{M}(\|\mathbb{E}x_0\| \right. \\
 &\quad \left. + \|\mathbb{E}(\mathcal{G}(x) - \mathcal{G}(0))\| + \|\mathbb{E}\mathcal{G}(0)\|) \right. \\
 &\quad \left. + \mathcal{M}_2\mathcal{M}K_1 \right] \\
 &\leq \frac{\mathcal{M}_1\mathcal{M}_2\mathcal{M}}{\lambda} \left[ \|x^b\| + \mathcal{M}_2\mathcal{M}(\|\mathbb{E}x_0\| \right. \\
 &\quad \left. + L_2r + \|\mathbb{E}\mathcal{G}(0)\|) + \mathcal{M}_2\mathcal{M}K_1 \right] \\
 &:= K_2,
 \end{aligned} \tag{11}$$

and from (8), (11), we obtain

$$\begin{aligned}
 (F_\lambda x)(t) &= \mathcal{V}(t, 0)\mathbb{E}(x_0 - \mathcal{G}(x)) \\
 &\quad + \int_0^t \mathcal{V}(t, \eta)\mathcal{F}(\eta, x(\eta))d\eta \\
 &\quad + \int_0^t \mathcal{V}(t, \eta)\mathbb{B}u_\lambda(\eta, x)d\eta
 \end{aligned}$$

**Step II:**  $\Phi_\lambda : \Omega_R \rightarrow \Omega_R$  is contraction.

For  $x, y \in \Omega_R$  and  $t \in J$ , using (H2) and (H3) we obtain

$$\begin{aligned}
 \|(\Phi_\lambda x)(t) - (\Phi_\lambda y)(t)\| &\leq \|\mathcal{V}(t, 0)\mathbb{E}(\mathcal{G}(x) \\
 &\quad - \mathcal{G}(y))\| \\
 &\quad + \int_0^t \|\mathcal{V}(t, s)\| \\
 &\quad \|\mathcal{F}(s, x(s)) \\
 &\quad - \mathcal{F}(s, y(s))\| ds \\
 &\leq \mathcal{M}_2\mathcal{M}L_2\|x - y\| \\
 &\quad + \mathcal{M}_2\mathcal{M} \\
 &\quad \int_0^t L_1\|x - y\| ds \\
 &\leq \mathcal{M}_2\mathcal{M}L_2\|x - y\| \\
 &\quad + \mathcal{M}_2\mathcal{M}L_1b\|x - y\| \\
 &\leq \mathcal{M}_2\mathcal{M}(L_2 + L_1b) \\
 &\quad \|x - y\| \\
 &= \Lambda\|x - y\|.
 \end{aligned} \tag{13}$$

Since  $\Lambda < 1$ , therefore  $\Phi_\lambda$  is contraction.

**Step III:**  $\Psi_\lambda$  is continuous in  $\Omega_R$ .

Consider  $\{x_n\}$  be a sequence in  $\Omega_R$  with  $\lim_{n \rightarrow \infty} x_n = x$  in  $\Omega_R$ . From continuity of non-linear term  $\mathcal{F}$  with respect to state variable, we have

$$\lim_{n \rightarrow \infty} \mathcal{F}(\eta, x_n(\eta)) = \mathcal{F}(\eta, x(\eta)), \quad \text{for each } \eta \in J.$$

So, we can conclude that

$$\sup_{\eta \in J} \|\mathcal{F}(\eta, x_n(\eta)) - \mathcal{F}(\eta, x(\eta))\| \rightarrow 0 \quad \text{as } n \rightarrow \infty. \tag{14}$$

For  $t \in J$ , (S1), (H3), and (14) yield the following

$$\begin{aligned}
 \|p(x_n) - p(x)\| &\leq \mathcal{M}_2\mathcal{M}\|\mathbb{E}\mathcal{G}(x_n) - \mathbb{E}\mathcal{G}(x)\| \\
 &\quad + \mathcal{M}_2\mathcal{M} \int_0^b \|\mathcal{F}(\zeta, x_n(\zeta)) \\
 &\quad - \mathcal{F}(\zeta, x(\zeta))\| d\zeta \\
 &\leq \mathcal{M}_2\mathcal{M}\|\mathbb{E}\mathcal{G}(x_n) - \mathbb{E}\mathcal{G}(x)\| \\
 &\quad + \mathcal{M}_2\mathcal{M}b \sup_{\zeta \in J} \|\mathcal{F}(\zeta, x_n(\zeta)) \\
 &\quad - \mathcal{F}(\zeta, x(\zeta))\| \\
 &\rightarrow 0 \text{ as } n \rightarrow \infty, \tag{15}
 \end{aligned}$$

therefore (6) implies that

$$\|u_\lambda(\eta, x_n) - u_\lambda(\eta, x)\| \rightarrow 0 \text{ as } n \rightarrow \infty, \tag{16}$$

and so

$$\begin{aligned}
 \|(\Psi_\lambda x_n)(t) - (\Psi_\lambda x)(t)\| &\leq \mathcal{M}_2\mathcal{M}\mathcal{M}_1b \\
 &\quad \sup_{\eta \in J} \|u_\lambda(\eta, x_n) \\
 &\quad - u_\lambda(\eta, x)\| \\
 &\rightarrow 0 \text{ as } n \rightarrow \infty,
 \end{aligned}$$

which means  $\Psi_\lambda$  is continuous in  $\Omega_R$ .

**Step IV:**  $\Psi_\lambda : \Omega_R \rightarrow \Omega_R$  is compact. For this we need to show :

(i): The set  $\{(\Psi_\lambda x)(\varrho) : x \in \Omega_R\}$  is relatively compact subset of  $X$ , for each  $\varrho \in J$ . For  $\varrho = 0$ , obviously the set  $\{(\Psi_\lambda x)(0) : x \in \Omega_R\} = \{0\}$  is compact subset of  $X$ . For fixed  $\varrho \in (0, b]$ , and  $\xi \in (0, \varrho)$ , consider an operator  $\Psi_\lambda^\xi$  on  $\Omega_R$  as following

$$\begin{aligned}
 (\Psi_\lambda^\xi x)(\varrho) &= \int_0^{\varrho-\xi} \mathcal{V}(\varrho, \eta) \mathbb{B}u_\lambda(\eta, x) d\eta \\
 &= \int_0^{\varrho-\xi} \mathbb{E}^{-1}\mathcal{S}(\varrho, \varrho - \xi) \\
 &\quad \mathcal{S}(\varrho - \xi, \eta) \mathbb{B}u_\lambda(\eta, x) d\eta \\
 &= \mathbb{E}^{-1}\mathcal{S}(\varrho, \varrho - \xi) \\
 &\quad \int_0^{\varrho-\xi} \mathcal{S}(\varrho - \xi, \eta) \mathbb{B}u_\lambda(\eta, x) d\eta \\
 &= \mathbb{E}^{-1}\mathcal{S}(\varrho, \varrho - \xi)y(\varrho, \xi).
 \end{aligned}$$

Since  $\mathbb{E}^{-1}$  and  $\mathcal{S}(\varrho, \varrho - \xi)$  are compact, and  $y(\varrho, \xi)$  is bounded on  $\Omega_R$ , we get  $\{(\Psi_\lambda^\xi x)(\varrho) : x \in \Omega_R\}$  is relatively compact subset of  $X$ . Also

$$\begin{aligned}
 \|(\Psi_\lambda x)(\varrho) - (\Psi_\lambda^\xi x)(\varrho)\| &\leq \int_{\varrho-\xi}^{\varrho} \|\mathcal{V}(\varrho, \eta) \mathbb{B} \\
 &\quad u_\lambda(\eta, x)\| d\eta \\
 &\leq \mathcal{M}_2\mathcal{M}\mathcal{M}_1\xi \|u_\lambda\| \\
 &\rightarrow 0 \text{ as } \xi \rightarrow 0.
 \end{aligned}$$

Hence,  $\{(\Psi_\lambda x)(\varrho) : x \in \Omega_R\}$  is relatively compact subset of  $X$ .

(ii): Now, we show  $\{\Psi_\lambda x : x \in \Omega_R\}$  is equicontinuous. For any  $x \in \Omega_R$  and  $0 \leq \varrho_1 < \varrho_2 \leq b$ , we have

$$\begin{aligned}
 \|(\Psi_\lambda x)(\varrho_2) - (\Psi_\lambda x)(\varrho_1)\| &= \left\| \int_0^{\varrho_2} \mathbb{E}^{-1}\mathcal{S}(\varrho_2, \eta) \right. \\
 &\quad \mathbb{B}u_\lambda(\eta, x) d\eta \\
 &\quad - \int_0^{\varrho_1} \mathbb{E}^{-1}\mathcal{S}(\varrho_1, \eta) \\
 &\quad \left. \mathbb{B}u_\lambda(\eta, x) d\eta \right\| \\
 &\leq \left\| \int_0^{\varrho_1} \mathbb{E}^{-1}[\mathcal{S}(\varrho_2, \eta) \right. \\
 &\quad - \mathcal{S}(\varrho_1, \eta)] \\
 &\quad \left. \mathbb{B}u_\lambda(\eta, x) d\eta \right\| \\
 &\quad + \left\| \int_{\varrho_1}^{\varrho_2} \mathbb{E}^{-1}\mathcal{S}(\varrho_2, \eta) \right. \\
 &\quad \left. \mathbb{B}u_\lambda(\eta, x) d\eta \right\| \\
 &\leq J_1 + J_2.
 \end{aligned}$$

For  $\varrho_1 = 0$ , it is easy to see that  $J_1 = 0$ . When  $\varrho_1 > 0$ , let  $\varepsilon > 0$  small enough, we obtain

$$\begin{aligned}
 J_1 &\leq \left\| \int_0^{\varrho_1-\varepsilon} \mathbb{E}^{-1}[\mathcal{S}(\varrho_2, \eta) - \mathcal{S}(\varrho_1, \eta)] \right. \\
 &\quad \left. \mathbb{B}u_\lambda(\eta, x) d\eta \right\| \\
 &\quad + \left\| \int_{\varrho_1-\varepsilon}^{\varrho_1} \mathbb{E}^{-1}[\mathcal{S}(\varrho_2, \eta) - \mathcal{S}(\varrho_1, \eta)] \right. \\
 &\quad \left. \mathbb{B}u_\lambda(\eta, x) d\eta \right\| \\
 &\leq \mathcal{M}_2\mathcal{M}_1(\varrho_1 - \varepsilon)\|u_\lambda\| \\
 &\quad \sup_{\eta \in [0, \varrho_1-\varepsilon]} \|\mathcal{S}(\varrho_2, \eta) - \mathcal{S}(\varrho_1, \eta)\| \\
 &\quad + 2\mathcal{M}_2\mathcal{M}\mathcal{M}_1\varepsilon\|u_\lambda\| \\
 J_2 &\leq \mathcal{M}_2\mathcal{M}\mathcal{M}_1\|u_\lambda\|(\varrho_2 - \varrho_1)
 \end{aligned}$$

Hence,  $J_1, J_2 \rightarrow$  as  $\varrho_2 \rightarrow \varrho_1, \varepsilon \rightarrow 0$ . As a result  $\|(\Psi_\lambda x)(\varrho_2) - (\Psi_\lambda x)(\varrho_1)\| \rightarrow 0$  independently of  $x \in \Omega_R$  as  $\varrho_2 \rightarrow \varrho_1$ , which means that  $\Psi_\lambda : \Omega_R \rightarrow \Omega_R$  is equicontinuous. Thus, by Arzela-Ascoli theorem,  $\Psi_\lambda$  is compact on  $\Omega_R$ .

Therefore Krasnoselskii fixed point theorem implies that  $F_\lambda$  has a fixed point, which is a mild solution to the problem (1).  $\square$

Now, we are ready to discuss the approximate controllability of the system (1). In order to prove it, the following hypotheses are also required:

(H5)  $\delta R(\delta, \Gamma_0^b) \rightarrow 0$  whenever  $\delta \rightarrow 0^+$  in strong operator topology.

(H6) There exist constants  $L_3 > 0$  and  $L_4 > 0$ , such that

$$\|\mathbb{E}\mathcal{G}(x)\| \leq L_3, \quad \forall x \in \mathcal{C}(J, X),$$

$$\|\mathcal{F}(t, x)\| \leq L_4, \quad \forall (t, x) \in J \times X.$$

**Theorem 5.** *If the assumptions of Theorem 4 as well as hypotheses (H5) and (H6) are satisfied, then (1) is approximately controllable on  $J$ .*

**Proof.** Theorem 4 guaranteed that  $F_\lambda$  has a fixed point in  $\Omega_R$ . Let  $x_\lambda$  is a mild solution of (1) under the control  $u_\lambda(t, x_\lambda)$  given by (6) and satisfies

$$\begin{aligned} x_\lambda(b) &= \mathcal{V}(b, 0)\mathbb{E}(x_0 - \mathcal{G}(x_\lambda)) \\ &\quad + \int_0^b \mathcal{V}(b, \eta)[\mathcal{F}(\eta, x_\lambda(\eta)) \\ &\quad + \mathbb{B}u_\lambda(\eta, x_\lambda)]d\eta \\ &= x^b - p(x_\lambda) + \int_0^b \mathcal{V}(b, \eta) \\ &\quad \mathbb{B}u_\lambda(\eta, x_\lambda)d\eta \\ &= x^b - p(x_\lambda) + \int_0^b \mathcal{V}(b, \eta) \\ &\quad \mathbb{B}\mathbb{B}^*\mathcal{V}^*(b, \eta)R(\lambda, \Gamma_0^b)p(x_\lambda)d\eta \\ &= x^b - p(x_\lambda) + \Gamma_0^b R(\lambda, \Gamma_0^b)p(x_\lambda) \\ &= x^b - [I - \Gamma_0^b(\lambda I + \Gamma_0^b)^{-1}]p(x_\lambda) \\ &= x^b - \lambda R(\lambda, \Gamma_0^b)p(x_\lambda), \end{aligned} \quad (17)$$

where

$$\begin{aligned} p(x_\lambda) &= x^b - \mathcal{V}(b, 0)\mathbb{E}(x_0 - \mathcal{G}(x_\lambda)) \\ &\quad - \int_0^b \mathcal{V}(b, \eta)\mathcal{F}(\eta, x_\lambda(\eta))d\eta. \end{aligned}$$

According to the compactness of  $\mathbb{E}^{-1}$ ,  $\mathcal{S}(t, s)$ , and the uniform boundedness of  $\mathbb{E}\mathcal{G}$ , we see that there exists a subsequence of  $\{\mathcal{V}(b, 0)\mathbb{E}\mathcal{G}(x_\lambda) : \lambda > 0\}$ , still denoted by it, converges to some  $x_g \in X$  as  $\lambda \rightarrow 0$ . Since  $\mathcal{F}$  is uniformly bounded, we get

$$\int_0^b \|\mathcal{F}(\eta, x_\lambda(\eta))\|^2 d\eta \leq L_4^2 b.$$

Hence  $\mathcal{F}(\cdot, x_\lambda(\cdot))$  is a bounded sequence in  $L^2(J, X)$ . So,  $\{\mathcal{F}(\cdot, x_\lambda(\cdot)) : \lambda > 0\}$  has a subsequence, still denoted by it, converges weakly to some  $\mathcal{F}(\cdot) \in L^2(J, X)$ . Define

$$\varpi = x_b - \mathcal{V}(b, 0)\mathbb{E}x_0 + x_g - \int_0^b \mathcal{V}(b, s)\mathcal{F}(s)ds.$$

Now, we get

$$\begin{aligned} \|p(x_\lambda) - \varpi\| &\leq \|\mathcal{V}(b, 0)\mathbb{E}\mathcal{G}(x_\lambda) - x_g\| \\ &\quad + \mathcal{M} \int_0^b \|\mathcal{F}(s, x_\lambda(s)) - \mathcal{F}(s)\|ds \\ &\rightarrow 0 \quad \text{as } \lambda \rightarrow 0^+. \end{aligned} \quad (18)$$

From (17), (18), and (H5), we obtain

$$\begin{aligned} \|x_\lambda(b) - x^b\| &\leq \|\lambda R(\lambda, \Gamma_0^b)p(x_\lambda)\| \\ &\leq \|\lambda R(\lambda, \Gamma_0^b)\varpi\| \\ &\quad + \|\lambda R(\lambda, \Gamma_0^b)\| \|p(x_\lambda) - \varpi\| \\ &\leq \|\lambda R(\lambda, \Gamma_0^b)\varpi\| + \|p(x_\lambda) - \varpi\| \\ &\rightarrow 0 \quad \text{as } \lambda \rightarrow 0^+. \end{aligned}$$

Hence, (1) is approximately controllable.  $\square$

#### 4. Example

Consider a control system governed by the following partial differential equation :

$$\begin{aligned} \frac{\partial}{\partial t}[x(t, z) - x_{zz}(t, z)] + [a(t, z) + \frac{\partial^2}{\partial z^2}]x(t, z) \\ = \mu(t, z) + \sin x(t, z), \\ z \in (0, \pi), \quad t \in (0, 1]; \\ x(t, 0) = x(t, \pi) = 0, \quad t \in [0, 1]; \\ x(0, z) + \frac{e^t}{c(1 + e^t)} \cos x(t, z) = x_0(z), \\ z \in (0, \pi); \end{aligned} \quad (19)$$

where  $X = \mathbb{U} = \mathcal{L}^2([0, 1] \times [0, \pi], \mathbb{R})$ ,  $x_0(z) \in D(\mathbb{E})$ ,  $a(t, z) \in C^1([0, \pi] \times [0, 1], \mathbb{R})$ ,  $J = [0, 1]$ , i.e.  $b = 1$ , and  $c$  is positive constant. Define

$$\begin{aligned} \mathbf{A}(t)x(t, z) &= [a(t, z) + \frac{\partial^2}{\partial z^2}]x(t, z), \\ \mathbb{E}x &= x - x_{zz}, \end{aligned} \quad (20)$$

where  $D(\mathbf{A}(t))$ ,  $D(\mathbb{E})$  is given by  $H^2(0, \pi) \cap H_0^1(0, \pi)$ . Therefore,  $-\mathbf{A}(t)$  generates a compact evolution system of bounded linear operators  $W(t, s)$  on  $X$  and is given by (see [19])

$$W(t, s)x = T(t - s)e^{\int_s^t a(\tau)d\tau} x, \quad x \in D(\mathbf{A}(t)). \tag{21}$$

Here

$$T(t)x = \sum_{n=1}^{\infty} e^{-n^2 t} \langle x, e_n \rangle e_n,$$

with  $e_n(z) = \sqrt{\frac{2}{\pi}} \sin(nz), 0 \leq z \leq \pi, n = 1, 2, \dots$

The operator  $\mathbb{E}$  can be written as following (see [5])

$$\mathbb{E}x = \sum_{n=1}^{\infty} (1 + n^2) \langle x, e_n \rangle e_n, \quad x \in D(\mathbb{E}). \tag{22}$$

Furthermore for  $x \in X$ , we have

$$\mathbb{E}^{-1}x = \sum_{n=1}^{\infty} \frac{1}{1 + n^2} \langle x, e_n \rangle e_n, \tag{23}$$

which is compact. So, the operator  $-\mathbf{A}(t)\mathbb{E}^{-1}$  generates a compact evolution system of bounded linear operators that is given as

$$\mathcal{S}(t, s)x = U(t - s)e^{\int_s^t a(\tau)d\tau} x, \tag{24}$$

where

$$U(t)x = \sum_{n=1}^{\infty} e^{\frac{-n^2}{1+\epsilon}t} \langle x, e_n \rangle e_n.$$

Hence assumptions (H1), (H4) hold. By putting  $x(t) = x(t, \cdot)$  which means  $x(t)(z) = x(t, z), t \in [0, 1], z \in [0, \pi]$  and  $u(t) = \mu(t, \cdot)$  is continuous. Let the bounded linear operator  $\mathbb{B} : \mathbb{U} \rightarrow X$  is defined as  $\mathbb{B}u(t)(z) = \mu(t, z)$ . Further

$$\begin{aligned} \mathcal{F}(t, x(t))(z) &= \sin x(t, z), \\ \mathcal{G}(x) &= \frac{e^t}{c(1 + e^t)} \cos x. \end{aligned}$$

So, the system (19) can be formulated into the abstract form of (1). Note that  $\mathbb{E}\mathcal{G}(x) = \frac{2e^t}{c(1+e^t)} \cos x$ . Observe that the functions  $\mathcal{F}, \mathcal{G}$  satisfies the assumptions (H2), (H3), and also  $\mathcal{F}, \mathbb{E}\mathcal{G}$  are uniformly bounded. Now it is needed to check the approximately controllability of the associated linear system, for this we show that

$$\mathbb{B}^* \mathcal{V}^*(b, s)x = 0, \quad s \in [0, b) \Rightarrow x = 0, \tag{25}$$

where  $\mathcal{V}(t, s) = \mathbb{E}^{-1}\mathcal{S}(t, s)$ . Notice that  $\mathcal{S}$  and  $\mathbb{E}^{-1}$  are self adjoint. Indeed,

$$\begin{aligned} \mathbb{B}^* \mathcal{V}^*(b, s)x &= \mathcal{V}^*(b, s)x = \mathcal{S}^*(b, s)(\mathbb{E}^{-1})^*x \\ &= \mathcal{S}(b, s)\mathbb{E}^{-1}x \\ &= e^{\int_s^b a(\tau)d\tau} \sum_{n=1}^{\infty} e^{\frac{-n^2}{1+n^2}(b-s)} \\ &\quad \langle \mathbb{E}^{-1}x, e_n \rangle e_n \\ &= e^{\int_s^b a(\tau)d\tau} \sum_{n=1}^{\infty} \frac{1}{1 + n^2} e^{\frac{-n^2}{1+n^2}(b-s)} \\ &\quad \langle x, e_n \rangle e_n. \end{aligned} \tag{26}$$

This implies that the condition (25) holds, and hence the assumption (H5). Thus by Theorem 5, the system (19) is approximately controllable on  $J$ .

### 5. Conclusion

In this work, we have obtained that the mild solutions for non-autonomous Sobolev differential equations with nonlocal condition exist mainly by the help of evolution system of bounded linear operators and Krasnoselskii fixed point technique. Also we have determined the sufficient conditions for approximate controllability by using the controllability of corresponding linear system. The results developed in this article can be extended to the study of existence of mild solutions and approximate controllability for neutral and impulsive differential systems. Moreover the obtained results also can be generalized for fractional Sobolev, neutral and impulsive differential systems.

### References

- [1] Chen, P.J., & Gurtin, M.E. (1968). On a theory of heat conduction involving two temperatures. *Zeitschrift für angewandte Mathematik und Physik*, 19(4), 614-627.
- [2] Barenblatt, G.I., Zheltov, I.P., & Kochina, I.N. (1960). Basic concepts in the theory of seepage of homogeneous liquids in fissured rocks. *Journal of Applied Mathematics and Mechanics*, 24, 1286-1303.
- [3] Taylor, D. (1952). *Research on Consolidation of Clays*. Massachusetts Institute of Technology Press, Cambridge.
- [4] Brill, H. (1977). A semilinear Sobolev evolution equation in a Banach space. *Journal of Differential Equations*, 24, 412-425.
- [5] Lightbourne, J.H., & Rankin, S.M. (1983). A partial differential equation of Sobolev type. *Journal of Mathematical Analysis and Applications*, 93, 328-337.

- [6] Byszewski, L. (1991). Theorem about the existence and uniqueness of solutions of a semi-linear evolution nonlocal Cauchy problem. *Journal of Mathematical Analysis and Applications*, 162, 494-505.
- [7] Curtain, R.F., & Zwart, H. (1995). *An Introduction to Infinite-Dimensional Linear Systems Theory*. Springer-Verlag, New York.
- [8] Mahmudov, N.I. (2003). Approximate controllability of semilinear deterministic and stochastic evolution equations in abstract spaces. *SIAM Journal on Control and Optimization*, 42(5), 1604-1622.
- [9] Shaktivel, R., Ren, Y., & Mahmudov, N.I. (2011). On the approximate controllability of semilinear fractional differential systems. *Computers and Mathematics with Applications*, 62, 1451-1459.
- [10] Mahmudov, N.I., & Zorlu, S. (2013). Approximate controllability of fractional integro-differential equations involving nonlocal initial conditions. *Boundary Value Problems*, 2013(118), 1-16.
- [11] Mahmudov, N.I., & Zorlu, S. (2014). On the approximate controllability of fractional evolution equations with compact analytic semigroup. *Journal of Computational and Applied Mathematics*, 259, 194-204.
- [12] Balasubramaniam, P., Vembarasan, V., & Senthilkumar, T. (2014). Approximate controllability of impulsive fractional integro-differential systems with nonlocal conditions in Hilbert Space. *Numerical Functional Analysis and Optimization*, 35(2), 177-197.
- [13] Zhang, X., Zhu, C., & Yuan, C. (2015). Approximate controllability of fractional impulsive evolution systems involving nonlocal initial conditions. *Advances in Difference Equations*, 2015(244), 1-14.
- [14] Yan, Z. (2009). On solutions of semilinear evolution integro-differential equations with nonlocal conditions. *Tamkang Journal of Mathematics*, 40(3), 257-269.
- [15] Haloi, R., Pandey, D.N., & Bahuguna, D. (2012). Existence uniqueness and asymptotic stability of solutions to non-autonomous semi-linear differential equations with deviated arguments. *Nonlinear Dynamics and Systems Theory*, 12(2), 179-191.
- [16] Chadha, A., & Pandey, D.N. (2015). Mild solutions for non-autonomous impulsive semi-linear differential equations with iterated deviating arguments. *Electronic Journal of Differential Equations*, 2015(222), 1-14.
- [17] Ahmed, H.M. (2012). Controllability for Sobolev type fractional integro-differential systems in a Banach space. *Advances in Differences Equations*, 2012(167), 1-10.
- [18] Mahmudov, N.I. (2013). Approximate controllability of fractional Sobolev type evolution equations in Banach space. *Abstract and Applied Analysis*, 2013, doi:10.1155/2013/502839.
- [19] Haloi, R. (2017). Approximate controllability of non-autonomous nonlocal delay differential equations with deviating arguments. *Electronic Journal of Differential Equations*, 2017(111), 1-12.
- [20] Friedman, A. (1997). *Partial Differential Equations*. Dover publication.
- [21] Pazy, A. (1993). *Semigroup of Linear Operators and Applications to Partial Differential Equations*. Applied Mathematical Sciences, Springer-Verlag, New York.
- [22] Granas, A., & Dugundji, J. (2003). *Fixed Point Theory*. Springer-Verlag, New York.

*Arshi Meraj* obtained her Master's degree in Mathematics from Indian Institute of Technology Kanpur and pursuing Ph.D. in the department of Mathematics at Indian Institute of Technology Roorkee. Her research interests include fractional differential equations and control theory.

*Dwijendra Narain Pandey* received his Master's and Ph.D. degree from Indian Institute of Technology Kanpur. Currently he is Associate Professor in the department of Mathematics at Indian Institute of Technology Roorkee. His area of research interests are functional evolution equations, theory of semigroup of operators, control theory, fractional differential equations and numerical methods for solving differential equations.



This work is licensed under a Creative Commons Attribution 4.0 International License. The authors retain ownership of the copyright for their article, but they allow anyone to download, reuse, reprint, modify, distribute, and/or copy articles in IJOCTA, so long as the original authors and source are credited. To see the complete license contents, please visit <http://creativecommons.org/licenses/by/4.0/>.

## RESEARCH ARTICLE

## A Boiti-Leon Pimpinelli equations with time-conformable derivative

Kamal Ait Touchent<sup>a</sup>, Zakia Hammouch<sup>\*a</sup>, Toufi Mekkaoui<sup>a</sup> and Canan Unlu<sup>b</sup>

<sup>a</sup>Department of Mathematics, FSTE Moulay Ismail University, Morocco

<sup>b</sup>Department of Mathematics Istanbul University, Turkey

kamaldemnite@gmail.com, z.hammouch@fste.umi.ac.ma, toufikmekkaoui@yahoo.fr, cunlu@istanbul.edu.tr

## ARTICLE INFO

## Article History:

Received 02 January 2019

Accepted 27 July 2019

Available 13 September 2019

## Keywords:

Sinh-Gordon expansion method

(2 + 1)- Boiti-Leon Pimpinelli equations

Conformable derivative

Jacobi Elliptic functions

AMS Classification 2010:

35Qxx; 26A33

## ABSTRACT

In this paper, we derive some new soliton solutions to (2 + 1)-Boiti-Leon Pimpinelli equations with conformable derivative by using an expansion technique based on the Sinh-Gordon equation. The obtained solutions have different expression such as trigonometric, complex and hyperbolic functions. This powerful and simple technique can be used to investigate solutions of other nonlinear partial differential equations.



### 1. Introduction

Partial differential equations play an important role in interpretation and modeling of many phenomena appearing in applied mathematics and physics including fluid mechanics, electrical circuits, diffusion, damping laws, relaxation processes, optimal control theory, solid mechanics, propagation of waves, chemistry, biology, and so on. Therefore, seeking solutions for partial differential equations is an important aspect of scientific research.

Besides, many scientists have focused on new findings to the nonlinear partial differential equations, such as traveling wave solutions, complex functions, trigonometric functions, Jacobi elliptic functions, and so on. For constructing such solutions, there exist numerous efficient techniques. For example, Sumudu homotopy perturbation transform method [1]- [4], Lie symmetry method [5],  $\tan(\phi(\xi)/2)$ - expansion method [6,7], generalized trigonometry functions [8], Riccati equation expansion technique [9], Jacobi elliptic function technique [10] and extended Jacobian

elliptic function technique [11], etc. For more informations about the analytical methods, we refer the reader to the following references [12]- [20].

In this article, we adopt a transformation method based on a sinh-Gordon expansion equation to obtain new soliton solutions of Boiti-Leon Pimpinelli equations (BLP) with conformable derivative. For more details on BLP equation we refer the reader to the references [21]- [23].

On the other hand, the following equation

$$\frac{\partial^2 u}{\partial x \partial t} = \alpha \sinh u, \quad (1)$$

is called Sinh-Gordon equation and arises in various areas of nonlinear sciences, where  $\alpha$  is an arbitrary constant.

Using the traveling wave transformation

$$\begin{cases} u(x, t) = U(\xi) \\ \xi = \mu(x + y - \lambda t), \end{cases} \quad (2)$$

equation (1) is converted to

\*Corresponding Author

$$\frac{\partial^2 U}{\partial \xi^2} = -\frac{\alpha}{\mu^2 \lambda} \sinh U, \tag{3}$$

where the coefficients  $\mu$  and  $\lambda$  stands for the wave number and wave speed, respectively. Now, integrating (3) yields to

$$\left(\frac{d}{d\xi} \frac{1}{2}U\right)^2 = -\frac{\alpha}{\mu^2 \lambda} \sinh^2 \left(\frac{1}{2}U\right) + c, \tag{4}$$

where  $c$  is an integration constant. Consider the following

$$c = 0, \alpha = -\mu^2 \lambda \quad \text{and} \quad \frac{1}{2}U = w,$$

equation (4) takes the form

$$\frac{dw(\xi)}{d\xi} = \sinh w(\xi). \tag{5}$$

To construct Jacobi elliptic function solutions, we convert equation (3) into the following

$$\frac{d^2 w}{d\xi^2} = \frac{1}{2} \sinh 2w, \tag{6}$$

under the assumptions  $\phi = 2w$  and  $-\frac{\alpha}{\mu^2 \lambda} = 1$ . Equation (6) can be also written as

$$\left(\frac{dw}{d\xi}\right)^2 = \sinh^2 w + c, \tag{7}$$

which can be used in the adopted method, where  $c$  is an integration constant. Therefore, Equation (7) has the following solutions

$$\sinh [w(\xi)] = \text{cs}(\xi; m), \tag{8}$$

$$\cosh [w(\xi)] = \text{ns}(\xi; m), \tag{9}$$

where  $m$  is the modulus of the Jacobian elliptic functions :

$$\text{cs}(\xi; m) = \frac{\text{cn}(\xi; m)}{\text{sn}(\xi; m)}$$

$$\text{ns}(\xi; m) = \frac{1}{\text{sn}(\xi; m)},$$

with the properties

$$\frac{d \text{cs}(\xi; m)}{d\xi} = -\text{ns}(\xi; m) \text{ds}(\xi; m),$$

$$\frac{d \text{ns}(\xi; m)}{d\xi} = -\text{cs}(\xi; m) \text{ds}(\xi; m).$$

Substitution of (8) and (9) in (7) reveals that the constant  $c$  must satisfy

$$c = 1 - m^2, \tag{10}$$

which is used throughout this work.

The plan of this paper is as follows: In section 2 some properties of conformable derivative are given. In section 3, we describe the sinh-Gordon expansion technique. Section 4 is devoted to construct exact solutions of (2+1)-Boiti-Leon Pimpinelli equations with time-conformable derivatives. Finally, a conclusion is given in section 5.

## 2. Conformable derivative

Recently, Khalil and his co-workers [24] presented a novel derivative called conformable. This section is devoted to provide some properties on it.

**Definition 1.** *The conformable derivative with order  $\alpha$  for a function  $f : [0, \infty) \rightarrow R$  is given by*

$$T_\alpha(f)(t) = \lim_{\epsilon \rightarrow 0} \frac{f(t + \epsilon t^{1-\alpha}) - f(t)}{\epsilon} \tag{11}$$

where  $t > 0, \alpha \in (0, 1)$ .

Now, we recall some of its properties :

$T_\alpha (af + bg) = aT_\alpha(f) + bT_\alpha(g)$  for all real constant  $a$  and  $b$ ,

$$T_\alpha (fg) = fT_\alpha(g) + gT_\alpha(f),$$

$$T_\alpha (t^r) = rt^{r-\alpha} \text{ for all } r,$$

$$T_\alpha \left(\frac{g}{f}\right) = \frac{fT_\alpha(g) - gT_\alpha(f)}{f^2},$$

$T_\alpha(C) = 0$ . Where  $C$  is a constant.

Moreover, if  $f$  is differentiable, then

$$T_\alpha(f) = t^{1-\alpha} \frac{df}{dt}(t).$$

**Theorem 1.** *Suppose that  $f : [0, \infty)$  is differentiable and conformable-differentiable with order  $\alpha$  and the function  $g$  is also differentiable. Then, we have the next property*

$$T_\alpha (f \circ g) = t^{1-\alpha} g'(t) f'(g(t)). \tag{12}$$

## 3. Description of the method

The analytical method, called sinh-Gordon equation expansion technique [25], is an efficient tool

to construct new explicit solutions for many problems arising in various branches of sciences and engineering. The algorithm of this method is based on equation (6) or equation (7) and it can be described as follows

- Consider the following nonlinear equation in the sense of conformable derivative:

$$\mathbf{N}(u, T_t^\alpha u, T_x^\alpha u, T_y^\alpha u, \dots) = 0. \quad (13)$$

- Using the following transformation

$$u(x, y, t) = U(\xi), \quad \xi = \mu \left( \frac{x^\alpha}{\alpha} + \frac{y^\alpha}{\alpha} - \lambda \frac{t^\alpha}{\alpha} \right).$$

Equation (13) is converted to an ordinary differential equation

$$\mathbf{Q}(U, U', \mu U', -\lambda U', U'', \mu^2 U'', \dots) = 0. \quad (14)$$

- Now, we assume that the solution of (14) is as follows

$$U(w) = A_0 + \sum_{i=1}^n \cosh^{i-1} w [A_i \sinh w + B_i \cosh w], \quad (15)$$

where  $w = w(\xi)$  satisfies (6) or (7) and (10),  $A_i, B_i$  for  $i = 0, 1, 2, \dots, n$ , are constants to be fixed later.

- By virtue of the balance principle, we take the nonlinear terms and the highest-order derivatives in (14) to determine the value of integer  $n$ . Now, let the coefficients of  $\sinh^i w \cosh^j w$  that have same power to be zero, to get a system of equations with the unknowns:

$$\mu, \lambda, A_i \text{ and } B_j \text{ for } i = 0, 1, \dots, n.$$

- Finally, we solve the obtained system with Maple software, then we substitute  $A_0, A_1, B_1, \dots, A_n, B_n, \mu$  and  $\lambda$  in (15).

**Remark 1.** When  $m \rightarrow 1$ , we have

$$\text{cs}(\xi, m) \rightarrow \text{csch}(\xi), \quad \text{ns}(\xi, m) \rightarrow \text{coth}(\xi), \quad (16)$$

Similarly, when  $m \rightarrow 0$ , it comes

$$\text{cs}(\xi, m) \rightarrow \cot(\xi), \quad \text{ns}(\xi, m) \rightarrow \csc(\xi). \quad (17)$$

## 4. Application of the method

In this section, we apply the above described method to solve the (2 + 1)-Boiti-Leon Pimpinelli equations defined as follows [26]:

$$\begin{cases} T_t^\alpha u_y = (u^2 - u_x)_{xy} + 2v_{xxx}, \\ T_t^\alpha v_y = v_{xx} + 2uv_x. \end{cases} \quad (18)$$

Accordingly, we consider the following wave transformation

$$\begin{cases} u(x, y, t) = U(\xi), \\ v(x, y, t) = V(\xi), \\ \xi = \mu(x + y - \lambda \frac{t^\alpha}{\alpha}), \end{cases} \quad (19)$$

where  $\lambda, \mu$  are constants to be fixed later.

The previous wave transformation reduces (20) to the following system of ODEs

$$\begin{cases} T_t^\alpha(u_y) = -\lambda\mu^2 U'', \\ (u^2 - u_x)_{xy} = \mu^2 [(U^2)'' - \mu U'''], \\ 2v_{xxx} = 2\mu^3 V''', \\ T_t^\alpha v = -\lambda\mu V', \\ v_{xx} = \mu^2 V'', \\ 2uv_x = 2\mu UV'. \end{cases} \quad (20)$$

Then, the new system becomes

$$\begin{cases} -\lambda\mu^2 U'' = \mu^2 (U^2)'' - \mu^3 U''' + 2\mu^3 V''', \\ -\lambda\mu V' = \mu^2 V'' + 2\mu UV'. \end{cases} \quad (21)$$

After simplification, we get

$$-\lambda U'' = (U^2)'' - \mu U''' + 2\mu V''', \quad (22)$$

$$-\lambda V' = \mu V'' + 2UV'. \quad (23)$$

integrating equation (22) twice and taking zero as constants of integration, yields to

$$V' = \frac{U'}{2} - \frac{U^2 + \lambda U}{2\mu}. \quad (24)$$

Injecting equation (24) into equation (23), gives the following nonlinear differential equation

$$\mu^2 U'' - 2U^3 - 3\lambda U^2 - \lambda^2 U = 0. \quad (25)$$

Now, balancing the terms  $U''$  and  $U^3$ , yields  $n = 1$ . Therefore, the solutions of equation (25) is converted to the following form

$$U(\xi) = A_0 + A_1 \sinh(w(\xi)) + B_1 \cosh(w(\xi)). \tag{26}$$

Substituting (26) into (25), we get a set of algebraic equations for  $\lambda, \mu, A_0, A_1$ , and  $B_1$  as follows

$$\begin{cases} eq1 = -6 A_1^2 B_1 - 2 B_1^3 + 2 B_1 \mu^2, \\ eq2 = -2 A_1^3 - 6 A_1 B_1^2 + 2 A_1 \mu^2, \\ eq3 = -6 A_0 A_1^2 - 6 A_0 B_1^2 - 3 A_1^2 \lambda - 3 B_1^2 \lambda, \\ eq4 = -12 A_0 A_1 B_1 - 6 A_1 B_1 \lambda, \\ eq5 = B_1 c \mu^2 - 6 A_0^2 B_1 - 6 A_0 B_1 \lambda + 6 A_1^2 B_1 \\ \quad - 2 B_1 \mu^2 - B_1 \lambda^2, \\ eq6 = A_1 c \mu^2 - 6 A_0^2 A_1 - 6 A_0 A_1 \lambda + 2 A_1^3 \\ \quad - A_1 \mu^2 - A_1 \lambda^2, \\ eq7 = -2 A_0^3 - 3 \lambda A_0^2 + 6 A_0 A_1^2 - \lambda^2 A_0 \\ \quad + 3 \lambda A_1^2. \end{cases} \tag{27}$$

Solving the set of above equations, we get

**Case I:**

$$\begin{cases} A_0 = -\frac{\lambda}{2}, & B_1 = \frac{\lambda}{\sqrt{2m^2+2}}, \\ \mu = -\frac{\lambda}{\sqrt{2m^2+2}}, & A_1 = 0. \end{cases}$$

By using (28) and (26), we attain

$$U_1(\xi) = -\frac{1}{2} \lambda + \frac{\lambda \operatorname{ns}(\xi, m)}{\sqrt{2m^2+2}}, \tag{28}$$

and

$$\begin{aligned} V_1(\xi) = & -1/4 \frac{\lambda m^2 \xi}{\sqrt{2m^2+2}} - 1/2 \frac{\lambda \operatorname{dn}(\xi, m) \operatorname{cn}(\xi, m)}{\sqrt{2m^2+2} \operatorname{sn}(\xi, m)} \\ & - 1/2 \frac{\lambda \operatorname{E}(\operatorname{sn}(\xi, m), m)}{\sqrt{2m^2+2}} + 1/4 \frac{\lambda \xi}{\sqrt{2m^2+2}} \\ & + 1/2 \frac{\lambda}{\sqrt{2m^2+2} \operatorname{sn}(\xi, m)}. \end{aligned} \tag{29}$$

where  $\xi = \mu(x + y - \lambda \frac{t^\alpha}{\alpha})$ .

**Case II:**

$$\begin{cases} A_0 = -\frac{\lambda}{2}, & A_1 = \frac{\lambda}{\sqrt{2m^2-4}}, \\ \mu = -\frac{\lambda}{\sqrt{2m^2-4}}, & B_1 = 0. \end{cases} \tag{30}$$

From (30) and (26), yields

$$U_2(\xi) = -\frac{1}{2} \lambda + \frac{\lambda \operatorname{cs}(\xi, m)}{\sqrt{2m^2-4}}, \tag{31}$$

and

$$\begin{aligned} V_2(\xi) = & -1/2 \frac{\lambda m^2 \operatorname{cn}(\xi, m) \operatorname{sn}(\xi, m)}{\sqrt{2m^2-4} ((\operatorname{dn}(\xi, m))^2 - 1)} + 1/8 \frac{\lambda^2 \xi}{\mu} \\ & + 1/4 \frac{\lambda^2 \sqrt{2m^2-4} \ln(\operatorname{ns}(\xi, m) - \operatorname{ds}(\xi, m))}{\mu (m^2 - 2)} \\ & + 1/4 \frac{\lambda^2 \operatorname{ds}(\xi, m) \operatorname{cs}(\xi, m)}{\mu (m^2 - 2) \operatorname{ns}(\xi, m)} + 1/4 \frac{\lambda^2 \operatorname{E}(\operatorname{sn}(\xi, m), m)}{\mu (m^2 - 2)} \\ & - 1/2 \frac{\lambda^2 \ln(\operatorname{ns}(\xi, m) - \operatorname{ds}(\xi, m))}{\mu \sqrt{2m^2-4}}, \end{aligned} \tag{32}$$

where  $\xi = \mu(x + y - \lambda \frac{t^\alpha}{\alpha})$ .

**Case III:**

$$\begin{cases} A_0 = -\frac{1}{2} \lambda, & A_1 = \frac{1}{2} \frac{\lambda}{\sqrt{2m^2-1}}, \\ B_1 = \frac{1}{2} \frac{\lambda}{\sqrt{2m^2-1}}, & \mu = \frac{\lambda}{\sqrt{2m^2-1}}. \end{cases} \tag{33}$$

By using (33) and (26), we get

$$U_3(\xi) = -\frac{1}{2} \lambda + \frac{1}{2} \frac{\lambda \operatorname{cs}(\xi, m)}{\sqrt{2m^2-1}} + \frac{1}{2} \frac{\lambda \operatorname{ns}(\xi, m)}{\sqrt{2m^2-1}}, \tag{34}$$

where  $\xi = \mu(x + y - \lambda \frac{t^\alpha}{\alpha})$ .

**Remark 2.** The expression of  $V_3$  is too long to be mentioned here.

If  $m \rightarrow 0$ , the following solitary wave solutions of (20) are generated from (28),(31) and (34), namely

$$U_4(\xi) = -\frac{1}{2} \lambda + \frac{1}{2} \lambda \operatorname{csc}(\xi) \sqrt{2}, \tag{35}$$

$$\begin{aligned} V_4(\xi) = & \frac{1}{4} \lambda \operatorname{csc}(\xi) \sqrt{2} - \frac{1}{8} \lambda \sqrt{2} \xi \\ & - \frac{1}{2} \lambda \ln(\operatorname{csc}(\xi) - \cot(\xi)) \\ & - \frac{1}{4} \frac{\lambda \sqrt{2} \cos(\xi)}{\sin(\xi)} - \frac{1}{2} \lambda \ln(\operatorname{csc}(\xi) + \cot(\xi)), \end{aligned} \tag{36}$$

$$U_5(\xi) = -\frac{1}{2} \lambda - \frac{1}{2} i \lambda \cot(\xi), \tag{37}$$

$$V_5(\xi) = -\frac{1}{4}i\lambda\xi - \frac{1}{8}i\lambda\pi + \frac{1}{4}i\lambda\operatorname{arccot}(\cot(\xi)) + \frac{1}{4}\lambda\ln\left((\cot(\xi))^2 + 1\right) + \frac{1}{2}\lambda\ln(\sin(\xi)), \quad (38)$$

$$U_6(\xi) = -\frac{1}{2}\lambda - \frac{1}{2}i\lambda\cot(\xi) - \frac{1}{2}i\lambda\csc(\xi), \quad (39)$$

$$V_6(\xi) = \frac{1}{4}i\lambda\xi - \frac{3}{8}i\lambda\cot(\xi) + \frac{1}{8}i\lambda\pi - \frac{1}{4}i\lambda\operatorname{arccot}(\cot(\xi)) - \frac{1}{4}i\lambda\csc(\xi) - \frac{\frac{1}{4}i\lambda}{\sin(\xi)} - \frac{\frac{1}{8}i\lambda\cos(\xi)}{\sin(\xi)} + \frac{1}{4}\lambda\ln(\csc(\xi) - \cot(\xi)) + \frac{1}{4}\lambda\ln(\csc(\xi) + \cot(\xi)), \quad (40)$$

where  $\xi = \mu(x + y - \lambda\frac{t^\alpha}{\alpha})$ .

If  $m \rightarrow 1$ , we get from (28),(31) and (34), new solutions of (20)

$$U_7(\xi) = -\frac{1}{2}\lambda + \frac{1}{2}\lambda\coth(\xi), \quad (41)$$

$$V_7(\xi) = -1/4\lambda\xi + 1/8\lambda\ln(\cosh(\xi) - \sinh(\xi)) + 3/8\lambda\ln(\cosh(\xi) + \sinh(\xi)), \quad (42)$$

$$U_8(\xi) = -\frac{1}{2}\lambda - \frac{1}{2}i\lambda\operatorname{csch}(\xi)\sqrt{2}, \quad (43)$$

$$V_8(\xi) = -1/4i\lambda\sqrt{2}\operatorname{csch}(\xi) - 1/8i\lambda\sqrt{2}\xi + \lambda\operatorname{arctanh}(e^\xi) + \frac{1/4i\lambda\sqrt{2}\cosh(\xi)}{\sinh(\xi)} + 1/2\lambda\ln\left(\frac{\cosh(\xi)-1}{\sinh(\xi)}\right). \quad (44)$$

$$U_9(\xi) = -\frac{1}{2}\lambda + \frac{1}{2}\lambda\operatorname{csch}(\xi) + \frac{1}{2}\lambda\coth(\xi), \quad (45)$$

$$V_9(\xi) = 1/4\lambda\operatorname{csch}(\xi) + 1/4\lambda\xi + 3/8\lambda\coth(\xi) + \lambda/8(\ln(\coth(\xi) - 1) - \ln(\coth(\xi) + 1)) - 1/2\lambda\operatorname{arctanh}(e^\xi) + 1/8\frac{\lambda\cosh(\xi)}{\sinh(\xi)} + 1/4\frac{\lambda(\cosh(\xi))^2}{\sinh(\xi)} - 1/4\lambda\sinh(\xi) - 1/4\lambda\ln\left(\frac{\cosh(\xi)-1}{\sinh(\xi)}\right), \quad (46)$$

where  $\xi = \mu(x + y - \lambda\frac{t^\alpha}{\alpha})$ .

## 5. Conclusion

In this paper, we have obtained some new solitary wave solutions to the (2 + 1)-dimensional-Boiti-Leon Pimpinelli equations with time-conformable derivative. It is clear to see that our obtained solutions through the suggested method are interesting and new comparing to the existing literature. Moreover, the obtained solitons have various structures such hyperbolic, trigonometric and complex, which signifies that they have an important physical meanings.

## Acknowledgments

The authors thank the anonymous referee for their careful reading of our manuscript and their many insightful comments and suggestions. This research was supported by The Research Project-UMI2016.

## References

- [1] Singh, J., Kumar, D. & Kılıcman, A. (2013). Homotopy perturbation method for fractional gas dynamics equation using Sumudu transform. *Abstract and Applied Analysis*. Vol.2013.
- [2] Ait Touchent, K. & Belgacem, F. (2015). Nonlinear fractional partial differential equations systems solutions through a hybrid homotopy perturbation Sumudu transform method. *Nonlinear Studies*, 22, 591-600.
- [3] Dinkar, S., Singh, P. & Chauhan S. (2016). Homotopy Perturbation Sumudu Transform Method with He's Polynomial for Solutions of Some Fractional Nonlinear Partial Differential Equations. *International Journal of Nonlinear Science*, 21, 91-97.
- [4] Youssif, E., & Hamed, S. (2014). Solution of nonlinear fractional differential equations using the homotopy perturbation Sumudu

- transform method. *Applied Mathematical Sciences*, 8, 2195-2210.
- [5] Buckwar, E. & Luchko, Y. (1988). Invariance of a partial differential equation of fractional order under the Lie group of scaling transformations. *J. Math. Anal. Appl.*, 227, 81-97.
- [6] Hammouch, Z., Mekkaoui, T. & Agarwal, P. (2018). Optical solitons for the Calogero-Bogoyavlenskii-Schiff equation in (2+1) dimensions with time-fractional conformable derivative. *European Physical Journal Plus*, 133:248.
- [7] Manaf an, J. & Foroutan, M. (2016). Application of  $\tan(\phi(\xi)/2)$ -expansion method for solving the Biswas–Milovic equation for Kerr law nonlinearity. *Optik-International Journal for Light and Electron Optics*, 127, 2040-2054.
- [8] Hammouch, Z. & Mekkaoui, T. (2012). Travelling-wave solutions for some fractional partial differential equation by means of generalized trigonometry functions. *International Journal of Applied Mathematical Research*, 1, 206-212.
- [9] Rezazadeh, H., Korkmaz, A., Eslami, M., Vahidi, J., & Asghari, R. (2018). Traveling wave solution of conformable fractional generalized reaction Duffing model by generalized projective Riccati equation method. *Optical and Quantum Electronics*, 50(3), 150.
- [10] Tasbozan, O., Cenesiz, Y., & Kurt, A. (2016). New solutions for conformable fractional Boussinesq and combined KdV-mKdV equations using Jacobi elliptic function expansion method. *The European Physical Journal Plus*, 131(7), 244.
- [11] Zhu, J. & Ma, Z. (2005). An extended Jacobian elliptic function method for the discrete mKdV lattice. *Chinese Physics*, 14, 17.
- [12] Hammouch, Z. & Mekkaoui, T. (2013). Approximate analytical and numerical solutions to fractional KPP-like equations. *General Mathematics Notes*, 14(2), 1-9.
- [13] Hammouch, Z. & Mekkaoui, T. (2015). Control of a new chaotic fractional-order system using Mittag-Leffler stability. *Nonlinear Studies*, 22(4), 565-577.
- [14] Hammouch, Z. & Mekkaoui, T. (2013). Approximate analytical solution to a time-fractional Zakharov-Kuznetsov equation. *Int. J. Eng. Tech.*, 1, 1-13.
- [15] Mekkaoui, T. & Hammouch, Z. (2012). Approximate analytical solutions to the Bagley-Torvik equation by the Fractional Iteration Method. *Annals of the University of Craiova-Mathematics and Computer Science Series*, 39(2), 251-256.
- [16] Baskonus, H. et al. (2015). Active control of a chaotic fractional order economic system. *Entropy*, 17(8), 5771-5783.
- [17] Yavuz, M. (2017). Novel solution methods for initial boundary value problems of fractional order with conformable differentiation. *An International Journal of Optimization and Control: Theories & Applications*, 8(1), 1-7.
- [18] Yavuz, M. & Ozdemir N. (2017). New numerical techniques for solving fractional partial differential equations in conformable sense. *Non-Integer Order Calculus and its Applications*, Springer Cham., 49-62.
- [19] Yavuz, M. & Yaskiran, B. (2018). Conformable derivative operator in modelling neuronal dynamics. *Applications & Applied Mathematics*, 13(2), 803-817.
- [20] Yavuz, M. & Ozdemir N. (2018). On the solutions of fractional Cauchy problem featuring conformable derivative. *ITM Web of Conferences*, Vol. 22. EDP Sciences.
- [21] Yu, J., Liu, X. & Wang, T. (2010). Exact solutions and conservation laws of (2+1)-dimensional Boiti–Leon–Pempinelli equation. *Applied Mathematics and Computation*, 216(8), 2293-2300.
- [22] Dai, C. & Wang, Y. (2009). Periodic structures based on variable separation solution of the (2+1)-dimensional Boiti–Leon–Pempinelli equation. *Chaos, Solitons Fractals*, 39, 350–355.
- [23] Huang, D.J. & Zhang, H-Q. (2004). Exact travelling wave solutions for the Boiti–Leon–Pempinelli equation. *Chaos Solitons and Fractals*, 22, 243–247.
- [24] Khalil, R., Al Horani, M., Yousef, A. & Sababheh, M. (2014). A new definition of fractional derivative. *Journal of Computational and Applied Mathematics*, 264, 65-70.
- [25] Yan, Z. (2003). A sinh-Gordon equation expansion method to construct doubly periodic solutions for nonlinear differential equations. *Chaos, Solitons and Fractals*, 16(2), 291-297.
- [26] Qi, J., et al. (2014). Some new traveling wave exact solutions of the (2 + 1)-dimensional Boiti–Leon–Pempinelli equations. *The Scientific World Journal*, Vol.2014.

**Kamal Ait Touchent** received his B.S. degree in Applied Mathematics from Sultan Moulay Sliman University, Morocco. Currently, he is a Secondary School Teacher at Errich city and Ph.D. student at Moulay Ismail University. His research interests include Fractional calculus, Traveling waves, and Homotopy methods.

**Zakia Hammouch** received her M.S. in Applied Mathematics and Ph.D. degree in Applied Mathematics and Mechanical Engineering from University of Picardie Jules Verne France. She received habilitation degree from Moulay Ismail University, Morocco in 2015. She is currently Associate Professor at Faculty of Sciences and Techniques University of Moulay Ismail, Morocco. Prof Zakia Hammouch has published over 60 journal papers and chapters in reputed journals and books. She is editorial member of more than 10 international journals, a reviewer of 35 international journals of mathematics and mechanical engineering and a member of scientific committee of more than 20 international conferences. Her research interests include : Computational mathematics, biomathematics, nonlinear dynamics, fractional calculus, chaos theory, control and synchronization, fluid dynamics, heat and mass transfer, soliton theory.

**Toufik Mekkaoui** received his M.S. in Mathematics and Ph.D. degrees in Numerical Analysis from Orsay University Paris 11 France. He received habilitation degree from Moulay Ismail University, Morocco in 2008. He is currently Full Professor at Faculty of Sciences and Techniques University of Moulay Ismail, Morocco. His research interests include : Computational mathematics, Homogenization, Partial Differential Equations, Numerical Analysis.

**Canan Unlu** received her M.S. in Mathematical Analysis from Department of Mathematics of Ataturk university, and PhD degree in Applied mathematics from Istanbul university Istanbul, Turkey. Her research fields are: Decomposition methods, traveling waves and biomathematics.

An International Journal of Optimization and Control: Theories & Applications (<http://ijocta.balikesir.edu.tr>)



This work is licensed under a Creative Commons Attribution 4.0 International License. The authors retain ownership of the copyright for their article, but they allow anyone to download, reuse, reprint, modify, distribute, and/or copy articles in IJOCTA, so long as the original authors and source are credited. To see the complete license contents, please visit <http://creativecommons.org/licenses/by/4.0/>.

## **INSTRUCTIONS FOR AUTHORS**

### **Aims and Scope**

An International Journal of Optimization and Control: Theories & Applications (IJOCTA) shares the research carried out through different disciplines in regards to optimization, control and their applications.

The basic fields of this journal are linear, nonlinear, stochastic, parametric, discrete and dynamic programming; heuristic algorithms in optimization, control theory, game theory and their applications. Problems such as managerial decisions, time minimization, profit maximizations and other related topics are also shared in this journal.

Besides the research articles expository papers, which are hard to express or model, conference proceedings, book reviews and announcements are also welcome.

### **Journal Topics**

- Applied Mathematics,
- Financial Mathematics,
- Control Theory,
- Game Theory,
- Fractional Calculus,
- Fractional Control,
- Modeling of Bio-systems for Optimization and Control,
- Linear Programming,
- Nonlinear Programming,
- Stochastic Programming,
- Parametric Programming,
- Conic Programming,
- Discrete Programming,
- Dynamic Programming,
- Optimization with Artificial Intelligence,
- Operational Research in Life and Human Sciences,
- Heuristic Algorithms in Optimization,
- Applications Related to Optimization on Engineering.

### **Submission of Manuscripts**

#### New Submissions

Solicited and contributed manuscripts should be submitted to IJOCTA via the journal's online submission system. You need to make registration prior to submitting a new manuscript (please [click here](#) to register and do not forget to define yourself as an "Author" in doing so). You may then click on the "New Submission" link on your User Home.

**IMPORTANT:** If you already have an account, please [click here](#) to login. It is likely that you will have created an account if you have reviewed or authored for the journal in the past.

On the submission page, enter data and answer questions as prompted. Click on the "Next" button on each screen to save your work and advance to the next screen. The names and contact details of at least four internationally recognized experts who can review your manuscript should be entered in the "Comments for the Editor" box.

You will be prompted to upload your files: Click on the "Browse" button and locate the file on your computer. Select the description of the file in the drop down next to the Browse button. When you have selected all files you wish to upload, click the "Upload" button. Review your submission before sending to the Editors. Click the "Submit" button when you are done reviewing. Authors are responsible for verifying all files have uploaded correctly.

You may stop a submission at any phase and save it to submit later. Acknowledgment of receipt of the manuscript by IJOCTA Online Submission System will be sent to the corresponding author, including an

assigned manuscript number that should be included in all subsequent correspondence. You can also log-on to submission web page of IJOCTA any time to check the status of your manuscript. You will receive an e-mail once a decision has been made on your manuscript.

Each manuscript must be accompanied by a statement that it has not been published elsewhere and that it has not been submitted simultaneously for publication elsewhere.

Manuscripts can be prepared using LaTeX (.tex) or MSWord (.docx). However, manuscripts with heavy mathematical content will only be accepted as LaTeX files.

Preferred first submission format (for reviewing purpose only) is Portable Document File (.pdf). Please find below the templates for first submission.

[Click here](#) to download Word template for first submission (.docx)

[Click here](#) to download LaTeX template for first submission (.tex)

### Revised Manuscripts

Revised manuscripts should be submitted via IJOCTA online system to ensure that they are linked to the original submission. It is also necessary to attach a separate file in which a point-by-point explanation is given to the specific points/questions raised by the referees and the corresponding changes made in the revised version.

To upload your revised manuscript, please go to your author page and click on the related manuscript title. Navigate to the "Review" link on the top left and scroll down the page. Click on the "Choose File" button under the "Editor Decision" title, choose the revised article (in pdf format) that you want to submit, and click on the "Upload" button to upload the author version. Repeat the same steps to upload the "Responses to Reviewers/Editor" file and make sure that you click the "Upload" button again.

To avoid any delay in making the article available freely online, the authors also need to upload the source files (Word or LaTeX) when submitting revised manuscripts. Files can be compressed if necessary. The two-column final submission templates are as follows:

[Click here](#) to download Word template for final submission (.docx)

[Click here](#) to download LaTeX template for final submission (.tex)

Authors are responsible for obtaining permission to reproduce copyrighted material from other sources and are required to sign an agreement for the transfer of copyright to IJOCTA.

### **Article Processing Charges**

There are no charges for submission and/or publication.

### **English Editing**

Papers must be in English. Both British and American spelling is acceptable, provided usage is consistent within the manuscript. Manuscripts that are written in English that is ambiguous or incomprehensible, in the opinion of the Editor, will be returned to the authors with a request to resubmit once the language issues have been improved. This policy does not imply that all papers must be written in "perfect" English, whatever that may mean. Rather, the criteria require that the intended meaning of the authors must be clearly understandable, i.e., not obscured by language problems, by referees who have agreed to review the paper.

### **Presentation of Papers**

#### Manuscript style

Use a standard font of the **11-point type: Times New Roman** is preferred. It is necessary to single line space your manuscript. Normally manuscripts are expected not to exceed 25 single-spaced pages

including text, tables, figures and bibliography. All illustrations, figures, and tables are placed within the text at the appropriate points, rather than at the end.

During the submission process you must enter: (1) the full title, (2) names and affiliations of all authors and (3) the full address, including email, telephone and fax of the author who is to check the proofs. Supply a brief **biography** of each author at the end of the manuscript after references.

- Include the name(s) of any **sponsor(s)** of the research contained in the paper, along with **grant number(s)**.
- Enter an **abstract** of no more than 250 words for all articles.

#### Keywords

Authors should prepare no more than 5 keywords for their manuscript.

Maximum five **AMS Classification number** (<http://www.ams.org/mathscinet/msc/msc2010.html>) of the study should be specified after keywords.

#### Writing Abstract

An abstract is a concise summary of the whole paper, not just the conclusions. The abstract should be no more than 250 words and convey the following:

1. An introduction to the work. This should be accessible by scientists in any field and express the necessity of the experiments executed.
2. Some scientific detail regarding the background to the problem.
3. A summary of the main result.
4. The implications of the result.
5. A broader perspective of the results, once again understandable across scientific disciplines.

It is crucial that the abstract conveys the importance of the work and be understandable without reference to the rest of the manuscript to a multidisciplinary audience. Abstracts should not contain any citation to other published works.

#### Reference Style

Reference citations in the text should be identified by numbers in square brackets "[ ]". All references must be complete and accurate. Please ensure that every reference cited in the text is also present in the reference list (and vice versa). Online citations should include date of access. References should be listed in the following style:

##### *Journal article*

Author, A.A., & Author, B. (Year). Title of article. Title of Journal, Vol(Issue), pages.

Castles, F.G., Curtin, J.C., & Vowles, J. (2006). Public policy in Australia and New Zealand: The new global context. *Australian Journal of Political Science*, 41(2), 131–143.

##### *Book*

Author, A. (Year). Title of book. Publisher, Place of Publication.

Mercer, P.A., & Smith, G. (1993). *Private Viewdata in the UK*. 2nd ed. Longman, London.

##### *Chapter*

Author, A. (Year). Title of chapter. In: A. Editor and B. Editor, eds. Title of book. Publisher, Place of publication, pages.

Bantz, C.R. (1995). Social dimensions of software development. In: J.A. Anderson, ed. *Annual review of software management and development*. CA: Sage, Newbury Park, 502–510.

##### *Internet document*

Author, A. (Year). Title of document [online]. Source. Available from: URL [Accessed (date)].

Holland, M. (2004). Guide to citing Internet sources [online]. Poole, Bournemouth University. Available from: [http://www.bournemouth.ac.uk/library/using/guide\\_to\\_citing\\_internet\\_sourc.html](http://www.bournemouth.ac.uk/library/using/guide_to_citing_internet_sourc.html) [Accessed 4 November 2004].

#### *Newspaper article*

Author, A. (or Title of Newspaper) (Year). Title of article. Title of Newspaper, day Month, page, column.

Independent (1992). Picking up the bills. Independent, 4 June, p. 28a.

#### *Thesis*

Author, A. (Year). Title of thesis. Type of thesis (degree). Name of University.

Agutter, A.J. (1995). The linguistic significance of current British slang. PhD Thesis. Edinburgh University.

#### Illustrations

Illustrations submitted (line drawings, halftones, photos, photomicrographs, etc.) should be clean originals or digital files. Digital files are recommended for highest quality reproduction and should follow these guidelines:

- 300 dpi or higher
- Sized to fit on journal page
- TIFF or JPEG format only
- Embedded in text files and submitted as separate files (if required)

#### Tables and Figures

Tables and figures (illustrations) should be embedded in the text at the appropriate points, rather than at the end. A short descriptive title should appear above each table with a clear legend and any footnotes suitably identified below.

#### Proofs

Page proofs are sent to the designated author using IJOCTA EProof system. They must be carefully checked and returned within 48 hours of receipt.

#### Offprints/Reprints

Each corresponding author of an article will receive a PDF file of the article via email. This file is for personal use only and may not be copied and disseminated in any form without prior written permission from IJOCTA.

### **Submission Preparation Checklist**

As part of the submission process, authors are required to check off their submission's compliance with all of the following items, and submissions may be returned to authors that do not adhere to these guidelines.

1. The submission has not been previously published, nor is it before another journal for consideration (or an explanation has been provided in Comments for the Editor).
2. The submission file is in Portable Document Format (.pdf).
3. The ORCID profile numbers of "all" authors are ready to enter in the step of Article Metadata (visit <https://orcid.org> for more details).
4. The text is single line spaced; uses a 11-point font; employs italics, rather than underlining (except with URL addresses); and all illustrations, figures, and tables are placed within the text at the appropriate points, rather than at the end.
5. The text adheres to the stylistic and bibliographic requirements outlined in the Author Guidelines, which is found in "About the Journal".
6. Maximum five AMS Classification number (<http://www.ams.org/mathscinet/msc/msc2010.html>) of the study have been provided after keywords.
7. After the acceptance of manuscript (before copy editing), Word (.docx) or LaTeX (.tex) version of the paper will be presented.
8. The names and email addresses of at least four (4) possible reviewers have been indicated in "Comments for the Editor" box in Paper Submission Step 1. Please note that at least two of the recommendations should be from different countries. Avoid suggesting reviewers who are at arms-length from you or your co-authors. This includes graduate advisors, people in your current department, or any others with a conflict of interest.

## Peer Reviewing Process

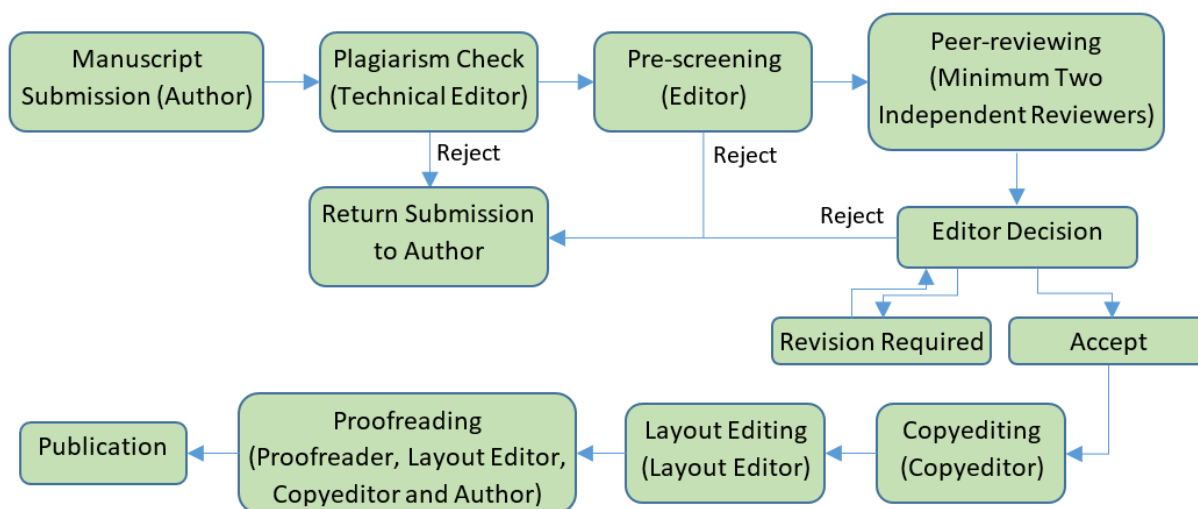
All contributions, prepared according to the author guidelines and submitted via IJOCTA online submission system are evaluated according to the criteria of originality and quality of their scientific content. The corresponding author will receive a confirmation e-mail with a reference number assigned to the paper, which he/she is asked to quote in all subsequent correspondence.

All manuscripts are first checked by the Technical Editor using plagiarism detection software (iThenticate) to verify originality and ensure the quality of the written work. If the result is not satisfactory (i.e. exceeding the limit of 30% of overlapping), the submission is rejected and the author is notified.

After the plagiarism check, the manuscripts are evaluated by the Editor-in-Chief and can be rejected without reviewing if considered not of sufficient interest or novelty, too preliminary or out of the scope of the journal. If the manuscript is considered suitable for further evaluation, it is first sent to the Area Editor. Based on his/her opinion the paper is then sent to at least two independent reviewers. Each reviewer is allowed up to four weeks to return his/her feedback but this duration may be extended based on his/her availability. IJOCTA has instituted a blind peer review process where the reviewers' identities are not known to authors. When the reviews are received, the Area Editor gives a decision and lets the author know it together with the reviewer comments and any supplementary files.

Should the reviews be positive, the authors are expected to submit the revised version usually within two months the editor decision is sent (this period can be extended when the authors contact to the editor and let him/her know that they need extra time for resubmission). If a revised paper is not resubmitted within the deadline, it is considered as a new submission after all the changes requested by reviewers have been made. Authors are required to submit a new cover letter, a response to reviewers letter and the revised manuscript (which ideally shows the revisions made in a different color or highlighted). If a change in authorship (addition or removal of author) has occurred during the revision, authors are requested to clarify the reason for change, and all authors (including the removed/added ones) need to submit a written consent for the change. The revised version is evaluated by the Area editor and/or reviewers and the Editor-in-Chief brings a decision about final acceptance based on their suggestions. If necessary, further revision can be asked for to fulfil all the requirements of the reviewers.

When a manuscript is accepted for publication, an acceptance letter is sent to the corresponding author and the authors are asked to submit the source file of the manuscript conforming to the IJOCTA two-column final submission template. After that stage, changes of authors of the manuscript are not possible. The manuscript is sent to the Copyeditor and a linguistic, metrological and technical revision is made, at which stage the authors are asked to make the final corrections in no more than a week. The layout editor prepares the galley and the authors receive the galley proof for final check before printing. The authors are expected to correct only typographical errors on the proofs and return the proofs within 48 hours. After the final check by the layout editor and the proofreader, the manuscript is assigned a DOI number, made publicly available and listed in the forthcoming journal issue. After printing the issue, the corresponding metadata and files published in this issue are sent to the databases for indexing.



## **Publication Ethics and Malpractice Statement**

IJOCTA is committed to ensuring ethics in publication and quality of articles. Conforming to standards of expected ethical behavior is therefore necessary for all parties (the author, the editor(s), the peer reviewer) involved in the act of publishing.

### International Standards for Editors

The editors of the IJOCTA are responsible for deciding which of the articles submitted to the journal should be published considering their intellectual content without regard to race, gender, sexual orientation, religious belief, ethnic origin, citizenship, or political philosophy of the authors. The editors may be guided by the policies of the journal's editorial board and constrained by such legal requirements as shall then be in force regarding libel, copyright infringement and plagiarism. The editors may confer with other editors or reviewers in making this decision. As guardians and stewards of the research record, editors should encourage authors to strive for, and adhere themselves to, the highest standards of publication ethics. Furthermore, editors are in a unique position to indirectly foster responsible conduct of research through their policies and processes.

To achieve the maximum effect within the research community, ideally all editors should adhere to universal standards and good practices.

- Editors are accountable and should take responsibility for everything they publish.
- Editors should make fair and unbiased decisions independent from commercial consideration and ensure a fair and appropriate peer review process.
- Editors should adopt editorial policies that encourage maximum transparency and complete, honest reporting.
- Editors should guard the integrity of the published record by issuing corrections and retractions when needed and pursuing suspected or alleged research and publication misconduct.
- Editors should pursue reviewer and editorial misconduct.
- Editors should critically assess the ethical conduct of studies in humans and animals.
- Peer reviewers and authors should be told what is expected of them.
- Editors should have appropriate policies in place for handling editorial conflicts of interest.

### *Reference:*

*Kleinert S & Wager E (2011). Responsible research publication: international standards for editors. A position statement developed at the 2nd World Conference on Research Integrity, Singapore, July 22-24, 2010. Chapter 51 in: Mayer T & Steneck N (eds) Promoting Research Integrity in a Global Environment. Imperial College Press / World Scientific Publishing, Singapore (pp 317-28). (ISBN 978-981-4340-97-7) [[Link](#)].*

### International Standards for Authors

Publication is the final stage of research and therefore a responsibility for all researchers. Scholarly publications are expected to provide a detailed and permanent record of research. Because publications form the basis for both new research and the application of findings, they can affect not only the research community but also, indirectly, society at large. Researchers therefore have a responsibility to ensure that their publications are honest, clear, accurate, complete and balanced, and should avoid misleading, selective or ambiguous reporting. Journal editors also have responsibilities for ensuring the integrity of the research literature and these are set out in companion guidelines.

- The research being reported should have been conducted in an ethical and responsible manner and should comply with all relevant legislation.
- Researchers should present their results clearly, honestly, and without fabrication, falsification or inappropriate data manipulation.
- Researchers should strive to describe their methods clearly and unambiguously so that their findings can be confirmed by others.
- Researchers should adhere to publication requirements that submitted work is original, is not plagiarised, and has not been published elsewhere.
- Authors should take collective responsibility for submitted and published work.
- The authorship of research publications should accurately reflect individuals' contributions to the work and its reporting.

- Funding sources and relevant conflicts of interest should be disclosed.
- When an author discovers a significant error or inaccuracy in his/her own published work, it is the author's obligation to promptly notify the journal's Editor-in-Chief and cooperate with them to either retract the paper or to publish an appropriate erratum.

*Reference:*

Wager E & Kleinert S (2011) *Responsible research publication: international standards for authors. A position statement developed at the 2nd World Conference on Research Integrity, Singapore, July 22-24, 2010. Chapter 50 in: Mayer T & Steneck N (eds) Promoting Research Integrity in a Global Environment. Imperial College Press / World Scientific Publishing, Singapore (pp 309-16). (ISBN 978-981-4340-97-7) [Link].*

Basic principles to which peer reviewers should adhere

Peer review in all its forms plays an important role in ensuring the integrity of the scholarly record. The process depends to a large extent on trust and requires that everyone involved behaves responsibly and ethically. Peer reviewers play a central and critical part in the peer-review process as the peer review assists the Editors in making editorial decisions and, through the editorial communication with the author, may also assist the author in improving the manuscript.

Peer reviewers should:

- respect the confidentiality of peer review and not reveal any details of a manuscript or its review, during or after the peer-review process, beyond those that are released by the journal;
- not use information obtained during the peer-review process for their own or any other person's or organization's advantage, or to disadvantage or discredit others;
- only agree to review manuscripts for which they have the subject expertise required to carry out a proper assessment and which they can assess within a reasonable time-frame;
- declare all potential conflicting interests, seeking advice from the journal if they are unsure whether something constitutes a relevant conflict;
- not allow their reviews to be influenced by the origins of a manuscript, by the nationality, religion, political beliefs, gender or other characteristics of the authors, or by commercial considerations;
- be objective and constructive in their reviews, refraining from being hostile or inflammatory and from making libellous or derogatory personal comments;
- acknowledge that peer review is largely a reciprocal endeavour and undertake to carry out their fair share of reviewing, in a timely manner;
- provide personal and professional information that is accurate and a true representation of their expertise when creating or updating journal accounts.

*Reference:*

Homes I (2013). *COPE Ethical Guidelines for Peer Reviewers, March 2013, v1 [Link].*

**Copyright Notice**

Articles published in IJOCTA are made freely available online immediately upon publication, without subscription barriers to access. All articles published in this journal are licensed under the Creative Commons Attribution 4.0 International License ([click here](#) to read the full-text legal code). This broad license was developed to facilitate open access to, and free use of, original works of all types. Applying this standard license to your work will ensure your right to make your work freely and openly available.

Under the Creative Commons Attribution 4.0 International License, authors retain ownership of the copyright for their article, but authors allow anyone to download, reuse, reprint, modify, distribute, and/or copy articles in IJOCTA, so long as the original authors and source are credited.

The readers are free to:

- Share — copy and redistribute the material in any medium or format
- Adapt — remix, transform, and build upon the material

for any purpose, even commercially.

The licensor cannot revoke these freedoms as long as you follow the license terms.

Under the following terms:

- Attribution — You must give appropriate credit, provide a link to the license, and indicate if changes were made. You may do so in any reasonable manner, but not in any way that suggests the licensor endorses you or your use.
- No additional restrictions — You may not apply legal terms or technological measures that legally restrict others from doing anything the license permits.



This work is licensed under a [Creative Commons Attribution 4.0 International License](https://creativecommons.org/licenses/by/4.0/).

# An International Journal of Optimization and Control: Theories & Applications

Volume: 9 Number: 3  
December 2019 (Special Issue)



## CONTENTS

- 1 On the numerical solution for third order fractional partial differential equation by difference scheme method  
Mahmut Modanlı
- 6 Investment evaluation of wind turbine relocation  
Hasan Huseyin Yildirim, Sakir Sakarya
- 15 Simulation of glucose regulating mechanism with an agent-based software engineering tool  
Sevcan Emek, Vedat Evren, Şebnem Bora
- 21 A comparison of some control strategies for a non-integer order tuberculosis model  
Tuğba Akman Yıldız
- 31 A new auxiliary function approach for inequality constrained global optimization problems  
Nurullah Yılmaz, Ahmet Sahiner
- 39 Analysis of boride layer thickness of borided AISI 430 by response surface methodology  
Turker Turkoglu, Irfan Ay
- 45 An application of fuzzy linear modeling: prediction of uncertainty for beta-glucan content  
Özlem Türkşen, Suna Ertunç
- 52 On the explicit solutions of fractional Bagley-Torvik equation arises in Engineering  
Zehra Pinar
- 59 Application of precedence constrained travelling salesman problem model for tool path optimization in CNC milling machines  
Ilker Kucukoglu, Tulin Gunduz, Fatma Balkancioglu, Emine Chousein Topal, Oznur Sayim
- 69 Maintenance of the latent reservoir by pyroptosis and superinfection in a fractional order HIV transmission model  
Ana R Carvalho, Carla M Pinto, João N Tavares
- 76 The DRBEM solution of Cauchy MHD duct flow with a slipping and variably conducting wall using the well-posed iterations  
Cemre Aydin, Münevver Tezer-Sezgin
- 86 Approximate controllability of nonlocal non-autonomous Sobolev type evolution equations  
Arshi Meraj, Dwijendra Narain Pandey
- 95 A Boiti-Leon Pimpinelli equations with time-conformable derivative  
Kamal Ait Touchent, Zakia Hammouch, Toufik Mekkaoui, Canan Unlu

